

SOME ASPECTS OF THE GEOCHEMISTRY OF POTASSIUM,  
RUBIDIUM, CESIUM, AND THALLIUM IN SEDIMENTS.

by

FRANK COGSWELL CANNEY

S.B., Massachusetts Institute of Technology  
(1942)

SUBMITTED IN PARTIAL FULFILLMENT OF THE  
REQUIREMENTS FOR THE DEGREE OF  
DOCTOR OF PHILOSOPHY

at the

MASSACHUSETTS INSTITUTE OF TECHNOLOGY  
(1952)

MASS. INST. TECH.  
WITHDRAWN  
FROM  
MIT LIBRARIES

Signature of Author .....  
Department of Geology, May 4, 1952

Certified by .....  
.....  
.....  
..... Thesis Supervisors

.....  
Chairman, Departmental Committee on Graduate Students

Some Aspects of the Geochemistry of Potassium,  
Rubidium, Cesium, and Thallium in Sediments.

Frank Cogswell Canney

Submitted to the Department of Geology on May 4, 1952 in  
partial fulfillment of the requirements for the degree of  
Doctor of Philosophy.

The development of an accurate D. C. arc quantitative spectrochemical scheme of analysis for the determination of Rb, Cs, and Tl in sediments is described in Part I. Potassium, present as a structure constituent in a known concentration, was used as a variable internal standard. The following line pairs were used: Rb 7947/K 6939, Rb 7800/K 6939, Cs 8521/K 6939, and Tl 5350/K 4047. Excellent near 45° working curves were obtained in all cases. Standard deviations were: Rb ± 4.3%, Cs ± 8.2%, and Tl ± 8.0%. Average detection limits were: Rb - 0.0001%, Cs - 0.0001%, and Tl - 0.00001%. All analyses were calibrated in terms of the standard granite (G-1) and standard diabase (W-1) to reduce systematic errors.

In Part II, pertinent aspects of the geochemistry of K, Rb, Cs, and Tl are discussed in the light of data obtained from the analyses of 324 samples, the majority of which came from ten sedimentary geological formations. Abundance values are given for the above elements in the various formations and sedimentary rock types. Average abundance values for these elements in argillaceous sediments are: K<sub>2</sub>O - 1.96%, Rb<sub>2</sub>O - 0.031%, Cs<sub>2</sub>O - 0.00081%, and Tl<sub>2</sub>O - 0.000038%. Thallium is usually enriched in highly organic sediments.

The comparison of the  $\frac{\%K_2O}{\%Rb_2O}$ ,  $\frac{\%K_2O}{\%Cs_2O}$ ,  $\frac{\%K_2O}{\%Tl_2O}$ , and  $\frac{\%Rb_2O}{\%Tl_2O}$  abundance ratios in sediments with the average values of these ratios in igneous rocks shows that the order of relative enrichment of these elements in sediments is normally: Cs > Rb > K > Tl.

The conclusion is reached that the order of relative enrichment found is in excellent agreement with the theory that the adsorption affinity of a cation from aqueous solutions is believed to be proportional to the value of the positive electrostatic potential existing at the surface of the hydrated ion.

Thesis Supervisors:

Walter L. Whitehead  
Associate Professor of Geology

Louis H. Ahrens  
Assistant Professor of Geology

## Contents

Abstract .....	2
Acknowledgments .....	6

## Part I

I.	Introduction .....	8
II.	Instrumentation .....	10
	A. The Spectrographs .....	10
	B. The Microphotometer .....	11
III.	Choice of Optimum Operating Conditions .....	15
	A. Preliminary work .....	15
	B. Attainment of adequate spectral sensitivity .....	17
	C. Summary .....	19
IV.	Preparation of Samples .....	25
	A. General .....	25
	B. Ignition treatment .....	26
	C. Possible volatilization losses .....	27
	D. Weight losses .....	30
V.	Development of a Quantitative Method .....	33
	A. General .....	33
	B. Internal standardization .....	33
	(1) General .....	33
	(2) Suitability of potassium .....	34
	(3) Variation internal standard method .....	42
	C. Plate calibration .....	43
	(1) General .....	43
	(2) Frequency of calibration .....	44
	(3) Calibration method .....	45
	(4) Achievement of even slit illumination .....	47
	(5) Construction of characteristic curves .....	52
	(6) Calibration of 103-J type emulsion .....	56
	(7) Calibration of I-N type emulsion .....	60
	(8) Construction of accurate low density calibration curves .....	62
	(9) Accuracy of calibration .....	66

D.	Background .....	66
	(1) General .....	66
	(2) Background correction .....	68
	(3) Correction for "invisible" background .....	72
	(4) Effect on precision .....	76
	(5) Effect on minimum detectibility .	76
E.	Photographic development .....	77
	(1) General .....	77
	(2) Development .....	77
	(3) Fixing .....	80
	(4) Washing .....	81
	(5) Drying .....	82
F.	Preparation of standards .....	82
	(1) General .....	82
	(2) Preparation of synthetic base materials .....	83
	(3) Preparation of standards .....	86
G.	Construction of working curves .....	88
H.	Photometric procedure and calculations ...	93
I.	Precision and accuracy of analytical methods .....	94
	(1) General .....	94
	(2) Precision obtained .....	96
	(3) Discussion of precision obtained.	97
	(4) Accuracy of methods .....	101
J.	Discussion of errors .....	103
VI.	Analysis of Samples .....	105
	A. General discussion .....	105
	B. Interfering lines and bands .....	105

## Part II

VII.	Introduction .....	113
	A. Purpose of investigation .....	113
	B. Chemistry of thallium .....	118
	C. Location and description of formations ...	120
	(1) General .....	120
	(2) Miocene Modular Shale .....	122
	(3) Cherokee Shale .....	123
	(4) Woodford Shale .....	123
	(5) Upper Cretaceous formations .....	124
	D. Presentation of data .....	126
VIII.	The Abundance of K, Rb, Cs, and Tl .....	128
	A. General .....	128
	B. The abundance of potassium .....	129
	C. The abundance of rubidium .....	129

D.	The abundance of cesium .....	147
E.	The abundance of thallium .....	156
IX.	Discussion of the Abundance Ratios .....	164
A.	The ratios in igneous rocks .....	164
B.	The $K_2O/Rb_2O$ ratio in sediments .....	167
C.	The $K_2O/Cs_2O$ abundance ratio .....	173
D.	The $Rb_2O/Tl_2O$ abundance ratio .....	187
E.	The $K_2O/Tl_2O$ abundance ratio .....	194
X.	Discussion of Results .....	207

#### Appendixes

A.	Tables Giving Values of $D_0/D$ ( $D_0 = 100$ ) for Values of $D$ From 0 to 70 .....	213
B.	Tables Giving the Quantitative Analyses of All Samples Studied in This Investigation .....	216
C.	Tables Giving the Abundance Ratios for All Samples .....	231
D.	Location of Samples .....	245
	Biography .....	254
	Bibliography .....	255

Acknowledgements

I wish to thank Professor Walter L. Whitehead for permission to undertake this investigation while I was a Research Assistant on the American Petroleum Institute Research Project 430. His active interest and advice were indeed most helpful.

I also would like to extend my appreciation to Professor Louis H. Ahrens who generously spent many hours with me in discussing the numerous problems that arose during the course of this work. His many helpful suggestions and criticisms were extremely welcome.

The majority of the samples used in this investigation were obtained by the American Petroleum Institute Research Project 430 through the courtesy of the following oil companies: Carter Oil Company, Gulf Oil Company, Phillips Petroleum Company, and the Standard Oil Company of California.

Thanks again to my wife for all of her assistance and encouragement.

F. C. C.

May 1952

To my wife

## Part I

### The Development of a Quantitative Spectrochemical Method.

#### I. Introduction

This part discusses the methods used to develop an accurate quantitative spectrochemical method for the analysis of rubidium, cesium, and thallium in sediments. The reader may wonder why such a large part of this thesis is concerned with a discussion of the analytical techniques. However, considerable effort and time had to be spent on development of the methods for two reasons. First, the detection limits using standard methods were such that only rubidium, of the three analysis elements, was known to occur in the sediments in a quantity well above its detection limit. Cesium was a borderline case, whereas the average amount of thallium in the sediments was well below its ordinary detection limit. Consequently, attainment of adequate detection limits was vital if the majority of samples were to be successfully analyzed for cesium and thallium. Second, a high degree of precision in the analytical method was considered absolutely necessary if any significant and valid conclusions were to be drawn from the analytical results. For example, conclusions as to whether or not an element had concentrated in the sediments with respect to another element were drawn from a comparison of the ratios of these two



elements in igneous rocks and in sediments. A change in a ratio might have been extremely small but still would have been significant. The ability to detect a small change in a ratio depended of course on the precision of the analytical method, for small changes would have been masked by large analytical errors.

Three hundred and twenty-four sedimentary rock samples from ten geological formations were analyzed. They were all samples which had been analyzed for potassium with a Perkin-Elmer flame photometer by personnel of the American Petroleum Institute Research Project 43C. In fact, the existence of such a large collection of samples which had been accurately analyzed for potassium was the main reason why the writer undertook this investigation. The presence of potassium, which is a good internal standard for all of the analysis elements, as a structure constituent of the samples offered the opportunity of developing a really precise quantitative method.

The composition of the samples varied over a rather wide range, representing as they did, shales, sandstones, and limestones, although the majority of the samples were probably fairly similar in composition. No one method would have been the ideal method for every sample. Consequently, an attempt was made to develop a general scheme of analysis which would give the most precise results for the greatest number of samples.

## II. Instrumentation

### A. The Spectrographs

The instrument utilized for the determination of thallium was a 21 foot, 30,000 lines-per-inch concave grating spectrograph in a Wadsworth mounting. The arcing bench of this instrument is shown in Fig. 1. A complete description of this spectrograph has been given in several earlier theses and need not be repeated here. The use of this instrument was required to obtain the dispersion necessary to free the T15350.46A line from interference by Ca5349.47A and T15351.084A. At the setting used for the determination of thallium, the dispersion was 2.43A/mm. on the plate. The standard set-up on this instrument was to place the center of the plate holder at 4800A (Focus 1.75). One quarter of a type 103-J plate was placed to pick-up T15350A (230 mm. to left of the center) and another quarter plate placed to record K4044A and K4047A ( 318 mm. to right of the center).

The instrument used for the determination of rubidium and cesium was a Hilger model R478 large quartz and glass spectrograph in the Littrow mounting. Details of this type of mounting may be found in any of the more complete texts on spectroscopy. The instrument mounted in the Cabot Laboratory is shown in Fig. 2. With the glass optics, adequate dispersion was available to separate the cesium

and rubidium lines from any serious interference. For the determination of the alkali metals, the right end of the plate holder was placed at 10,000Å. A four by five plate (Type I-N) was placed 11/16 inches from the right end of the plate holder.

#### B. The Microphotometer

All photometric measurements were made on a Projection Comparison Microphotometer manufactured by the Jarrell-Ash Company. This instrument is shown in use in Fig. 3.



Fig. 1

Arcing bench of grating spectrograph.



Fig. 2

Hilger large quartz and glass spectrograph.



Fig. 3

Jarrell-Ash projection comparator microphotometer

### III. Choice of Optimum Operating Conditions

#### A. Preliminary work

At the start of this investigation it was hoped that it would be possible to analyze for all three elements simultaneously. The spectral lines of these elements which were considered sensitive enough to investigate are listed in Table 1. The material in this table is taken from the M. I. T. Wavelength Tables compiled by Dr. G. R. Harrison.

Table 1

<u>Rubidium</u>	<u>Intensity</u>	<u>Sensitivity</u>
7947.60	5000R	U2
7800.227	9000R	U1
4215.556	1000R	U4
4201.851	2000R	U3
 <u>Cesium</u>		
8943.50	2000R	U2
8521.10	5000R	U1
4593.177	1000R	U4
4555.355	2000R	U3
 <u>Thallium</u>		
5350.46	5000R	U1
3775.72	3000R	U2
3519.24	2000R	U3

Preliminary tests on the grating spectrograph soon revealed that the cesium and rubidium lines in the violet were not suitable. Lack of sufficient sensitivity and excessive interference from strontium, iron, and titanium

lines ruled out any possible consideration of their use. Tl 3775 seemed to be highly sensitive, provided cyanogen emission was quenched.

The preliminary work on the prism instrument showed that Rb 7800, Rb 7947, and Cs 8521 were highly sensitive provided a panchromatic emulsion was used. Cs 8943 was not useable due to poor emulsion sensitivity at this wavelength with Type I-N plates. Tl 5350 also proved not to be useable on this instrument due to direct interference by Ca 5349 (See Fig.27, pg.109). As a result of this finding, it became necessary to analyze each sample twice, once on the prism instrument for rubidium and cesium and once on the grating instrument for thallium.

On the grating instrument, Tl 3775 seemed to be slightly more sensitive than Tl 5350 although the latter line is generally reported as being the most sensitive. However, Tl 5350A was selected for use for two reasons. First, a CN band component is coincidental with Tl 3775 and this meant that unless CN emission was completely quenched, a process that is not always easy to do, direct interference from CN would result. Second, interference from Ni 3775.572 with Tl 3775 was considered possible due to the fact that many of the samples had been ground in a nickel-steel mortar with the probable resulting contamination of these samples with traces of nickel.



The spectrograph is similar to many other types of detection devices in that the limit of detection depends upon a "signal to noise ratio". In spectroscopy, this "noise" is the intensity of the background radiation while the "signal" is the intensity of the sought for radiation. It will be pointed out in the section on background that a line can be used provided its intensity is 0.2 to 0.3 times the intensity of the background. Thus attempts to

ordinary detection limits for cesium and thallium were about 0.0003% and 0.0001% respectively. The experimentation was required to accomplish this end. The particularly thallium, had to be increased. Considerable thallium, the spectral sensitivities of those two elements, samples were to be successfully analyzed for cesium and as mentioned in the introduction, in the majority of

B. Attainment of adequate spectral sensitivity

Element	Line Pair
Thallium	$\frac{71\ 5350}{K\ 4047}$
Cesium	$\frac{68\ 8521}{K\ 6939}$
Rubidium	$\frac{7947\ Rb}{7800\ Rb}\ \frac{K\ 6939}{K\ 6939}$

Following line pairs seemed to be the most suitable: as a result of these preliminary experiments, the

improve sensitivity are generally centered around methods which increase the intensity of a line relative to that of the background. In attempting to obtain maximum line-to-background intensity ratios and resulting lower detection limits, the writer used the following facts as a general guide. The analysis elements are all extremely volatile and their spectral lines emit their peak intensity early in the arcing cycle. The intensity of the continuous radiation, on the other hand, remains fairly constant, at least during the first part of the arcing period. Thus it seemed that maximum line-to-background intensity ratios would result by arranging the operating conditions so as to boil off the greater percentage of the analysis elements in as short a period as possible. This could be effected by the proper selection of sample size, electrode design, amperage, and arcing time.

The decisions on these various questions were made empirically. The general procedure adopted was to arc a sample a number of times on the same plate with all the variables held constant, except one, which was systematically varied from exposure to exposure. The setting for that particular variable which gave the maximum line-to-background intensity ratio was then determined visually.

The slit width was also quite critical. Continuous background on the plate is merely a series of overlapped

slit images and therefore its intensity is closely proportional to the slit width. Line intensity, on the other hand, increases as the slit is widened only up to a certain critical width, after which there is no appreciable increase in line intensity with further widening of the slit. Thus the optimum slit width for obtaining maximum line-to-background intensity ratios is close to this critical value.

The emulsion types selected were those which were specially sensitized for the wavelength regions in which they were used. Contrary to general opinion, use of a more sensitive emulsion does not increase the limit of detection of an element because increased sensitivity merely increases the intensities of both lines and background proportionally. It does decrease the exposure time and sample size required to produce a useable line image.

### C. Summary

The operating conditions selected are listed in Tables 2 and 3. The actual detection limits attained were somewhat variable, depending to some extent on the background. The following might be considered as average values:

Tl	-	0.00001%
Rb	-	0.0001%
Cs	-	0.0001%

These detection limits were found to be adequate for the majority of the samples.

The improvement in the case of cesium was not as great as had been hoped for, but this was offset to a considerable extent by the fact that the average cesium content of the sediments was found to be somewhat higher than had been expected.

Table 2

Operating conditions for the determination  
of thallium

Spectrograph	- 21 ft. concave grating instrument. Center of plate holder at 4800A (Focus 1.75). Two 3" x 4" plates placed to record K 4047 and Tl 5350.
Optical arrangement	- Short focus spherical condenser focused on slit.
Excitation	- Anode, 220-230 <sup>v</sup> D. C., 6 amperes.
Analytical gap	- 4-5 mm.
Electrode type	- Anode - 3/16" regular carbon rod, 1" long, with a cavity 1/8" in dia. and 1/4" deep. Cathode - 3/16" carbon rod pointed at one end.
Emulsion	- Eastman 103-J.
Slit width	- 0.025 mm.
Slit height	- 6 mm.
Exposure time	- 45 seconds.
Weight of charge	- ~50 mg.
Composition of charge	- Undiluted sample.
Sectoring	- Special stepped sector, 3 steps: 1:2, 1:32, 1:64, plus 1:1 step.
Development	- 4 1/2 minutes in Eastman D-19 (Dil. 1:1 with H <sub>2</sub> O) at 20°C.
Line pair	- <u>Tl 5350</u> K 4047
Samples per plate	- Six in duplicate

Precautions taken - Upper electrode holder cleaned  
between samples - clean anode  
for every sample.

Operating conditions for the determination  
of thallium

Table 2 - continued

Table 3

Operating conditions for the determination  
of the alkali metals

Spectrograph	- Hilger Prism Instrument. Glass optics. Focus 4-3. Shutter setting - 12 mm. Right end of plate holder at 10,000A. 4" x 5" plate placed 11/16" from right end of plate holder.
Optical arrangement	- Short focus spherical condenser focused on slit.
Excitation	- Anode, 220-230 <sup>V</sup> D. C., 6 amperes.
Analytical gap	- 4-5 mm.
Electrode type	- Anode - 3/16" regular carbon rod, 1" long, with a cavity 1/8" in dia. and 1/4" deep.  Cathode - 3/16" carbon rod pointed at one end.
Emulsion	- Eastman I-N.
Slit width	- 5 divisions(0.025 mm.).
Slit height	- 11 mm.
Exposure time	- 45 seconds
Weight of charge	- ~ 50 mg.
Composition of charge	- Undiluted sample.
Sectoring	- Seven step sector, 1:2, 1:4, 1:8, 1:16, 1:32, 1:64, 1:128.
Development	- 4 1/2 minutes in Eastman D-19 (Dil. 1:1 with H <sub>2</sub> O) at 20°C.

Table 3 - Continued

Operating conditions for the determination  
of the alkali metals

Line pairs	- Rubidium $\frac{\text{Rb } 7800}{\text{K } 6939}$ , $\frac{\text{Rb } 7947}{\text{K } 6939}$ .
	Cesium $\frac{\text{Cs } 8521}{\text{K } 6939}$ .
Samples per plate	- Six.
Precautions taken	- Clean cathode used for every sample. Upper electrode holder cleaned between samples.



#### IV. Preparation of Samples

##### A. General

The samples used in this investigation came from the extensive collection of sedimentary rock samples available in the M. I. T. Geology Department where they had been used in the API Research Project 43C. The majority of samples used in this work were already ground to a satisfactory degree of fineness and only a very occasional sample required further grinding.

As a general rule, untreated sedimentary rock samples behave very badly in the D. C. arc. This is due to the fact that many sediments contain appreciable quantities of organic matter, water, and carbonates. These materials decompose when the arc is struck and release large quantities of gas which tends to blow the sample out of the electrode. In some cases, complete loss of sample occurs within a few seconds; in others, the sample remains but the burn is quite erratic, and excessive spectral background results from the many incandescent particles being wafted up into the arc column. A preliminary survey of the arcing qualities of the selected samples disclosed the expected poor behavior in the arc. Consequently it was clear that some treatment would be necessary if a satisfactory smoothness of burn was to be attained.

## B. Ignition treatment

The first expedient tried, which proved successful enough to be adopted, was to remove the organic matter and adsorbed water by heating the samples in an electrically operated muffle furnace. When any ignition procedure like this is used, one has to consider possible losses of analysis elements by volatilization during the sintering process. The boiling points of all alkali metal compounds were high enough to obviate any concern for them so thallium remained the critical element. It was noted that Rankama (18) predicted the possibility that thallium was present in sediments as thallic chloride (B.P. -  $720^{\circ}\text{C}$ ) so it seemed that  $700^{\circ}\text{C}$  would be the ceiling temperature for any sintering process.

A series of experiments was conducted to decide on the best sintering temperature and time. The material used was a black highly organic shale from Big Marsh, Nova Scotia. Samples of this shale were placed in small porcelain crucibles and sintered at varying temperatures and for different times. The best compromise between the lowest possible ignition temperature and destruction of the organic matter within a reasonable period of time seemed to be one hour at a temperature of  $450^{\circ}\text{C}$ . As a result of this, all samples used in this investigation were sintered for one hour at  $450^{\circ}\text{C}$ . After sintering,

the samples were stored in tightly corked glass vials to prevent them from picking up any moisture. Mitchell (15) also found a temperature of 450°C to be the most suitable for the dry ashing of organic materials.

This sintering greatly improved the arcing qualities of the majority of the samples. In fact, less than 5% of the 324 sintered samples could still be classified as really "bad actors", and these were samples containing a very high percentage of calcium carbonate which, of course, was not decomposed at the ignition temperature used. It was found that losses during arcing of samples high in calcium carbonate could generally be avoided by momentarily reducing the amperage at critical points in the burn - a point that had to be learned by experience. Fig. 4 shows how sintering lessened the background. There it may be seen how much less intense the background is in the 500° sample than in the other two.

### C. Possible volatilization losses

To check on the possible loss of any of the analysis elements during sintering, a series of Big Marsh shale samples were sintered at the following temperatures: 105°, 300°, 500°, 700°, and 1000°C. Each of the resulting samples was then analyzed using both standard operating methods and the following intensity ratios determined for each sample:  $\frac{Tl\ 5350}{K\ 4047}$ ,  $\frac{Rb\ 7947}{K\ 6939}$ , and  $\frac{Cs\ 8521}{K\ 6939}$ . Any change

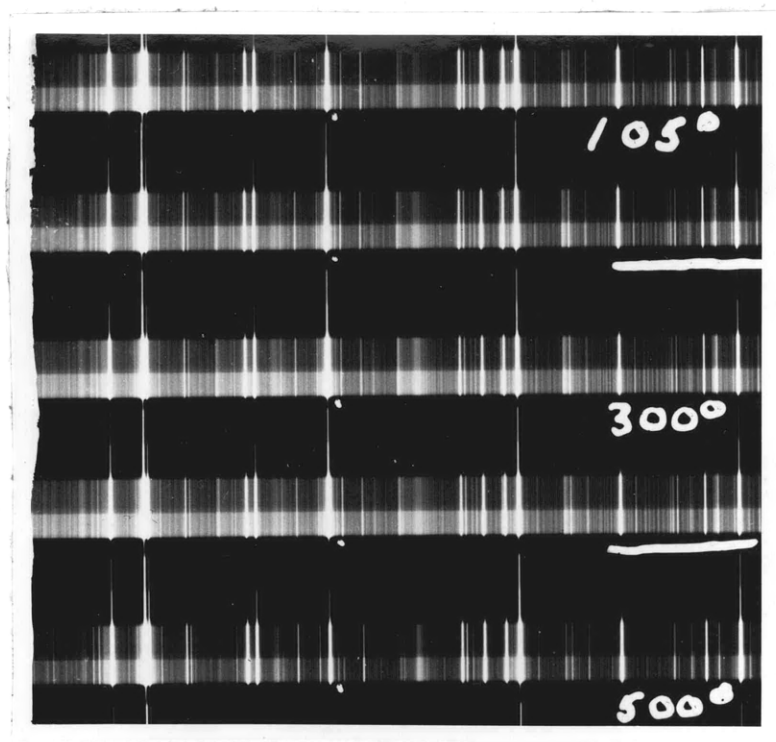


Fig. 4

Reduction of background by destruction of  
organic matter.

found in a given ratio outside of experimental error would, of course, indicate volatilization losses. The rubidium and cesium ratios in all samples were found to be constant within the limits of experimental error. For thallium though, the ratios for the 105° and 300° samples were slightly higher than the ratios for the three remaining samples, thus indicating a possible partial loss of thallium. However, in view of the rather large standard deviation for thallium and the probable even larger deviation in the case of the poorer burning 105° and 300° samples, it was statistically impossible with the data available to definitely conclude whether or not any loss of thallium had occurred. All that could be said on the basis of this evidence was that if a loss did occur, it was not large. In connection with a possible thallium loss, the following interesting facts were noted during the analysis for thallium of the Miocene Nodular shale samples. Samples from this formation occasionally carried appreciable quantities of fluorine as evidenced by the presence of strong CaF bands with main band head at 5291A (See Fig. 26, pg.108). There seemed to be a rough correlation between the presence and intensity of this band and the intensity or absence of the thallium line, although it was rather hard to prove the presence or absence of thallium whenever the CaF bands were intense, as the tail of this band blanketed the region of the

thallium line. After making this observation, the volatilities of all thallium compounds were rechecked and it was noted that thallium fluoride has a boiling point of 300°C, 150° below the sintering temperature used. Thus it seems entirely possible that some thallium might have been lost during sintering from those samples which were high in fluorine. On checking back to the Big Marsh samples, a slight development of CaF bands was noticed there. Consequently, the change in the  $\frac{Tl\ 5350}{R\ 4047}$  intensity ratio which was discussed before might be a valid change due to a slight loss of thallium as thallium fluoride. Further experiments though would be necessary to completely prove or disprove this point. Cholak (6) states that no thallium losses occurred during experiments in the dry ashing of organic matter. In any event, even if losses did occur, less than ten percent of all samples would have been affected by this source of error as this was about the number of samples which showed any development of the CaF band.

#### D. Weight losses

Another point checked was the magnitude of the weight loss during the sintering process. This was accomplished by actually determining the percent weight loss on twenty-one samples of Cherokee shale which had varying organic carbon contents. The results which are plotted in Fig. 5

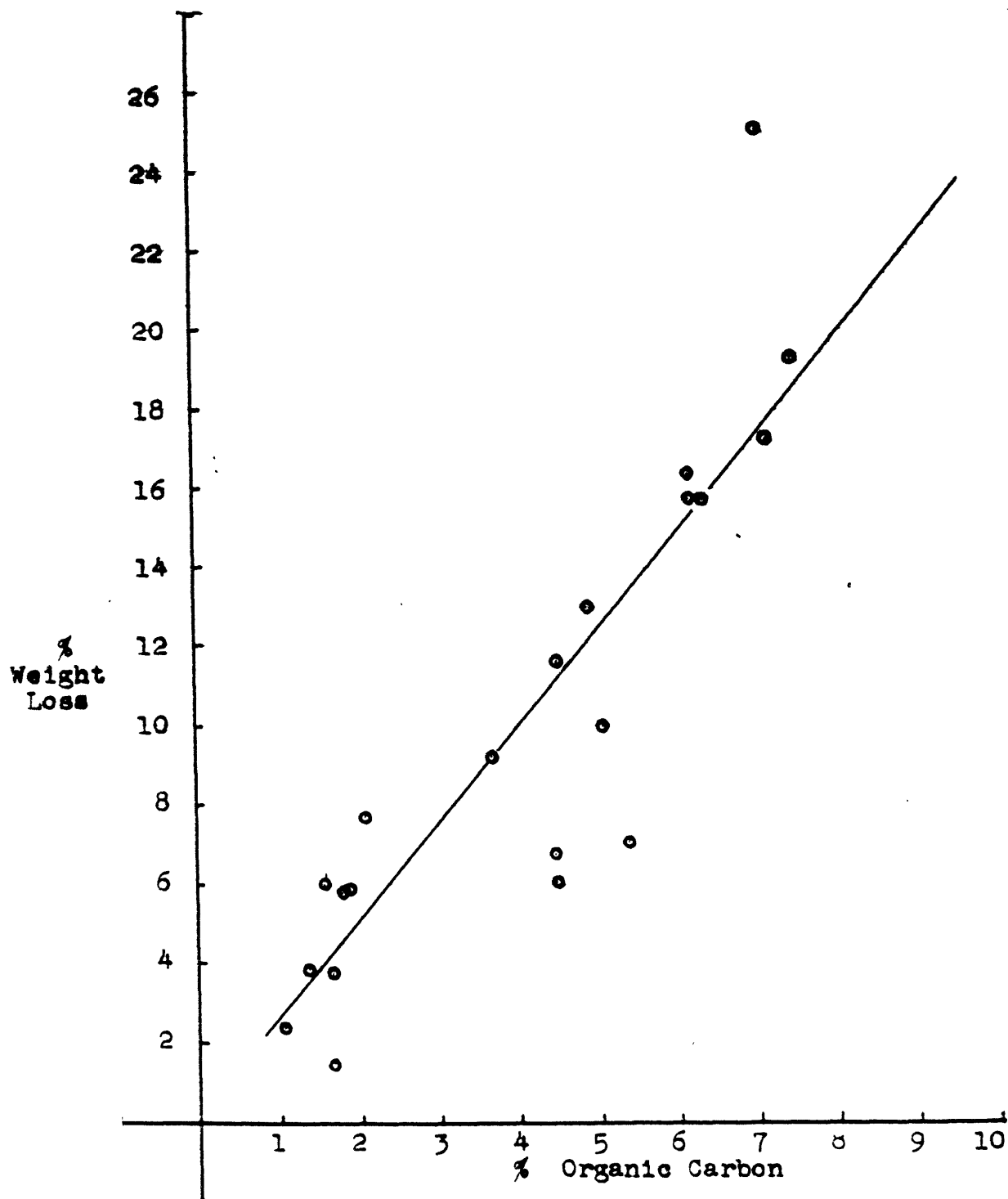


Fig. 5

Relationship between % weight loss and % organic carbon in 21 samples of Cherokee shale. All samples sintered for one hour at 450°C.

show that there is a fair linear correlation between percent weight loss and percent organic carbon. Information about the magnitude of weight losses was desired because of the resulting increase in the percentages of all elements remaining in the sintered samples. For example, K 4047A, the internal standard line for thallium, begins to self-absorb under the operating conditions used at about 5%  $K_2O$ . Consequently, if weight losses had been of such a magnitude that the  $K_2O$  percentages in the sintered samples would have been radically increased, errors due to self-absorption by the internal standard line might have resulted. However, the average weight loss was small enough so that this potential source of error could be disregarded.

The fact that the potassium values were based on the original unsintered samples meant that this applied an automatic correction for weight losses in the computation of the analytical results. Therefore, all reported percentages for rubidium, cesium, and thallium are those existing in the original samples.



## V. Development of a Quantitative Method

### A. General

Quantitative spectrochemical analysis is based upon the fact that when a sample is volatilized in an arc, most elements present in the sample emit radiation in the form of light. For any given element the intensity of this radiation is a function of the concentration of that element. However, the matter is complicated by the fact that many factors beside element concentration influence line intensity as recorded on the spectrogram. For a much fuller discussion of the basis for quantitative spectrochemical analysis, the reader is referred to any of the general texts on spectroscopy.

### B. Internal standardization

#### (1) General

It is generally recognized today that some form of internal standardization must be employed to attain the highest precision in a quantitative method. An internal standard method is one where the concentration of an element is determined through its relationship to the intensity ratio of a line of the element to be determined and a line of another element present in constant or known amount. Its general superiority is due to the fact that it is assumed that all the variables other than concentration affect

the intensities of the analysis line and internal standard line in a similar manner. The most precise results are obtained in any method employing internal standards when the internal standard and analysis element have similar characteristics. The factors which must be considered in the choosing of an internal standard have been thoroughly discussed by Ahrens ( 2 ) and need not be repeated here.

## (2) Suitability of potassium

It was mentioned earlier that one of the major factors which influenced the writer to undertake this investigation was the presence of a large number of samples which had been analyzed for potassium. This was because potassium was known to be a satisfactory internal standard for the other alkali metals, and the writer believed that it would also be at least a fair internal standard for thallium. Nevertheless, it was considered necessary to check its effectiveness as an internal standard under the operating conditions used for the analysis of the samples.

The volatilization rates of potassium, rubidium, and cesium from both a typical sample and a synthetic mixture were determined by arcing each sample in the usual manner except that the plate was racked down at the end of each five second interval. The resulting plots of intensity versus time are shown in Fig. 6. It is seen that all three elements volatilize in a very similar manner both

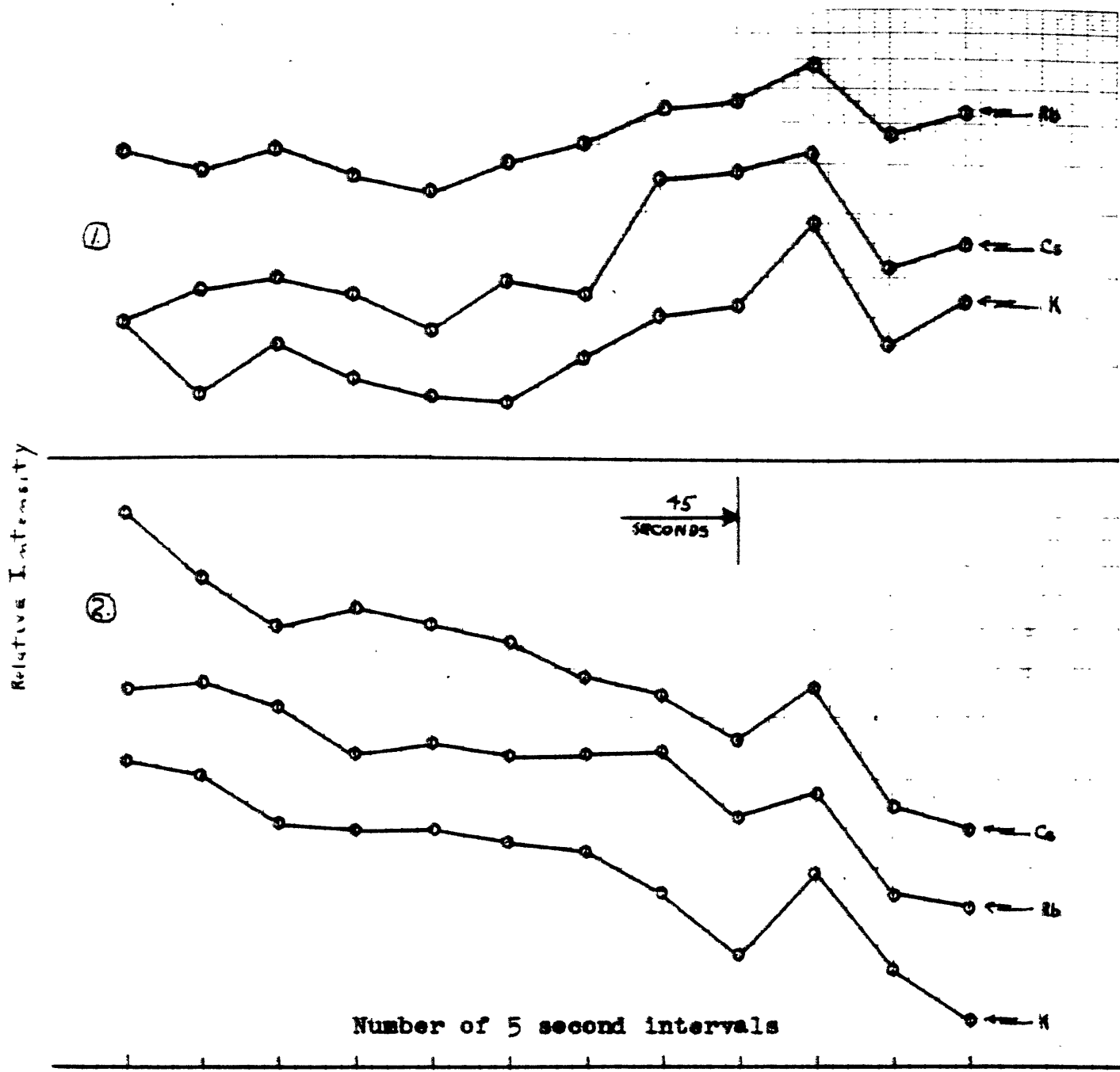


Fig. 6

Volatilization plots for rubidium, cesium, and potassium from a synthetic mixture (No. 1) and sample 45125 (No. 2). Some intensities have been multiplied by a constant factor for convenience in plotting

from the sample and the synthetic mix, thus indicating that good reproducibility was to be expected. It is interesting to note that while peak alkali emission from sample 45125 occurred extremely early during the arcing period, peak emission from the synthetic standard mix occurred towards the end of the period. This accounted for the fact noted during the preparation of the working curves, that the lines from the synthetic standards were always weaker than those lines from natural materials with the same element concentration, due to peak alkali emission from the standards never being recorded on the plate when the standard procedure with its arcing period of 45 seconds was used. Satisfactory volatilization curves for thallium could not be obtained due to the slowness of the plate racking mechanism on the grating instrument. However, thallium is known to be as volatile, if not more so, than the alkali metals.

Except in the immediate vicinity of the electrodes, excitation in the D. C. arc is largely thermal. The temperature also varies longitudinally in the arc column, and this causes a longitudinal variation in the exciting power of the arc. The stability of the various line pairs to changing excitation conditions was checked by plotting the longitudinal intensity distribution of the various lines. Standard operating conditions were used except that the entire slit was sectorized by a constant amount. The

resultant lines were divided into 1.5 mm. long segments, and the intensity of each segment determined in the usual fashion. The plots of the longitudinal intensity distribution for all the lines are shown in Figs. 7 and 8. Due to fairly similar excitation characteristics, all the intensity distribution curves are seen to be very similar. The intensity ratios of the various line pairs were therefore largely unaffected by changing excitation conditions in the arc. The longitudinal positioning of the arc image on the slit was also less critical.

Checks showed that the internal standard lines K 4047 and K 6939 would be free of self-absorption at the concentration of potassium existing in practically all of the samples. K 6939 was found to be free of self-absorption at any concentration, while K 4047 was reasonably safe provided the potassium concentration was not over about five percent.

The effectiveness of potassium as an internal standard element is shown in Figs. 9 and 10. From these plots one can observe how satisfactory the compensation was for each line pair. It is seen to be practically perfect for the potassium-rubidium pair; satisfactory for potassium-cesium; and only fair for potassium-thallium. This is also the order of increasing standard deviations, as would be expected. The effectiveness of potassium as an internal standard for thallium was probably, as a general rule, somewhat better

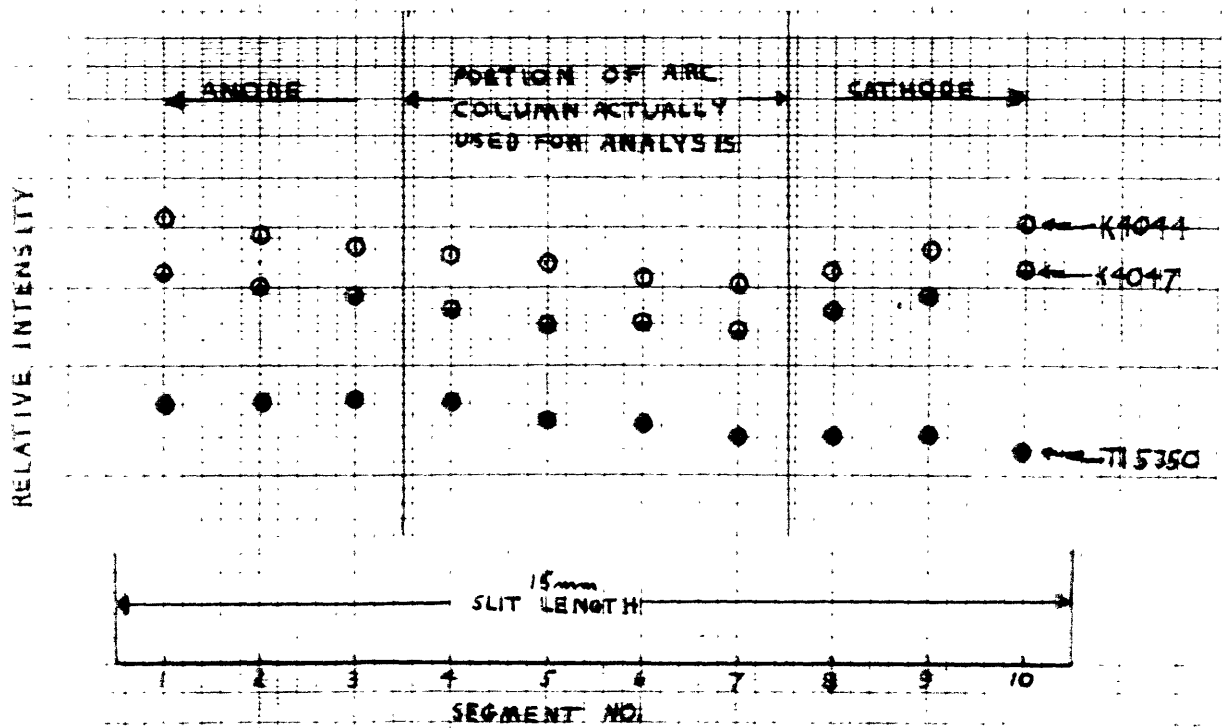


FIG. 7

Longitudinal intensity distribution in  
arc of K 4044, K 4047, and Tl 5350

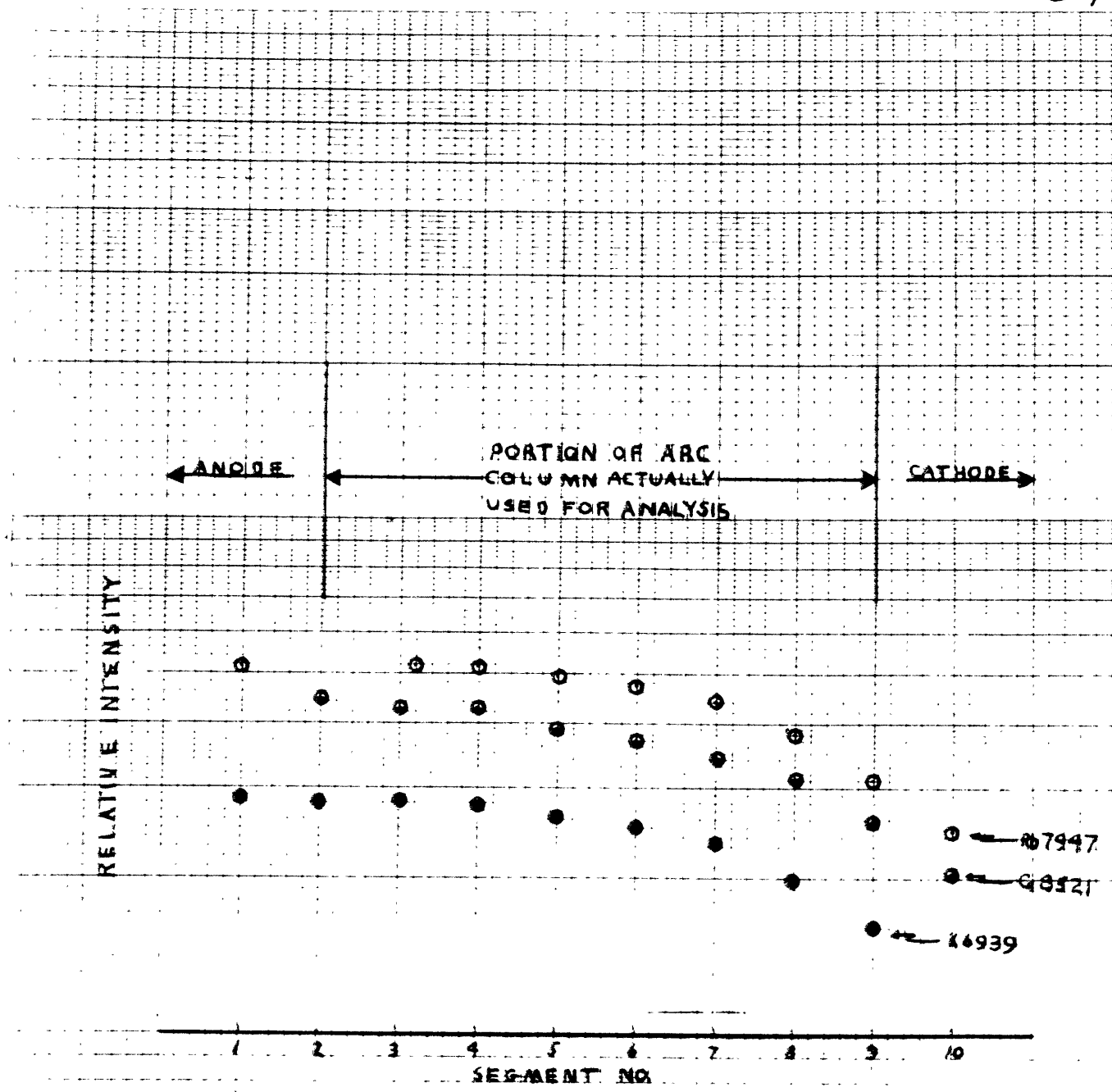


Fig. 8

Longitudinal intensity distribution in arc of Rb 7947, Cs 8521, and K 6939

PRINTED IN U. S. A.

1 CENTIMETER X 10 DIVISIONS

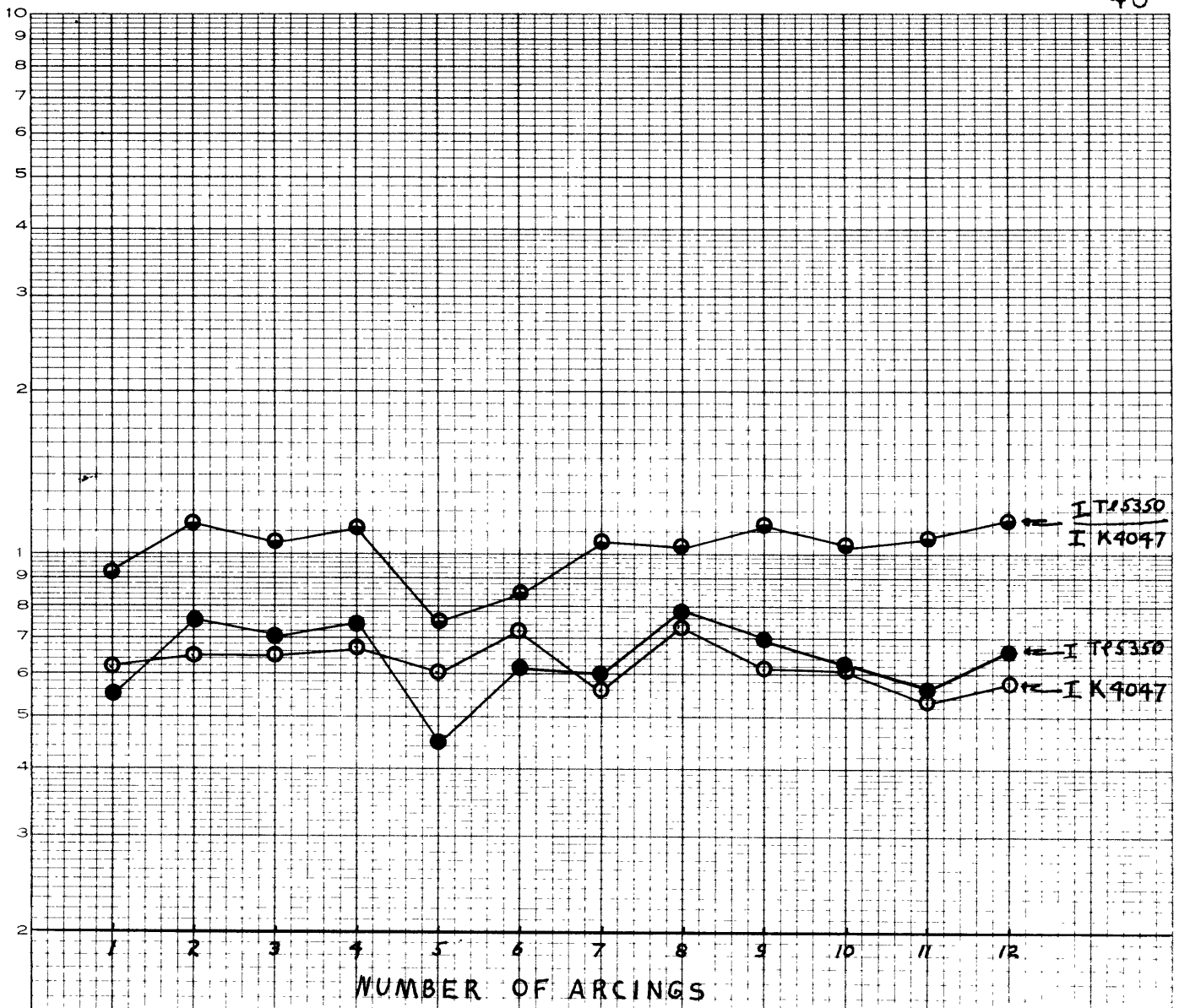
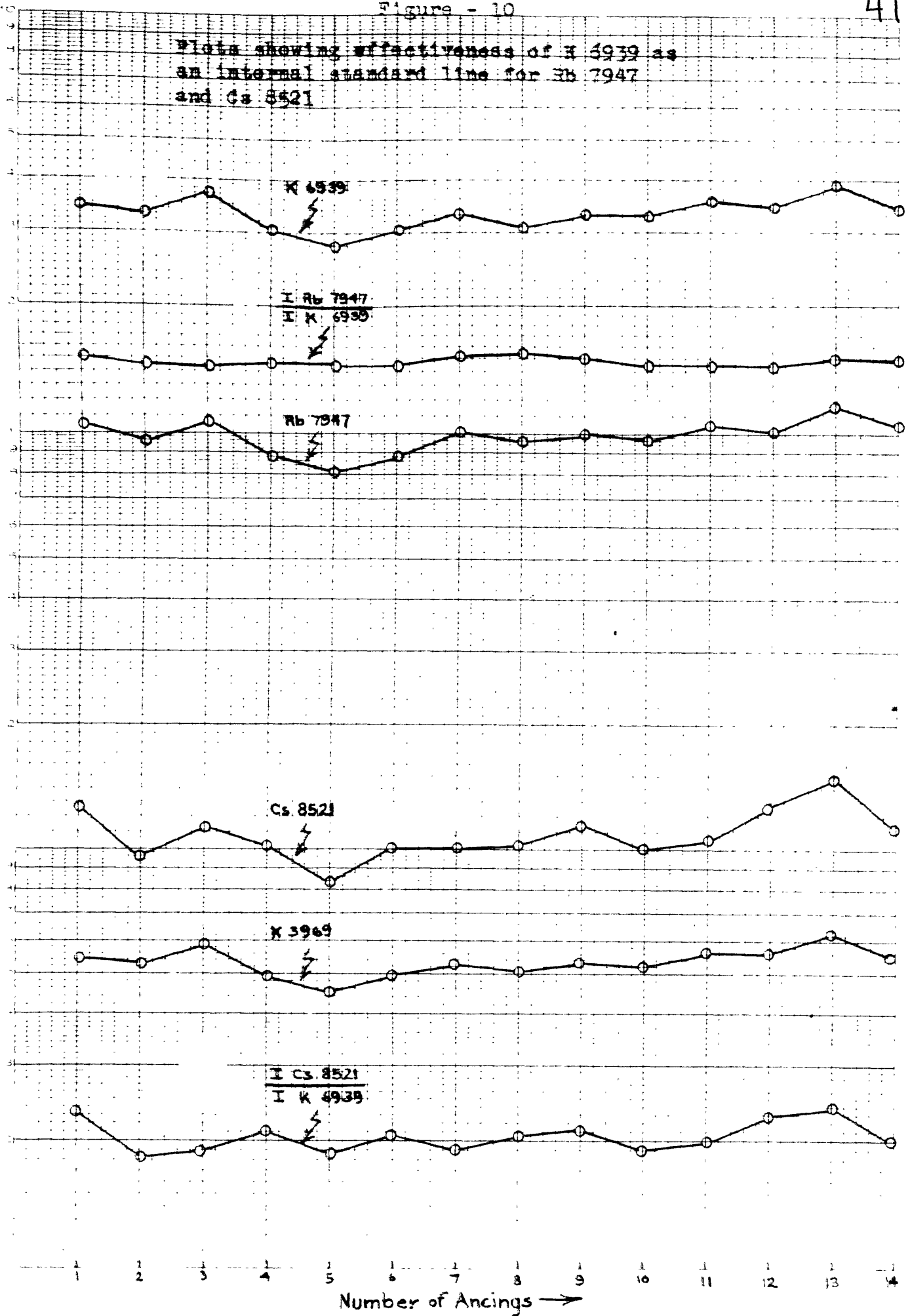


Fig. 9

Plot illustrating effectiveness of K 4047 as an internal standard line for Tl 5350



Plots showing effectiveness of K 6939 as  
an internal standard line for Rb 7947  
and Cs 8521



than the rather large standard deviation would indicate, but there would be occasional samples where potassium afforded absolutely no compensation. These occasional wild fluctuations in the intensity of the thallium line were attributed to the fact that the lower level of Tl 5350A is a metastable one.

Standard deviations with and without internal standardization were computed for all the analysis elements. Use of an internal standard improved the reproducibility in all cases.

### (3) Variation internal standard method

An internal standard is usually thought of as an element which is present in constant amount. In the majority of methods this is so, but it need not be, for it can be present in a variable amount providing it is a known amount. Such methods are known as variation internal standard methods, and the writer had to use such a type in this investigation. The only difference between a method of this type and the conventional type is that in constructing the working curve, the intensity ratio of the line pair is plotted against the concentration ratio of the analysis element and internal standard element instead of just versus the percentage of the analysis element.

The resulting working curves are similar to the ordinary

types, except that measurements should generally be restricted to the straight line portions of the curves. Self-absorption by the analysis line flattens the upper sections of both types of working curves. With an ordinary type of working curve, this "shoulder" can be used, although accuracy is considerably reduced. With a variation method though, such a shoulder can be used only when the percentage of internal standard in the samples is approximately equal to the internal standard content of the standards.

### C. Plate calibration

#### (1) General

The intensity of radiation emitted from the arc column is a function of the concentration of the element emitting the radiation. However, the quantity measured by the spectrographer is the density of the spectral line produced by that radiation. Usually this relationship is shown in the form of a curve where density is plotted against the logarithm of the light intensity. This curve is called the characteristic curve of the photographic emulsion under the given conditions. The logarithm of the light intensity is generally used as this results in a curve having a considerable straight line portion. The relationship between density and intensity of incident radiation is quite complicated and dependent upon many factors. The whole course of the characteristic curve

must be obtained experimentally as there is no simple mathematical relationship between these two quantities.

Plate calibration refers to the science of determining the response of a photographic emulsion to incident light. The nature of this problem has been adequately covered in many recent books on spectroscopy and will only be summarized briefly here. The problem of accurate plate calibration must be faced by every spectrographer who desires to obtain precise quantitative results.

The more important of the many factors which influence this relationship are: intensity and wavelength of the radiation; intermittancy effect; failure of the reciprocity law; Eberhard effect; time of exposure; type of exposure; temperature and type of developer; and time of development. Some of these are, of course, under the direct control of the spectrographer and can be held essentially constant during any investigation. The effect of other variables can often be minimized by producing the calibration spectra in the same exposure time and in the same manner as is used for the unknown samples.

## (2) Frequeney of calibration

There is no unanimity of opinion on this subject. Opinions range from those spectrographers who believe that not only should every plate be calibrated, but different parts of the same plate should be calibrated separately;

to others who believe that only one plate from a given batch should be calibrated. Of course, frequency of calibration really depends upon the precision desired; how closely the variables are controlled; and the uniformity of the emulsion.

The writer found the emulsion types used in this work to have an extremely uniform contrast from plate to plate provided the processing conditions were closely controlled. In view of this and of the fact that accurate calibration methods are somewhat time consuming, it was decided to calibrate carefully each lot of emulsion bearing the same emulsion number and use the same characteristic curve for all plates with that emulsion number. All analysis and calibration plates were processed in an identical manner as possible. This method gave very satisfactory and consistent results, and the writer believes that it resulted in better precision than would have been the case had each plate been calibrated separately using a faster but less accurate method.

### (3) Calibration method

There are many possible ways of calibrating an emulsion, and the interested reader is again referred to any general spectroscopic text where these various methods are discussed. The method used by the writer was one which is in

wide use today due to its relative simplicity. It consisted of placing a rapidly rotating stepped sector immediately in front of the evenly illuminated slit of the spectrograph. The stepped sector used was of the double symmetrical type with its edge cut back in steps of increasing depth. The step factor, which is the relation between the exposures given by two adjacent steps, was two. Since a line is merely an image of the slit, and the number of flashes for all steps is the same, each spectral line thus shows a graduated series of exposures whose relative values are known.

The stepped sector method has been criticized in the past as not providing a valid method of plate calibration due to possible errors arising from failure of the reciprocity law and the intermittency effect. However, later workers have justified its use provided it is used with care and within the limitations imposed by the reciprocity law. The writer feels that it provided a valid calibration method because exposure times and conditions for both calibrating and unknown exposures were approximately the same; thus minimizing any possible errors due to failure of the reciprocity law or the intermittency effect. An indication of its validity was that two calibration curves resulting from two exposures made with the same exposure times but different source intensities could be overlapped satisfactorily.

The optical arrangement used for the calibration of the type I-N plates with the Hilger prism instrument is shown in FIG. 11. A long focus spherical lens was mounted immediately in front of the slit, and the source placed at such

used. available, the equipment available dictated the ones to be illumination would be ensured. Although many methods are fore, to use an optical arrangement whereby even slit illumination of the arc column. It was thought advisable, therefore, the slit - reflects any intensity variations along the the unknown samples - an image of the source focused on unless this is so. The normal set-up for the analysis of be seen that incorrect calibration patterns will result slit be evenly illuminated from end to end. It can easily a stepped sector calibration method requires that the

#### (4) Achievement of even slit illumination

was produced as described in the following section. The way in which a relatively background free spectrum accurate background corrections could not have been made, a background free spectrum, for unless this was done, it was necessary that the calibration curves be made from spectral regions be accurate at low densities. Consequently, it was essential that the calibration curves used in those had to be made in the thallium and cesium determinations, where a considerable number of background corrections

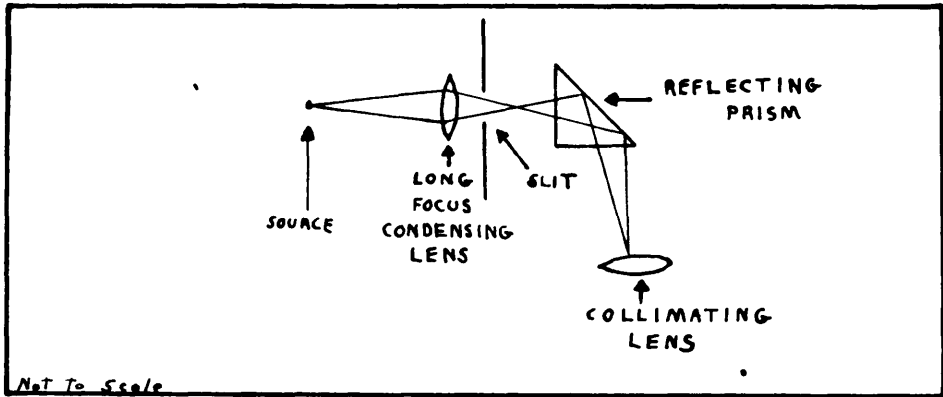


Fig. 11

Optical arrangement used to achieve even slit illumination on prism spectrograph

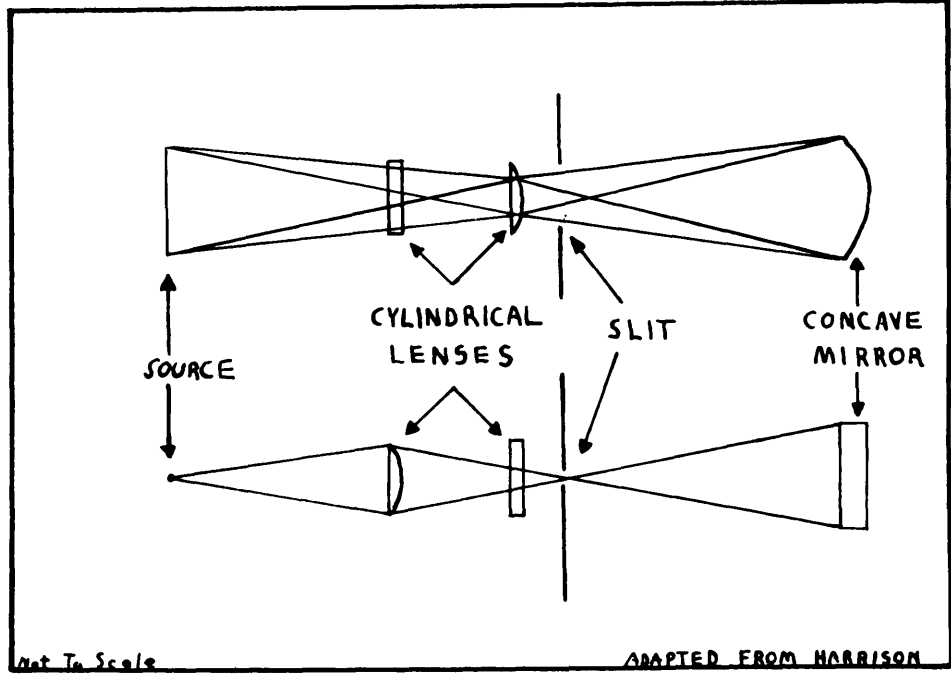


Fig. 12

Optical arrangement used to achieve even slit illumination on grating spectrograph

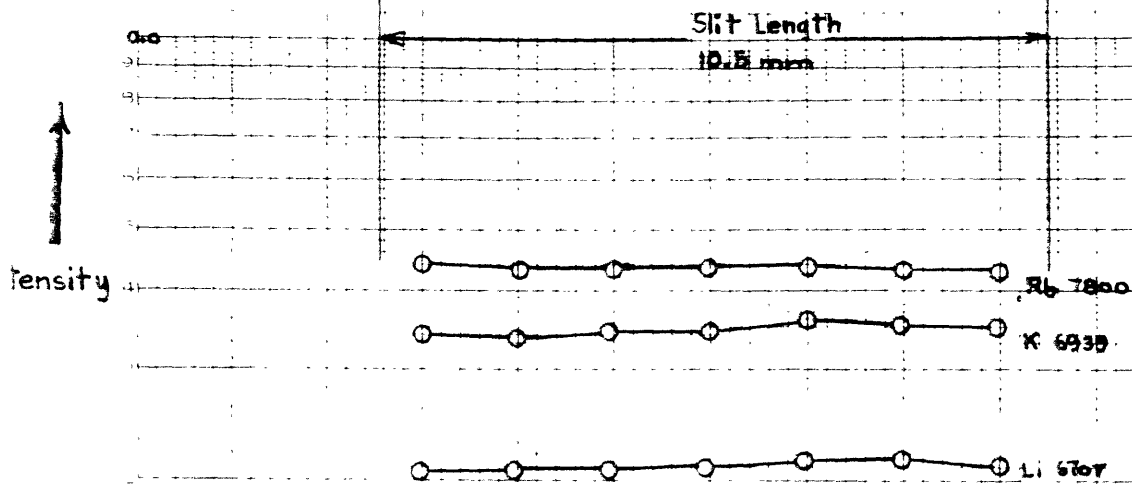


a distance from this lens that an image of the source was formed on the collimator. Because each point of the source illuminates the entire length of the slit, reasonably even illumination results. To prevent background-producing continuous radiation from entering the system, the images of the glowing electrode tips were masked off by placing masking strips at the top and bottom of the collimator. A 35 mm. horizontal strip was left unmasked. When the analytical gap was maintained at not less than 10 mm., no continuous radiation could enter the system. To control the position of the arc column continuously during a calibration exposure, an additional spherical lens was placed alongside the arc in the proper position to project an image of the arc onto the laboratory wall. This, combined with the use of properly placed reference marks, made possible the continuous maintenance of the proper arc gap and position.

A photographic check of the evenness of slit illumination was made. The check lines were each divided into seven 1.5 mm. long segments, and then photometered. The results are shown in Fig. 13. The evenness of illumination is seen to be quite satisfactory, as the few small variations are quite random. This photographic check was made using the same exposure time as was used for the calibrating exposures. The only difference between the two set-ups was that a sector which sectored the entire length of

Figure - 13

Photographic check of evenness of slit illumination on Hilger spectrograph



Number of Segments

the slit was used in place of the step sector.

The optical arrangement used to provide even slit illumination on the grating instrument is shown in Fig. 12 . Two cylindrical lenses were mounted between the source and the slit. The short focus lens nearest the source had its axis vertical and threw a vertical line of light onto the slit focussed only in a horizontal plane. The long focus lens at the slit with its axis horizontal projected an image of the source onto the collimating mirror as a horizontal band of light focussed in the vertical plane only. As first set-up, this arrangement gave very satisfactory and uniform slit illumination provided the optical system was properly aligned. However, considerable background always seemed to be present in the steps with a large sector aperture (See Photograph B in Fig. 14 ). This was very noticeable when carbon electrodes were used instead of iron electrodes. A critical review of the optical system revealed that any continuous radiation from the glowing electrode tips could enter the system, because the first cylindrical lens focussed only in the horizontal plane. To eliminate the entry of this continuous radiation into the system, this short focus lense was completely masked except for a horizontal strip approximately 4 mm. wide at its center. This masking, combined with maintaining the arc gap as great as possible without causing an unsteady arc, proved extremely successful in screening out

all the continuous radiation coming from the glowing electrode tips. Before and after photographs are shown in Fig. 14 . Operating conditions and exposure times were the same in both cases.

(5) Construction of characteristic curves

All the characteristic curves used for the various spectral regions were constructed in the same manner. As described previously, a rotating stepped sector was used to provide a uniformly graded series of exposures. Although seven steps were available on the sector, generally only 3 or 4 points for each line fell in the useable density range. Consequently, no one line gave a sufficient number of points for accurately plotting the whole curve. However, a complete curve was obtained by laterally shifting two or more partial curves until they overlapped. This could be done since relative rather than absolute intensities were desired, and when two lines of different intensities but approximately the same wavelength are plotted, the two calibration curves are displaced due to the different intensity scales. The ~~degree of~~ separation of the curves gives the intensity ratio of the two lines.

As all the curves were plotted in a similar manner, construction details will be given for only one curve, that used for calibrating emulsion type 103-J at a wavelength of 5350Å. To obtain calibration data, a 103-J

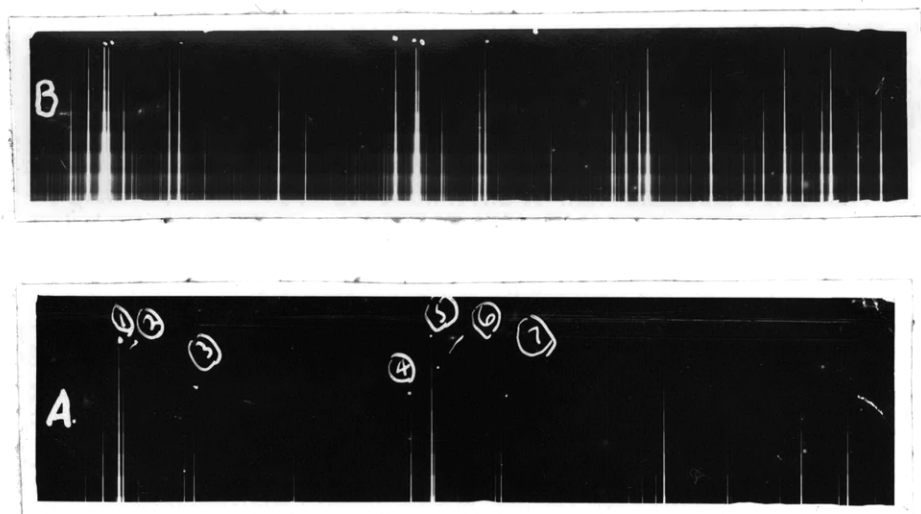


Fig. 14

Reduction of background by proper  
masking of lens.

A. Masked. B. Not masked.

plate was exposed for 45 seconds to the radiation from an iron arc run at 3 amperes. The previously described arrangement of two cylindrical lenses was used to insure even slit illumination. Other operating conditions were identical with those listed in Table 2 except that a seven step sector with a step factor of two was used in place of the special three step sector. Six iron lines having an appropriate range of intensities and lying within 25A of 5350A were then photometered in the usual fashion, and the opacities of all measurable steps calculated. The results are listed below:

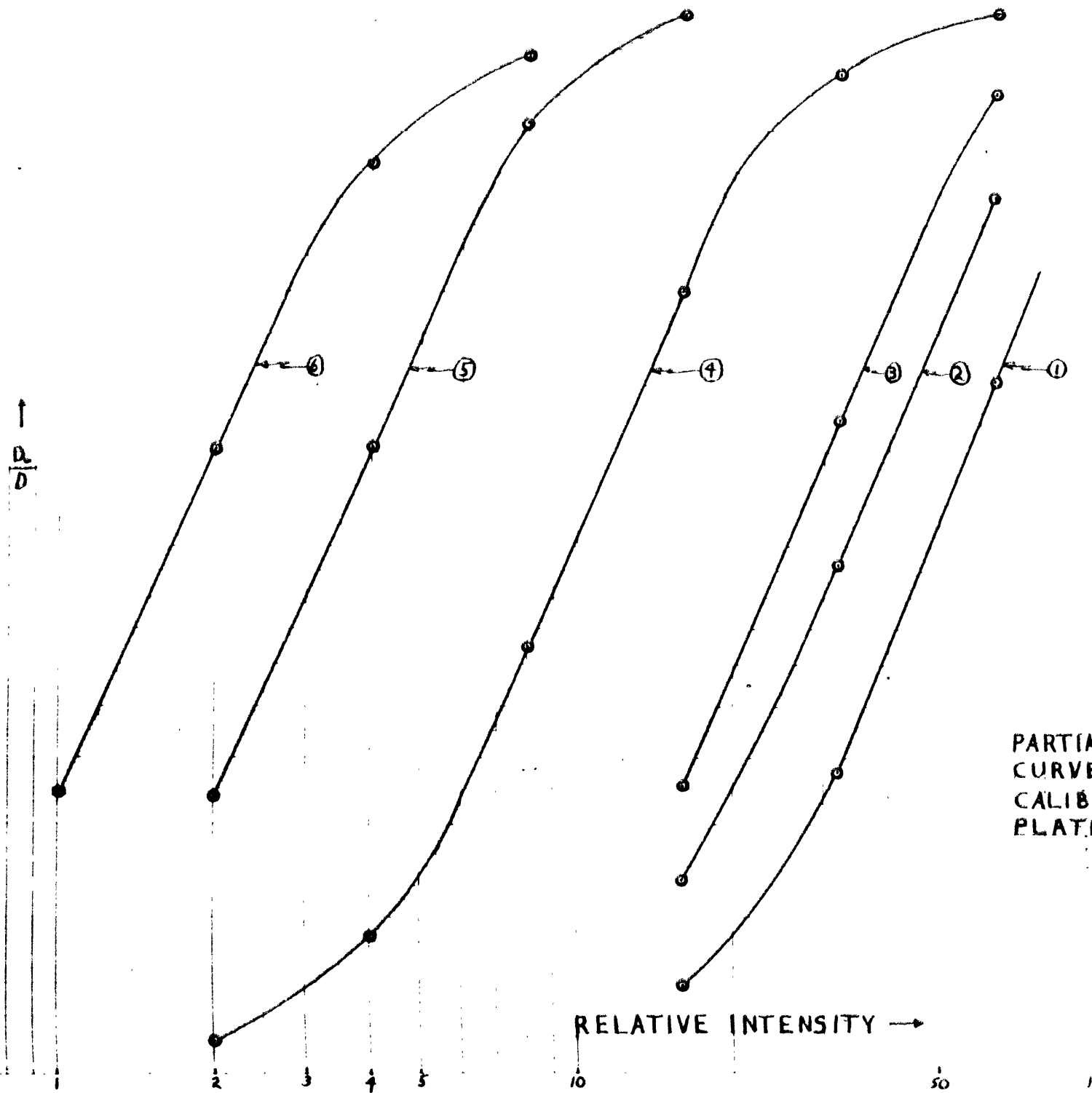
<u>Sector</u> <u>Aperture</u>	<u>Relative</u> <u>Intensity</u>	<u>Opacity</u>					
		<u>Line</u>					
		1	2	3	4	5	6
1:2	64	20.8	45.5	71.4	100.0	-	-
1:4	32	3.82	9.25	17.2	76.9	-	-
1:8	16	1.49	2.35	3.52	30.3	100.0	-
1:16	8	1.11	1.26	-	6.50	62.5	83.3
1:32	4	-	-	-	1.85	15.4	52.6
1:64	2	-	-	-	1.16	3.40	15.2
1:128	1	-	-	-	-	1.42	3.46

These data were then plotted in the usual fashion, and the resulting partial characteristic curves are shown in Fig.15 . The relative intensities of these six lines were determined by measuring the separation of these partial

$\uparrow$   
 $\frac{D_0}{D}$

RELATIVE INTENSITY  $\rightarrow$

FIG.-15  
PARTIAL CALIBRATION  
CURVES USED IN THE  
CALIBRATION OF 103-J  
PLATES AT  $\lambda = 5350 \text{ \AA}$



curves. Line 4 was arbitrarily assigned an intensity of one. The next step was to combine this family of curves into one curve based on the curve for line 4. This was accomplished by multiplying the value of the relative intensity for each step of each line by the relative intensity of that line compared with line 4. For example, the intensity ratio of line 5 to line 4 is 2.98, and consequently the curve for line 5 will come into coincidence with the curve for line 4 if the opacities for line 5 are plotted against the following corrected relative intensities.

<u>Corrected</u> <u>Relative Intensity</u>	<u>Opacity</u>
16 x 2.98	100.0
8 x 2.98	62.5
4 x 2.98	15.4
2 x 2.98	3.4
1 x 2.98	1.42

The resultant composite calibration curve is shown in Fig. 16. The scattering of points in the higher density region is believed due to errors caused by stray light in the microphotometer. This was not serious though, because by selection of the proper sector step, use of this section of the curve could generally be avoided.

#### (6) Calibration of 103-J type emulsion

This emulsion type was calibrated for the wavelength



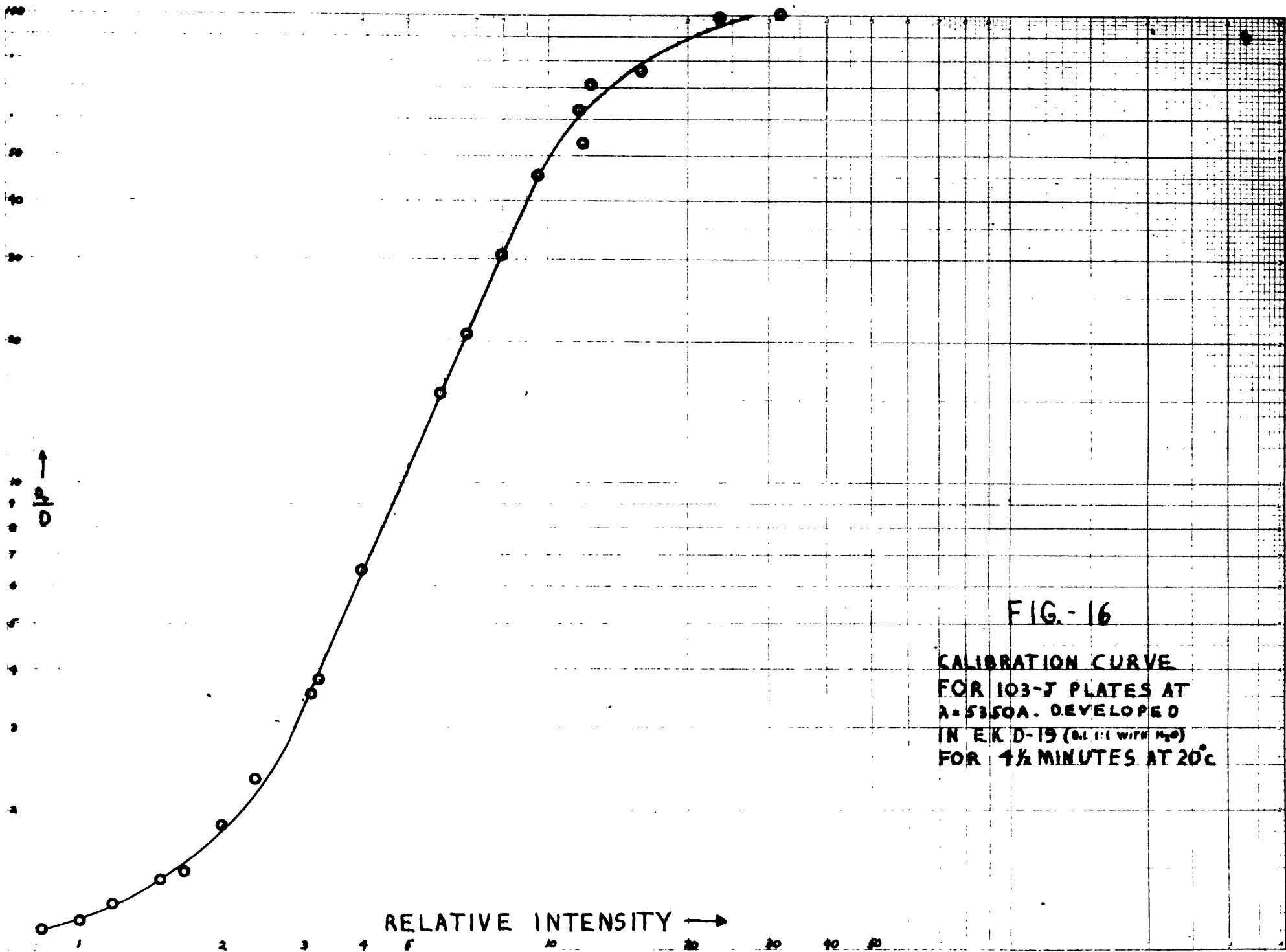


FIG.-16

CALIBRATION CURVE  
FOR 103-J PLATES AT  
 $\lambda = 5350\text{\AA}$ . DEVELOPED  
IN E.K. D-19 (dil. 1:1 with  $H_2O$ )  
FOR  $1\frac{1}{2}$  MINUTES AT  $20^\circ\text{C}$

region in the vicinity of the thallium line at 5350A and for the region near the potassium line at 4047A. The construction of the calibration curve for the 5350A region has already been described. The 4047A region was calibrated in a similar fashion, and the characteristic curve shown in Fig. 17.

The contrast for the 5350A spectral region ( $\gamma = 2.3$ ) was considerably higher than the contrast for the 4047A region ( $\gamma = 1.7$ ). This was not unexpected though as the contrast in the region of optical sensitization is frequently higher than in the blue or violet. It did mean though that both curves had to be used for the thallium determinations. The determination of correct intensity ratios for two lines of widely varying wavelength is really a problem of heterochromatic photometry and requires a calibration source where the intensity distribution as a function of wavelength is known so that the proper separation for the two calibration curves can be determined. However, such sources are rather hard to obtain and are really not necessary for practical work. The solution adopted by the writer was to let the two calibration curves cross at an arbitrary point. The resulting thallium-potassium intensity ratios were then purely arbitrary but were significant so long as the two calibration curves were maintained in the same relative positions when referring to working curves derived from them.

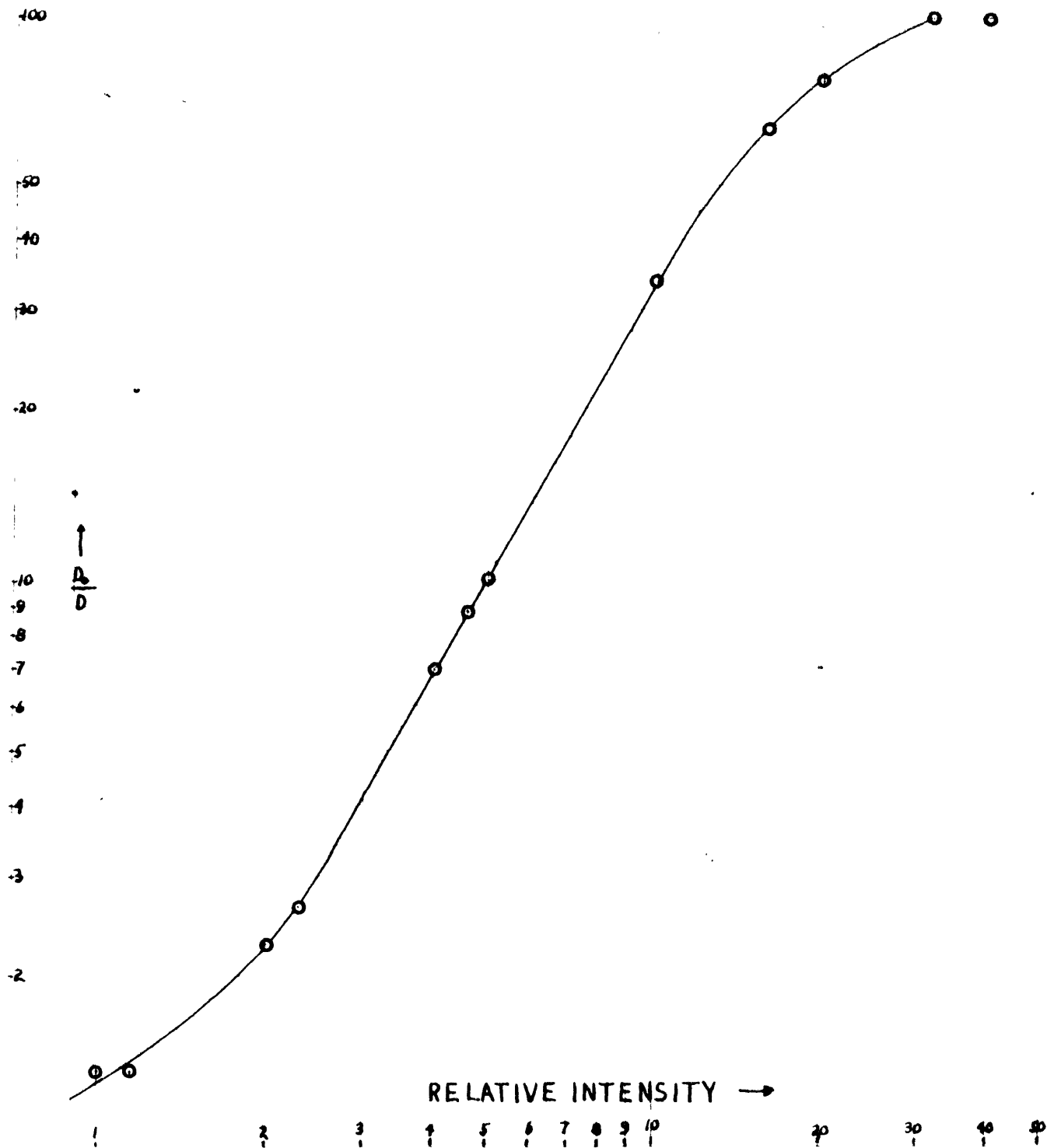


FIG.-17

CALIBRATION CURVE  
 FOR 103-J PLATES AT  
 $\lambda = 4045\text{\AA}$ . DEVELOPED  
 IN E.K. D-19 (D.I. 1:1 WITH  $H_2O$ )  
 FOR  $4\frac{1}{2}$  MINUTES AT  $20^\circ\text{C}$ .

(7) Calibration of I-N type emulsion

The I-N type emulsion was calibrated like the 103-J type with one exception. Instead of an iron arc, a series of standards containing varying amounts of the analysis elements were used to provide the calibration data. The only difference from the standard alkali set-up was the optical arrangement used to provide even slit illumination. Thus, the I-N plates were calibrated under conditions which were almost precise duplicates of those which were used for the analyses. Errors due to calibration were thus reduced to a minimum by this procedure.

The composite calibration curve obtained for the I-N emulsion is shown in Fig. 18. The contrast ( $\gamma = 3.17$ ) was found to be constant within the experimental error of determination in the wavelength region from 5600Å to 8600Å. The slope of the straight line portion averaged  $72.5^\circ \pm 1/2^\circ$ . Slopes outside of this range were very rare and were probably due to microphotometric errors in the determination of line density.

As a result of this constant contrast, only one calibration curve was used for this region. The employment of a single calibration curve is strictly valid only in a spectral region where both plate contrast and plate sensitivity are constant. Determination of plate sensitivity as a function of wavelength again requires a source whose

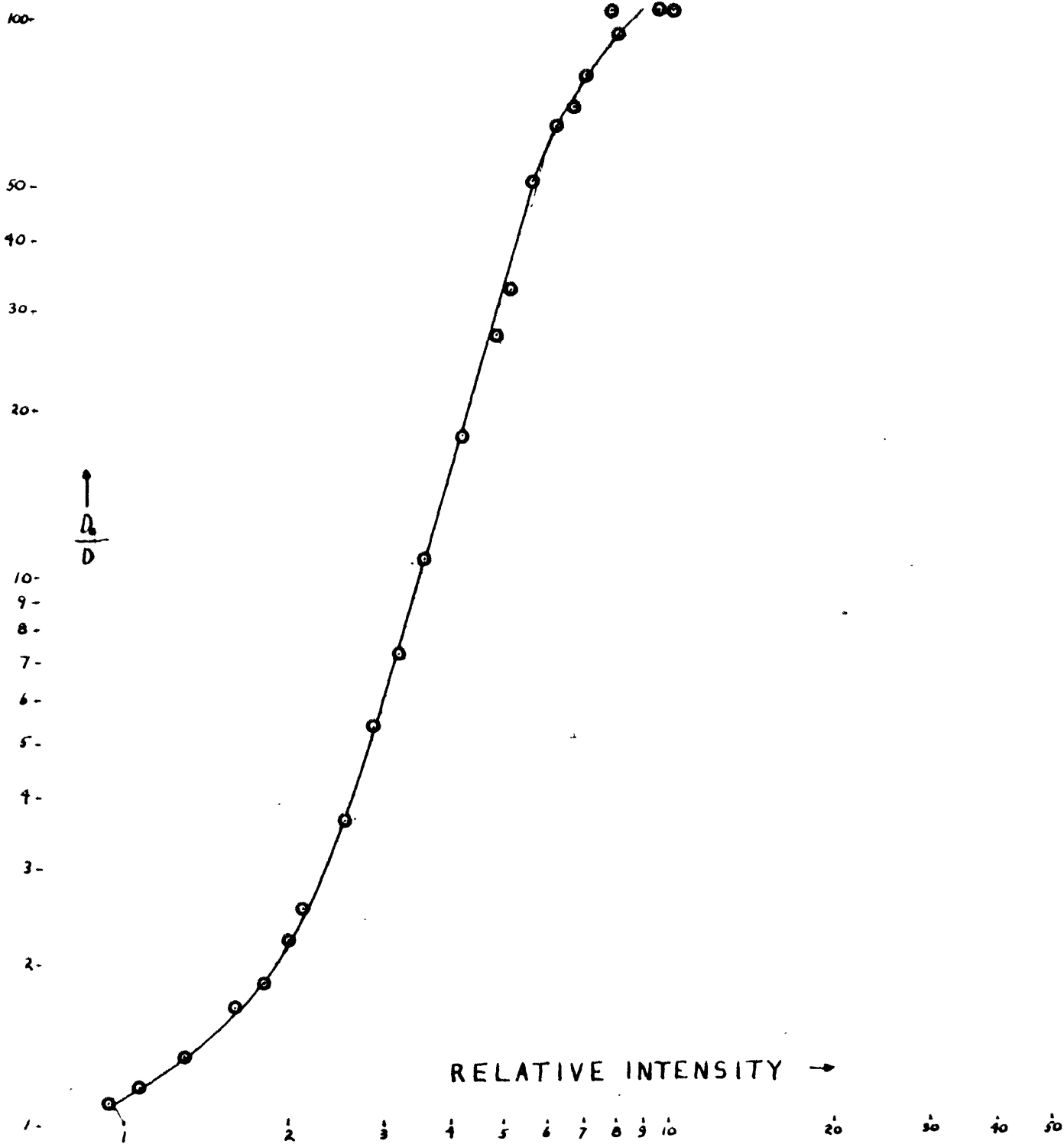


FIG.-18

CALIBRATION CURVE  
 FOR I-N PLATES IN  
 5600A - 8600A REGION,  
 DEVELOPED IN E.K. D-19  
 (D.L. 1:1 WITH H<sub>2</sub>O) FOR 4½  
 MINUTES AT 20°C.

intensity as a function of wavelength is known. However, this type of calibration was not considered necessary, as a constant variation in sensitivity would merely result in incorrect intensity ratios; yet would have no effect on the accuracy of the determinations for this variation in sensitivity would be compensated for in the working curve.

Spot checks made on quite a number of routine analysis plates showed that the processing procedure maintained a very reproducible contrast.

(8) Construction of accurate low density calibration curves

As can be seen in Figs. 16, 17, and 18; the typical characteristic curve has a pronounced "toe" at low density values. The flatness of this type of curve at low intensity values tends to make calibration rather inaccurate in this region. This caused considerable concern at first, because if a satisfactory precision was to be attained in the thallium and cesium determinations, accurate background corrections were essential. This in turn demanded accurate low-density calibration curves.

A suitable plate calibration function was found in the Seidel function which is defined as follows:

$$\text{Seidel Function} = \frac{D_0}{D} - 1$$

This function has been discussed by Kaiser (12). The

lower portion of the characteristic curve becomes a straight line when it is used in place of the density. The writer does not believe that there is any fundamental increase in accuracy when this Seidel function is used. However, it is much easier to fit a curve accurately to data which follows a linear trend than to data which does not, and it is probably for this reason that use of this function increases the accuracy of calibration at low densities.

Plots of the Seidel function versus relative exposure for both emulsion types are shown in Figs. 19 and 20. It can be seen that a perfectly straight line between 2% and 95% transmission is the result in both cases. The writer believes that use of the Seidel function for the determination of background intensities in the thallium and cesium determinations substantially increased the precision.

Early experiments by the writer on the use of the Seidel function generally showed the presence of a small "toe". However, this "toe" disappeared, at least down to the lowest measurable density, when suitable precautions were taken to eliminate continuous radiation from the calibrating spectrum; thus indicating a possible connection between background and the presence of this "toe". If this is correct, then the Seidel function would be a useful way of determining whether a calibrating spectrum was free of error-producing background radiation.

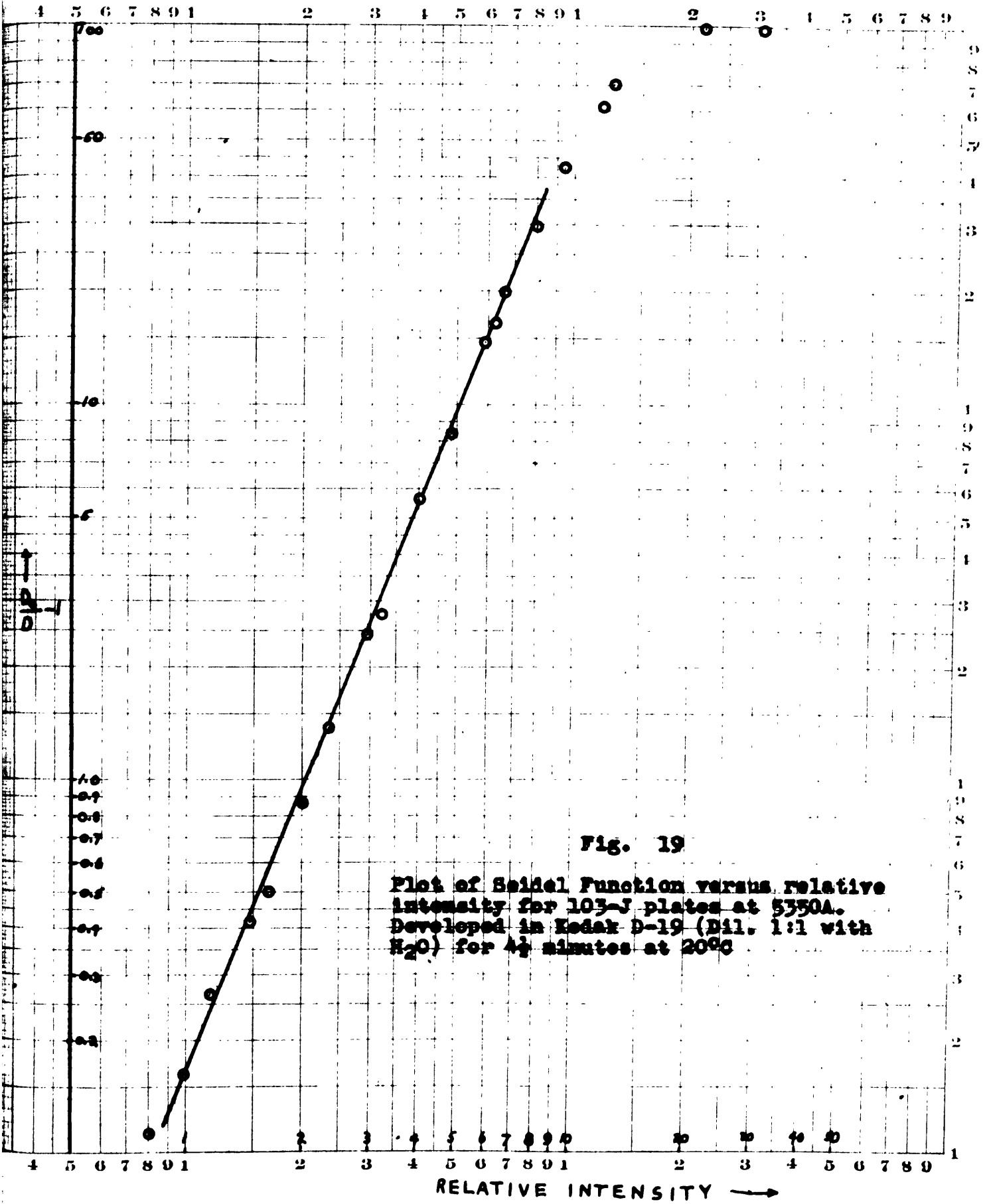


Fig. 19

Plot of Seidel Function versus relative intensity for 103-J plates at 5350A. Developed in Kodak D-19 (Dil. 1:1 with H<sub>2</sub>O) for 4½ minutes at 20°C



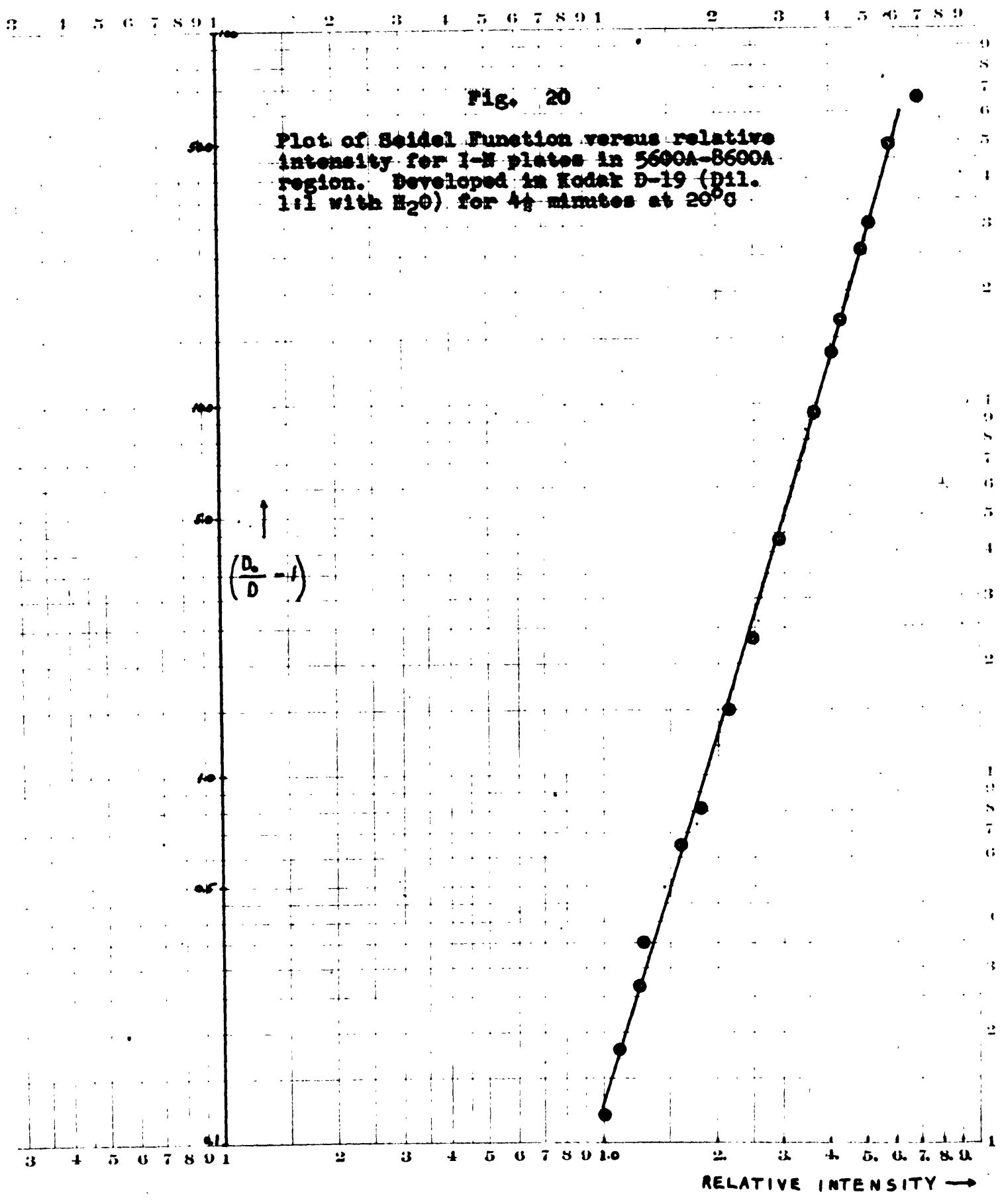


Fig. 20

Plot of Seidel Function versus relative intensity for I-N plates in 5600A-8600A region. Developed in Kodak D-19 (Dil. 1:1 with H<sub>2</sub>O) for 4½ minutes at 20°C

RELATIVE INTENSITY →

### (9) Accuracy of calibration

According to Sawyer (19), one of the best checks on the accuracy of any calibration method is to prove that it is self-consistent. Earlier in this section, it was mentioned that the calibration methods used in this work had been proven to be reasonably self-consistent through the fact that the partial characteristic curves could be satisfactorily overlapped. In this respect, the I-N emulsion was a little better than the 103-J emulsion although both were satisfactory.

Another check is that inaccurate calibration will affect the slope of the working curve. Thus the fact that the slopes of all working curves were practically equal to the theoretical  $45^\circ$  once the necessary background corrections had been made indicated that the calibration methods were reasonably accurate.

### D. Background

#### (1) General

On most spectrograms it is possible to observe a general overall blackening superimposed on the line spectra. This is spectral background and it is due to the effect of continuous radiation which generally comes from several sources. Among the most important are the incandescent tips of electrodes, incandescent particles of sample and carbon which are

wafted up into the arc column, and scattered light from various components of the optical system. Heavy background poses a rather serious problem as the resulting density of a spectral line is due not just to the intensity of the line, but rather to the intensity of the line plus the intensity of the background at the wavelength of the line. Fairly heavy background can be ignored in quantitative spectroscopy only in a few selected cases; thus the problem which usually faces the analyst is how to correct for the presence of this background.

Of course the best solution is to try to select the operating conditions in such a manner that the background intensity is reduced to a negligible level. Occasionally though, in spite of selecting the optimum conditions, the background intensity is still appreciable. This was true for the thallium determinations where background corrections had to be made on every sample.

Uncorrected background causes a working curve to depart from a straight line at low concentrations and approach the concentration axis asymptotically. Neglecting the presence of the background and plotting the working curve with a "toe" would, of course, be one way of compensating for the presence of background provided its intensity was fairly reproducible from sample to sample. However, background intensities were found to be extremely variable not only

from sample to sample but also in separate exposures of the same sample. This fact was particularly noticeable in the thallium determinations. Two duplicate samples would occasionally give extremely smooth and identical burns, at least as far as could be visually determined, and yet the background densities would be radically different.

## (2) Background correction

There are a large number of references in the literature pertaining to the general subject of background correction which indicates that this is a subject of major concern to spectrographers. This literature is also extremely vague on the subject of just when to apply a background correction. However, the writer believed that it should be possible to make a more precise statement as to when a correction should be applied. The overall level of the background density did not seem to be as important as its effect on the intensity ratio of the analysis line to the internal standard line. Also, it seemed important that the standard deviation of a method due to random errors other than background should be considered along with the effect of background on the intensity ratio of the line pair. As a result of these two considerations, it seemed logical to state that a background correction should be applied whenever the percentage

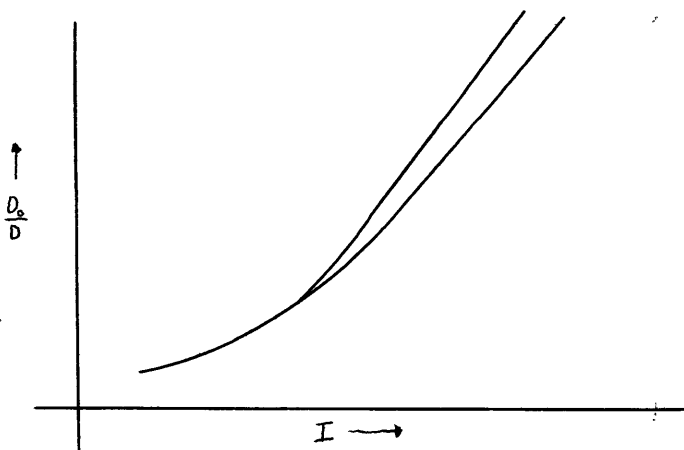
error in the determination of the intensity ratio of the line pair due to spectral background is greater than the standard deviation to be expected from the other random errors inherent in the method. The foregoing criterion was used throughout this investigation.

Early workers in the field used to correct for background by subtracting the background density from the combined line plus background density. The incorrectness of this method is clearly evident when one looks at the characteristic curve that connects plate response and intensity of incident light. Nachtrieb (16) has shown mathematically as well that subtraction of densities is equivalent to dividing the line-plus-background intensity by the background intensity. He has also shown that the sometimes used practice of "zeroing" the microphotometer in the background is equivalent to performing a subtraction of densities.

The most accurate method for making background corrections is the one used by the writer in this investigation. This consisted of converting the density of the background to intensity by use of the emulsion characteristic curve and then subtracting its value from the total intensity of the line-plus-background. This is a rather time consuming method but is probably sufficiently accurate provided the following two assumptions are true. First,

it is assumed that the background intensity underlying the line is the same as in the immediate neighborhood where the background reading was taken; this is probably justified in the great majority of cases. Second, the assumption is made that the response of a photographic emulsion to a continuum is the same as it is to monochromatic radiation. It is on this second point that there still is considerable controversy among spectrographers. Stroock (20) and others have reported that the slope of the characteristic curve for a continuum is less than the slope for monochromatic radiation. Other spectrographers have reported that there were no slope differences for the two types of radiation. Those who reported finding such differences attributed the reason to the Eberhard effect. Although the writer made no detailed investigation into this problem, a qualitative appraisal of the more than 400 background corrections made during the determination of thallium indicated that, at least for 103-J plates at 5350A, the characteristic curves for continuous and monochromatic radiation would not have coincided in their entirety. It was hard to obtain an accurate picture due to the somewhat variable nature of the background itself, and time did not permit experiments to determine the true shape of the characteristic curve for continuous radiation at 5350A. All background corrections were made using the characteristic curve for monochromatic radiation at 5350A.

If the two curves are identical, then the ratio of the background intensities of two neighboring steps should be equal to the step factor of two. For low and medium density values this was generally found to be true. For increasing values of density though, there seemed to be a rough correlation between the overall level of the background density and the magnitude of the deviation from two. This would indicate that the slope of the characteristic curve for a continuum was less than the slope for the monochromatic curve in agreement with the findings of Stroock and others. It is assumed here, of course, that errors in the determination of the intensity ratio due to failure of reciprocity law and the intermittancy effect were negligible as the calibrating exposures had been proven to be self-consistent. The following sketch illustrates what the writer believes to be the relationship between the two curves, at least for 103-J plates at 5350A.



As the two curves probably coincide for densities up to about 0.5 (transmission = 30%), no errors will result by

using the monochromatic curve for determination of background intensities up to this density level. In the thallium determinations, the majority of background deflections fell in the region where the two curves coincided.

In the photometry of all lines the general practice was to record the background deflection immediately after the deflection of the line plus background had been recorded. Where possible, background deflections were taken far enough away from the line to avoid possible errors from the Eberhard effect. Both sides of a line were scanned and if the background seemed at all variable an attempt was made to strike a mental average. If background measurements had been made on two steps, the one with the lower density was generally selected to compute the background correction.

### (3) Correction for "invisible" background

Every photographic plate has a "threshold" intensity level due to the inertia of the emulsion. Light whose intensity is below this "threshold" value will leave no visible effect on the plate in the form of increased density. This fact can occasionally result in fairly large errors in the determination of the intensity of weak spectral lines. For example, spectral background may be just below the "threshold" value and by itself would produce no effect, but the intensity of spectral lines will be increased by the



addition of this "invisible" background. For a very weak spectral line, the percentage error in the determination of its intensity may be quite large. The writer has frequently heard complaints by co-workers in the Cabot Laboratory that background corrections often seemed to be of excessive magnitude. It is believed that this is often the result of a worker not appreciating the significance of the fact that each emulsion does have a "threshold" level. For example, when a line which has been placed on a plate with a step sector is photometered, there are frequently three or more steps where the line is of the proper density to be measured. If background is visible in some steps and not in others, the analyst will frequently mistakenly believe that a background correction can be avoided by photometering the line in the step where no background is visible. This is manifestly an incorrect procedure because sectoring does not change the line-background ratio. In the step where background has seemingly vanished, all that has happened is that the background intensity has fallen below the "threshold" level of the emulsion and leaves no visible record except that all spectral lines have an increased density. If background is present in any step to the extent that a correction is considered necessary, then every step will require a correction. If, in a series of stepped spectra, background corrections are considered necessary but it is

considered more accurate to measure the line plus background response in a step where there is no visible background, the proper amount of background correction can be calculated by measuring its density in a step where it is visible and multiplying the result by the proper step factor.

The complaint that background corrections are frequently excessive results from the analyst photometering lines in the steps where no background is visible even though the background-to-line intensity ratio is such that a correction is required. In a series of standards where the intensity of the analysis line gradually diminishes, the background intensity generally remains at a fairly constant level with a consequent increase in the background-to-line intensity ratio with diminishing concentration of the analysis element. On photometering the standard plates, the analyst, by selecting the proper step, often does not consider a background correction necessary until the lowest standard or two when there is no question but that a correction is required. When this is made it frequently amounts to 50% or so of the line plus background intensity, and the analyst then begins to wonder about the validity of this method of background correction.

The following example is given to show the effect of neglecting this background in the construction of a working curve. This example is taken from the writer's work

in the construction of a working curve for thallium where the significance of "invisible" background first became apparent.

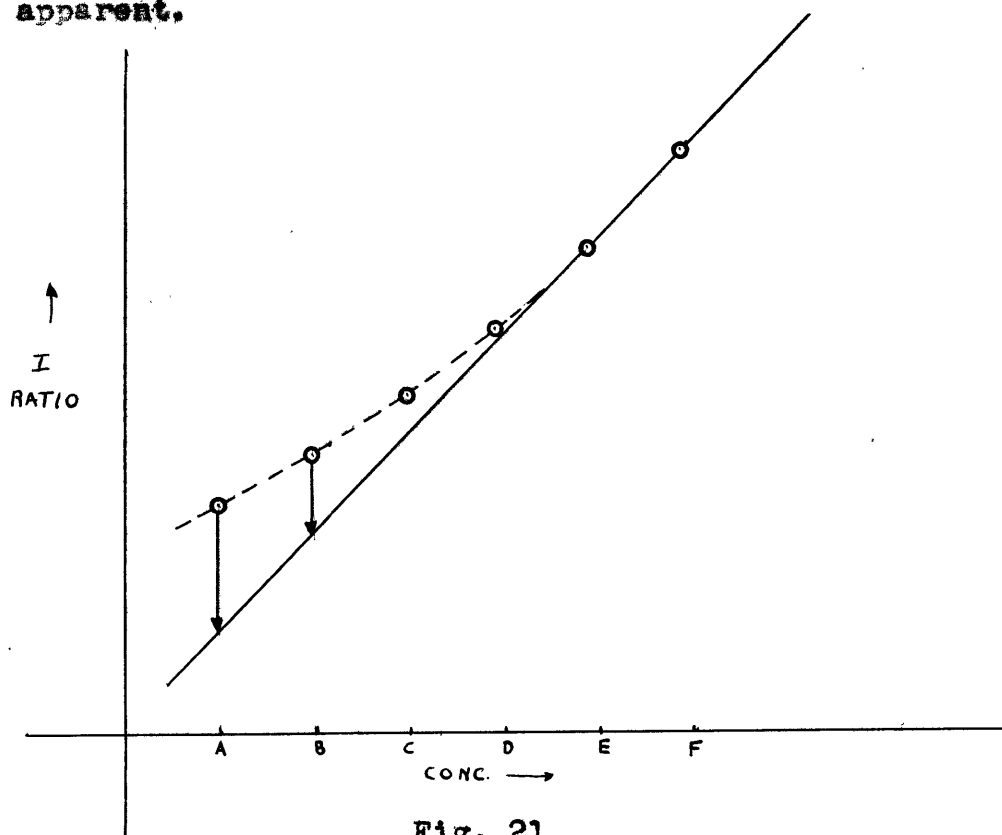


Fig. 21

The dashed line in Fig. 21 shows the approximate shape of the working curve before any background corrections had been applied. Standards A and B obviously required background corrections and, when these were made, the intensity ratios decreased as indicated. At C and D it was possible to measure the line intensities in steps where no background was visible; therefore no correction was considered necessary at first. When an attempt was made to draw a corrected working curve, however, it was found that the values for the intensity ratios at points A, B, E, and F

could be connected by a straight line of approximately  $45^\circ$  slope, but the values at C and D fell above this line. As soon as the significance of the photographic "threshold" level was realized, the requisite amount of background correction was calculated by determining its intensity in a step where it was visible and multiplying the result by the proper step factor. When this correction was applied, the values of the intensity ratios at C and D were reduced by the proper amount and fell nicely onto the line that connected the remaining points.

(4) Effect on precision

It is hard to assess exactly the effect of background on precision, but there is little doubt that precision and accuracy diminish whenever background corrections are made due to some or all of the following factors: possible errors in calibration, possible differences in the slopes of calibration curves for monochromatic radiation and continuum, variable background, Eberhard effect, and micro-photometric errors. The writer believes that precision lessens as the line-to-background ratio decreases.

The samples used in experiments to obtain precision data gave an average amount of background.

(5) Effect on minimum detectability

The statement has been made in the literature that a

line is useable in quantitative analysis provided its intensity is at least 0.1 to 0.3 times the background intensity. The writer verified this statement for type 103-J plates where the minimum useable ratio was found to be 0.2 to 0.3. The minimum useable ratio should also depend on plate contrast, diminishing as plate contrast increases. As a result of this ratio, it is easily seen that detection limits will increase as background intensity increases. A slight amount of background is necessary to ensure that the maximum desirable exposure has been reached, but heavy background is always undesirable as it lowers precision and increases the detection limit.

#### E. Photographic development

##### (1) General

The development process is one of the variables which influences the slope of the characteristic curve. Therefore, where only one calibration curve was constructed for a given emulsion lot, every effort was made to provide identical development conditions for all important plates, so that errors due to the development process would be kept at a minimum.

##### (2) Development

All plates were developed in Eastman Kodak developer D-19 (diluted 1:1 with water) for 4 1/2 minutes. One

gallon lots of D-19 stock solution were made up according to the manufacturer's directions and were stored in the refrigerator. For day to day use, a small portion of this stock solution was diluted with an equal quantity of distilled water and stored in one pint stoppered bottles. To avoid variations in the development process due to depletion of the developer, each pint bottle was generally used to develop the equivalent of three 4 x 10 plates and then discarded.

Tray development at a temperature of 20°C was used. Although thermostatic control of developer temperature was not available, developer temperatures generally deviated less than  $\pm 1^\circ\text{C}$  except during periods of unusually hot or cold darkroom temperatures. Whenever it was known that the variation would be greater than  $\pm 1^\circ\text{C}$ , some compensation was attempted by adjusting the initial temperature of the developer to be slightly greater or less than 20°C. Then, as its temperature either fell or rose during the course of development, the average temperature tended to approximate 20°C.

For the most consistent results in the development of quantitative plates, some form of developer agitation such as rocking the tray or brushing the emulsion is usually recommended. Failure to agitate the developer can lead to local depletion of developing agents and consequent under-

development of certain portions of the plate. This is usually called the Eberhard effect. A reduced density in the center of a dense spectral line and also in the background density immediately adjoining a dense line is the usual result of the Eberhard effect. Just how important this effect is as a variable in the photographic process is not yet thoroughly established. Some spectrographers feel that it is a relatively minor one compared to the other variables. However, it is within the writer's experience on plates developed without agitation that the background density immediately adjoining a strong line is sometimes considerably less than the average background density. This is an important point to keep in mind when background corrections are necessary.

There are many suggestions in the literature concerning the proper method of agitation. The two most common non-mechanical methods are rocking the tray and brushing the surface of the emulsion with a wide camel's hair brush. Both are designed to remove the bromide-rich depleted developer from the surface of emulsion and introduce fresh developer there. Harrison (10) claims that simple motion of the developer by rocking the tray will not remove an extremely thin layer of depleted developer that clings tightly to the surface of the emulsion. He further believes that the Eberhard effect results from this thin film, and that it can be removed only by constant brushing of the

emulsion surface during development. Other spectrographers while agreeing that brush development is probably the most satisfactory for extremely accurate work, nevertheless feel that "rocking the tray" methods can give highly satisfactory results provided the rocking cycle is not of such a type that standing waves of developer are set up in the tray with resulting under and over developed bands on the plate.

The writer initially planned to use brush development but abandoned this idea when it was found that camel's hair brushes of proper size (width greater than 4") were not available. An agitation method recommended by the Eastman Kodak Company in their data book "Processing & Formulas" ( 22 ) was then selected and used for all important quantitative plates. In addition the amount of developer used was kept to a minimum, and the area of the developing tray was just slightly larger than the area of the plates being developed.

### (3) Fixing

All plates were fixed in Kodak Acid Fixing bath for a minimum period of ten minutes plus clearing time. The fixer was reused until the clearing time reached twenty minutes when it was renewed. The temperature of the fixing bath, while not critical, nevertheless should not be radically different from that of the developer, otherwise reticulation



and peeling of the emulsion may result.

(4) Washing

Plates were washed by placing them emulsion side up at the bottom of a tray into which tap water was continuously introduced through a rubber hose in such a fashion that it did not fall directly on the emulsion. All plates were washed for at least thirty minutes. Reticulation and undue softening of the emulsion through use of too warm wash water was avoided by floating ice cubes in the wash water; this generally kept the water close to the proper temperature. At first a few plates were also spoiled by plunging them into much too cold wash water which resulted in a peeling of the emulsion due to the gelatin layer contracting faster than the glass plate. As it was impractical to warm the wash water, the following expedient was tried and found to work successfully whenever very cold wash water had to be used. Upon removing a plate from the fixing bath, a stream of cold water was run over the glass side for about a minute before placing it in the wash water. This allowed both the glass plate and gelatin layer to contract without setting up disruptive stresses between them.

Occasionally the 103-J plates would still have a slight yellowish tinge remaining after washing; this was attributed to residual traces of the special sensitizing dye used.

(5) Drying

After washing, the plates were "stripped" of the filmy layer deposited on them by the tap water by holding them under a gentle stream of water and carefully rubbing both sides with the palm of the hand. After "stripping", the plates were rinsed with distilled water and set aside to dry in a dust free location. Some of the earlier plates were swabbed with a moist viscose sponge to remove the layer of surface water remaining after rinsing, but this was later found to be unnecessary. No water marks resulted when this procedure was followed.

F. Preparation of standards

(1) General

Standards should, if at all possible, resemble closely the unknown samples both physically and in chemical composition. In particular it is desirable to have the elements to be determined exist in the same state in the standards as they are thought to exist in the unknown samples. Therefore the ideal standards for this work would have been a series of naturally occurring sedimentary samples that had been accurately analyzed by chemical methods for the elements to be determined. However, as is so often the case in spectrochemical analysis, such ideal standards were not available due to the nonexistence of accurate chemical methods

for the determination of traces of rubidium, cesium, and thallium. Consequently, it was necessary to resort to synthetic standards, and it is generally due to the use of such standards that quantitative spectrochemical results sometimes have a systematic bias.

(2) Preparation of synthetic base materials

For the base material of these standards, a mixture which resembled closely an average shale in gross chemical composition was synthesized. Rankama (18) lists the following analysis as being typical of the average shale. It is based on the analysis of a composite sample of 78 shales.

SiO <sub>2</sub>	-	58.38
Al <sub>2</sub> O <sub>3</sub>	-	15.47
FeO	-	6.07
MgO	-	2.45
CaO	-	3.12
Na <sub>2</sub> O	-	1.31
K <sub>2</sub> O	-	3.25
H <sub>2</sub> O	-	5.02
CO <sub>2</sub>	-	2.64
		<hr/>
		97.71

Twenty grams of base material were prepared as follows:

<u>Compound</u>	<u>Percentage</u>	<u>Quantity</u>
SiO <sub>2</sub>	60%	12 grams
Al <sub>2</sub> O <sub>3</sub>	15%	3 "
Fe <sub>2</sub> O <sub>3</sub>	5%	1 "
Na <sub>2</sub> CO <sub>3</sub>	10%	2 "
CaO	5%	1 "
MgO	5%	1 "

With the exception of the SiO<sub>2</sub>, all the components of this mixture were reagent grade chemicals used without further purification. The SiO<sub>2</sub> was obtained from naturally occurring quartz crystals ("Herkimer Diamonds").\*

All the components were thoroughly mixed by grinding them together in a mortar. The resulting mixture was then placed in a platinum crucible and sintered for five hours in a muffle furnace at a temperature of 925°C. This sintered material, after a second grinding, was used as the base for the preparation of the standard mixtures. A spectrographic examination of this base material showed it to be free from detectable amounts of thallium, rubidium, and cesium.

---

\* The quartz crystals were first handpicked to remove gross impurities. They were then heated to about 500-600°C and quenched in cold water to render them more amenable to crushing. After crushing them down to pea size on an anvil, and a second handpicking, they were ground down to a fine powder in a tungsten carbide mortar.

One requirement for the use of a variation internal standard method is that the working curves for different internal standard contents be parallel. To check this point it was considered necessary to make two sets of standards containing identical amounts of the analysis elements but with different amounts of potassium. Two sets containing 1% K and 2% K respectively were prepared as a large percentage of the unknown samples had potassium concentrations lying between these two values. These two mixtures were prepared by adding appropriate amounts of  $K_2CO_3$  (reagent grade) as follows:

	<u>1% K Mixture</u>	<u>2% K Mixture</u>
	6.7538 grams sintered base	6.8769 grams sintered base
	<u>0.2462</u> " $K_2CO_3$	<u>0.1231</u> " $K_2CO_3$
Total	7.0000 "	7.0000 "

For each mixture, the  $K_2CO_3$  was mixed with about 1-2 grams of the base and ground in an agate mortar for 5 minutes. The resulting mixture was then combined with the remainder of the base and mixed by grinding for 20 minutes in a small porcelain mortar.

Spectrographic examination of these two mixtures still showed no detectable traces of thallium and cesium, but a definite trace of rubidium was present, probably due to its presence as an impurity in the  $K_2CO_3$ . The amount present was later determined by use of an "addition method"

and taken into consideration when the working curves for rubidium were constructed.

(3) Preparation of standards

Considerable time was devoted to the preparation of the standard mixtures, because accurate standards were essential if significant and accurate results were to be achieved. The preparation of standards containing as little as 0.0001% of an element presents a problem, for at this level of concentration, the compound of the element added must have a particle size of a few microns or less, and be uniformly dispersed throughout the body of the mixture if fluctuations in composition are to be avoided. Any method of preparation selected must be such as to achieve this end.

The method selected by the writer for each of the standard mixtures was to prepare a primary standard containing all of the analysis elements at a concentration level of 10%; this avoided any significant weighing error. A series of the more dilute standards were then prepared by making successive dilutions with the pure matrix. Preparation in this fashion avoided non-uniformity due to large dilution factors. A dilution factor of 0.1 was chosen. This factor is frequently used by spectrographers as it has the advantage of giving an equal spacing of points along the concentration axis when a logarithmic scale is used.

All of the elements to be determined were incorporated into the base in the form of sulphates. The sulphate was selected because it decomposes into the oxide when heated. The primary standard (1% K), containing 10% of each analysis element calculated as the oxide, was constituted as follows:

242.1 mg. 1% synthetic base

118.8 "  $Tl_2SO_4$

367.9 "  $Li_2SO_4$

128.4 "  $Cs_2SO_4$

142.8 "  $Rb_2SO_4$

Total weight 1000.0 mg.

Lithium sulphate was also added because it was proposed to analyze for lithium at the time these standards were prepared.

The weaker standards were then prepared using the dilution factor of  $\sqrt{0.1}$  as follows:

<u>Standard No.</u>	<u>Percent Oxide</u>	
1	10.00	Primary standard (1% K)
2	1.00	100 mg. (1) std. + 900 mg. (1% K) base
3	0.316	316.2 mg. (2) " + 683.8 mg. " "
4	0.100	" " (3) " + " " " "
5	0.0316	" " (4) " + " " " "
6	0.0100	" " (5) " + " " " "
7	0.00316	" " (6) " + " " " "
8	0.00100	" " (7) " + " " " "
9	0.000316	" " (8) " + " " " "
10	0.000100	" " (9) " + " " " "
11	0.0000316	" " (10) " + " " " "
12	0.0000100	" " (11) " + " " " "

Each standard was mixed by grinding for ten minutes in an agate mortar. A relatively new mortar with an unworn grinding surface was used for all mixing. The mortar was thoroughly cleaned between standards\* to preclude contamination of a weaker standard with residual traces of a higher concentration standard. All the components of these standards were dried for one hour at 105°C before preparation. The standards were stored in a dessicator to prevent any pick-up of moisture.

### G. Construction of working curves

The working curves were constructed from data obtained by analyzing both sets of standards using the standard operating procedures listed in Tables 2 and 3. The intensity ratios for each line pair were then computed in the usual fashion and plotted against the concentration ratios. Line intensities were corrected for background where necessary. The four working curves used are shown in Figs. 22, 23, 24, and 25. The slopes of all working curves were within one degree of the theoretical 45° slope.

---

\* The agate mortar was cleaned between standards by:

1. Grinding a paste of "Ajax" plus water.
2. Water rinse (mortar remained slick even after the water rinse due to the base contained in the "Ajax").
3. Dilute HCl rinse.
4. Grinding a slurry of levigated alumina plus water.
5. Water rinse.
6. Acid rinse.
7. Final thorough water rinse.
8. Drying with a paper towel.



Figure - 22

Working curve for the determination of thallium using Tl 5350

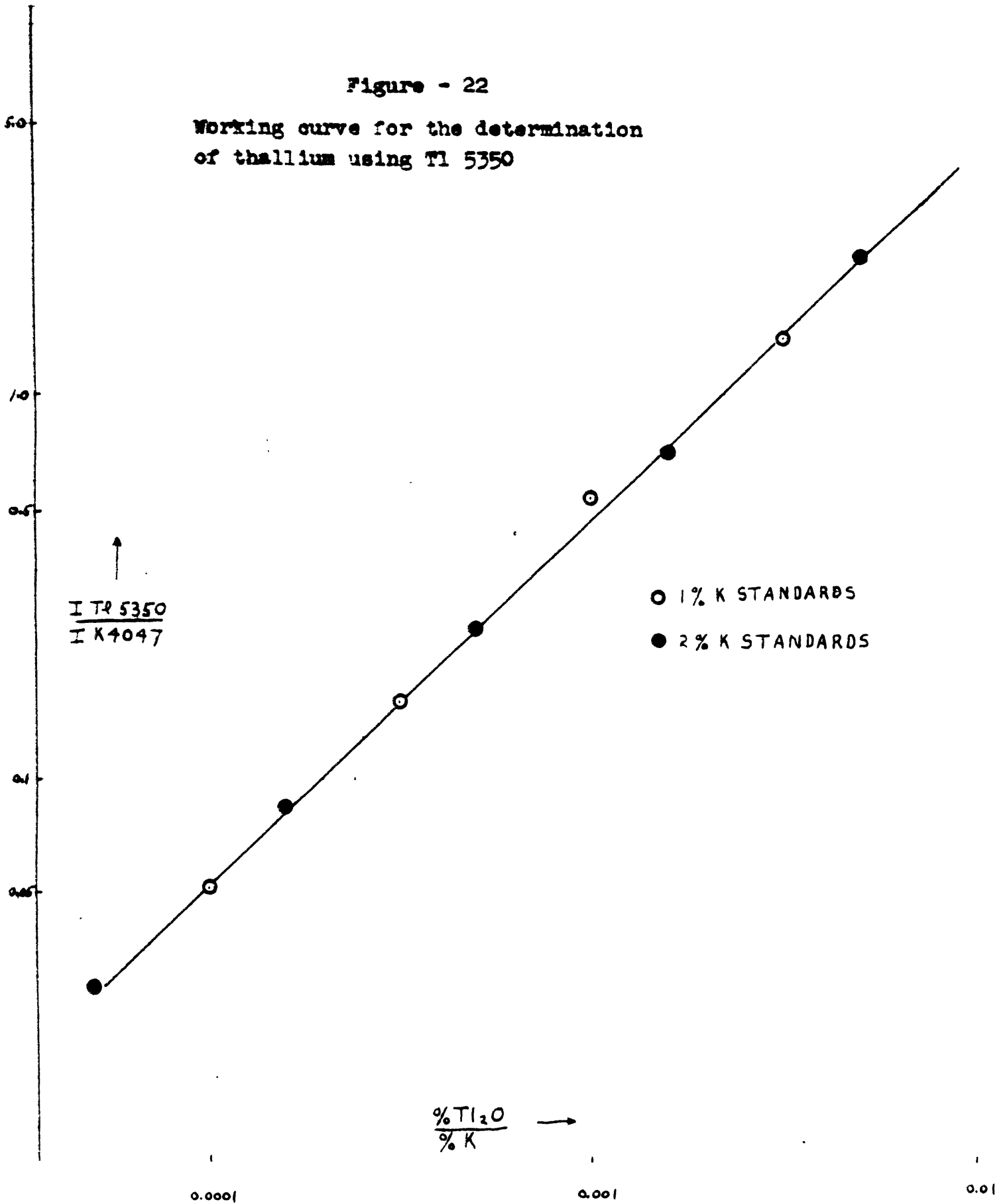
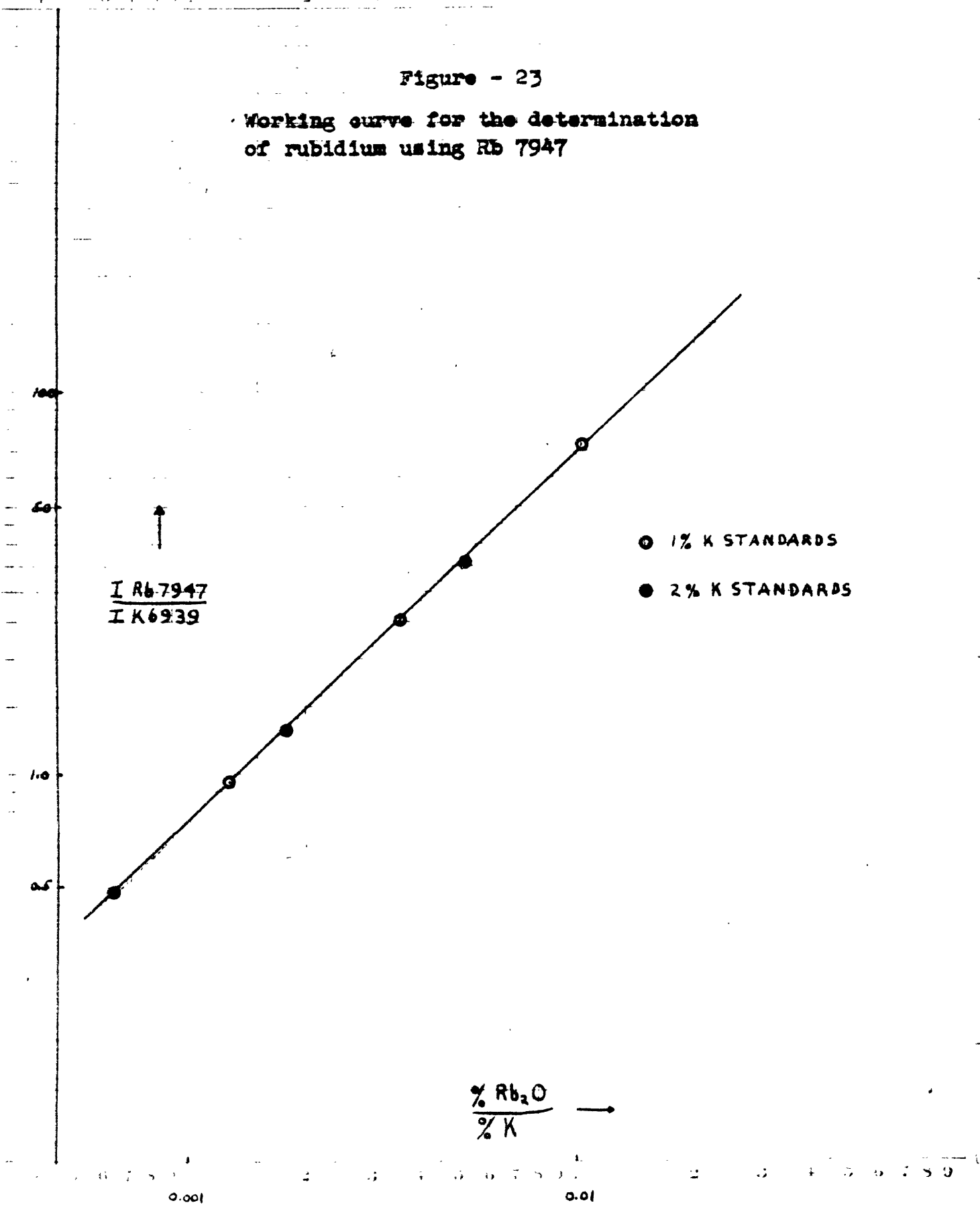


Figure - 23

Working curve for the determination of rubidium using Rb 7947

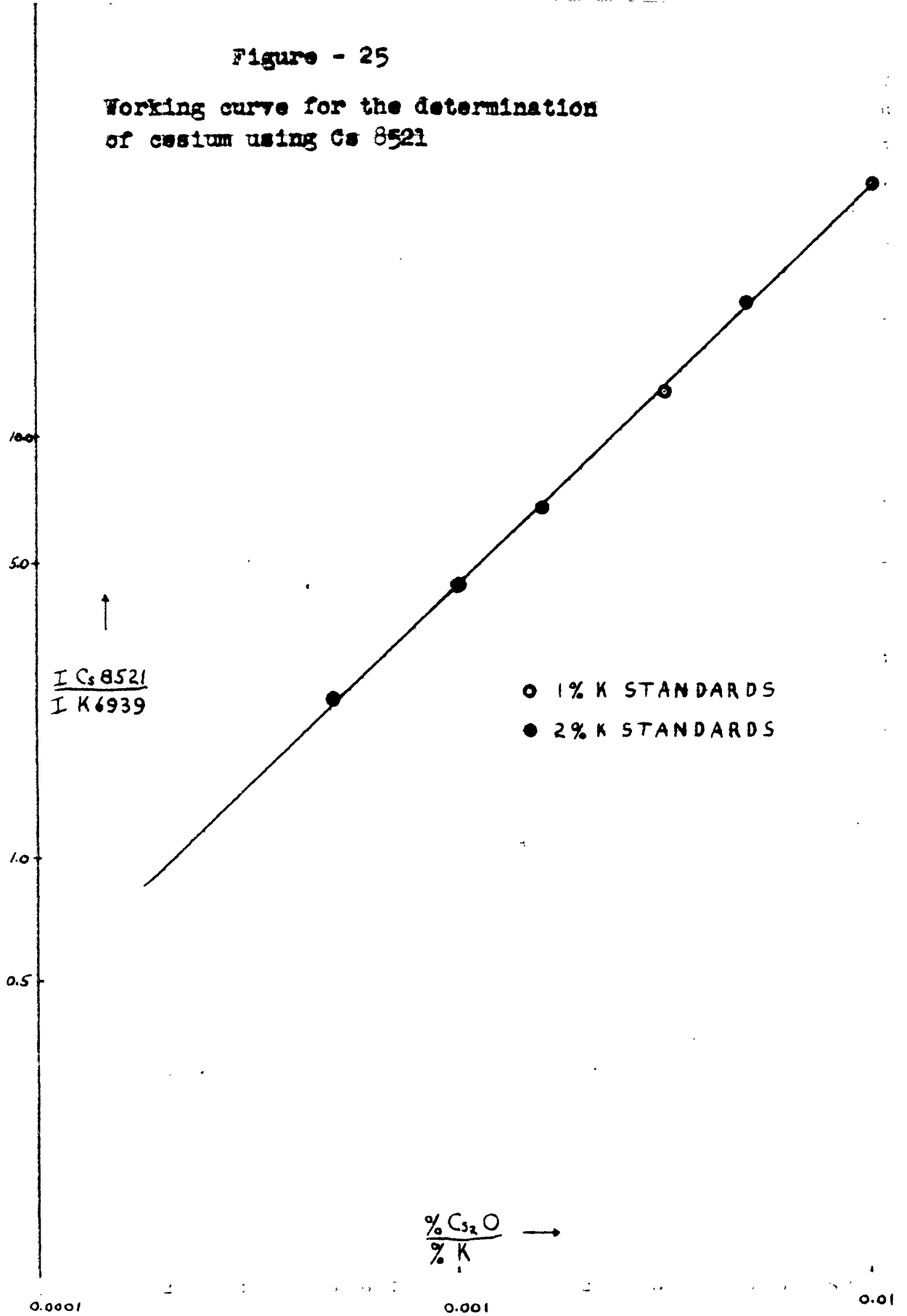


PAGES (S) MISSING FROM ORIGINAL

91

Figure - 25

Working curve for the determination of cesium using Cs 8521



The two sets of standards with different percentages of internal standard element gave coincidental working curves in each case. The attainment of near 45° working curves was significant for the following reasons: first, they showed that the standards were correctly made up and that the amount of any blank correction was of the proper magnitude; second, the methods used for emulsion calibration and background correction were reasonably correct; third, self-absorption over the concentration range plotted was probably nonexistent; and fourth, the use of potassium as a variable internal standard was valid. Of course the existence of compensating errors cannot be completely ruled out but this was considered unlikely.

#### H. Photometric procedure and calculations

The Jarrell-Ash microphotometer was the only type used in this investigation. Measurements were restricted to the one instrument because the shape and slope of a calibration curve are dependent to some extent on the instrument used in the preparation of that curve. Use of any other instrument would have necessitated the construction of a second set of calibration curves.

For measurements in the thallium determinations, a microphotometer slit width of approximately fifteen microns was used whereas a ten micron width was used for the other elements. The length of line photometered in all cases was

1 mm. The writer attempted to reproduce closely the slit widths for all measurements. The "clear plate" reading ( $D_0 \approx 100$ ) was set at the beginning of each plate and was occasionally checked during the course of the measurements; if any radical change was found, the entire plate was reread. When reading quite dense lines that had a low transmission value, a close watch was kept on the position of the scale zero because this is a potential source of major error when photometering dense lines.

Once a plate had been measured, the resulting transmission values were converted to opacities with the aid of the table in Appendix A that had been prepared by the writer to facilitate the calculations. The opacities were then converted to intensities by use of the appropriate calibration curve or curves, any necessary background corrections made, and the intensity ratios computed. Concentration ratios were obtained from intensity ratios by use of the working curves, and the percentages of the elements as oxides determined by multiplying the concentration ratios by the potassium percentages.

## I. Precision and accuracy of analytical methods

### (1) General

To have any real scientific value, all quantitative data should be accompanied by data that will give an

observer a general idea of its reliability. Replicate analyses of the same sample under supposedly identical operating conditions will rarely give values that are exactly alike due to the random errors inherent in the method. Precision is a measure of the ability of a method to reproduce a given value. It is generally expressed by means of the "average deviation" or "standard deviation". The average deviation represents the amount by which an average independent value differs from the most probable value. The standard deviation, however, provides a more useful measure of precision than the average deviation. It is the root-mean-square of the deviations from the arithmetic mean and is calculated by means of the following formula:

$$S. D. = \sqrt{\frac{\sum(d^2)}{n-1}}$$

where S. D. = standard deviation  
 d = deviations from arithmetic mean  
 n = number of analyses

The standard deviation is always larger than the average deviation and seems to present the data in a less favorable light, but it is much more useful as it enables a more complete and rigorous interpretation to be made. If the spectroscopic data follows a normal bell shaped distribution, the interval lying between plus or minus one standard deviation of the mean will include about 68% of the values, and about 95% of the values will be included in the interval between plus or minus two standard deviations

of the mean. Therefore it is seen that the standard deviation is more useful as a measure of precision than the average deviation because it is a measure of the spread of the values about the mean. The standard deviation is always larger than the average deviation because the squaring of all values places greater emphasis on extreme values.

The accuracy of the standard deviation depends upon the number of determinations and the magnitude of the standard deviation. Statisticians generally state that a minimum of 30 observations are required to give an accurate value. However, most spectrographers believe that 10 to 20 observations are sufficient to give a reasonably accurate answer.

## (2) Precision obtained

The precision of the analytical methods used in this investigation was determined by making a series of replicate analyses of the same sample. The operating conditions were the standard ones used for the analysis of all the unknown samples. Of course, the resulting precision data is true only for that one particular sample. It is not to be expected that every unknown sample was analyzed with that precision. For some samples the precision was better than the reported value, whereas for others it was undoubtedly much worse. Consequently, in selecting the samples to be used for the determination of precision data, an



attempt was made to select an "average" sample; that is one which burned about as smoothly and gave as much background as the majority of samples analyzed. Tables 4, 5, and 6 list the precision data obtained for thallium, rubidium, and cesium. The writer believes that the standard deviations reported in these tables give a good idea of the average reproducibility of the methods developed in this investigation.

### (3) Discussion of precision obtained

As is evident from Table 4 the best precision was obtained for rubidium. This was expected, as rubidium and potassium are known to be ideal internal standards for each other. In an earlier investigation (Canney, 1949, unpublished research) where rubidium was used as an internal standard for the determination of potassium in feldspars, a standard deviation of  $\pm 3.1\%$  was obtained using the line pair K 4047/Rb 4202. Consequently, in view of the facts that the excitation potentials of K 6939 (3.3 volts) and Rb 7947 (1.55 volts) are much further apart than are the potentials of K 4047 (3.05 volts) and Rb 4204 (2.94 volts), that there is a much greater wavelength separation of the two lines, and that these samples have poorer burning qualities, the attained standard deviation of  $\pm 4.5\%$  for the line pair Rb 7947/K 6939 was considered very good.

The standard deviation of  $\pm 8.2\%$  obtained for the

Table 4

Replicate analyses of  $\text{Rb}_2\text{O}$  in sample 46667

<u>Analysis No.</u>	<u>%<math>\text{Rb}_2\text{O}</math></u>	<u>D</u>	<u>%D</u>	<u>(%D)<sup>2</sup></u>
1	0.030	0.000	0.0	0.0
2	0.028	-0.002	6.7	45.0
3	0.028	-0.002	6.7	45.0
4	0.029	-0.001	3.3	9.0
5	0.029	-0.001	3.3	9.0
6	0.029	-0.001	3.3	9.0
7	0.030	0.000	0.0	0.0
8	0.030	0.000	0.0	0.0
9	0.030	0.000	0.0	0.0
10	0.029	-0.001	3.3	9.0
11	0.029	-0.001	3.3	9.0
12	0.028	-0.002	6.7	45.0
13	0.030	0.000	0.0	0.0
14	0.030	0.000	0.0	0.0
15	0.030	0.000	0.0	0.0
16	0.033	+0.003	10.0	100.0
17	0.033	+0.003	10.0	100.0
18	0.030	0.000	0.0	0.0

Average 0.030%  $\text{Rb}_2\text{O}$ Average Deviation  $\pm 3.1\%$ Standard Deviation  $\pm 4.5\%$

Table 5

Replicate analyses of  $\text{Ca}_2\text{O}$  in sample 46667

<u>Analysis No.</u>	<u>%<math>\text{Ca}_2\text{O}</math></u>	<u>D</u>	<u>%D</u>	<u>(%D)<sup>2</sup></u>
1	0.0012	+0.0001	9.1	80.3
2	0.0010	-0.0001	9.1	80.3
3	0.0010	-0.0001	9.1	80.3
4	0.0011	0.0000	0.0	00.0
5	0.0010	-0.0001	9.1	80.3
6	0.0011	0.0000	0.0	00.0
7	0.0010	-0.0001	9.1	80.3
8	0.0011	0.0000	0.0	00.0
9	0.0011	0.0000	0.0	00.0
10	0.0010	-0.0001	9.1	80.3
11	0.0011	0.0000	0.0	00.0
12	0.0012	+0.0001	9.1	80.3
13	0.0013	+0.0002	18.2	333.2
14	0.0011	0.0000	0.0	00.0
15	0.0010	-0.0001	9.1	80.3
16	0.0012	+0.0001	9.1	80.3
17	0.0012	+0.0001	9.1	80.3
18	0.0011	0.0000	0.0	00.0

Average 0.0011%  $\text{Ca}_2\text{O}$   
Average Deviation  $\pm 6.1\%$   
Standard Deviation  $\pm 8.2\%$

Table 6

Replicate determinations of the ratio  $I \frac{Tl\ 5350}{K\ 4047}$  in

Big Marsh oil shale

<u>Analysis No.</u>	<u>I <math>\frac{Tl\ 5350}{K\ 4047}</math></u>	<u>D</u>	<u>%D</u>	<u>(%D)<sup>2</sup></u>
1	0.009	-0.002	18.2	332
2	0.012	+0.001	9.1	83
3	0.012	+0.001	9.1	83
4	0.011	0.000	0.0	00
5	0.008	-0.003	27.3	745
6	0.009	-0.002	18.2	332
7	0.011	0.000	0.0	000
8	0.011	0.000	0.0	000
9	0.011	0.000	0.0	000
10	0.010	-0.001	9.1	83
11	0.011	0.000	0.0	000
12	0.011	0.000	0.0	000

Average Value of Ratio 0.011

Average Deviation  $\pm 7.6\%$

Standard Deviation  $\pm 12.2\%$

Standard Deviation  $\pm 8.0\%$   
(Mean of duplicate determination)

determination of cesium was still considered fairly good. Although potassium is probably not as good an internal standard for cesium as it is for rubidium, the major reason for the poorer precision in the cesium determinations was undoubtedly due to the necessity of having to correct for background. Background corrections were not necessary in the rubidium determinations. As mentioned in the section on background, there seems to be no question but that precision is lowered whenever background corrections have to be made regardless of how carefully these corrections are made.

The precision for thallium for a single determination ( $\pm 12.2\%$ ) was the poorest of the three. However, where all thallium determinations were made in duplicate and the values reported are the averages of duplicate determinations, the standard deviation reduces to  $\pm 8.8\%$ . Even more so than with cesium, large background corrections were necessary in all thallium determinations, and a considerable portion of the standard deviation can probably be attributed to this cause.

#### (4) Accuracy of methods

The accuracy of a method takes into consideration both precision and the tendency of the spectroscopic results to consistently run higher or lower than the chemical results due to the systematic errors inherent in the method. These

systematic errors are generally measured where possible by the "average bias", which is the difference between the chemical and the spectrographic results. An accurate method must be precise but the converse is not necessarily true; a very precise method may still have a large systematic bias.

In this investigation, as is so often the case in spectroscopic trace analysis, the complete absence of chemically analyzed standards prevented any assessment of the magnitude of the systematic bias. This was not too important as any constant bias would not, of course, affect the comparison of ratios. What was important, if the concentration ratios of elemental pairs in sediments were to be accurately compared with the same ratios in igneous rocks, was that the values for each element in sediments and igneous rocks have approximately the same bias. Neglect of this point could result in completely erroneous conclusions as to whether or not an element had concentrated in sediments.

To accomplish this standardization, mixtures of the standard granite (G-1) and the standard diabase (W-1) were analyzed using the standard operating conditions for the analysis of sediments. Any significant difference between the standard value of an element and the value obtained was used to compute the proper correction factor by which all values for the element were multiplied to bring them in

line with the standards. This was necessary because the methods used for the analysis of these elements in igneous rocks had been calibrated in terms of the standard granite and diabase. A large correction factor was only necessary in the case of rubidium. As a result of this standardization, the writer felt that any changes found in ratios between pairs of elements in igneous and sedimentary rocks would be significant and not due to different degrees of systematic error in the analytical methods.

#### J. Discussion of errors

The errors which enter into a spectrochemical method of analysis can be separated into two major classes: the systematic, and the accidental or random errors. The reproducibility of a method is dependent upon the magnitude and number of random errors whereas the systematic errors generally cause a systematic bias.

The random errors in any spectroscopic method are generally due to some or all of the following causes. No claim is made that all possible sources of error are listed.

1. Variations in emulsion sensitivity.
2. Plate grain.
3. Variations in plate processing conditions.
4. Inhomogeneity of samples.
5. Scratched and dirty plates.

6. Out of focus spectra.
7. Inability to sample same portion of arc column for each sample.
8. Influence of extraneous elements on intensity ratio of the line pair.
9. Influence of source fluctuations on intensity ratio of the line pair.
10. Faulty alignment of spectrograph and microphotometer optics.
11. Fluctuations in microphotometer light source.
12. Contamination of samples.
13. Uncorrected background.
14. Incorrect setting of instruments.
15. Errors in microphotometer measurements.
16. Errors in calculations.

The systematic errors generally arise from standardization. The use of synthetic standards instead of chemically analyzed natural materials is probably the major cause of spectroscopic results having a systematic bias. Other possible causes are:

1. Faulty emulsion calibration.
2. Incorrect values assigned to standards.
3. Uncorrected background.
4. Lateral shift in working curve.



## VI. Analysis of Samples

### A. General discussion

The degree of success in obtaining successful analyses may be seen from a perusal of Table 7. The highest percentage of successful analyses were for rubidium but this was because the average rubidium content was well above minimum detection limits. As mentioned before, the methods adopted were those which the writer believed would give successful results for the greater majority of the samples. Due to the large number of samples analyzed, every sample was analyzed in an identical fashion for time could not be spent in adjusting the operating conditions to be the most suitable for each sample. If this had been done, the writer feels that the percentage of successful analyses in the case of thallium and cesium could have been raised to at least 90%.

Some typical spectrograms are shown in Figs. 26, 27, 28, and 29. These show the analysis lines and the various types of interference encountered.

### B. Interfering lines and bands

In the thallium determinations no direct line interference was encountered but halation from Ca 5349A was occasionally intense enough to prevent an accurate determination. Ca 5349 is an atom line arising from a transition between two high energy levels; therefore its intensity is

Table 7

## Classification of results - 324 samples

	<u>Rb</u>		<u>Cs</u>		<u>Tl</u>	
	<u>No.</u>	<u>%</u>	<u>No.</u>	<u>%</u>	<u>No.</u>	<u>%</u>
Value reported	294	90.7	245	75.6	241	74.5
v.	12	3.7	25	7.7	24	7.4
n. d.	7	2.2	15	4.7	39	12.0
n. d. (1)	7	2.2	34	10.5	6	1.8
n. d. (2)	1	0.3	1	0.3	10	3.1
n. a.	3	0.9	4	1.2	4	1.2

## Explanation of symbols

- n. a. - not analyzed
- n. d. - not detected
- n. d. (1) - not detected - but excessive background  
and/or interference present
- n. d. (2) - not detected but burn was poor
- v. - faint line visible but background and/or  
interference generally of such nature  
that no accurate determination was possible

very dependent, percentage wise, on the arc temperature. The wide range of intensities which it exhibited due to this cause may be seen from the photographs in Figs. 26 and 27. There it is the line just to the left of the thallium line.

The CaF band with main head at 5291A occasionally swamped the region of the thallium line and made an analysis impossible. This band is shown in Fig. 26, sample 45133, and in more detail in Fig. 27, sample 45004. Luckily very few samples contained enough fluorine to cause an appreciable development of this band.

Sample 45134 in Fig. 26 illustrates the statement made in the section on background on how the same sample would occasionally give two apparently identical burns and yet the intensity of the continuous background would be radically different.

Fig. 28 shows a typical analysis plate for rubidium and cesium. Fig. 29 illustrates two extreme conditions. In exposure one in Fig. 29, conditions are ideally perfect whereas in the other exposures, there is an extensive development of interfering cyanogen red bands. These bands generally appeared whenever a sample contained extremely small amounts of the alkali metals. No line interference was encountered.

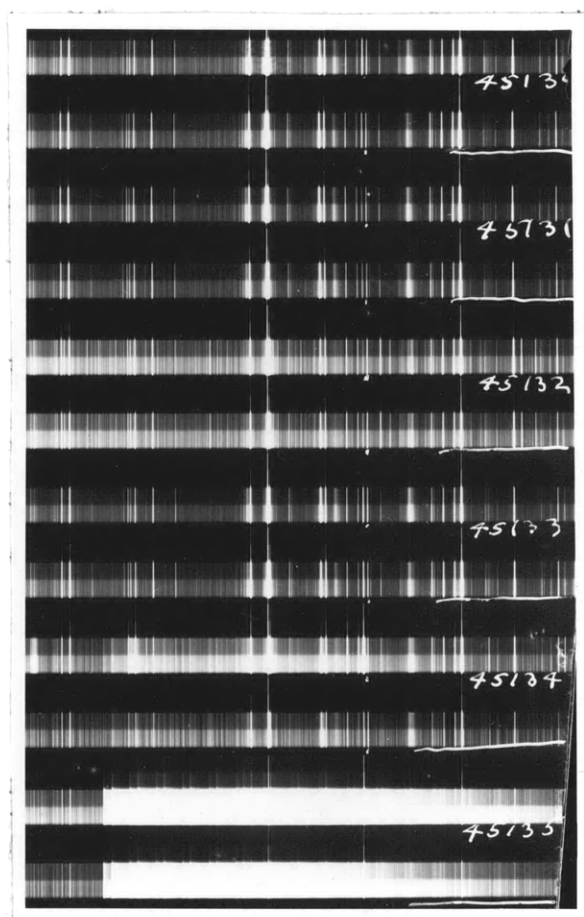


Fig. .26

A typical thallium plate.

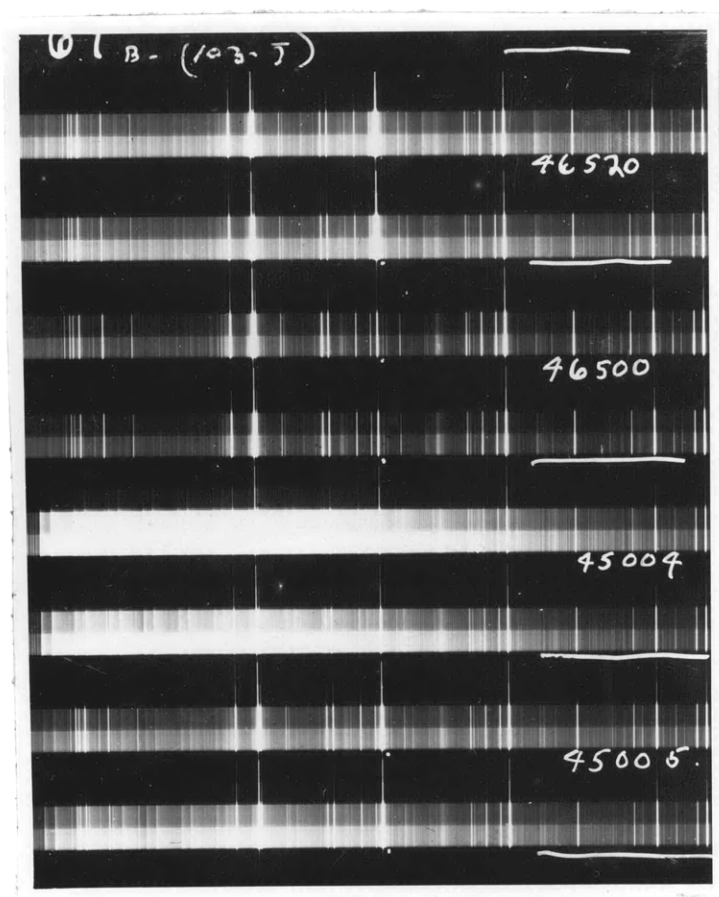


Fig. 27

The thallium line (5350A) and neighbors.

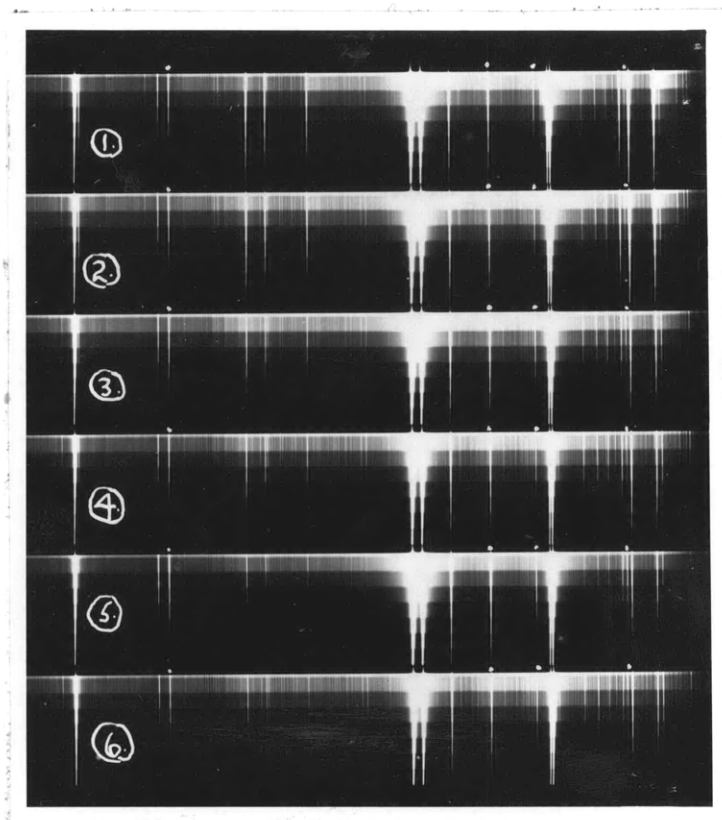
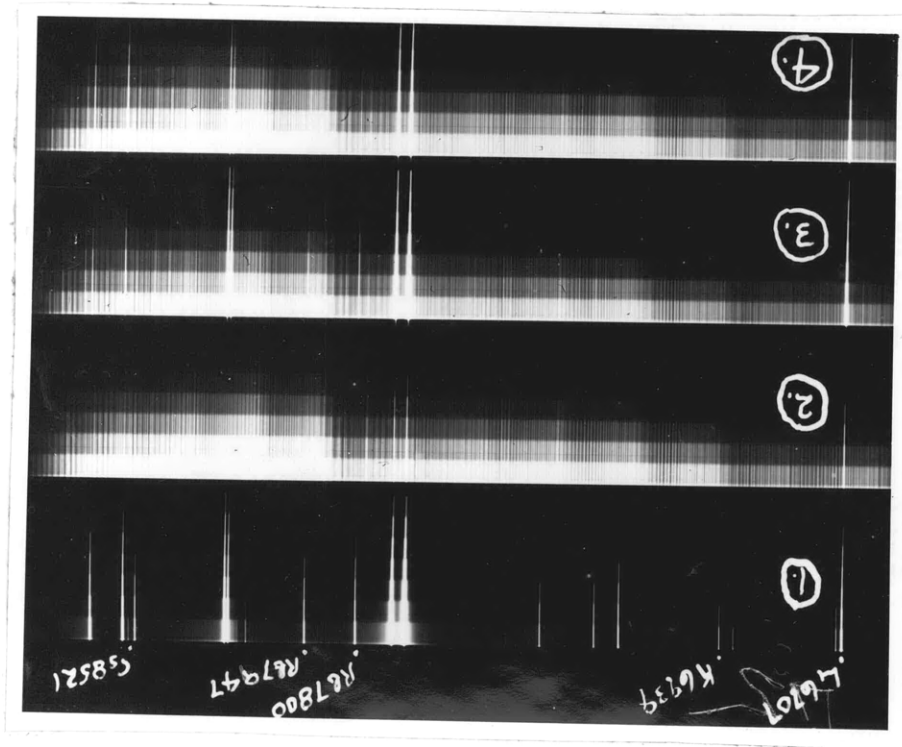


Fig. 28

A typical alkali plate

The alkali analysis lines (1)  
plus ON red bands (2) (3) (4)

FIG. 29



Part II



## VII. Introduction

### A. Purpose of investigation

This thesis had three main objectives:

1. To determine abundance values for rubidium, cesium, and thallium in sediments.
2. To compare the ratios  $K_2O/Rb_2O$ ,  $K_2O/Cs_2O$ ,  $K_2O/Tl_2O$ , and  $Rb_2O/Tl_2O$  in sediments with the corresponding ratios in igneous rocks to ascertain whether or not there had been any concentration of one element with respect to another during the sedimentary cycle.
3. To explain any changes found in the abundance ratios between igneous and sedimentary rocks on the basis of the physical and chemical properties of the elements involved.

There is a recognized need for abundance data for rubidium, cesium, and thallium in sediments. In their recent book on geochemistry Rankama and Sahama ( 18 ) state that the number of available analyses is still deplorably small. To the best of the writer's knowledge, our entire knowledge of the content of rubidium and cesium in sediments is based upon seven analyses of sedimentary materials by Goldschmidt, Bauer, and Witte ( 9 ). Thallium has even fewer recorded analyses; Preuss ( 17 ) reported the average content of thallium in two composite samples of German sand-

stones and shales.

In igneous rocks, potassium, rubidium, cesium, and thallium form a group of elements of varying degrees of coherency. Two elements are said to be geochemically coherent if they constantly follow one another in nature. The coherency of these four elements in igneous rocks will be more thoroughly discussed in a later section. However, once these elements are released from the igneous rocks by means of chemical weathering processes, they enter a quite different environment. In the sedimentary cycle, their migration will be governed by principles which are different than the laws governing their behavior during the crystallization of a magma. Their migration will be controlled by the physical and chemical laws that control their behavior in an essentially aqueous medium at the comparatively low temperatures and pressures existing at the surface of the earth. For example, it is a well known fact that while the sodium and potassium contents of igneous rocks are roughly similar, their different behavior during the sedimentary cycle results in a considerable degree of separation. The bulk of the sodium is carried to the ocean and remains there in the dissolved form while only a small proportion of the originally dissolved potassium remains in solution.

What will be the relationship between potassium, rubidium,

and cesium in sediments? The potassium-rubidium pair is a remarkably coherent one in igneous rocks. Will the same degree of coherency be exhibited in sedimentary rocks? It can be predicted on the basis of theory, which will be discussed in a later section, that rubidium and cesium will be adsorbed in argillaceous sediments even more strongly than is potassium. Cation-exchange experiments with clays and the scanty data on the rubidium and cesium content of sediments tended to verify this theory but the lack of an adequate number of analyses made it impossible to reach a definite conclusion.

Ahrens ( 1 ) has found a remarkably close association between thallium and rubidium in potash-rich silicate minerals. Will these two elements also be closely associated in sediments? As will be brought out in the following section, there are some significant differences in the chemistry of "thallous" thallium from that of rubidium which could under the proper conditions, it was believed, result in a quite complete separation of these two elements.

It was hoped that the results of this investigation would throw some welcome light on the above questions. No claims will be made for completeness in this work because several mechanisms for the fixation of elements in sediments still remain largely unknown. The effect of biological activity is one of the more important of these. In general, marine organisms possess a remarkable ability for extracting

various elements from the sea water and concentrating them in their bodies. After the death of the organism, this accumulated material is redissolved or falls to the bottom where it enters into the formation of the sedimentary rocks. On the basis of rather meager and somewhat contradictory data, it has been found that about forty elements are accumulated by marine organisms in various degrees of concentration. In connection with this problem of the fixation of elements by biological activity, the writer was fortunate in that a considerable number of the samples used in this investigation had been analyzed for organic carbon by personnel of the American Petroleum Institute Research Project 43C. Consequently, scatter diagrams of element concentration or abundance ratio versus percent organic carbon were made wherever possible to detect any possible relationship. These diagrams will be discussed in their proper place. Of course, whenever there seemed to be a correlation, one never could be certain that the organic matter itself was directly responsible, because the environmental conditions responsible for the preservation of the organic matter might also have caused the fixation of the element by some other mechanism.

Another largely unknown factor is the fixation of elements in authigenic minerals. These are minerals which form in sediments at the place of their occurrence. Important authigenic minerals that carry the alkali metals, mainly potassium, in structure sites are : glauconite

feldspar, and the "illite group" of clay minerals. The phenomena of authigenesis is still imperfectly understood. Its importance to this work might be summed up in the following question. What is the source of the alkali metals which are important constituents of these minerals? If these minerals are formed principally by alteration of existing materials; then of course, authigenesis will not appreciably affect alkali abundance values or ratios. However, if the alkali metals are extracted from the sea water as some authorities believe; then the alkali abundance values and ratios in sediments will be appreciably affected by the formation of authigenic minerals, since the content of rubidium and cesium in sea water is strongly reduced with respect to potassium. Unlike the problem of accumulation by biological activity, it should be quite easy to determine experimentally whether the source of the alkali metals which occupy essential structure sites in authigenic minerals is the sea water or the sediments. All that would be necessary would be to determine several alkali abundance ratios such as the K-Rb and K-Cs ones in a suitable selection of pure authigenic minerals. If the source is the sea water; then the values of these ratios should be equal to or close to the values of these ratios in sea water, which are considerably different from the values of these ratios in sediments and igneous rocks. On the other hand, values close to those existing in sediments would indicate a sedimentary source.

The writer believes that the chemical reactions which the alkali metals undergo in aqueous solutions are known well enough so that no discussion of this subject need be included here. However, the reader may well wonder why thallium, a group 3B element, is considered in this work which is essentially an investigation on the geochemistry of several of the alkali metals. Consequently, it was considered necessary to insert a short discussion on the chemistry of thallium.

#### B. Chemistry of thallium

Thallium is assigned to group 3B in the periodic classification of the elements along with boron, aluminum, gallium, and indium. All of these elements have three potential valence electrons, but the heavier members of the group exhibit variable valencies of one, two, or three due to the increased masking of the positive charge on the nucleus with increasing atomic number. A glance at the electronic configuration of the thallium atom shows completed K, L, M, N, and O shells plus three valence electrons in the P shell. However, the two 6S electrons in the P shell tend to act as an inert pair. The result of this is that thallium most commonly exhibits a valency of one. The trivalent state ("thallic" thallium) is known, but the univalent state ("thallous" thallium) is the stable one. Of great geochemical significance is the fact that the radius of the univalent thallium ion (1.49A) is equal to the radius of the

rubidium ion. As a result there is a close association between thallium and rubidium in potash-rich igneous minerals where they both proxy for potassium.

The aqueous chemistry of thallium is of more direct interest as thallium exhibits a rather striking dual behavior. On the one hand certain of its reactions are very similar to those of the alkali metals; on the other hand it resembles Ag, Pb, and Cu in many ways. Univalent thallium resembles the alkali metals in that its hydroxide, carbonate, and sulphate are soluble, and the chloroplatinate and cobaltinitrite are insoluble. The basic strength of thal-  
lous hydroxide is comparable with that of sodium hydroxide.

Univalent thallium differs from the alkali metals in several respects. The thal-  
lous halides exhibit the characteristic low solubility in water typical of the halides of univalent Cu, Ag, Au, and Hg, whereas halides of the alkali metals are all extremely soluble. Some authorities have predicted that the low solubility of thal-  
lous chloride should cause the precipitation of thallium as thal-  
lous chloride in marine sediments, but the writer could find no evidence that any such precipitation took place. Of course it would be possible to make some assumptions and calculate whether or not there was any possibility that the solubility product of thal-  
lous chloride in sea water could be exceeded. However, the writer believes such calculations would be meaningless because the activity coefficients for these ions

in sea water are unknown.

Another important difference between thallium and the alkali metals is the sparing solubility of its sulphide. The sulphides of Tl, Cu, Ag, Hg, and Pb are among the least soluble of all substances in all but strongly acid solutions. It is a well known fact that certain sedimentary environments contain rather high concentrations of hydrogen sulphide. Therefore it seems possible that the low solubility of thalious sulphide should influence the distribution of thallium in sediments. The writer believes that he obtained corroboratory evidence to support such a viewpoint, although the evidence is of a somewhat indirect nature. This evidence is considered in the section where the Rb-Tl abundance ratios are discussed.

### C. Location and description of formations

#### (1) General

The value of an investigation of this type increases almost in proportion to the number of samples and formations that can be analyzed. Therefore the writer attempted to analyze as many samples and formations as time and facilities would permit. A total of three hundred and twenty-four samples were analyzed. All except eleven of these came from the ten sedimentary formations that are listed in Table 8. The sample numbers and the formations from which they were taken are listed in Appendix D.



Table 8

## Formations studied

Formation	Number of Samples
Miocene Nodular Shale	43
Cherokee Shale	39
Lower Eutaw Shale	24
Eagle Ford Shale	28
Woodford Shale	13
Woodbine Sandstone	41
Tuscaloosa Sandstone	29
Frio Sandstone	12
Selma Chalk	33
Austin Chalk	51
Misc.	11
Total	<u>324</u>

The three types of sediments analyzed - shales, sandstones, and limestones - constitute more than 99 per cent of all sediments. These three types, however, are not equally abundant. All authorities agree that shales are by far the most common type followed by sandstones and limestones in that order, but they generally disagree on the proportions assigned to each type. This question of the relative proportions of the various types of sediments is important and always arises whenever some value such as the average content of an element in sedimentary rocks has to

be determined. In this investigation, average values for the rubidium, cesium, and thallium contents were determined for each formation. In computing an average value for an element in sediments, the question arose of whether to weight the value for each lithologic type in accordance with the relative abundance of that type. A decision against such a computational method was made for the following reason. The samples as received by the writer were already pulverized, and all that was generally known about a sample was its location and the fact that it came from a certain formation. Its exact lithologic type was generally unknown. Consequently, where many of the formations studied had a very variable lithology - particularly the Upper Cretaceous formations of the Gulf Series - one never could be certain that a particular sample was actually a shale or sandstone merely because it came from a shale or sandstone formation.

## (2) Miocene Nodular Shale

The Miocene Nodular Shale samples came from the Los Angeles Basin in California. The great majority of these samples were obtained from nine core sections varying in depth from 8090 feet to 8237 feet from a well in the Lawndale Oil Field. Megascopically this formation is generally described as consisting of hard black shale with a highly carbonaceous appearance. The black color is interrupted with tan-colored laminations and irregularly shaped nodules. The average organic carbon content of the samples used in this

investigation was 5.85 per cent. Hoots, Blount, and Jones ( 11 ) believe that this shale was deposited in an environment that supported an abundant plant and animal life. There is also excellent geological and chemical evidence that this formation was the source bed for the oil in the Playa Del Rey Field.

### (3) Cherokee Shale

The Pennsylvania Cherokee Shale samples were obtained from wells in and near the Burbank Field. It is quite generally believed that this formation was deposited in a lagoonal and shallow sea environment. The Cherokee Shale samples had an average organic carbon content of 3.34 per cent. Like the Miocene Nodular Shale, the Cherokee Shale is considered a likely source bed of petroleum.

### (4) Woodford Shale

The majority of the Woodford Shale samples came from a well in West Texas. A few samples which were included in this formation actually are samples of Chattanooga Shale. However, the Woodford of West Texas and Oklahoma is correlated with the Chattanooga Shale of Northern and Eastern areas. The Woodford Shale has generally been considered to be Lower Mississippian in age although recently it is usually placed in the Upper Devonian.

In West Texas, Barton ( 4 ) describes the Woodford as

a dark brown shale with considerable evidence of vegetable matter. Locally there are large developments of dark brown chert and pyrite. Descriptions from other areas are all quite similar and generally note the presence of much chert and pyrite.

The American Petroleum Institute Research Project 43C found the Woodford Shale to be by far the most radioactive of all the sedimentary geological formations studied. The writer also found this formation to be unusual in that most of the samples had an extremely high thallium content. The significance of this high thallium content will be discussed in a later section.

#### (5) Upper Cretaceous formations

Six Upper Cretaceous formations were studied. Samples of three of these - the Austin Chalk, Eagle Ford Shale, and Woodbine Sandstone - came from wells in or near the East Texas Oil Field. The majority of these East Texas samples came from Trask's collection ( 21 ) of oil well cuttings. The other three are corresponding formations from the Mississippi region of the Cretaceous. These were the Lower Eutaw Shale, Selma Chalk, and Tuscaloosa Sandstone.

These Cretaceous formations, as mentioned before, have a very varied lithology. Just how variable is the lithology can be seen from the description of the Eagle Ford - Woodbine

group by Minor and Hanna ( 14 ). The lower member of this group is the producing formation of the East Texas field. They describe it as being composed of black fissile shales, grey and greenish shales, mottled or red-bed shales, homogeneous and saccharoidal sands as well as silty and sandy conglomerates. The beds are predominately non-marine and very variable, both horizontally and vertically. They describe the Austin Chalk as usually consisting of hard chalk with minor amounts of chalky shale and shale.

The Mississippi Cretaceous samples were obtained from two wells in the Gwinville and Baxterville fields, which lie in the embayment area. No published descriptions of the formations in these fields were located, but they probably follow rather closely the descriptions given by McEllothlin ( 13 ), who studied these formations in the central counties. The following descriptions of the lithology of these formations are taken from his paper:

- Upper Tuscaloosa - Variegated purple red and grey waxy shales with abundant ankerite pellets.
- Lower Eutaw - Glauconitic sands and shales.  
Dark laminated shales.
- Selma - Chalks, marls, and calcareous shales.

#### D. Presentation of data

The problem of how to adequately present the large mass of data collected in this work caused a considerable amount of concern. The writer feels that there is nothing more monotonous in the body of a report than a large number of pages filled with tables. Therefore the writer decided to present as much of the data as possible in a graphical form. The two methods of graphic presentation adopted were histograms and scatter diagrams. Such methods tend to give a much better picture of the distribution of a variable than do columns of figures in a table. They are also ideal for comparison purposes.

The nature of these two types of graphs are well enough known so that no detailed explanation of the construction methods need be given. For constructing the histograms, a linear scale was not found to be suitable, owing to the large range of values which had to be plotted. Therefore it was necessary to use a geometric scale in setting up the class intervals. Such a scale uses larger intervals for the larger values and smaller intervals for the smaller values. The interval factors used to construct the various histograms presented in this report ranged from 1.10 to 1.40. The only basis used to select these factors was to attempt to cover a given range of values with ten to twenty class intervals. This is generally considered the most efficient number. Too much accuracy is lost when fewer than ten are

used, and the computations generally become too tedious with more than twenty. Histograms are occasionally criticized for the reason that the use of a different class interval might markedly change the form of a graph. However, such criticism is really valid only if too few classes are present or the size of the statistical sample is too small.

Tables were used only for summary purposes.

## VIII. The Abundance of K, Rb, Cs, and Tl

A. General

The material in this section is largely presented in the form of histograms and scatter diagrams. In general the following plots were made for each element:

1. Size-distribution in all sediments.
2. Comparison of the size-distributions in shales, limestones, and sandstones.
3. Comparison of the size-distributions in four shale formations.
4. Comparison of the size-distributions in two limestone formations.
5. Comparison of the size-distributions in two sandstone formations.
6. Relationship between element concentration and organic carbon content in the Cherokee Shale and Nodular Shale formations.

Although the potassium determinations were not performed by the writer, a section on the abundance and distribution of potassium is included for comparison purposes.

Appendix B lists the results of all determinations on all samples.



### B. The abundance of potassium

The average content of  $K_2O$  in each of the formations studied is presented in Table 9.

The average content of  $K_2O$  in shales (2.20%) is somewhat lower than previous published analyses. Clarke (7) reports the average shale to contain 3.24 per cent  $K_2O$ . No useful purpose would be served by comparing the average  $K_2O$  contents of the limestone and sandstone formations with published analyses because, as mentioned before, the exact lithology of many of the so-called limestone and sandstone samples was not known.

Histograms showing the size-distribution of  $K_2O$  content in the various formations and lithological types are presented in Figs. 30 to 35.

Fig. 36 illustrates the relationship between potassium content and organic carbon content in the Miocene Nodular Shale and Cherokee Shale. No apparent correlation is visible from these plots; yet, the possibility that there is a relationship will be discussed in the section on the K-Rb abundance ratio.

### C. The abundance of rubidium

Table 10 summarizes the average rubidium content of the various formations. This table shows that there is little variation among the different types of sediments.

Table 9

## Potassium content of sediments

Formation	Number of samples included in average and percentage of total	Average content K <sub>2</sub> O (%)
Miocene Nodular Shale	43 (100%)	1.33
Cherokee Shale	39 (100%)	2.98
Woodford Shale	13 (100%)	3.20
Lower Eutaw Shale	24 (100%)	2.13
Eagle Ford Shale	28 (100%)	1.84
Woodbine Sandstone	41 (100%)	1.05
Tuscaloosa Sandstone	29 (100%)	2.27
Frio Sandstone	12 (100%)	2.37
Selma Chalk	33 (100%)	2.30
Austin Chalk	51 (100%)	1.47
All Shales	154 (100%)	2.20
All Sandstones	82 (100%)	1.67
All Limestones	84 (100%)	1.80
All Samples	320 (98%)	1.96

### Size-Distribution of K<sub>2</sub>O Content in Argillaceous Sediments

Based on 320 Samples

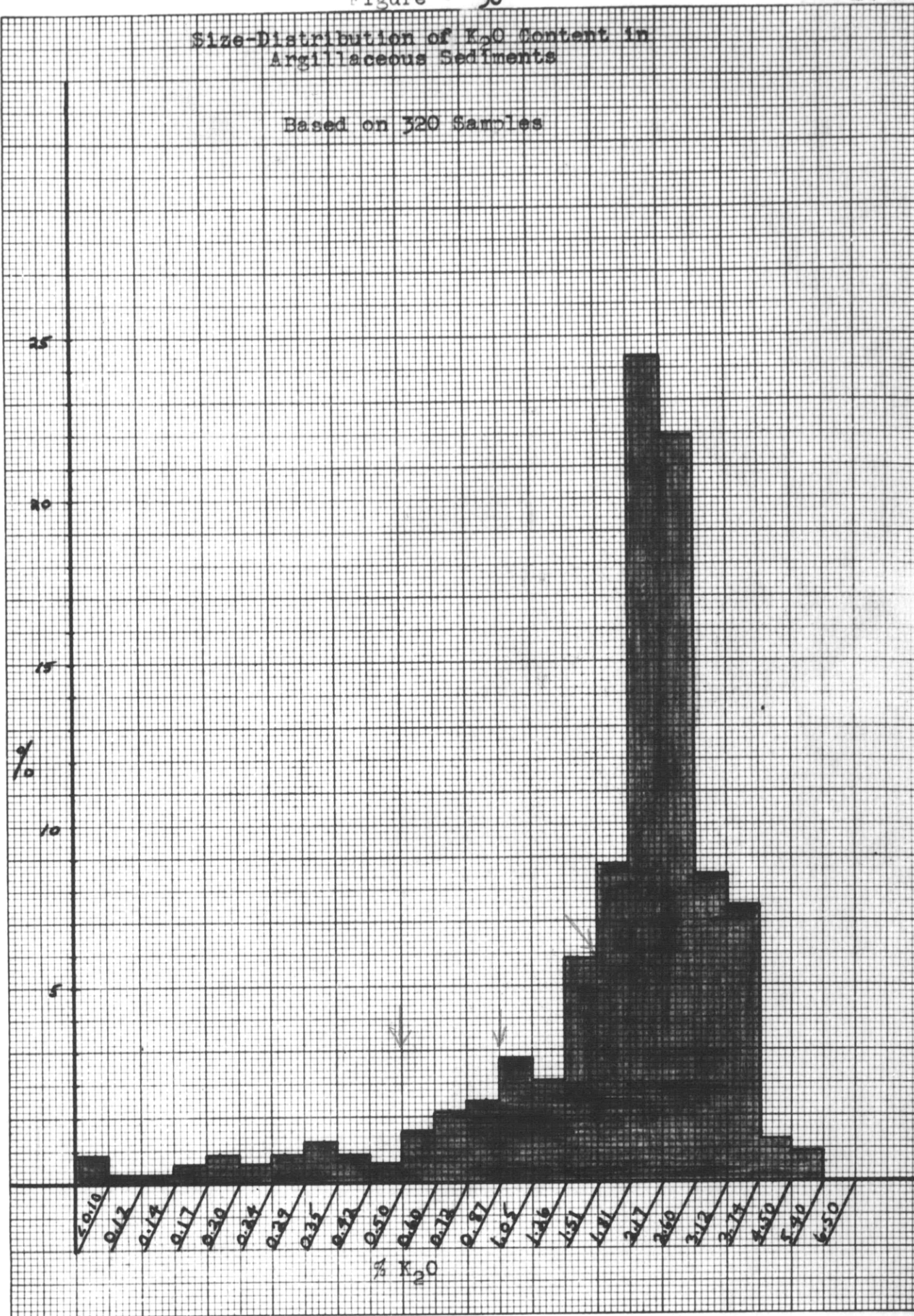
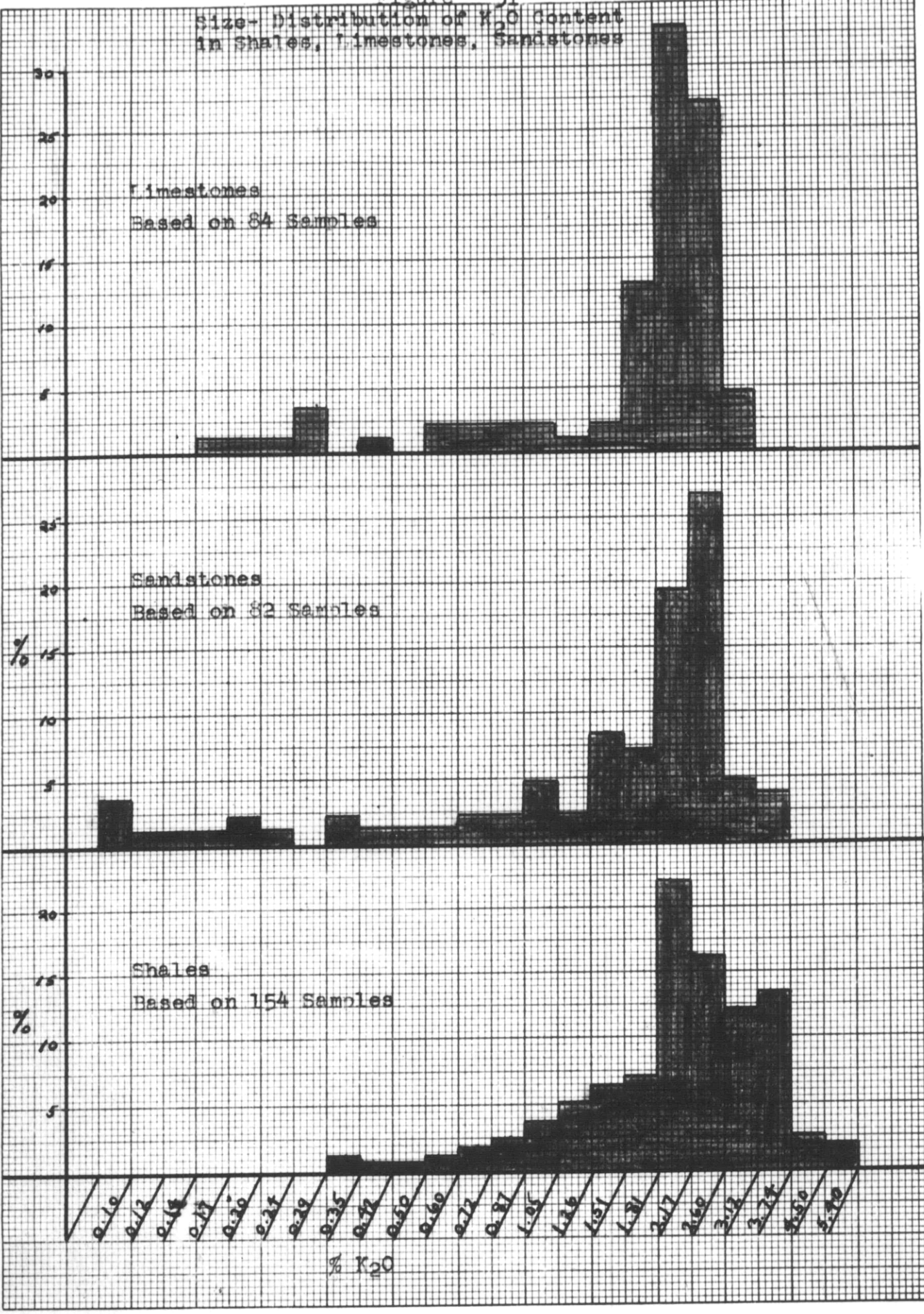
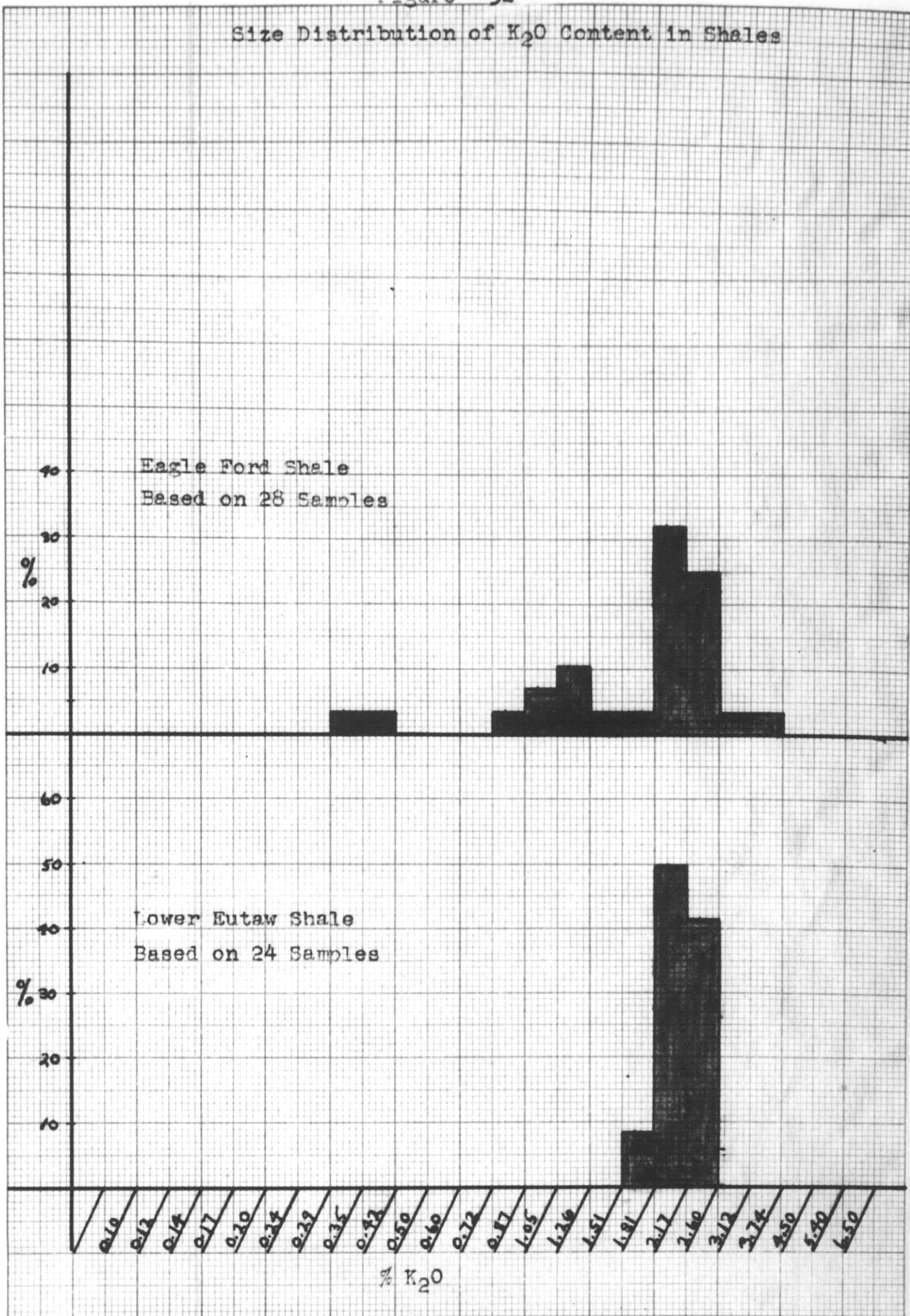


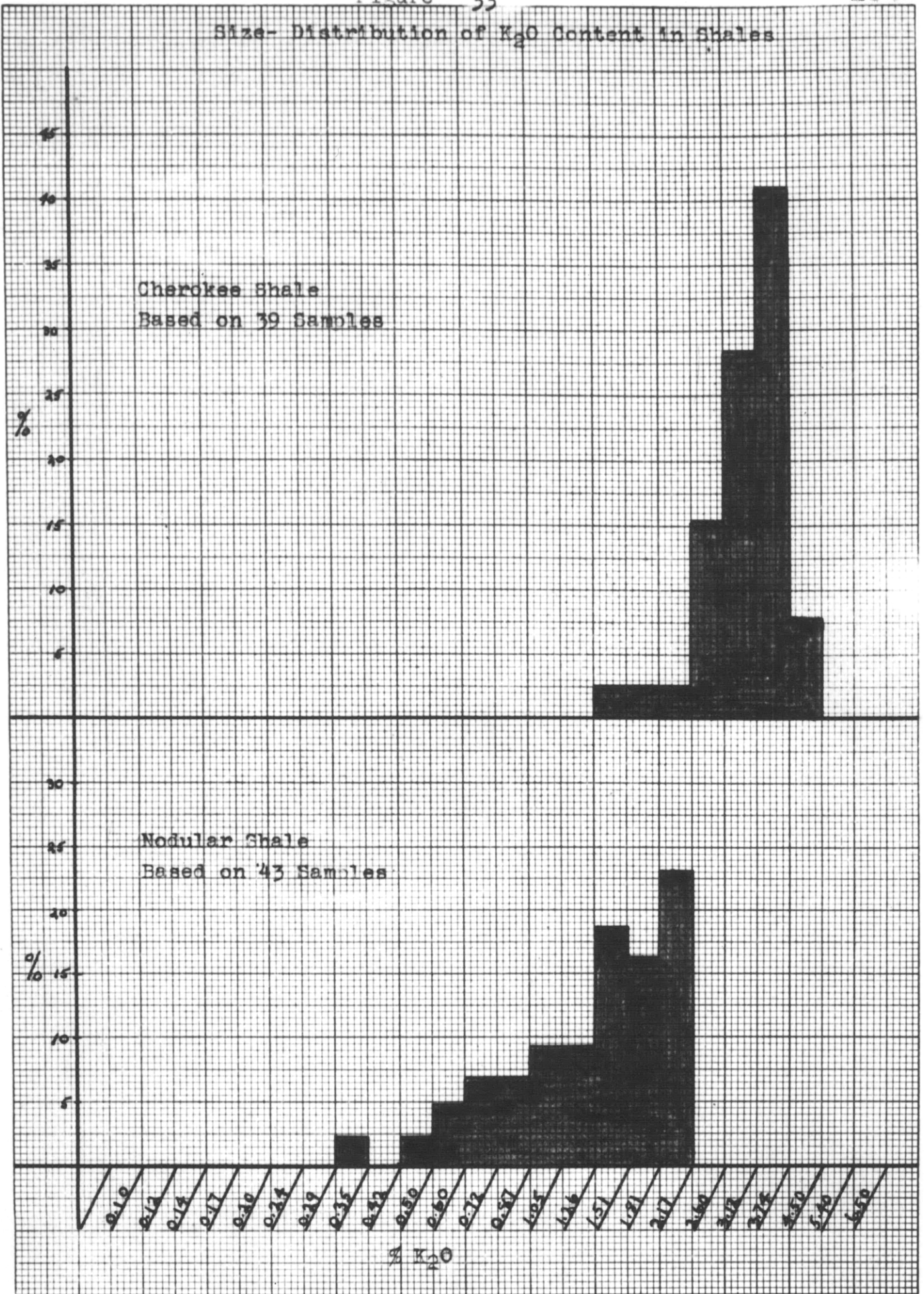
Figure - 31  
Size-Distribution of K<sub>2</sub>O Content  
in Shales, Limestones, Sandstones



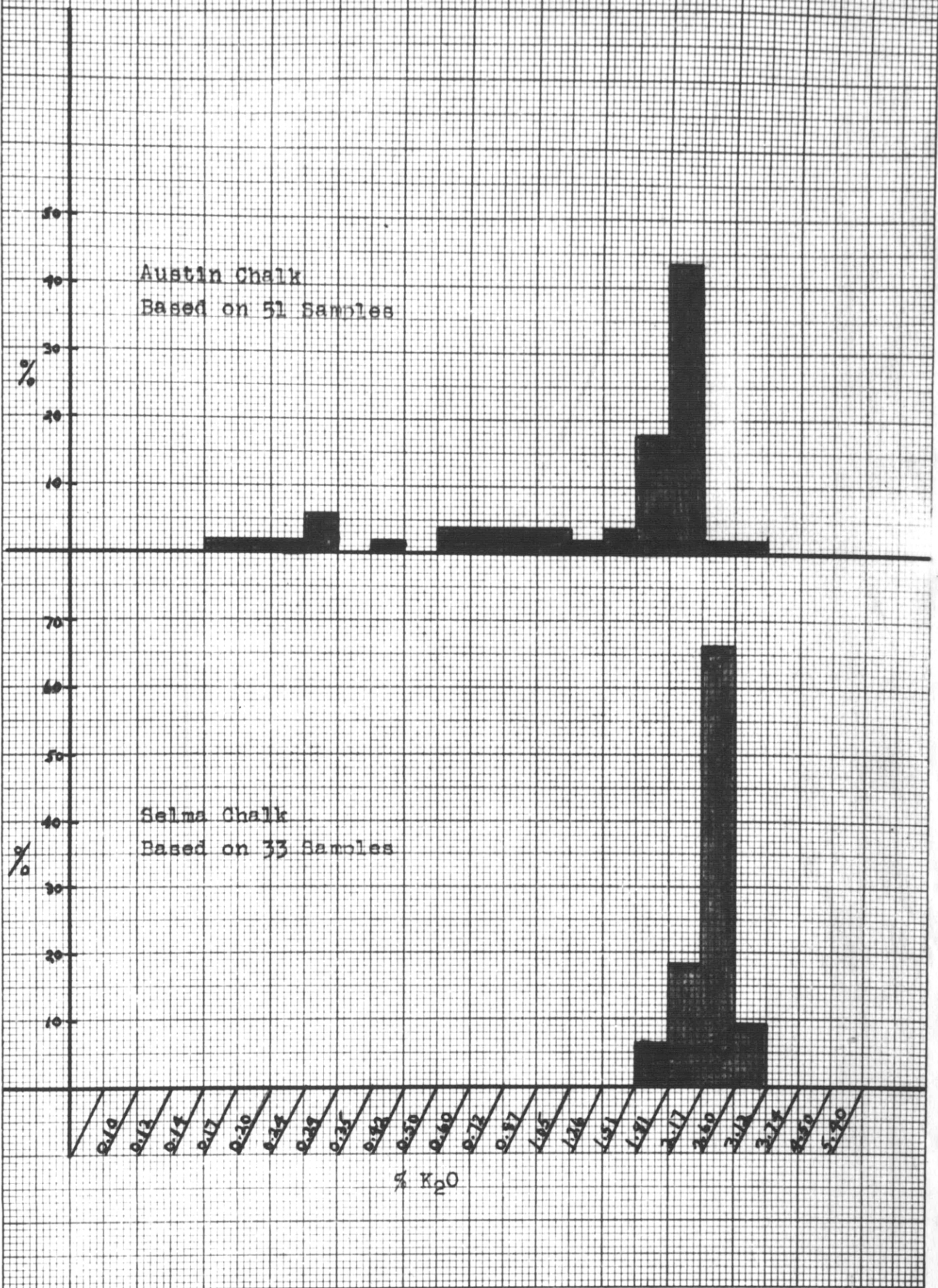
Size Distribution of K<sub>2</sub>O Content in Shales



Size- Distribution of K<sub>2</sub>O Content in Shales



Size Distribution of K<sub>2</sub>O Content in Ls.



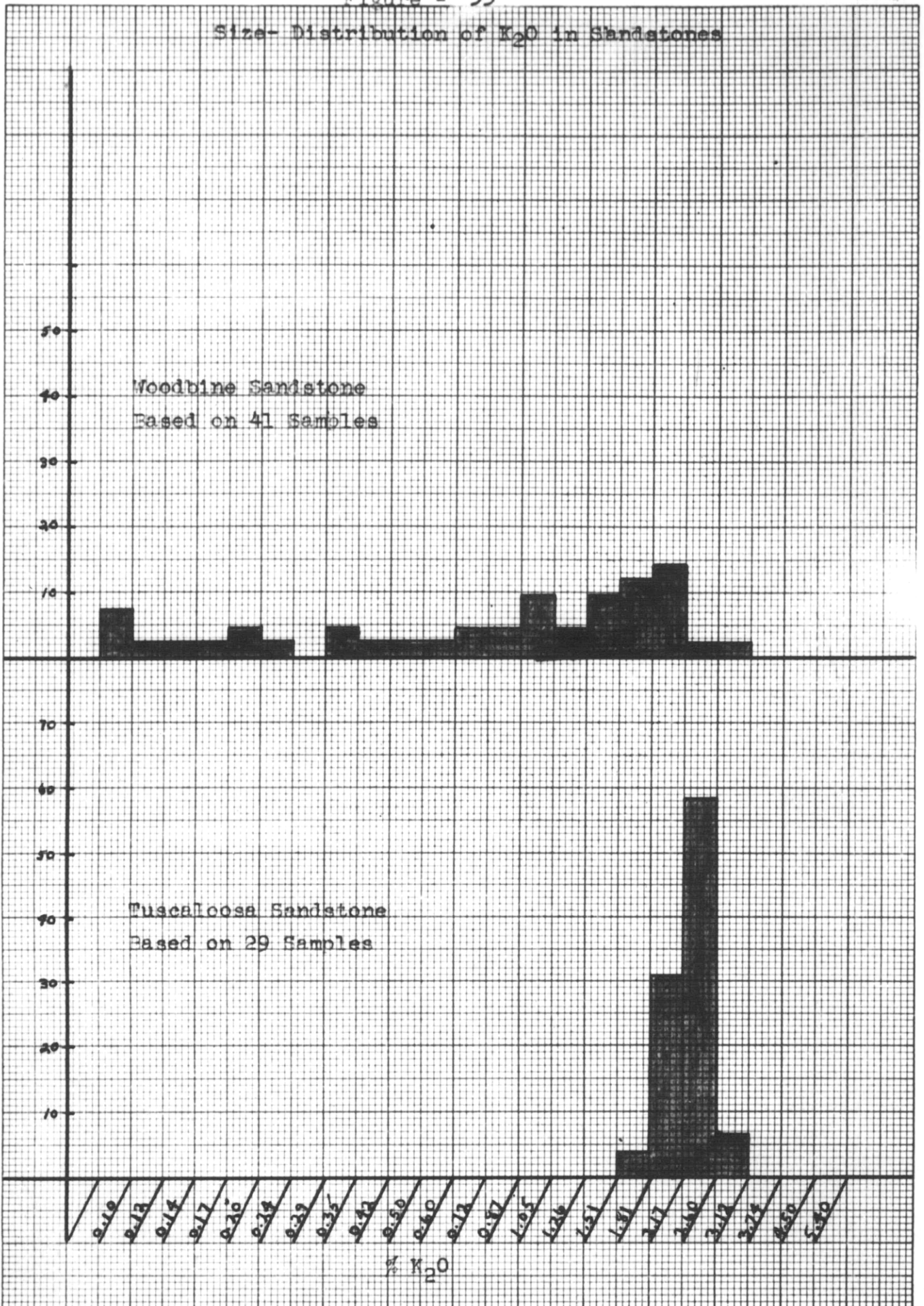
U.S. GEOLOGICAL SURVEY, WASHINGTON, D.C.

TECHNOLOGICAL STORE, R. O. 2.

FORM 1 H

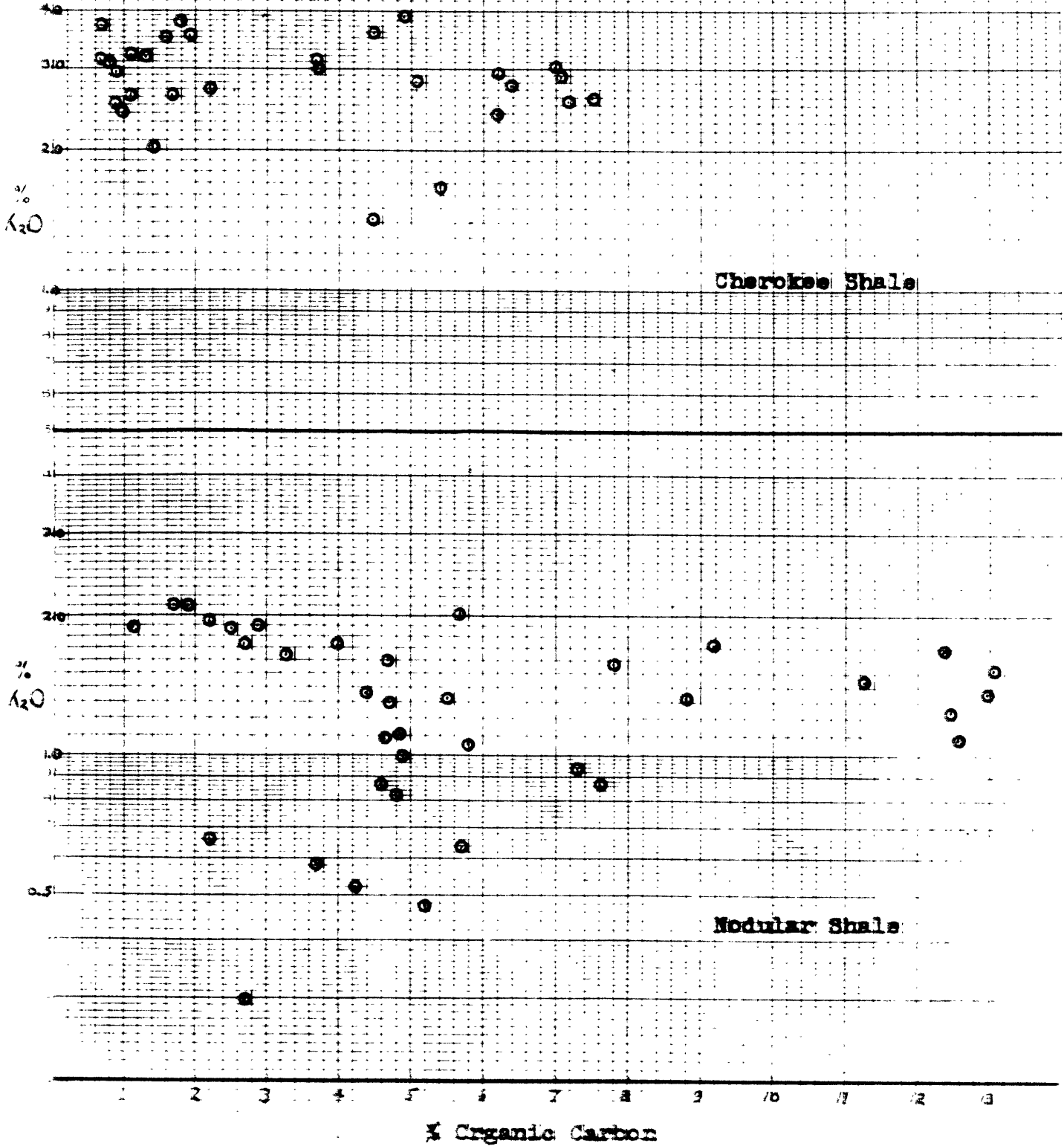
Figure - 35

Size- Distribution of K<sub>2</sub>O in Sandstones





Relationship between potassium and organic carbon  
in shales



All Mississippi Cretaceous formations have considerably higher rubidium contents than the corresponding Cretaceous formations from East Texas. However, the sample with the greatest concentration of rubidium (No. 45354 - 0.075%  $Rb_2O$ ) came from the Eagle Ford Shale. Also there is a considerable difference between the rubidium content of the Cherokee Shale from Oklahoma and the Miocene Modular Shale from California. The Woodford Shale, which carries a remarkably high content of thallium, is seen to have a quite average content of rubidium.

The only published analyses on the average content of rubidium in sediments are those by Goldschmidt, Bauer and Witte ( 9 ). They analyzed several composite samples of argillaceous sediments with the following results:

Material	Per Cent $Rb_2O$
European Paleozoic Shales	0.049
Japanese Paleozoic Shales	0.027
Japanese Mesozoic Shales	0.024
Red Deep-Sea Clay, Challenger 253	0.048
Red Deep-Sea Clay, Challenger 353	0.037

Their values compare very favorably with the results obtained by the writer.

Histograms showing the size-distribution of rubidium in the various formations are presented in Figs. 37 to 42 .

Table 10

## Rubidium content of sediments

Formation	Number of samples included in average and percentage of total	Average content Rb <sub>2</sub> O (%)
Miocene Nodular Shale	42 (97%)	0.019
Cherokee Shale	39 (100%)	0.042
Woodford Shale	12 (92%)	0.035
Lower Eutaw Shale	24 (100%)	0.034
Eagle Ford Shale	25 (89%)	0.031
Woodbine Sandstone	22 (54%)	0.026
Tuscaloosa Sandstone	29 (100%)	0.037
Frio Sandstone	12 (100%)	0.029
Selma Chalk	33 (100%)	0.035
Austin Chalk	46 (90%)	0.024
All Shales	149 (94%)	0.032
All Sandstones	63 (77%)	0.031
All Limestones	79 (94%)	0.028
All Samples	291 (93%)	0.031

### Size-Distribution of Rb<sub>2</sub>O Content in Argillaceous Sediments

Based on 291 Samples

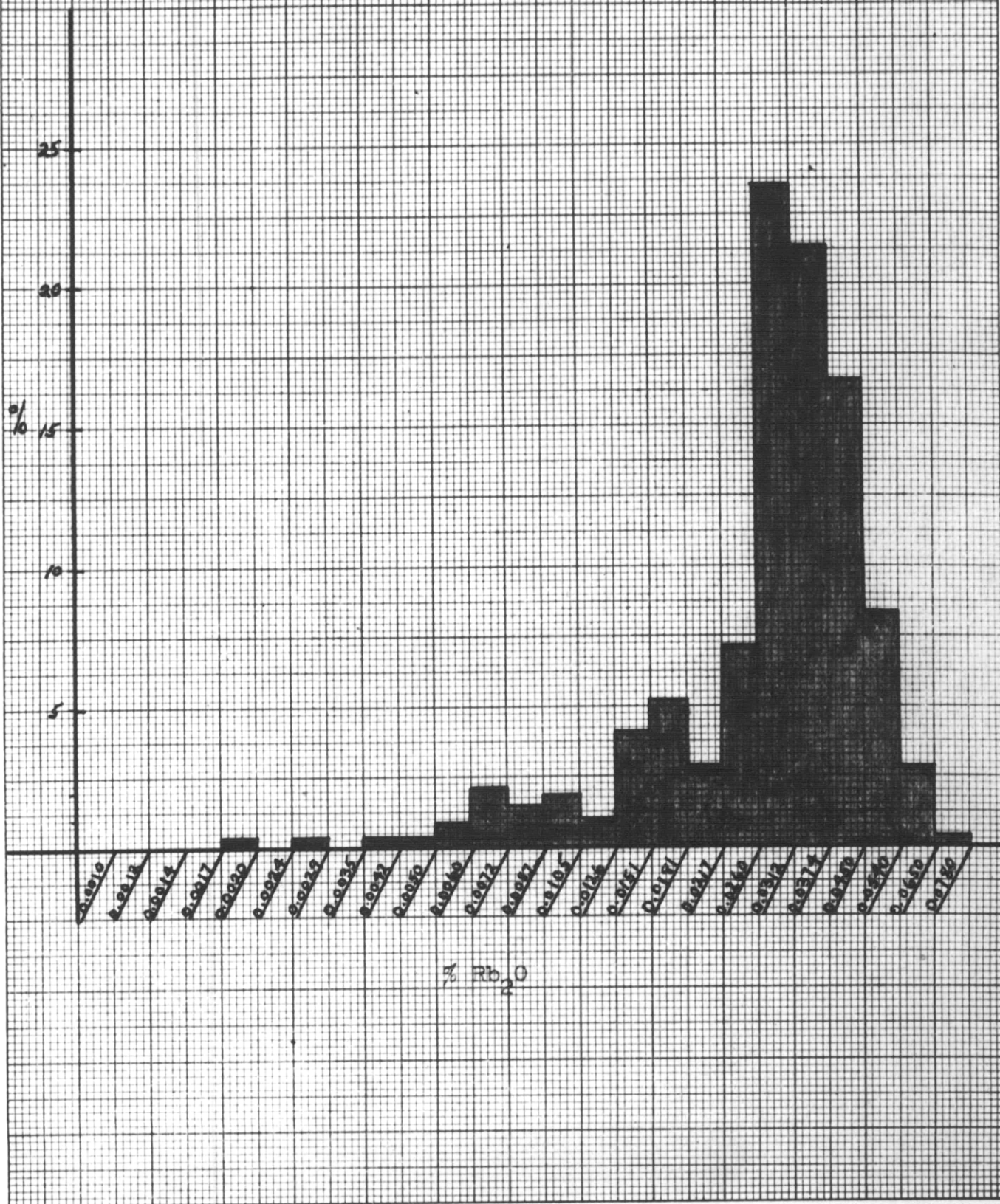
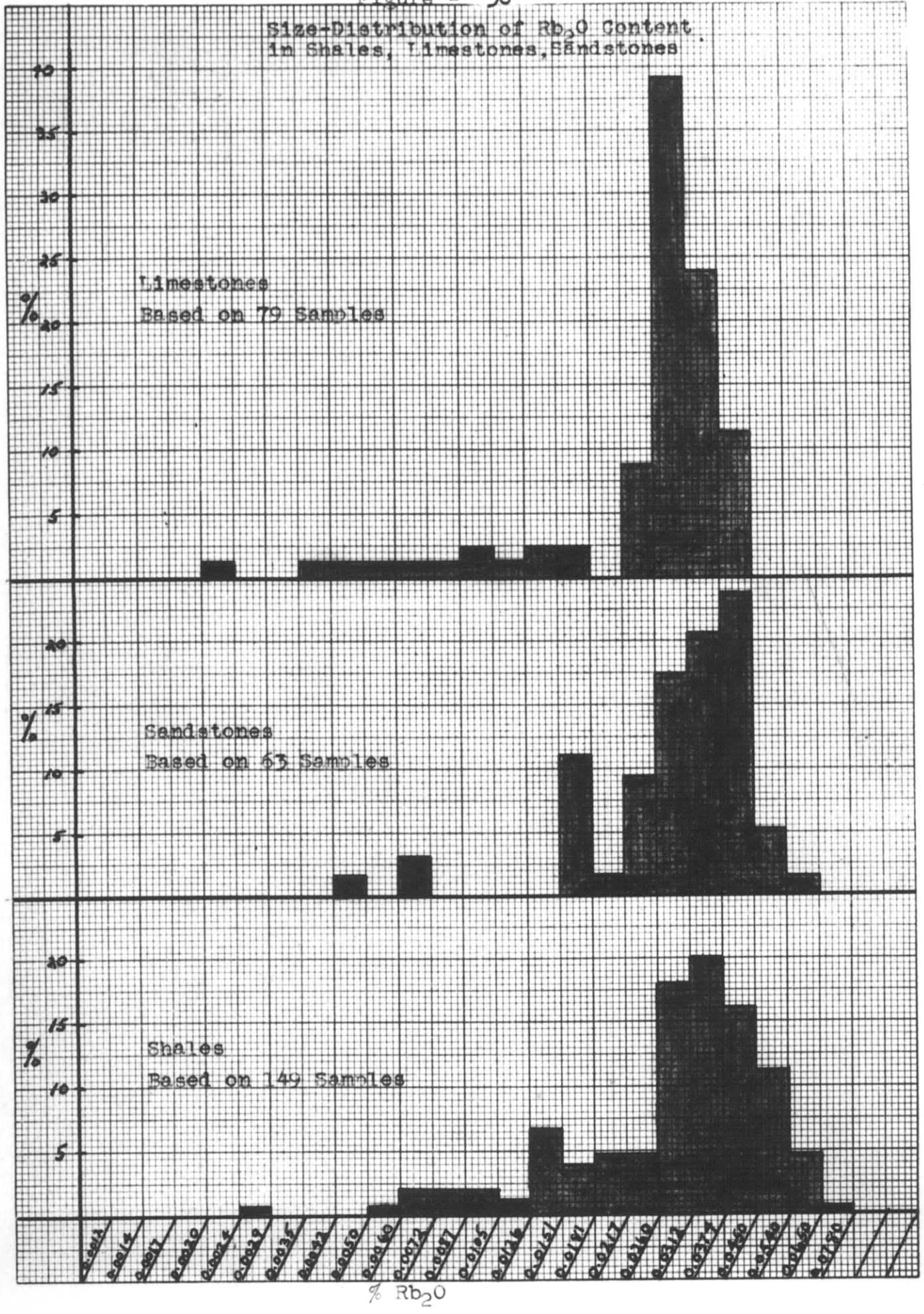


Figure - 38

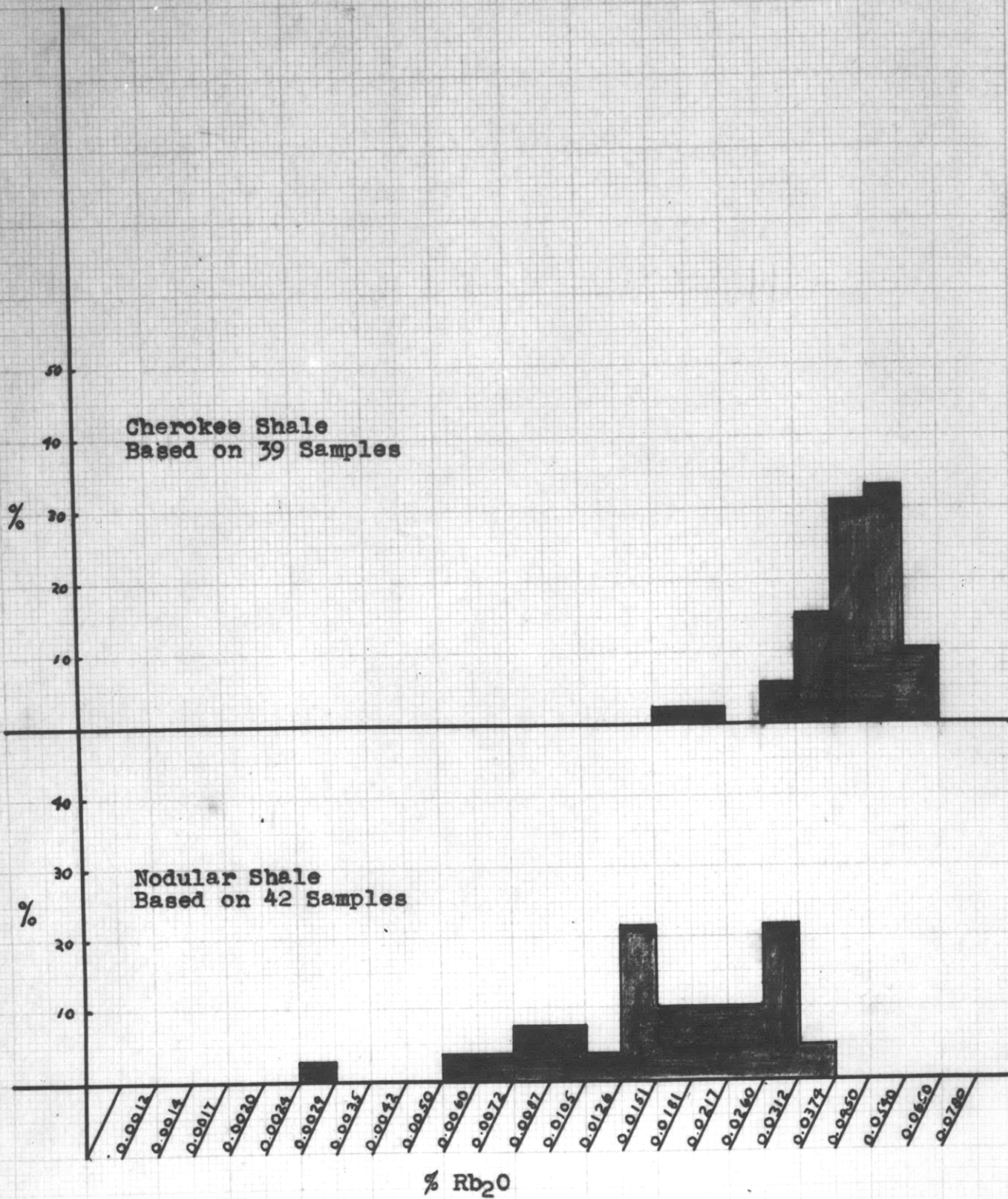
Size-Distribution of Rb<sub>2</sub>O Content in Shales, Limestones, Sandstones



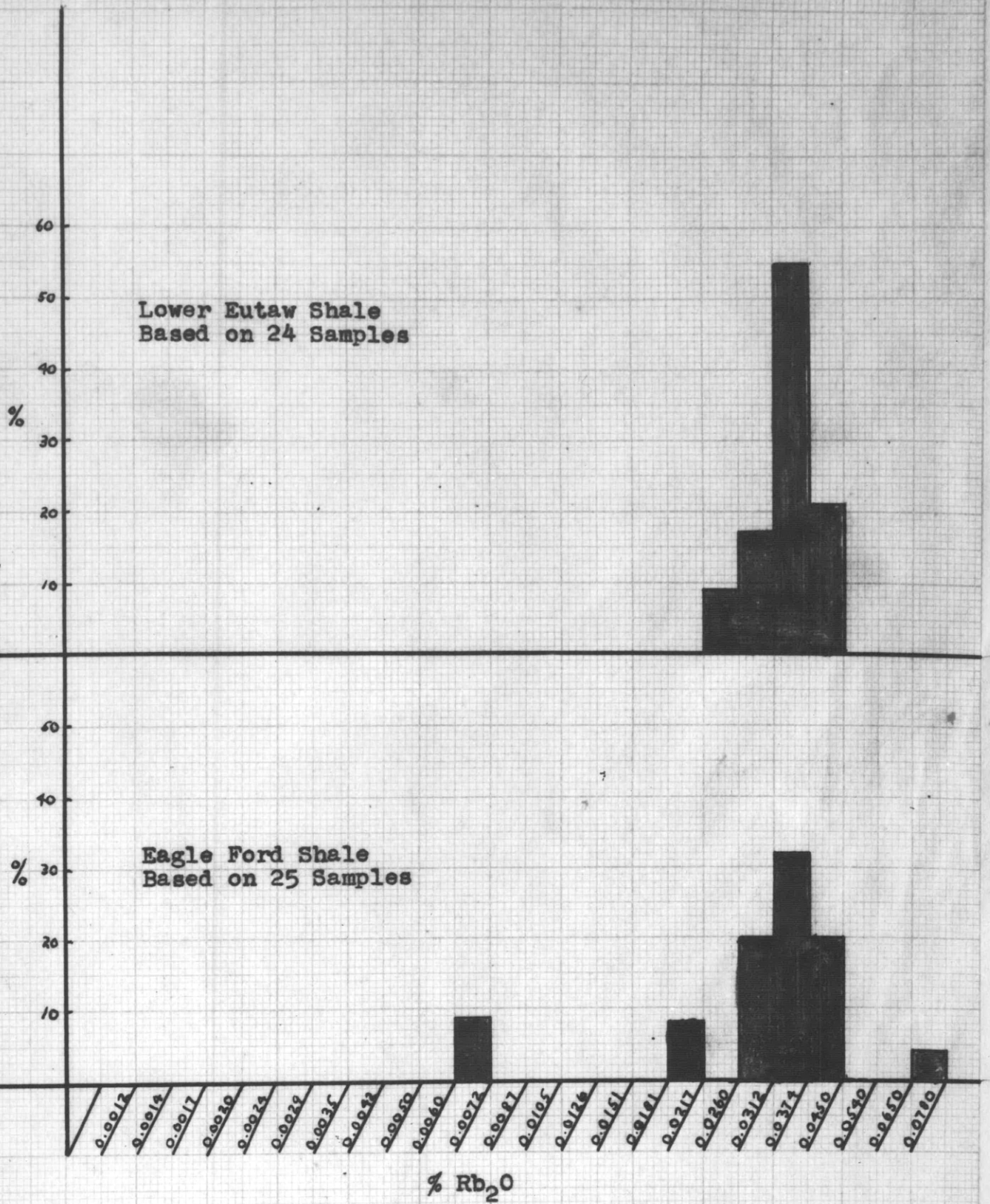
TECHNOLOGY STORE, H. C. S.

FORM I H

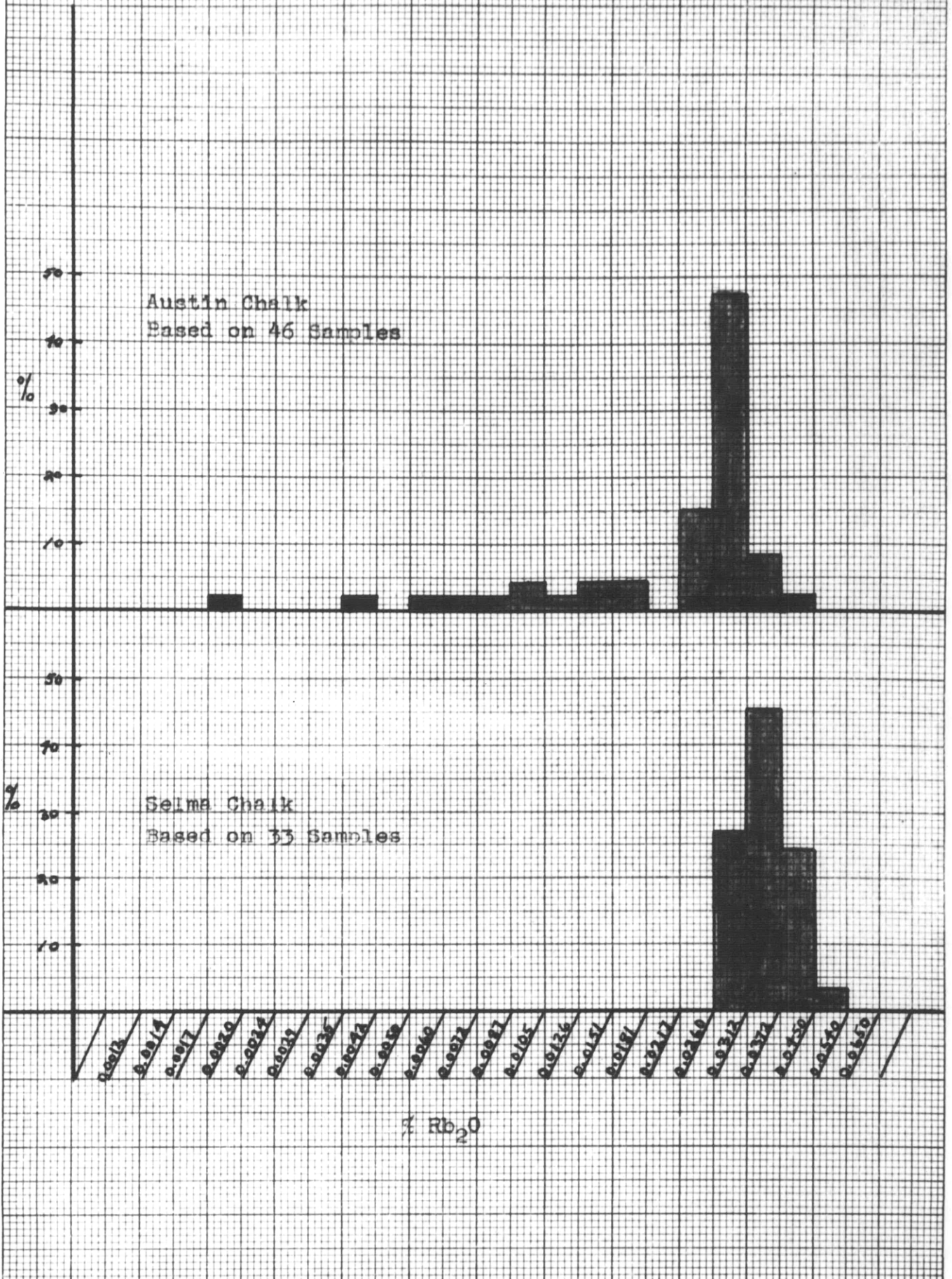
Size Distribution of Rb<sub>2</sub>O Content in Shales



### Size Distribution of Rb<sub>2</sub>O Content in Shales

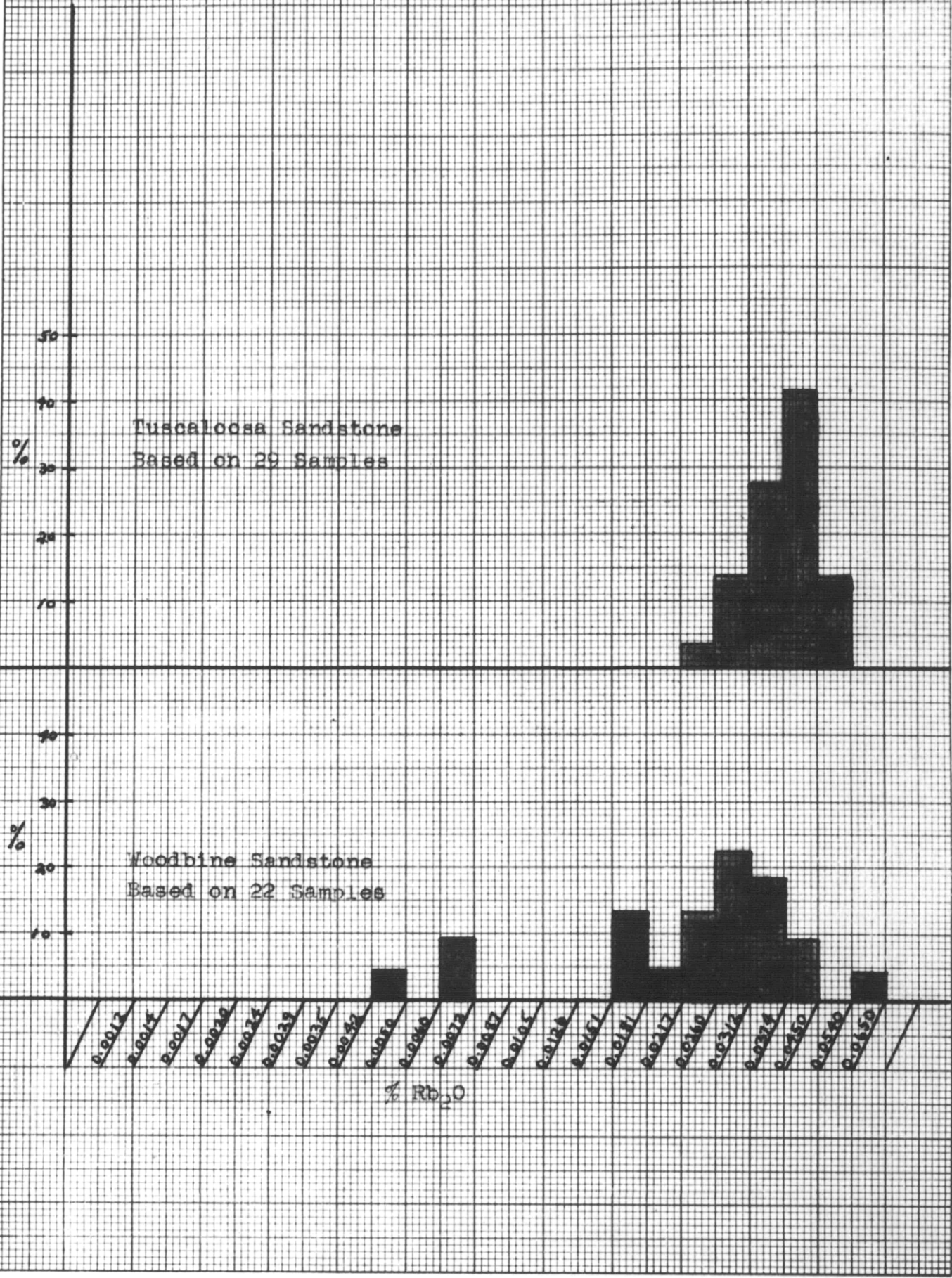


Size Distribution of  $Rb_2O$  Content in Limestones





Size-Distribution of Rb<sub>2</sub>O in Sandstones



40 MASS. AVE., CAMBRIDGE, MASS.

Relationship between rubidium and organic carbon  
in the Miocene Nodular Shale

EUGENE DIETZGEN CO.  
PRINTED IN U.S.A.

LOGARITHMIC 3 CYCLES X 10 DIVISIONS

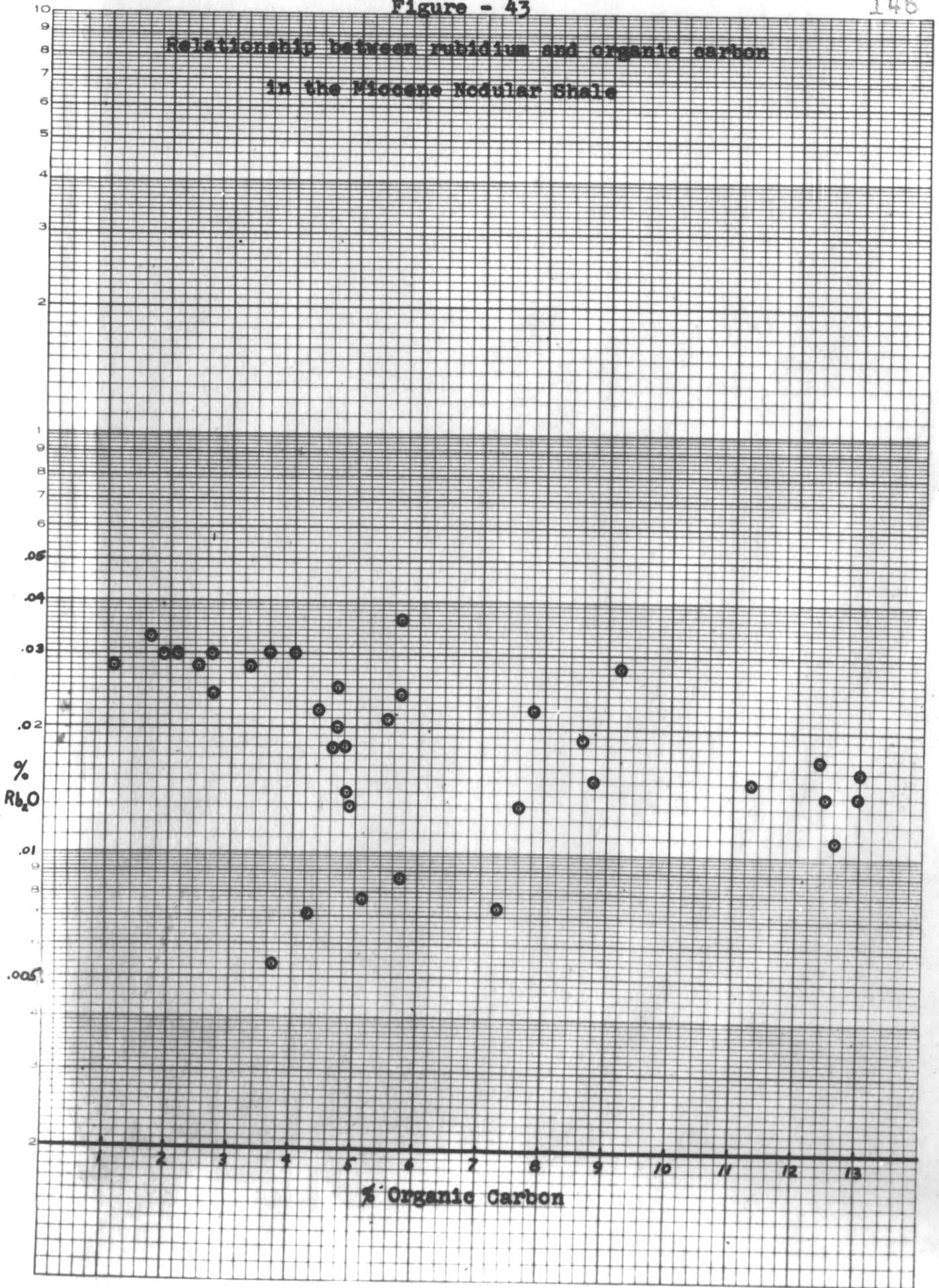


Figure 43 presents the relationship between organic carbon content and rubidium content in the Miocene nodular shale. No clean-cut correlation is visible but the possibility of a slight inverse relationship is present. The correlation is so weak, however, that it does not warrant further discussion.

D. The abundance of cesium

Table 11 summarizes the average cesium content of all the formations analyzed. These averages present the same type of picture as the rubidium values.

The only published information on the cesium content of sediments is again furnished by Goldschmidt and his co-workers. The following tabulation lists some of their results. They reported an accuracy of  $\pm 30\%$  for the cesium determinations.

Material	Per cent Cs20
European Paleozoic Shales	0.0025
Japanese Paleozoic Shales	0.0007
Japanese Mesozoic Shales	0.0008
Red Deep-Sea Clay, Challenger 253	0.0020
Red Deep-Sea Clay, Challenger 353	0.0007

In general their values seem to be in line with the average cesium content of American sediments with the exception of the sample of European shales which has a considerably higher cesium content.

Table II

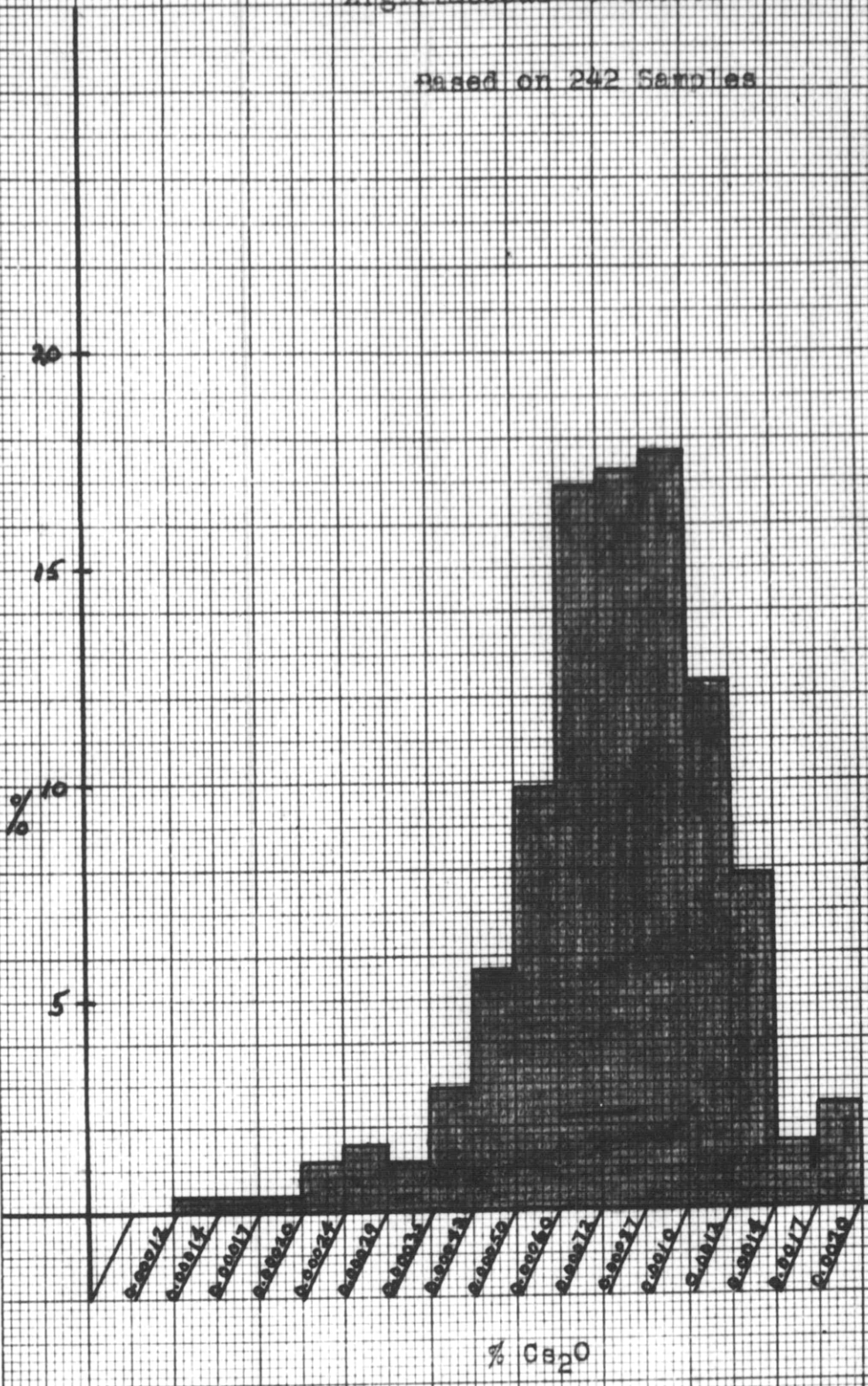
Calcium content of sediments

Formation	Number of samples included in average and percentage of total	Average content Ca <sub>2</sub> O (%)
Miocene nodular shale	31 (72%)	0.00055
Cherokee shale	39 (100%)	0.0010
Woodford shale	11 (85%)	0.0010
Lower Eutaw shale	24 (100%)	0.00086
Eagle Ford shale	19 (68%)	0.00073
Frio sandstone	3 (25%)	0.00064
Woodbine sandstone	10 (24%)	0.00069
Tuscaloosa sandstone	27 (93%)	0.00073
Austin chalk	40 (78%)	0.00066
Belma chalk	33 (100%)	0.0011
All shales	129 (82%)	0.00083
All sandstones	40 (49%)	0.00071
All limestones	73 (87%)	0.00083
All samples	242 (75%)	0.00081

Figure - 44

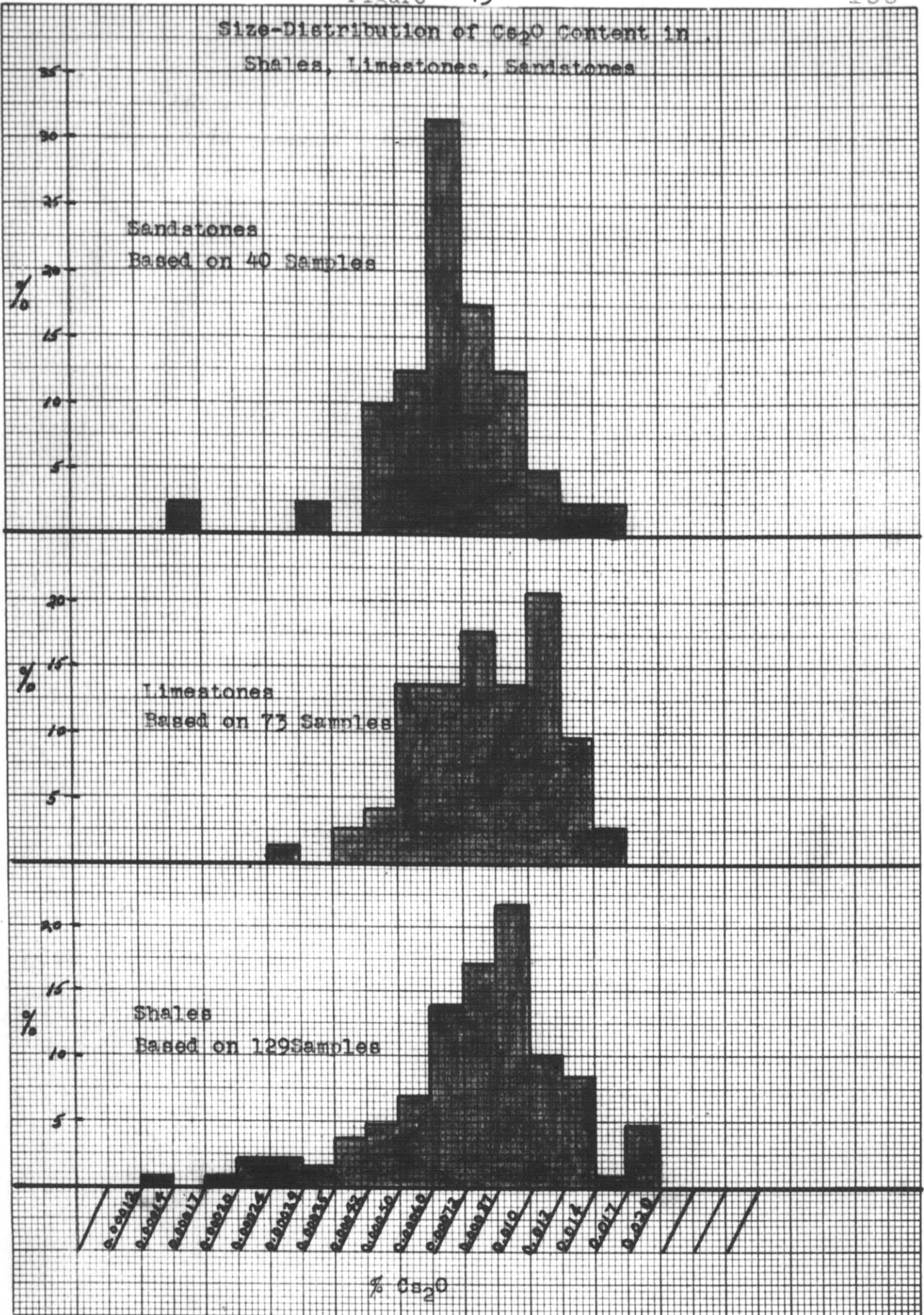
### Size-Distribution of Ca<sub>2</sub>O Content in Argillaceous Sediments

Based on 242 Samples



TECHNOLOGICAL SURVEY, 1955  
FORM 1-F

Size-Distribution of  $Ca_2O$  Content in  
Shales, Limestones, Sandstones



Size-Distribution of CaO Content in Shales

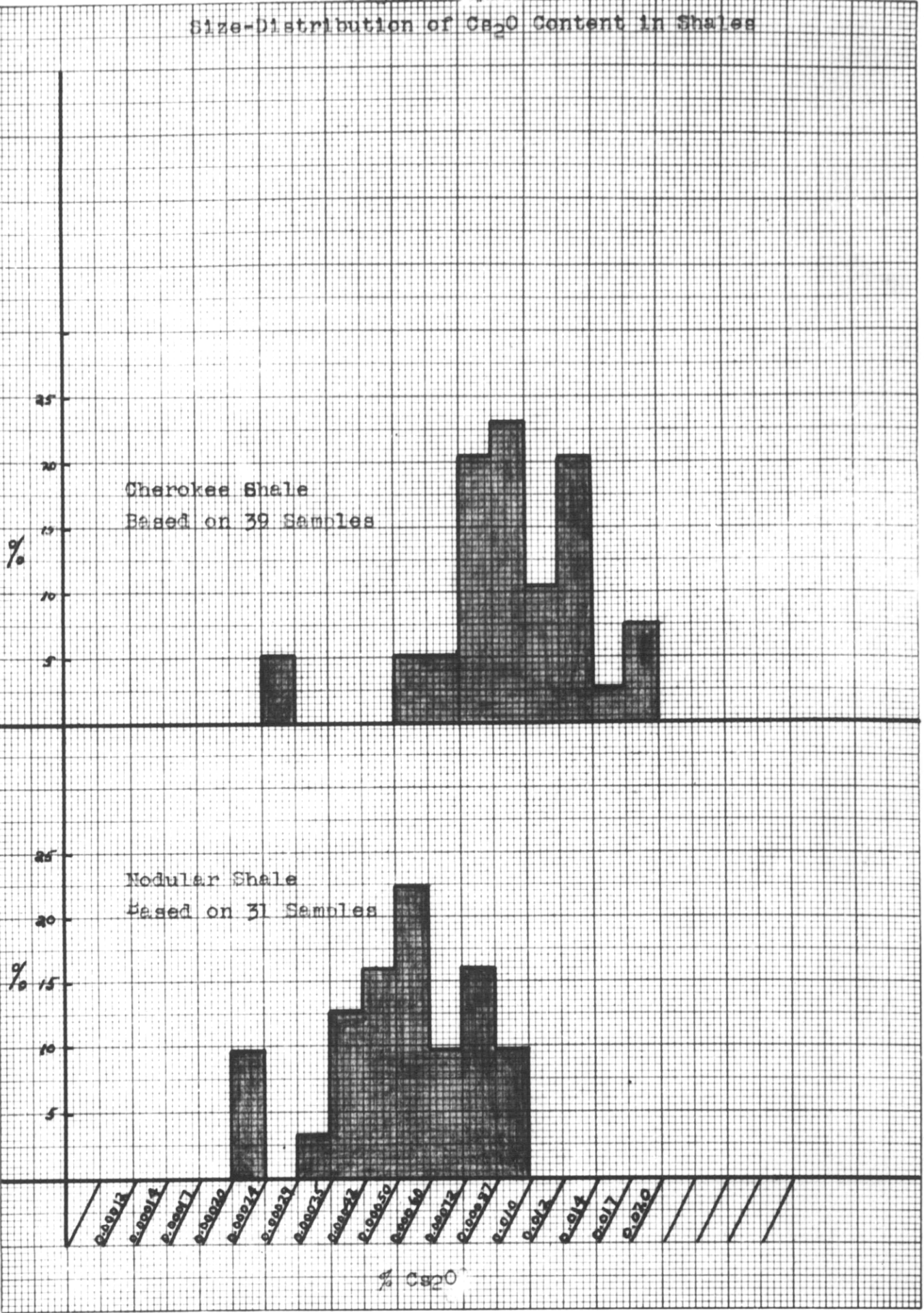
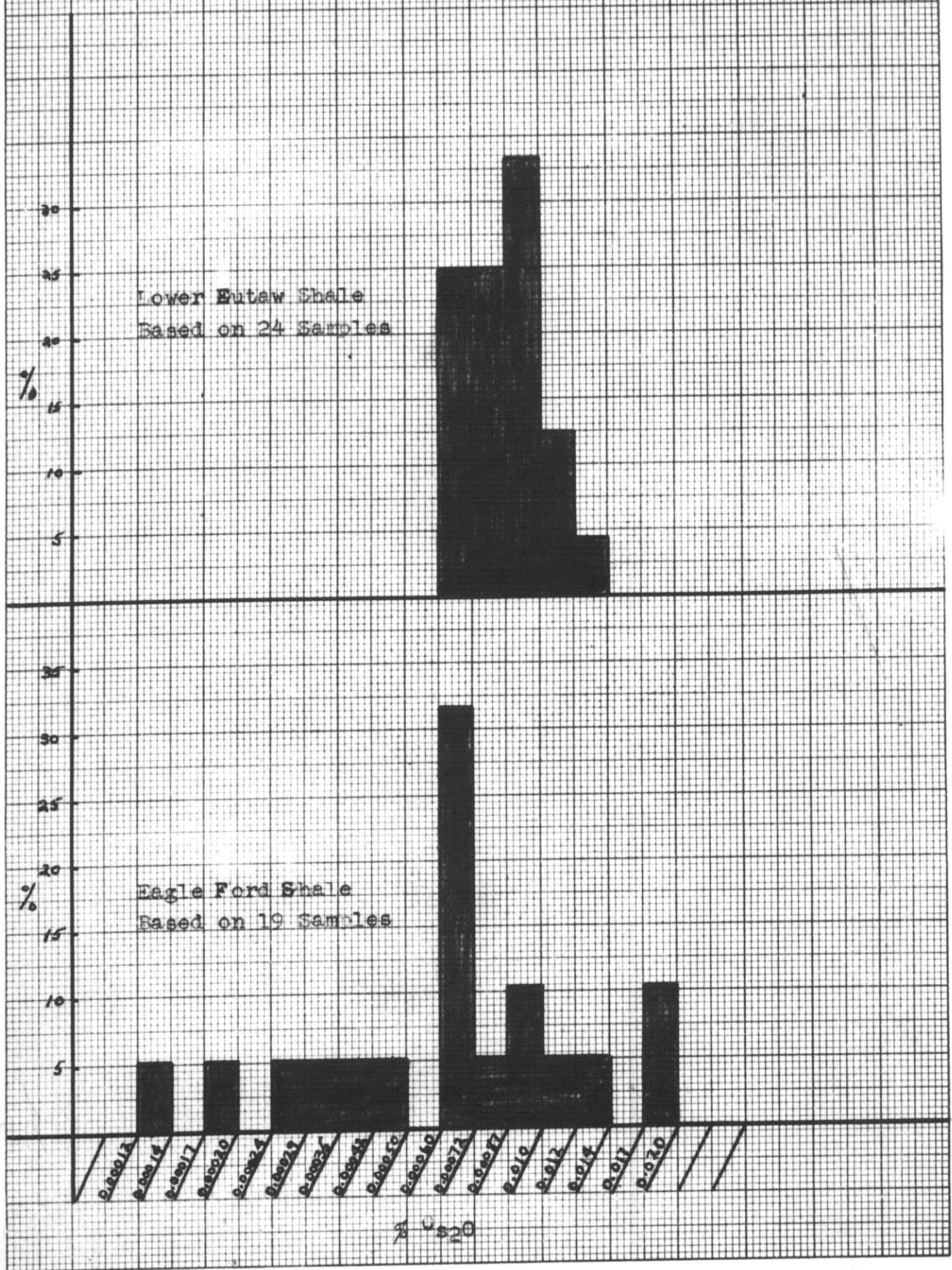


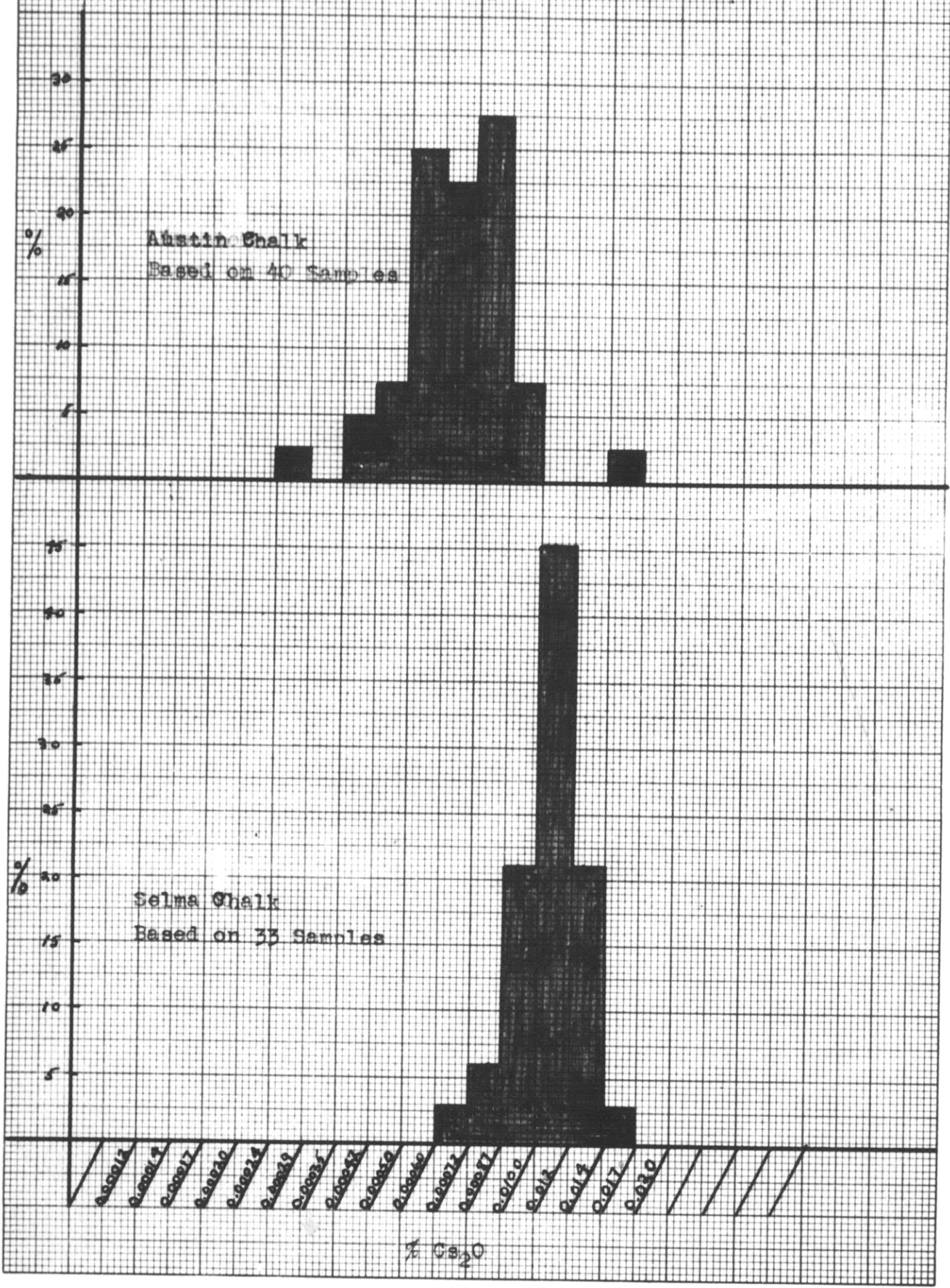
Figure - 47

Size-Distribution of Ca<sub>2</sub>O Content in Shales





Size-Distribution of  $Ca_2O$  in Limestones



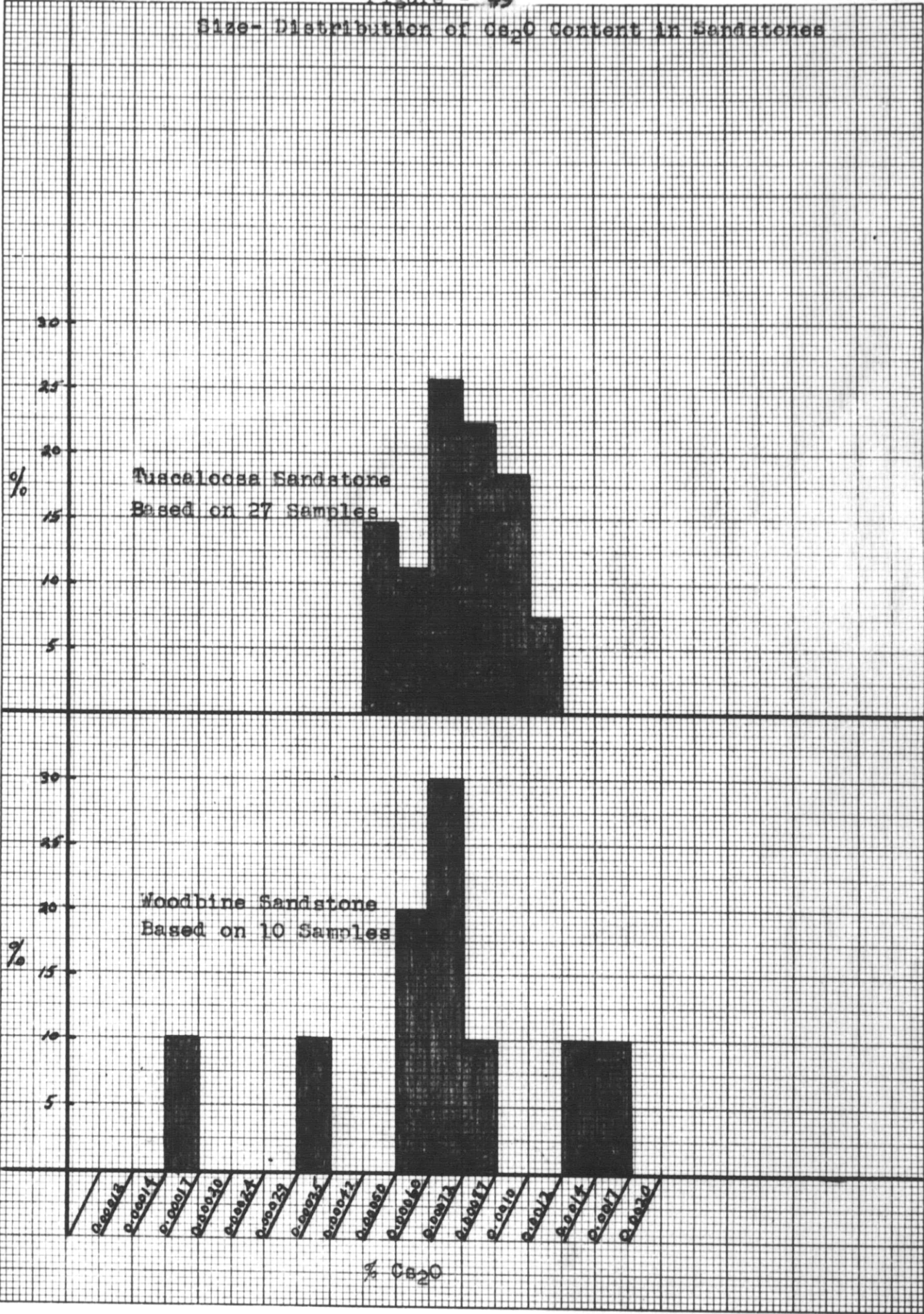
U.S. GEOLOGICAL SURVEY, WASHINGTON, D.C.

A-50012  
 A-50014  
 A-50017  
 A-50020  
 A-50024  
 A-50029  
 A-50037  
 A-50047  
 A-50050  
 A-50052  
 A-50053  
 A-50057  
 A-50060  
 A-50072  
 A-50077  
 A-50100  
 A-5013  
 A-5015  
 A-5017  
 A-5020

%  $Ca_2O$

Figure - 49

Size-Distribution of Ca<sub>2</sub>O Content in Sandstones

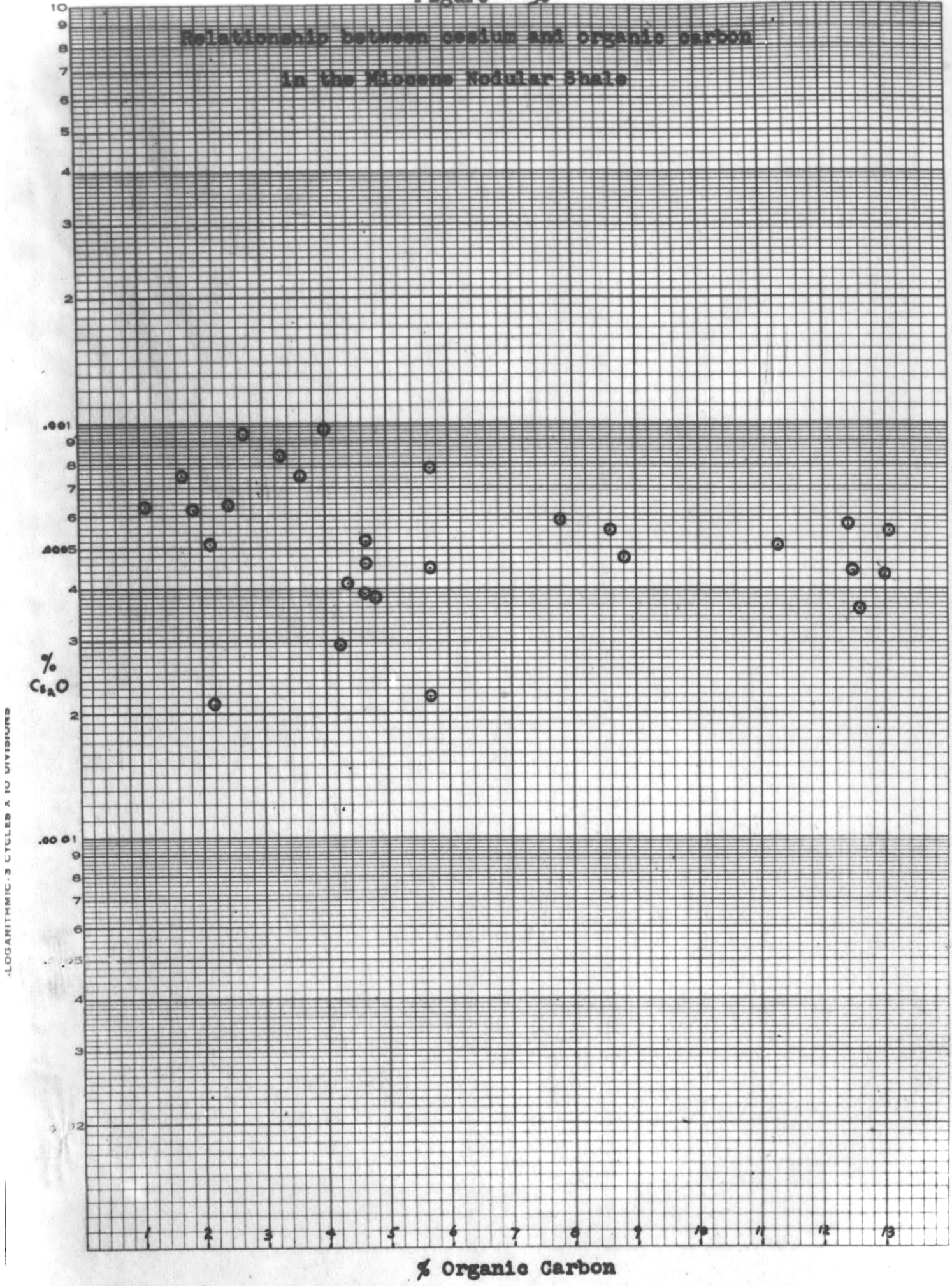


40 MASS. AVE., CAMBRIDGE, MASS.

TECHNOLOGY STORE, H. C. S.

FORM I H

Relationship between cesium and organic carbon  
in the Miocene Nodular Shale



LOGARITHMIC - 3 CYCLES X 10 DIVISIONS

Figures 44 to 49 present the size-distribution of cesium in the various formations and rock types.

The relationship between cesium content and organic matter is shown in Fig. 50. As was the case with rubidium, there is a possible slight inverse correlation.

#### E. The abundance of thallium

Table 12 tabulates data on the average thallium content of sediments. It presents about the same picture as did the rubidium and cesium contents with one striking exception. That is the extremely high thallium content of the Woodford Shale samples. The thallium content of the samples of the miscellaneous group, mostly consisting of black shales, was also considerably above the average. The sample with the highest thallium content was from the Woodford formation (No. 46667 - 0.0019%  $Tl_2O$ ). The writer believes that there is a plausible explanation for the high concentration of thallium in the Woodford Shale and other black shales. This will be discussed when the relationship between the Rb-Tl abundance ratio and organic carbon content is considered.

Preuss (17) determined the thallium content of two composite samples of German shales and sandstones. His results, which are tabulated below, are considerably higher than similar averages for American sediments.

Material	Per Cent Tl
Composite sample of 36 German shales	0.0002
Composite sample of 23 German (New Red) sandstones	0.0002

Figs. 51 to 55 present the size-distribution of thallium in the various formations.

Table 12

## Thallium content of sediments

Formation	Number of samples included in average and percentage of total	Average content Tl <sub>2</sub> O (%)
Miocene Nodular Shale	25 (58%)	0.000029
Cherokee Shale	39 (100%)	0.000059
Woodford Shale	13 (100%)	0.00075
Lower Eutaw Shale	24 (100%)	0.000037
Eagle Ford Shale	17 (61%)	0.000035
Frio Sandstone	11 (92%)	0.000031
Woodbine Sandstone	10 (24%)	0.000025
Tuscaloosa Sandstone	27 (93%)	0.000041
Austin Chalk	32 (63%)	0.000025
Selma Chalk	33 (100%)	0.000039
All Shales	125 (79%)	0.00013
All Shales (Except Woodford & misc. groups)	105 (76%)	0.00043
All Sandstones	48 (59%)	0.000035
All Limestones	65 (77%)	0.000032
All Samples	238 (74%)	0.000083
All Samples (Except Woodford & misc. groups)	218 (72%)	0.000038

Size-Distribution of  $Tl_2O$  in  
Argillaceous Sediments

Based on 218 Samples ( Woodford Shale Samples  
not included)

25

20

%

15

10

5

2.0000/0

2.0000/2

2.0020/2

2.0040/7

2.0060/20

2.0080/25

2.0100/27

2.0120/70

2.0140/20

2.0160/20

2.0180/10

2.0200/7

2.0220/10

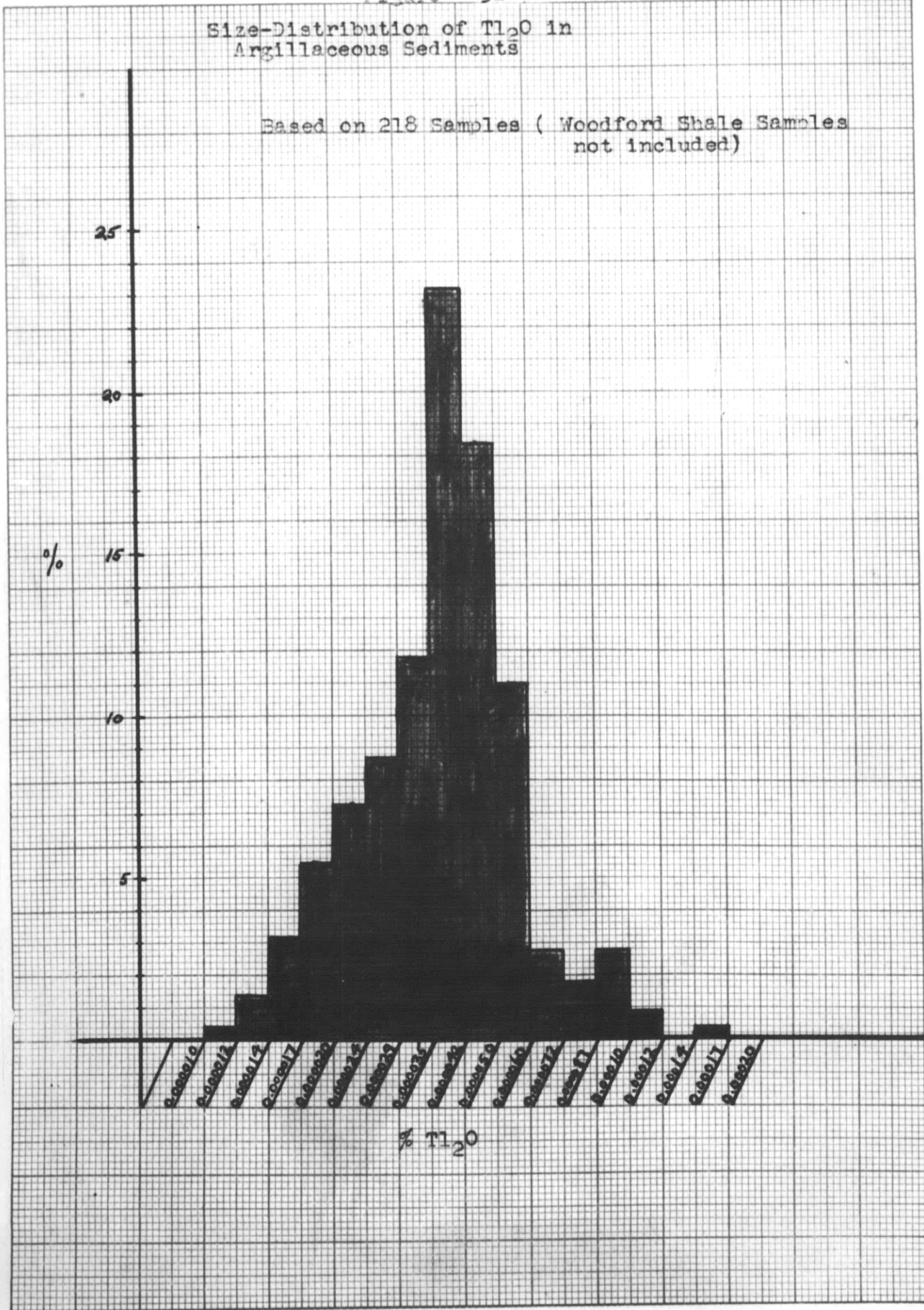
2.0240/12

2.0260/4

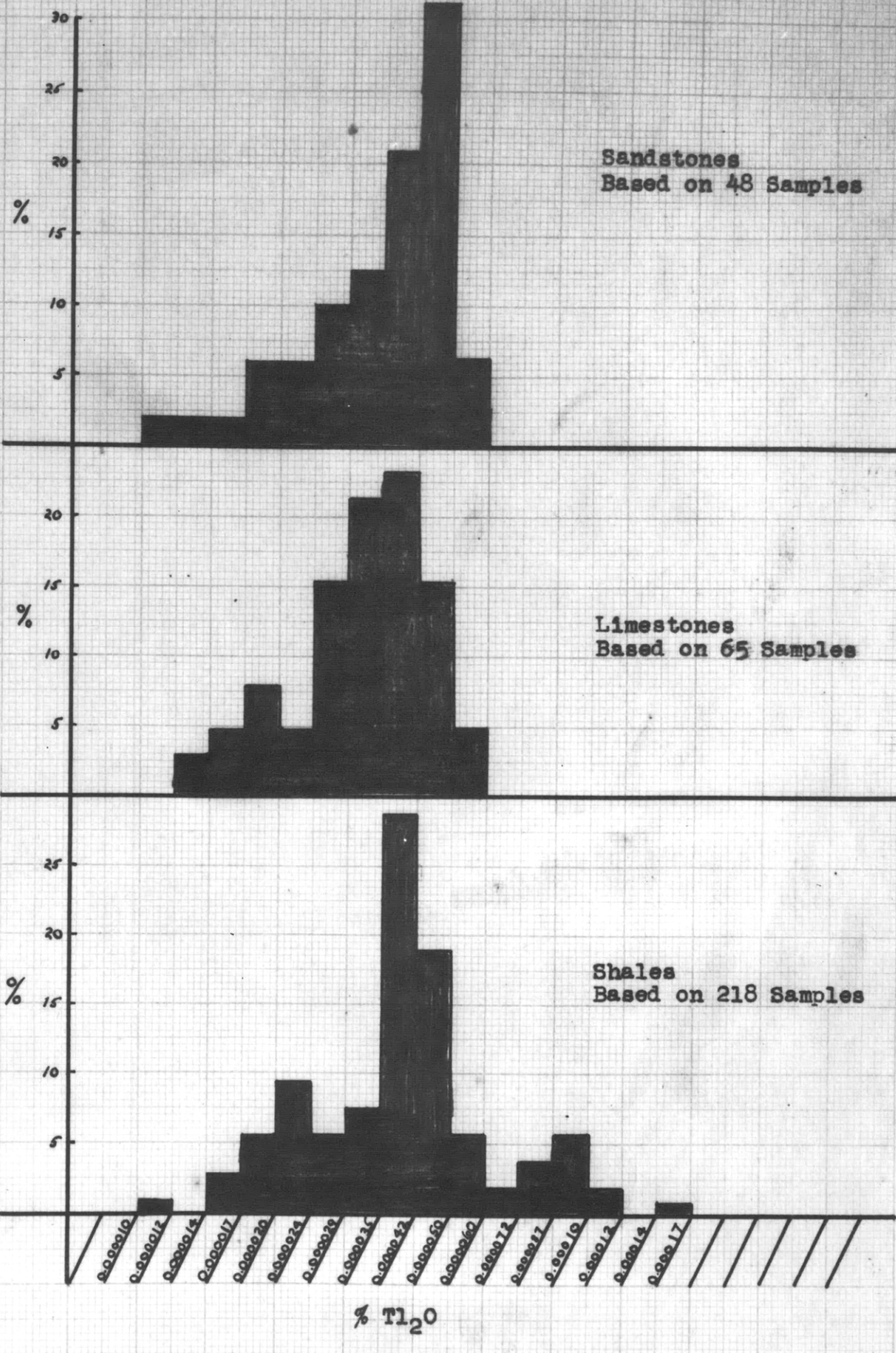
2.0280/7

2.0300/20

%  $Tl_2O$

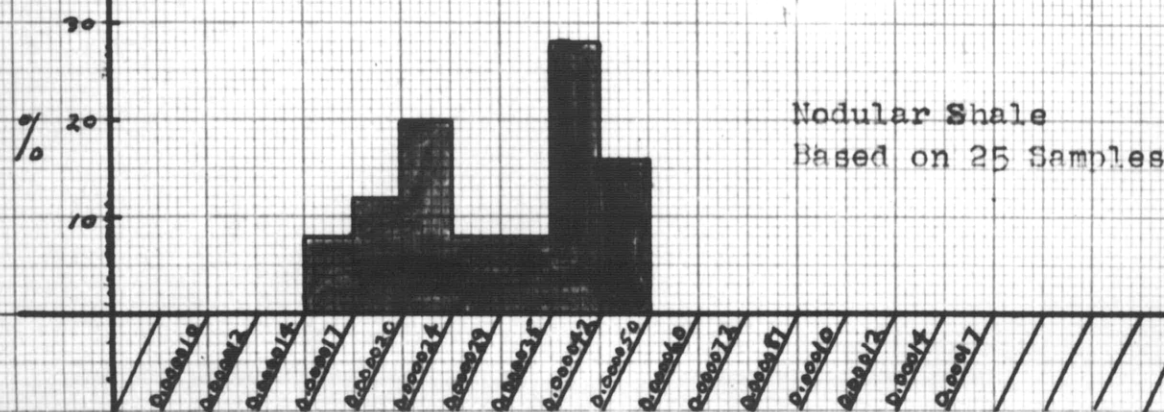
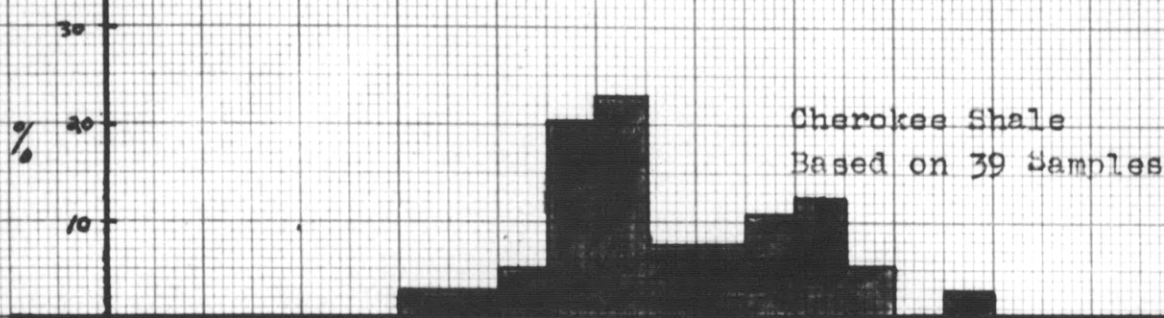
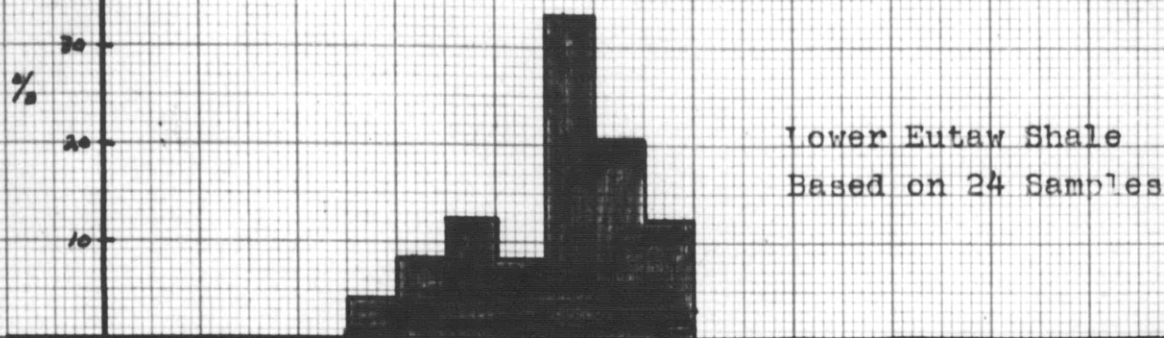
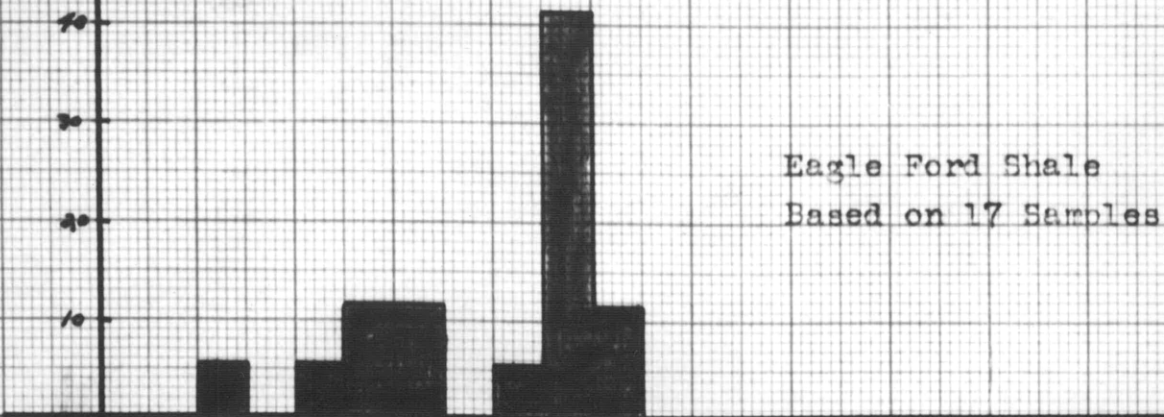


Distribution of  $Tl_2O$  in Shales, Sandstones, Limestones



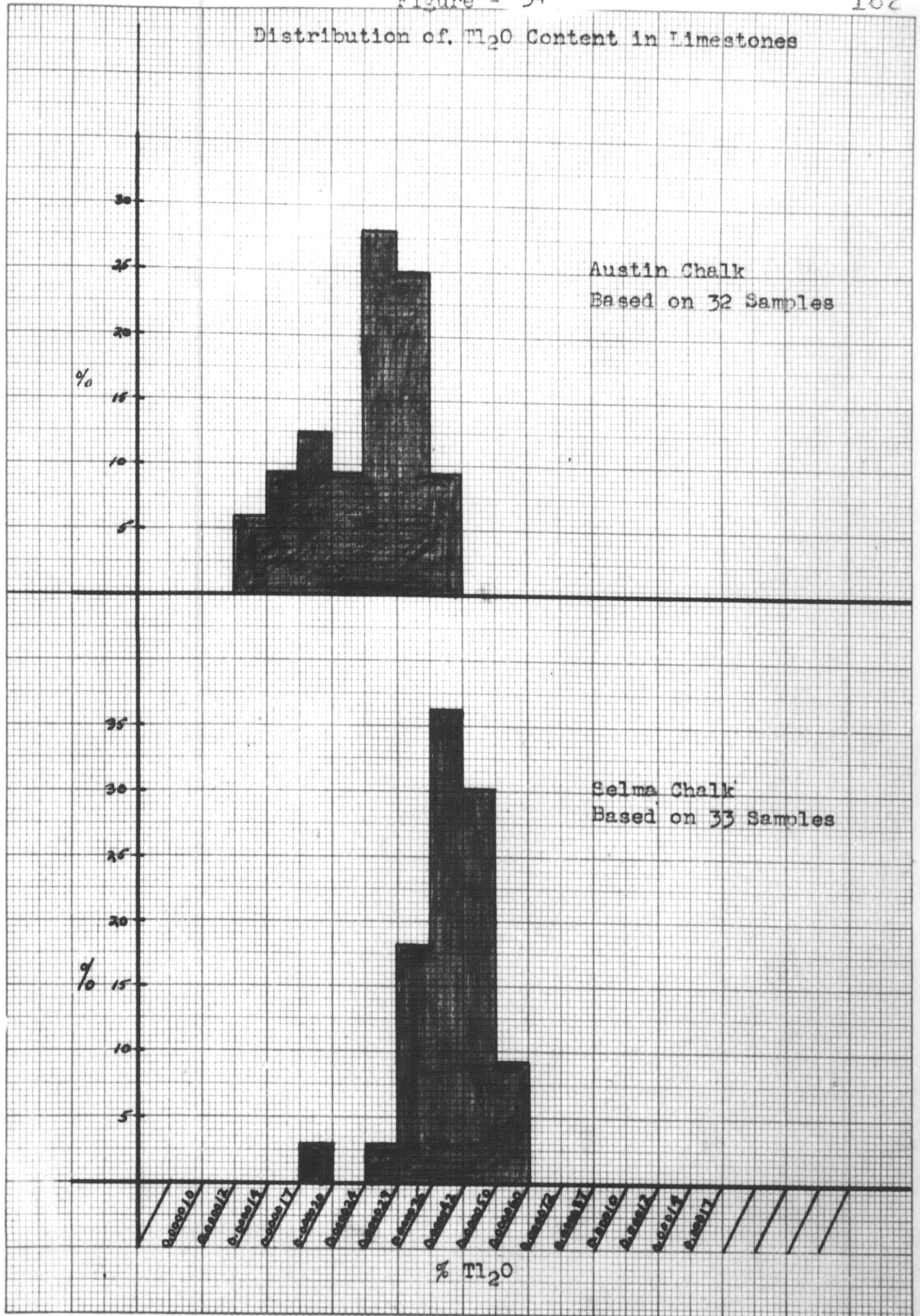


Distribution of  $TL_2O$  Content  
in Shales,

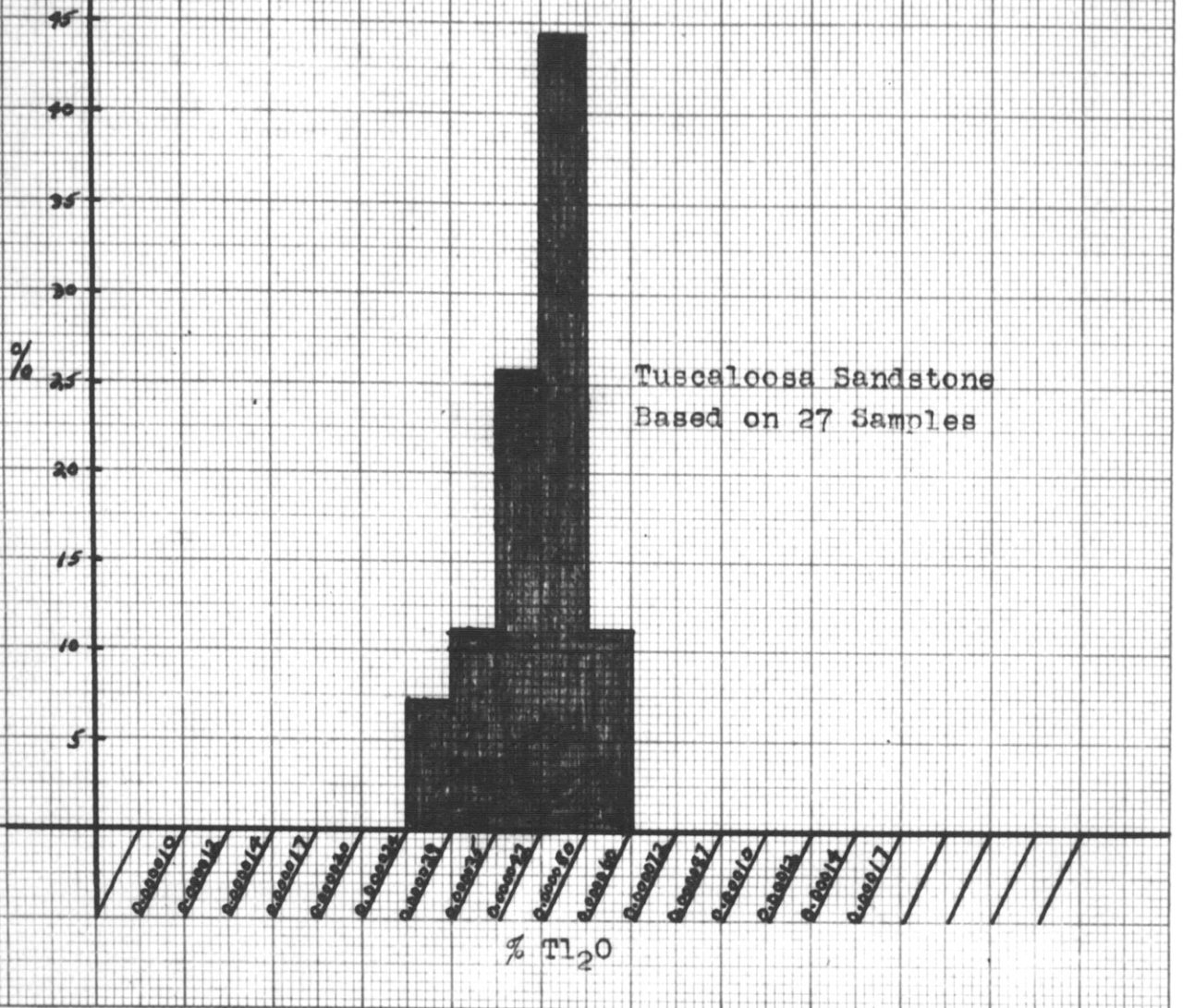
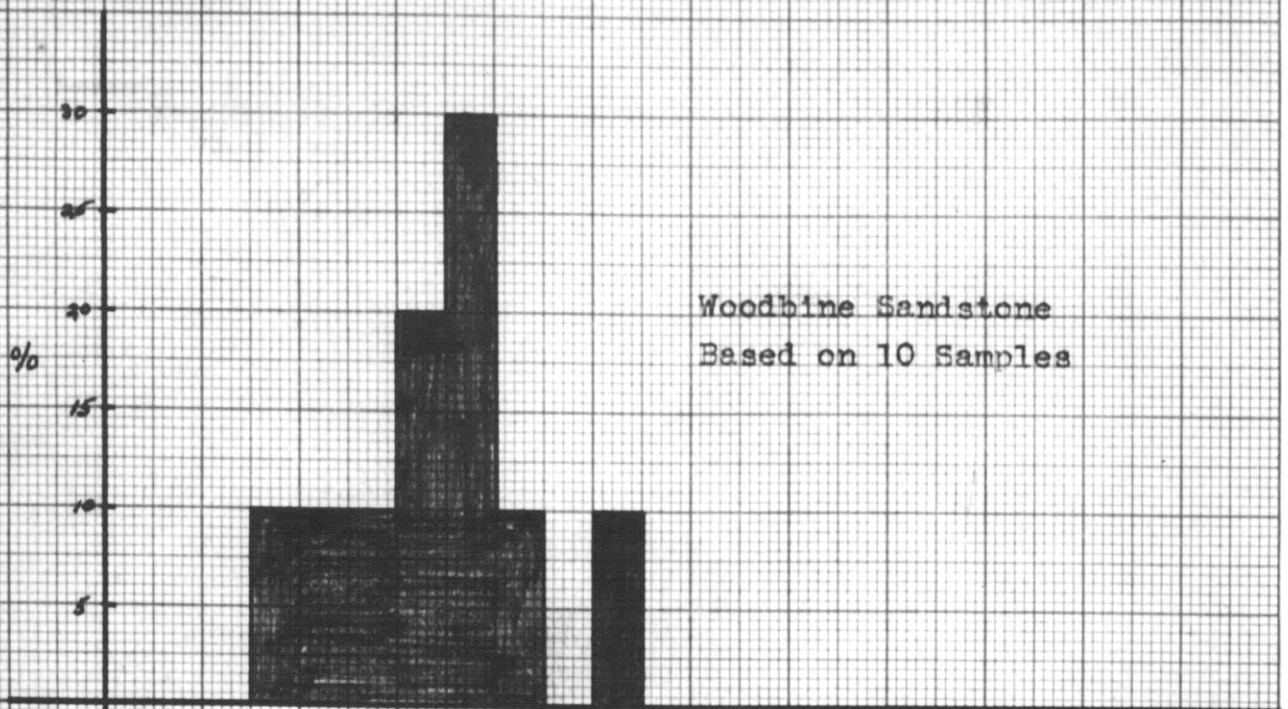


%  $TL_2O$

Distribution of  $\text{Ti}_2\text{O}$  Content in Limestones



Distribution of  $Tl_2O$  in Sandstones



%  $Tl_2O$

## IX. Discussion of the Abundance Ratios

### A. The ratios in igneous rocks

In the section where the objectives of this investigation were discussed, it was mentioned that the writer hoped to prove whether or not there had been any concentration of one element with respect to another during the sedimentary cycle. The general method of attack adopted was to compute for each sample wherever possible the values of the following four abundance ratios:  $K_2O/Rb_2O$ ,  $K_2O/Cs_2O$ ,  $K_2O/Tl_2O$ , and  $Rb_2O/Tl_2O$ . These were then compared with the average values of the corresponding ratios in igneous rocks and any change found outside of experimental error was of course significant.

These four abundance ratios in igneous rocks are known with varying degrees of accuracy. The K-Rb pair has probably been most thoroughly studied. Ahrens ( 3 ) and co-workers have determined this ratio in a large number of igneous rocks of various types and from different locations. Almost without exception the  $K_2O/Rb_2O$  ratio lies near 100, thus indicating a high degree of coherency between potassium and rubidium. This is to be expected though as their ionization potentials and ionic radii are quite similar, thereby allowing rubidium to proxy for potassium in silicate minerals.

The K-Cs pair in igneous rocks has been studied considerably less than the K-Rb pair. However, it is known to proxy

for potassium in silicate minerals to a slight extent. These two elements do not form a fully coherent pair though, owing to the fact that the cesium ion is considerably larger than the potassium ion.  $K_2O/Cs_2O$  abundance ratios have been determined in 27 specimens of granite from various localities in New England. These results are tabulated in Table 13. The locations of these granite specimens are listed in Appendix D. The  $K_2O/Cs_2O$  ratio is seen to be extremely variable, ranging from 2100 (No. 16A10) to 16000 (No. 15A2) and averaging at 8900.

The Rb/Tl pair is another highly coherent one, owing to the similarity in their ionic radii. Ahrens (1) has determined the  $Rb_2O/Tl_2O$  ratio in 167 specimens of potash-rich silicate minerals and found the mean ratio to be 100. However he did not determine the ratio in granites and other igneous rocks because their thallium content was below the limit of detection of the spectrographic method used. The sensitivity of the writer's method for thallium was such that it was possible to determine thallium in potash-rich igneous rocks such as granites. It was considered advisable, therefore, to determine the thallium contents in the suite of New England granites so that any possible systematic analytical errors would cancel out when the Rb/Tl ratios were compared. The determinations were made by the writer and the resulting  $Rb_2O/Tl_2O$  ratios are listed in Table 13. The values range from 180 (No. 15A2) to 830 (No. 15A19). However,

Table 13

The  $K_2O/CO_2$ ,  $Rb_2O/TL_2O$ , and  $K_2O/TL_2O$  abundance ratios in a suite of New England Granites

Sample No. \*  
Ratio

Sample No.	$K_2O$	$Rb_2O$	$K_2O$
	%	%	%
2A4	-	480	54000
6A8	15000	750	75000
15A2	16000	180	16000
15A19	5200	830	63000
15A35	3400	650	51000
16A10	2100	590	43000
16A12	4300	490	31000
16A13	9100	550	40000
16A16	12000	490	37000
16A22	9800	630	65000
16A28	15000	720	87000
18A18	16000	620	51000
18A25	15000	700	60000
19A5	15000	660	61000
19A8	12000	630	48000
19A13	3800	690	47000
19A22	12000	330	28000
20A11	3700	570	48000
20A26	5900	470	40000
21A1	2800	540	48000
21A7	10000	820	73000
21A11	5500	580	29000
21A16	3000	490	25000
22A11	11000	570	49000
22A4	8300	510	28000
24A20	5300	460	32000
24A24	8200	560	40000
25A12	9800	790	62000

\* Sample locations are listed in Appendix D

the majority of the values are clustered about the mean value of 580. The writer's value is considerably above the value determined by Ahrens. Further experimentation would be required to determine whether this is an actual difference or whether it is due to different degrees of systematic error in the two analytical methods employed.

The  $K_2O/Tl_2O$  abundance ratios were also computed and these are tabulated in Table 13. The mean  $K_2O/Tl_2O$  ratio is 48000.

B. The  $K_2O/Rb_2O$  ratio in sediments

The relationship between potassium and rubidium in argillaceous sediments is illustrated by means of the scatter diagram in Fig. 56. To avoid crowding only approximately one-third of the available values are plotted. A straight line of unit slope fits the points most satisfactorily. That there is a high degree of geochemical coherence between these two elements is evidenced by the scatter of points being confined to a relatively narrow path.

The average ratio was calculated to be 70. Table 14 tabulates the average ratios found in the various formations and rock types. All the ratios, with the exception of those for the Woodford and Frio formations, are seen to lie within  $\pm$  ten per cent of the general average of 70. It was mentioned earlier that the average  $K_2O/Rb_2O$  ratio in igneous rocks

Fig. 56

Relationship between potassium  
and rubidium in sediments

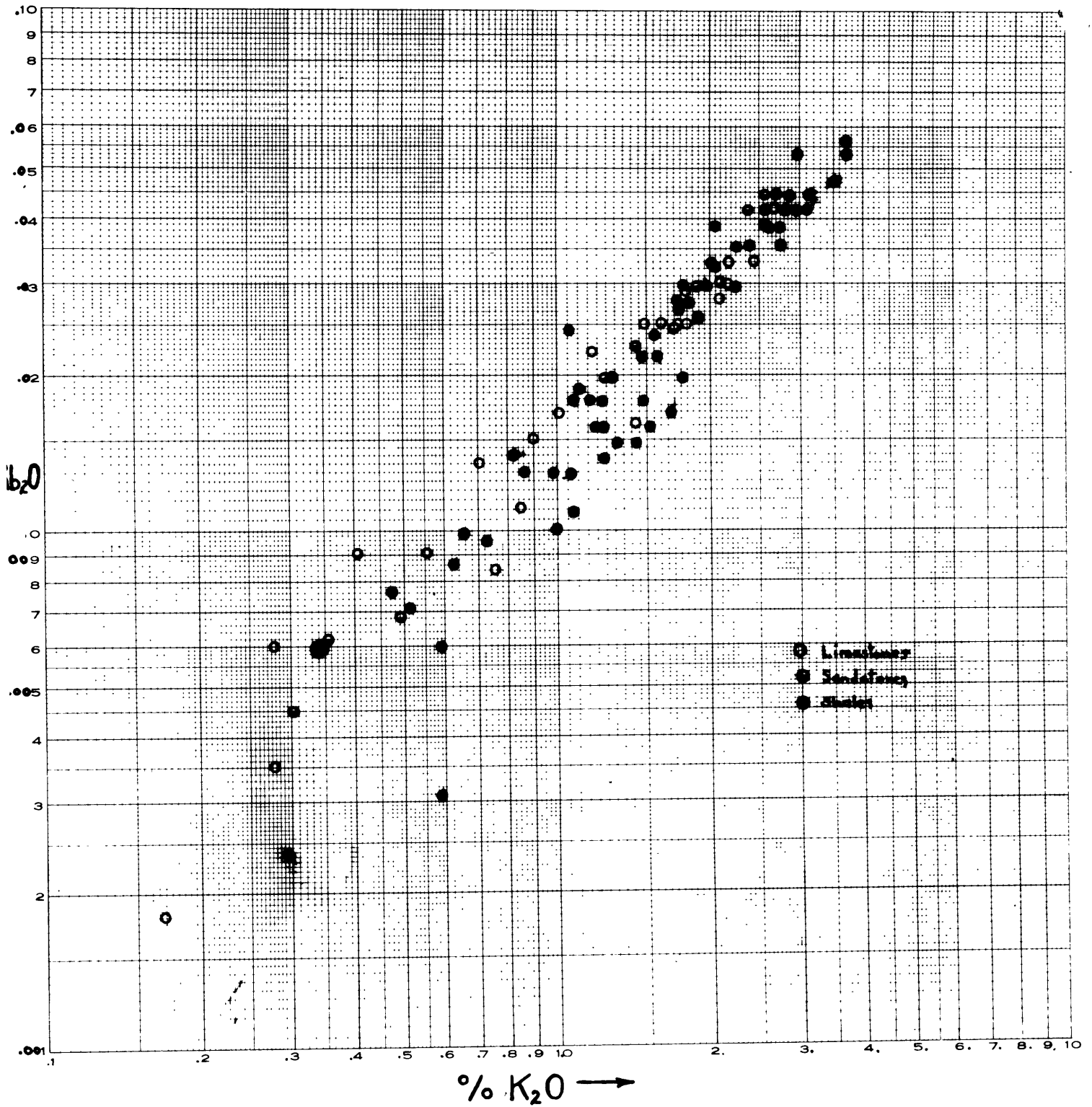


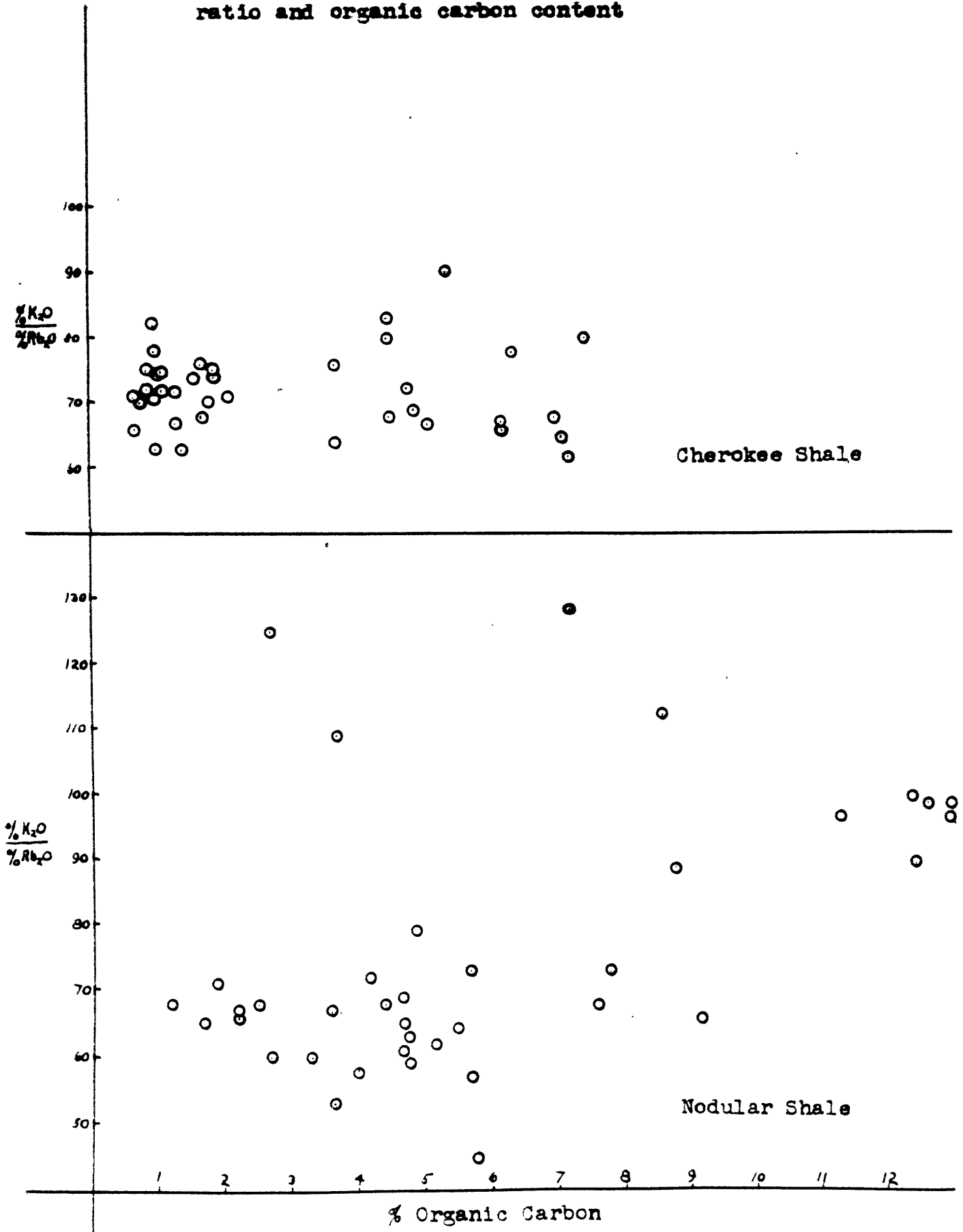


Table 14

The  $K_{20}/Rb_{20}$  abundance ratio in sediments

Formation	Number of samples included in average	Average value $\frac{K_{20}}{Rb_{20}}$
Modular shale	42 (97%)	76
Cherokee shale	39 (100%)	72
Woodford shale	12 (92%)	97
Lower Eutaw shale	24 (100%)	63
Eagle Ford shale	25 (89%)	63
Prle Sandstone	12 (100%)	86
Woodbine Sandstone	22 (54%)	63
Tuscaloosa Sandstone	29 (100%)	62
Austin Chalk	46 (90%)	67
Belm Chalk	33 (100%)	66
All Shales	149 (94%)	72
All Sandstones	63 (77%)	67
All Limestones	79 (94%)	67
All Samples	291 (93%)	70

Relationship between the  $\%K_2O/\%Rb_2O$  abundance ratio and organic carbon content



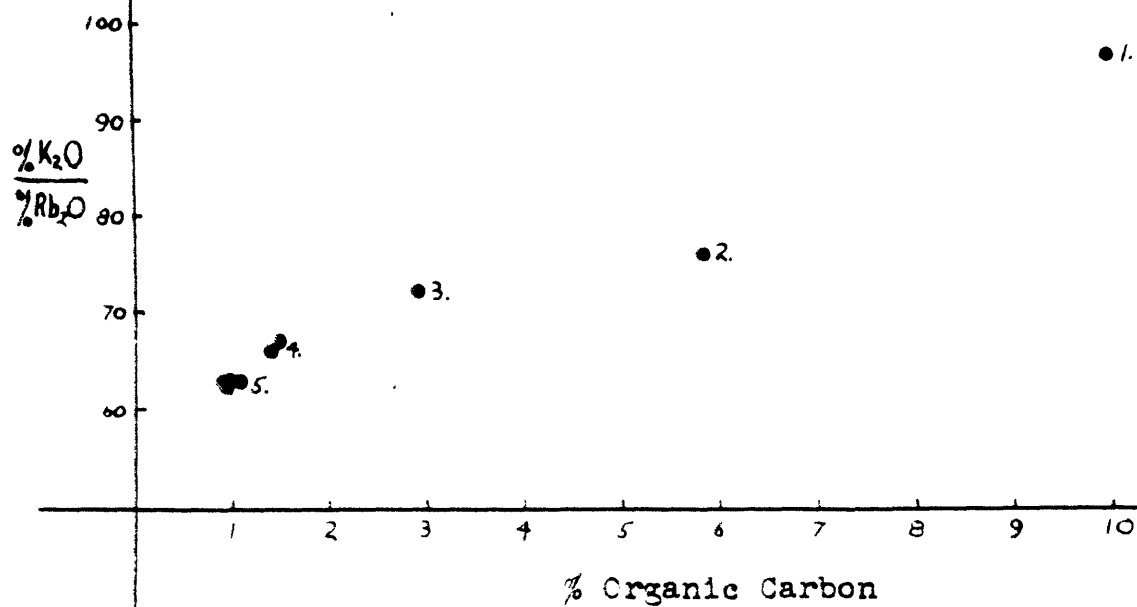
was known to be approximately 100. Thus it is clearly evident that rubidium is adsorbed in sediments to a greater extent than potassium by a factor of about one-third.

During this phase of the investigation the writer noted that there seemed to be a relationship between the value of the  $K_2O/Rb_2O$  ratio and the per cent organic carbon in the sample. Almost without exception the ratio was greater than about 90 whenever the sample contained more than 10 per cent organic carbon. It was decided to investigate whether or not there was any correlation between these two variables by making the usual scatter diagrams. Fig. 57 presents such diagrams for the Cherokee Shale and Nodular Shale formations. No correlation is visible in the Cherokee Shale but a weak correlation is evident in the Miocene Nodular Shale. It is seen there that while samples with a high organic content always have a high value for the ratio, the converse is not necessarily true. Fig. 58 presents a more convincing bit of evidence for a positive correlation between the value of the  $K_2O/Rb_2O$  ratio and the organic carbon content. This is a plot of the average organic carbon content of each formation versus the average  $K_2O/Rb_2O$  ratio and there appears to be a definite positive correlation between organic carbon content and the value of the  $K_2O/Rb_2O$  abundance ratio. The writer believes that the most plausible explanation for this relationship is that the marine organisms, whose remains are responsible for the organic carbon

Figure - 58

Relationship between average organic carbon content and average  $K_2O/Rb_2O$  abundance ratio

1. Woodford Shale
2. Nodular Shale
3. Cherokee Shale
4. Austin and Selma Chalk
5. Others



content of these samples, accumulated potassium. Many marine organisms, particularly the large algae, apparently have the ability of extracting potassium from their environment. If this is so, it does not necessarily mean that these organisms rejected rubidium, because the content of rubidium in sea water is extremely depleted with respect to that of potassium; consequently even if these organisms accepted potassium and rubidium ions impartially, the K/Rb ratio in their bodies would be equal to the extremely high ratio known to exist in sea water. Therefore any sediment which contained an appreciable quantity of organic remains should have a somewhat higher ratio than the same type of sediment without any organic matter.

Another reason for a higher than average ratio would be for a sample to contain a certain percentage of unweathered igneous minerals. A sediment composed exclusively of fragments of igneous minerals would of course have a K/Rb ratio typical of igneous rocks.

Histograms showing the distribution of the  $K_2O/Rb_2O$  abundance ratio in the various formations are presented in Figs. 59 to 63.

#### C. The $K_2O/Cs_2O$ abundance ratio

The degree of association between potassium and cesium in argillaceous sediments is illustrated in Fig. 64. The

### Distribution of $K_2O/Al_2O_3$ Abundance Ratio in Argillaceous Sediments

Based on 291 Samples

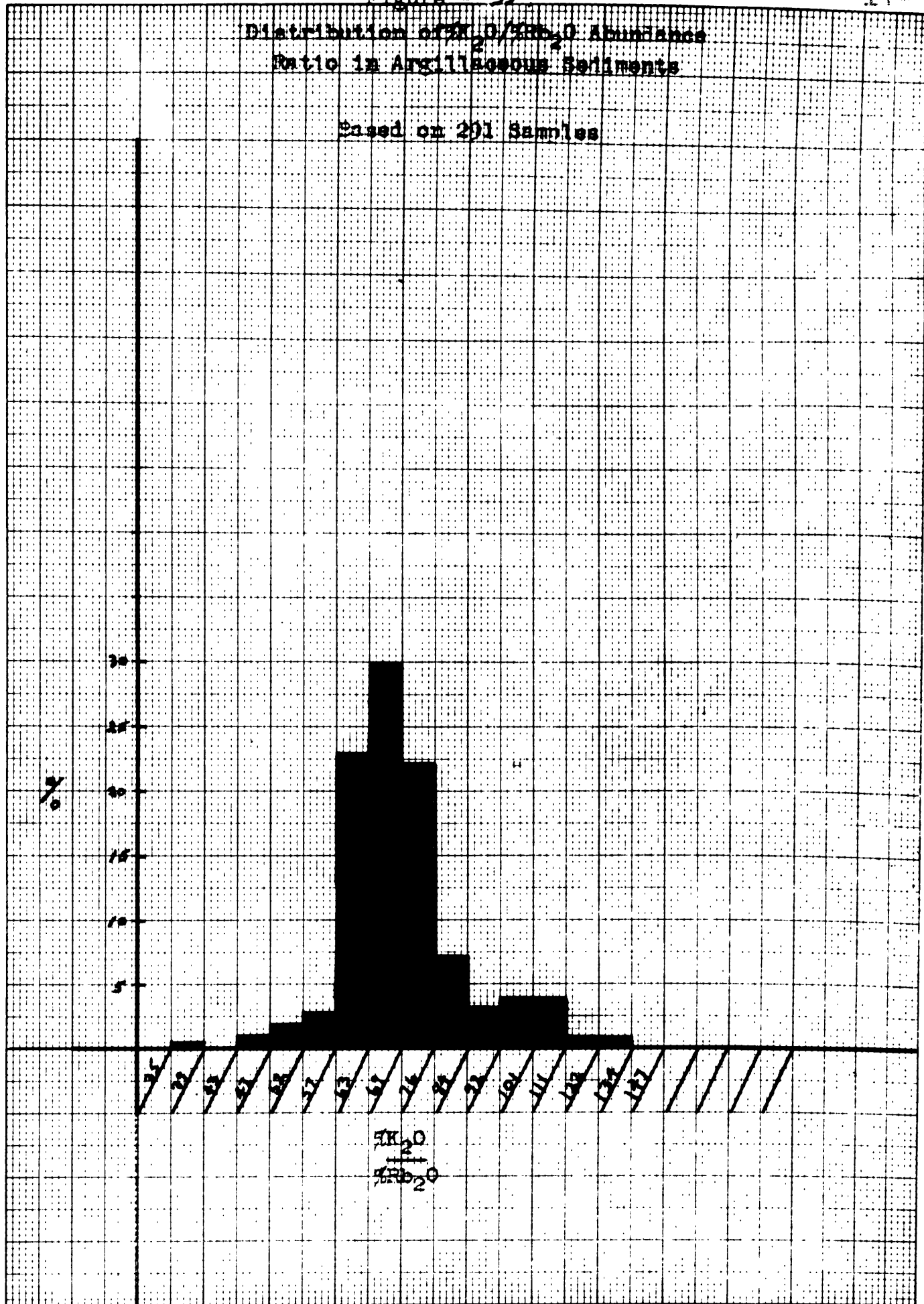
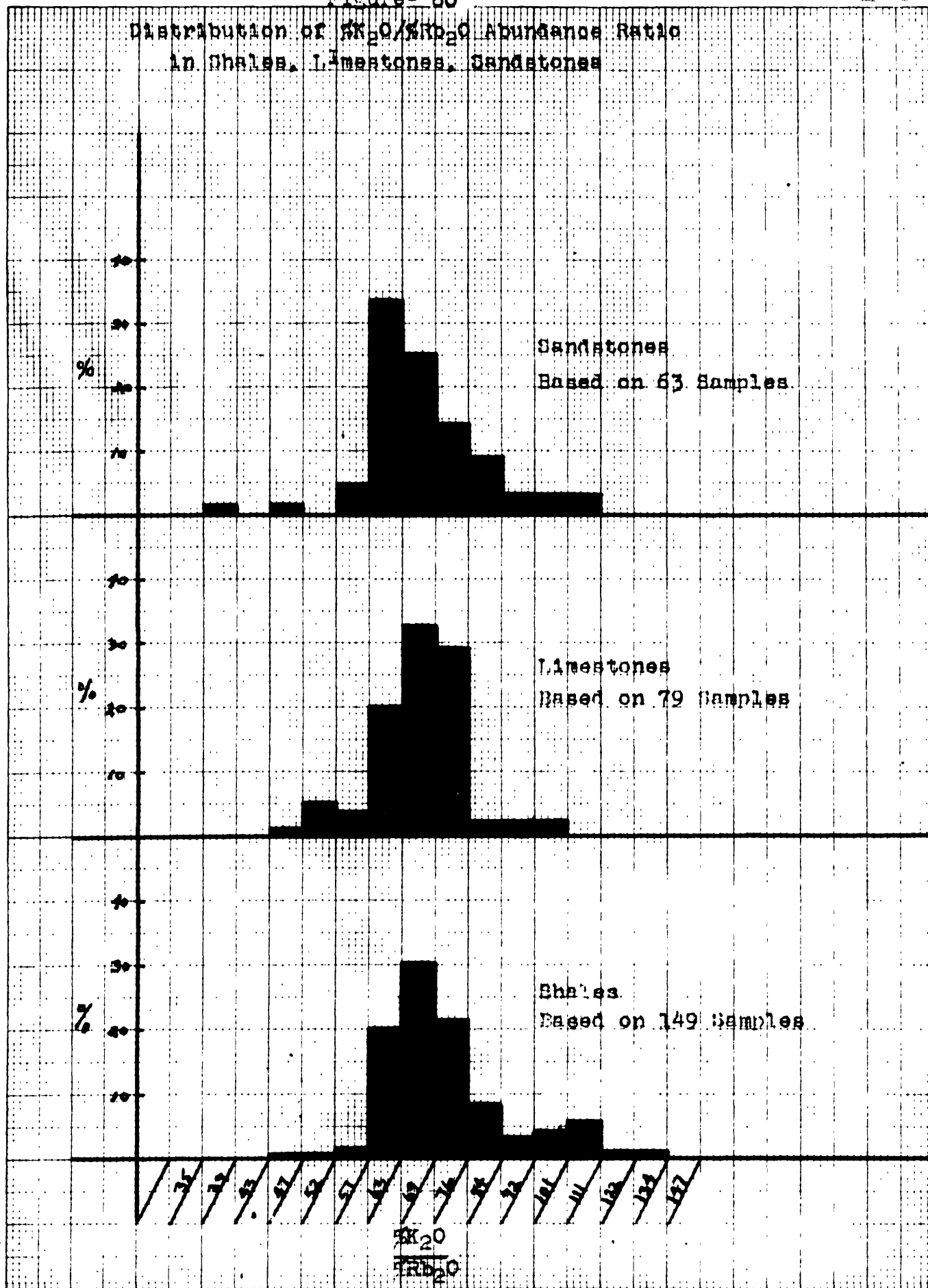


Figure- 60

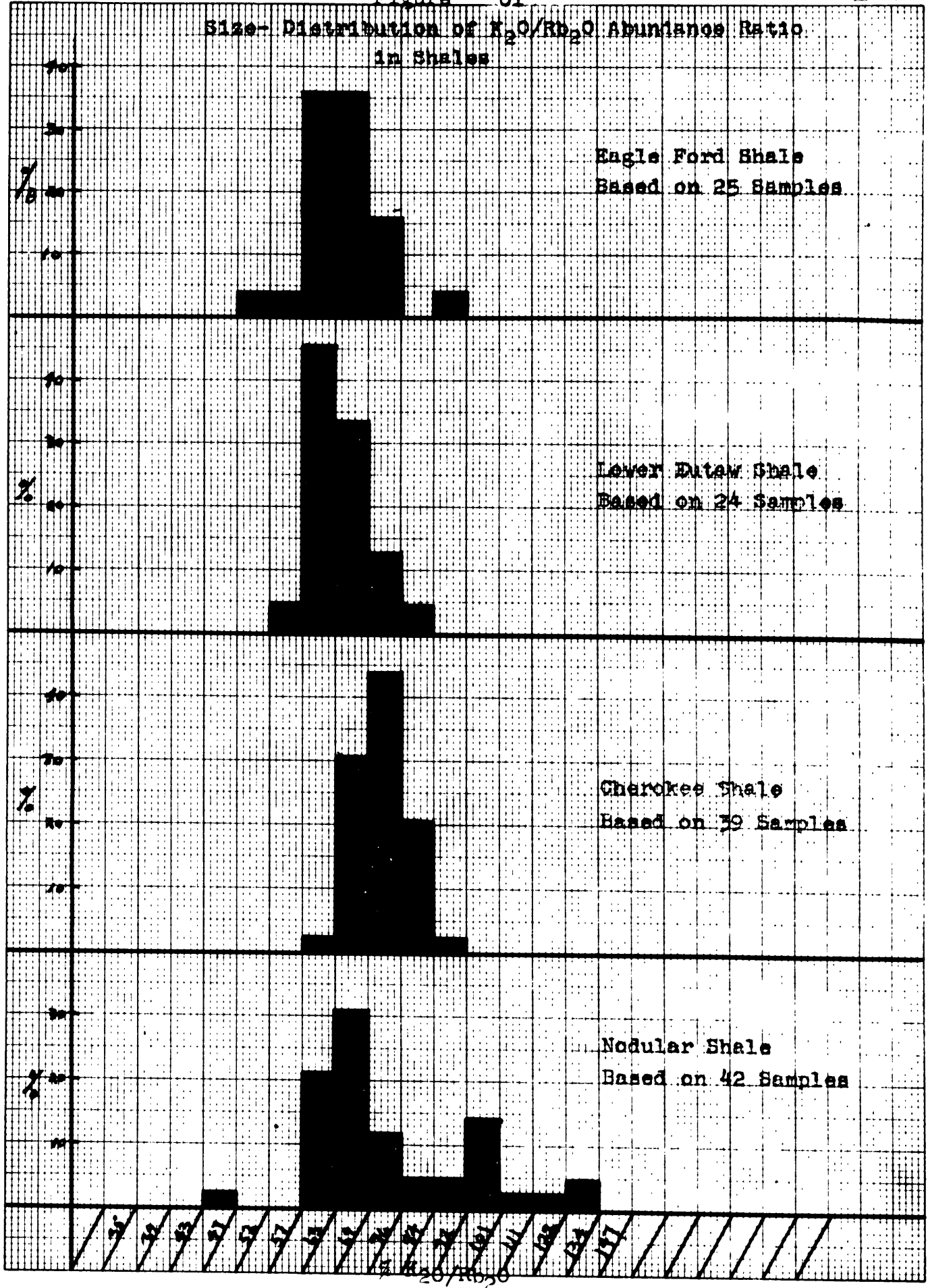
Distribution of  $K_2O/Na_2O$  Abundance Ratio  
In Shales, Limestones, Sandstones



80 MASS. AVE., CAMBRIDGE, MASS.

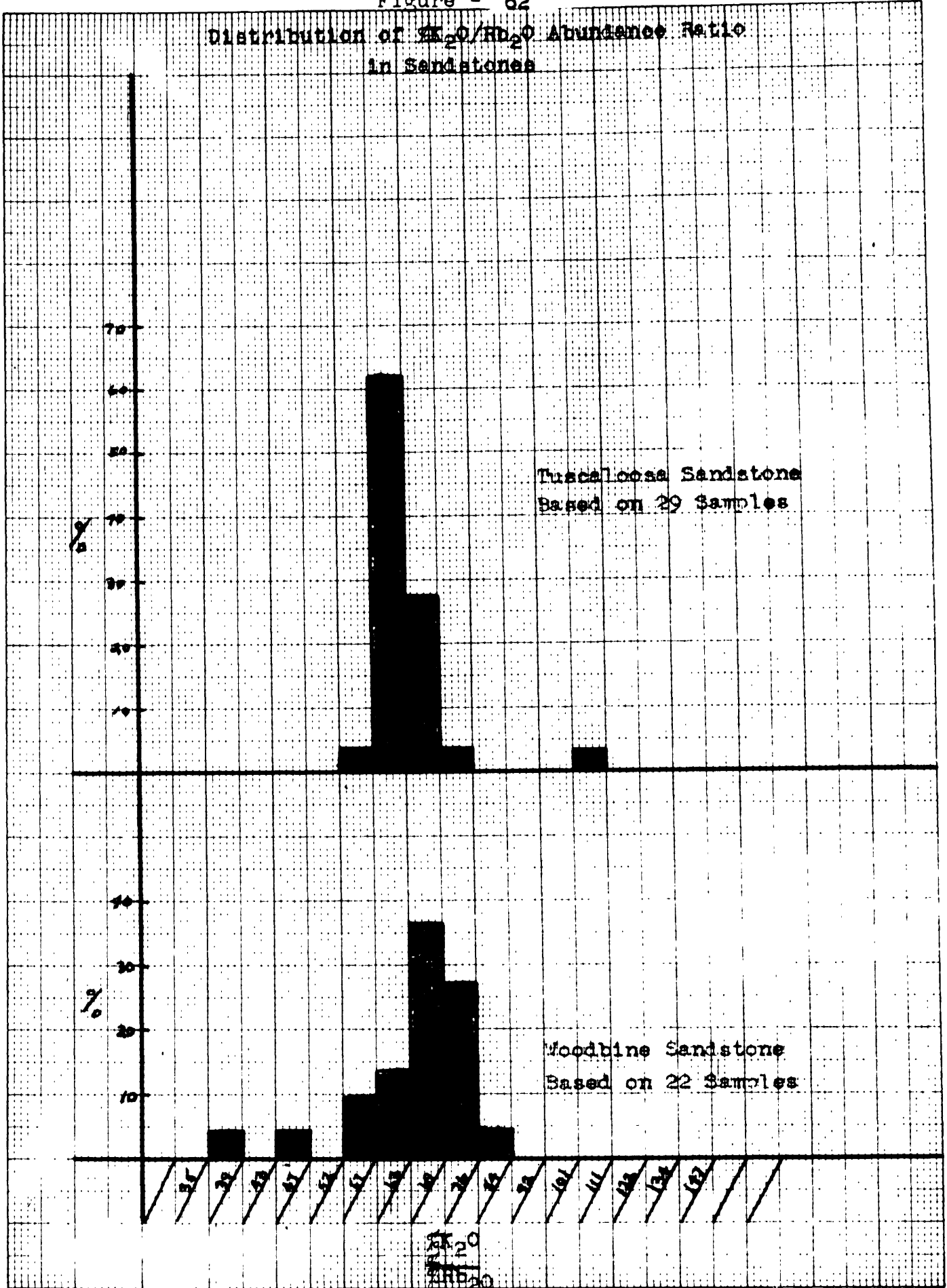
U.S. GEOLOGICAL SURVEY

### Size- Distribution of $K_2O/R_2O_3$ Abundance Ratio in Shales

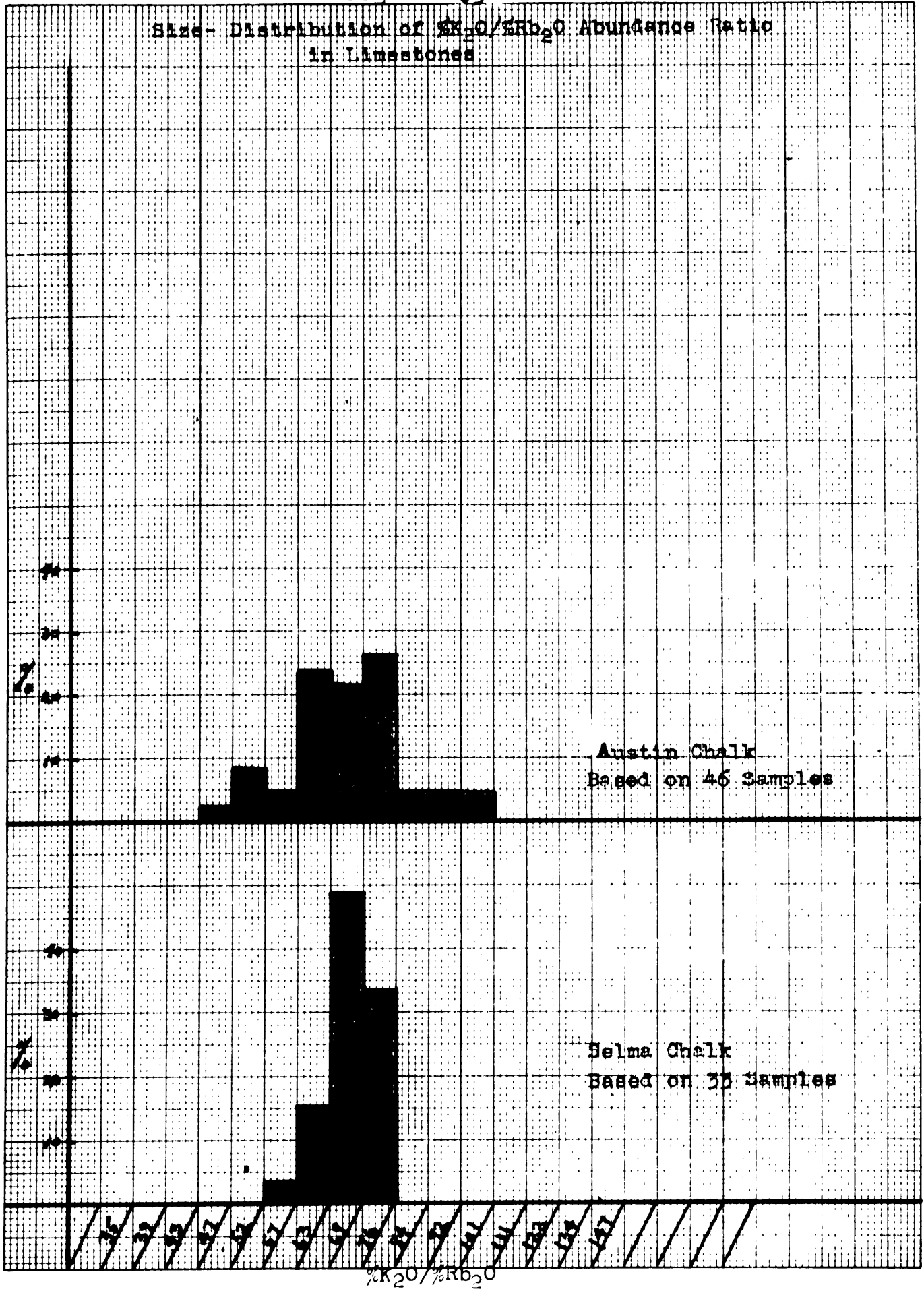




Distribution of  $K_2O/R_2O_3$  Abundance Ratio  
in Sandstones



Size-Distribution of  $K_2O/RO_2$  Abundance Ratio  
in Limestones



Austin Chalk  
Based on 46 Samples

Selma Chalk  
Based on 35 Samples

%K<sub>2</sub>O/%RO<sub>2</sub>

rather wide scatter of points indicates that the coherency between potassium and cesium is less perfect than the relationship between potassium and rubidium, thus paralleling the comparison between these two pairs in igneous rocks.

The average  $K_2O/Cs_2O$  abundance ratio was calculated to be 2900. The various averages for the different formations and rock types are listed in Table 15, where they are seen to vary from 2200 (Selma Chalk) to 3300 (Woodford Shale). In general these values are of the same order of magnitude as those reported by Goldschmidt, Bauer, and Witte ( 9 ). Their results are tabulated below.

Material	$\frac{\%K_2O}{\%Cs_2O}$
European Paleozoic Shales	1550
Japanese Paleozoic Shales	3900
Japanese Mesozoic Shales	3250
Deep-Sea Red Clay	2100

The average  $K_2O/Cs_2O$  ratio in a suite of New England granites was reported to be 3900. Therefore, if this average ratio is reasonably typical of igneous rocks in other provinces, it is clearly evident that cesium is adsorbed in sedimentary rocks to a greater extent than rubidium.

Figures 65 to 69 illustrate how this ratio is distributed among the various formations.

Fig. 64  
Relationship between potassium  
and cesium in sediments

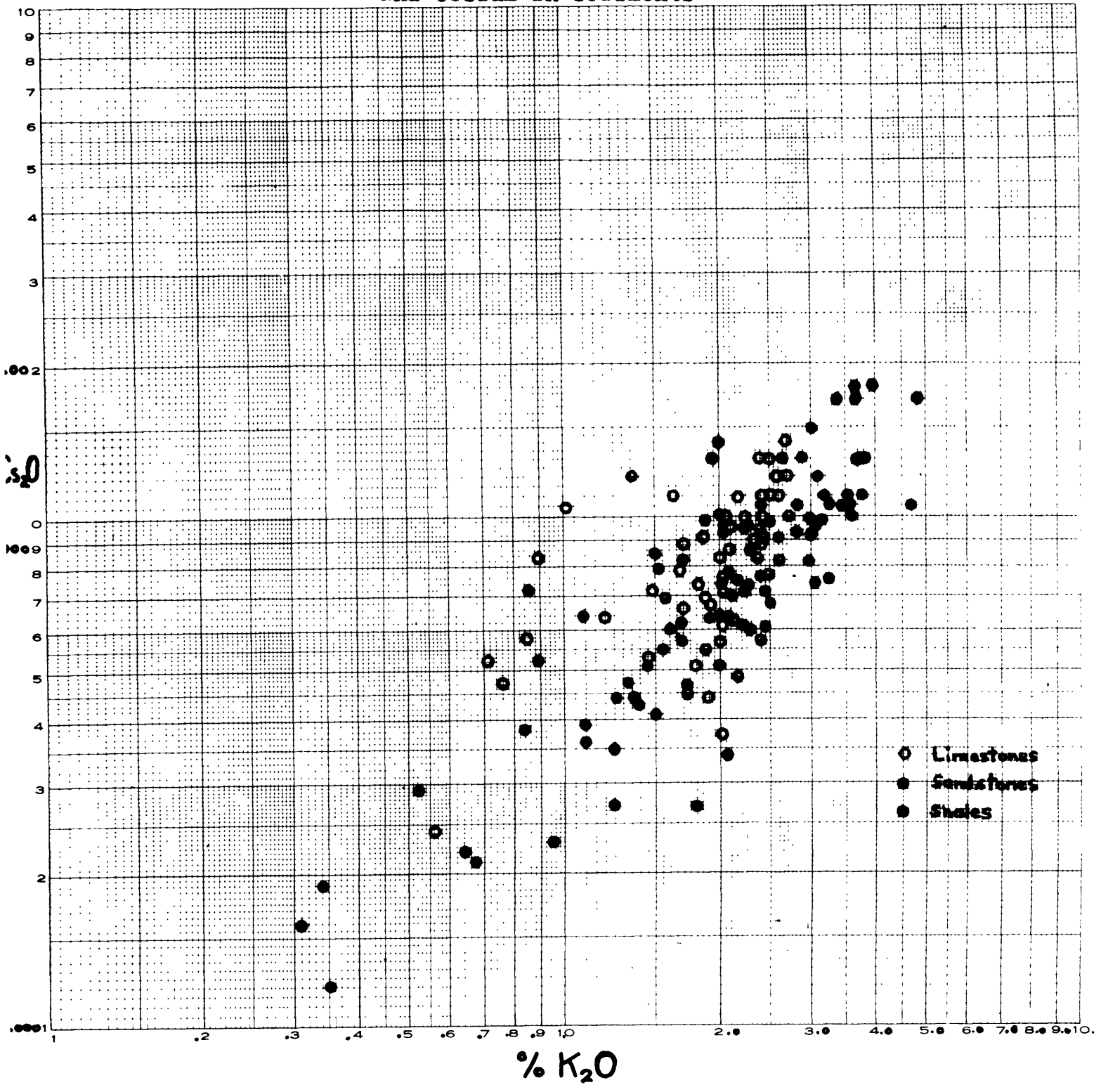


Table 15

The  $K_2O/Ca_2O$  abundance ratio in sediments

Formation	Number of samples included in average and percentage of total	Average value $\frac{\%K_2O}{\%Ca_2O}$
Nodular Shale	31 (76%)	2800
Cherokee Shale	39 (100%)	3200
Woodford Shale	11 (85%)	3300
Lower Eutaw Shale	24 (100%)	2600
Eagle Ford Shale	19 (68%)	3100
Woodbine Sandstone	10 (24%)	2400
Tuscaloosa Sandstone	27 (93%)	3300
Austin Chalk	40 (78%)	2900
Selma Chalk	33 (100%)	2200
All Shales	129 (82%)	3000
All Sandstones	40 (49%)	3200
All Limestones	73 (87%)	2600
All Samples	242 (75%)	2900

Size-Distribution of  $K_2O/K_2O$  Abundance Ratio in Argillaceous Sediments

Based on 242 Samples

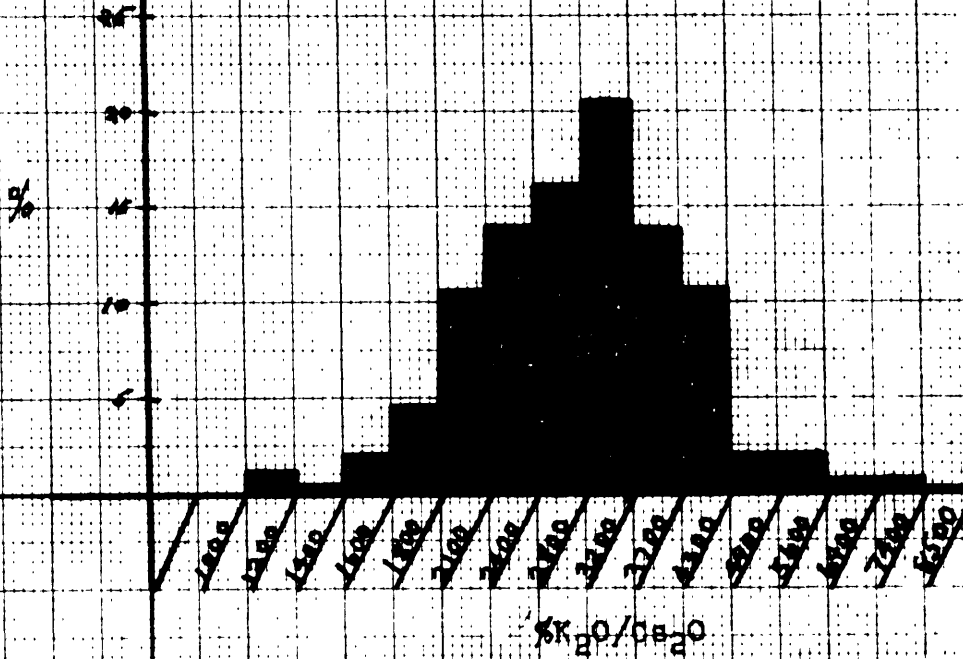
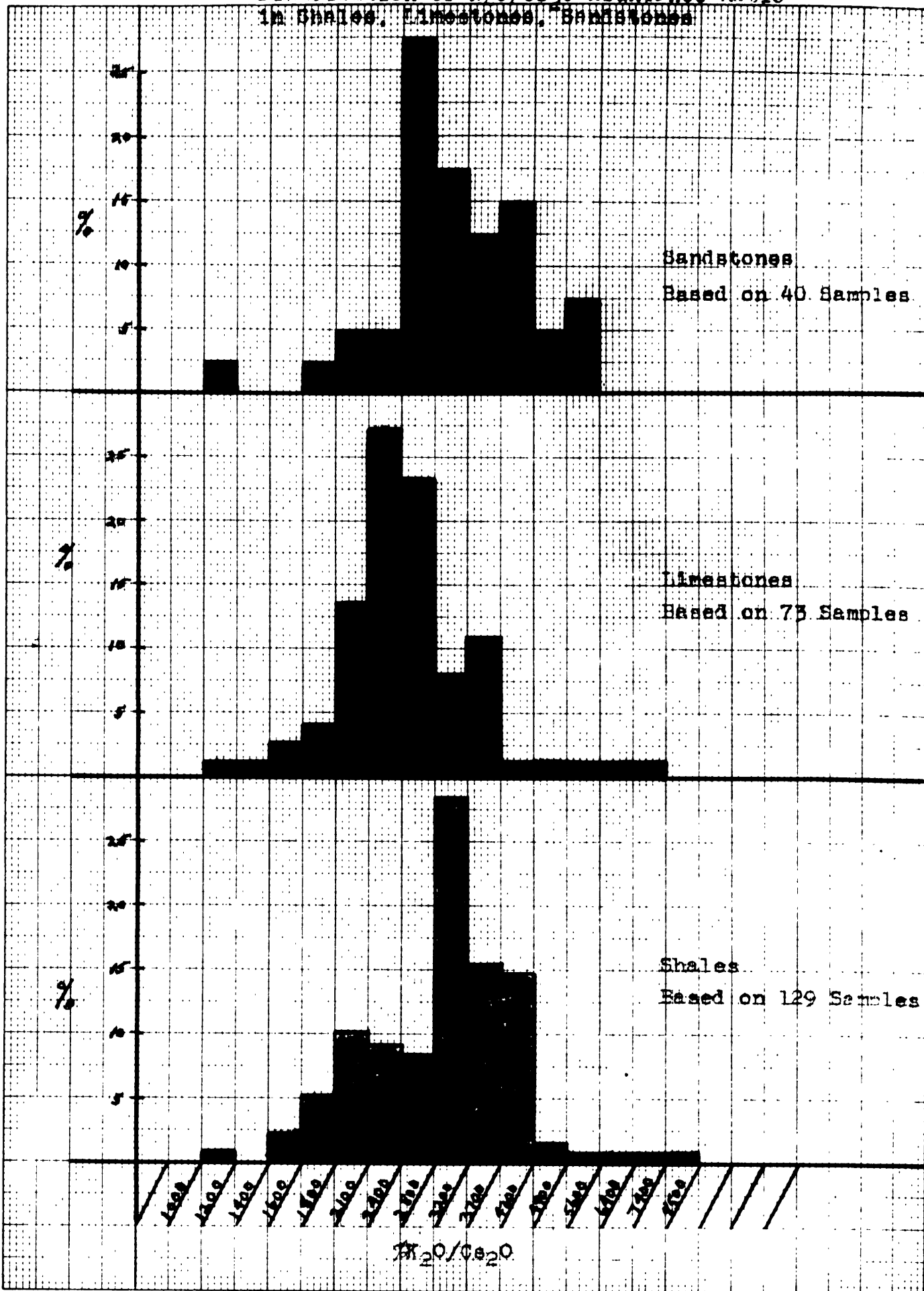
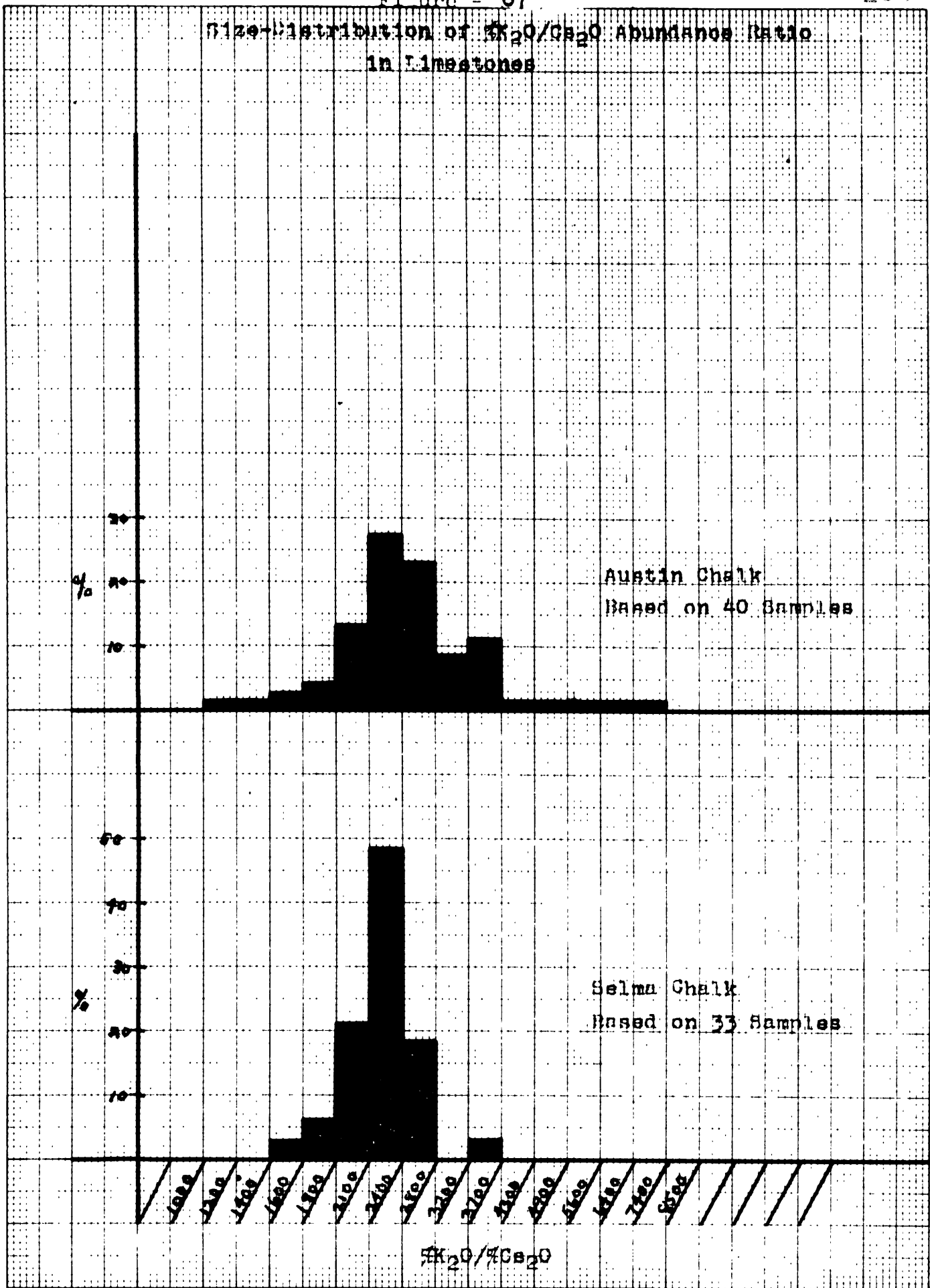


Figure - 66  
 Distribution of  $K_2O/Cs_2O$  Abundance Ratio  
 in Shales, Limestones, Sandstones

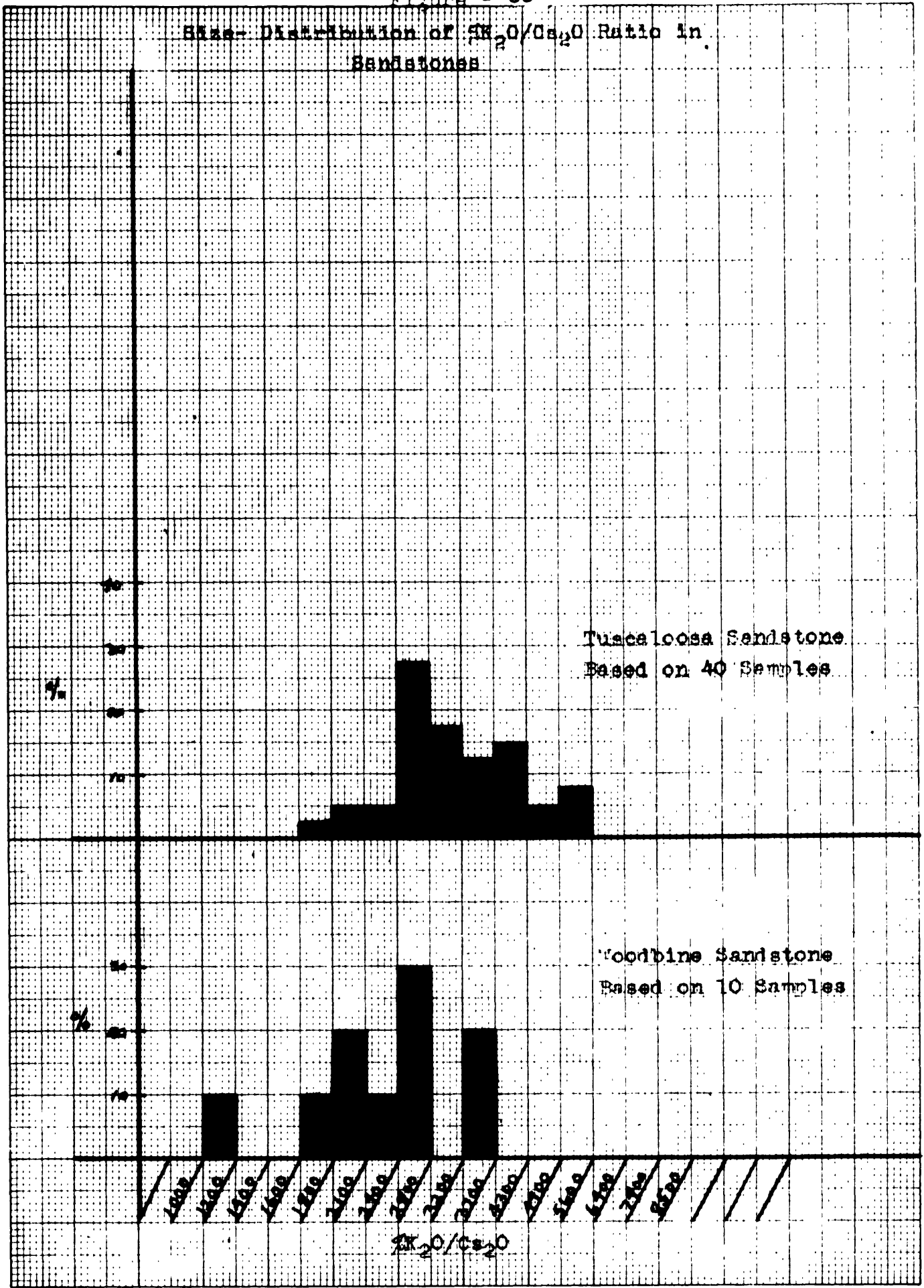


Size-Distribution of  $K_2O/CO_2O$  Abundance Ratio  
in Limestones





Base-Distribution of  $K_2O/Ca_2O$  Ratio in Sandstones





D. The  $\text{Rb}_2\text{O}/\text{Tl}_2\text{O}$  abundance ratio

The close association between rubidium and thallium in igneous rocks and more particularly in the potash-rich minerals of the late crystallites has been mentioned before. The question was also brought up as to whether these two elements would closely follow one another during the sedimentary cycle in view of the fact that there were some important differences in their chemical properties.

The relation between rubidium and thallium is illustrated by the scatter diagram in Fig. 70. The wide and rather erratic scatter of points shows that rubidium and thallium do not follow one another closely during the sedimentary cycle. It is evident that the coherency between these two elements in argillaceous sediments is much less perfect than is the case in igneous rocks. Table tabulates average  $\text{Rb}_2\text{O}/\text{Tl}_2\text{O}$  abundance ratios in the various formations and rock classes. The average ratio is seen to be 920 with a low of 110 in the Woodford Shale and a high of 1400 in the Woodbine Sandstone. When these values are compared with the average value of this ratio in igneous rocks (580), it is evident that there has been a definite partial separation of rubidium and thallium except in the Woodford Shale formation and a few other black shales where there has apparently been a concentration of thallium against rubidium. It is to be remembered that these two groups also carried an exceedingly high content of thallium.

Fig. 70

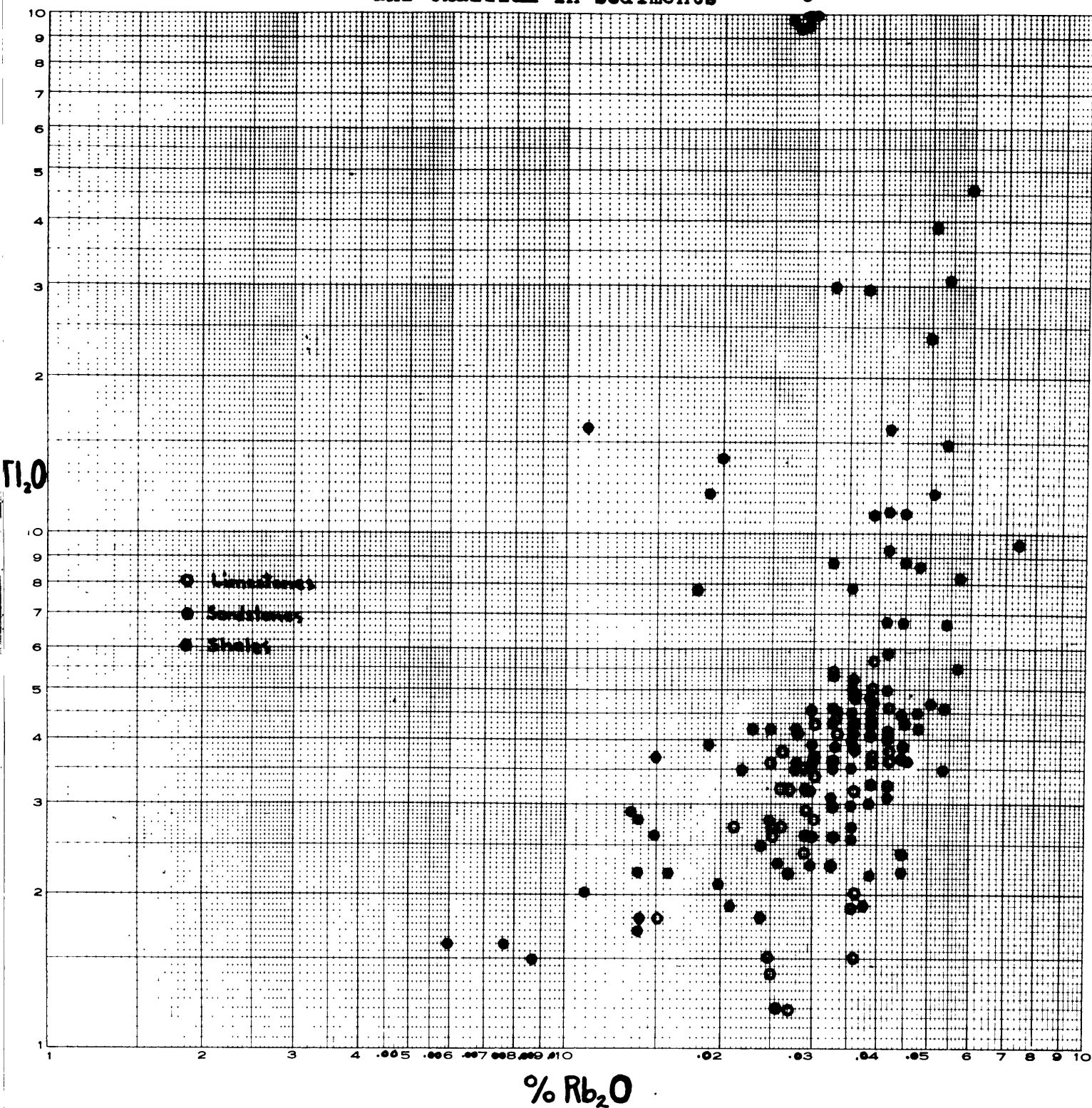
Relationship between rubidium  
and thallium in sediments

Table 16

The  $Rb_{20}/^{87}Sr_{20}$  abundance ratio in sediments

Formation	Number of samples included in average and percentage of total	Average value $\frac{Rb_{20}}{^{87}Sr_{20}}$
Nodular shale	24 (56%)	730
Cherokee shale	39 (100%)	880
Woodford shale	12 (92%)	110
Lower Kewanee shale	24 (100%)	960
Eagle Ford shale	16 (57%)	1100
Miss. Group Black Shales 7 (64%)		200
Woodbine Sandstone	10 (24%)	1400
Gasconade Sandstone	27 (93%)	950
Beina Chalk	33 (100%)	920
Austin Chalk	31 (61%)	1200
All shales	122 (77%)	780
All shales (Except Woodford & Miss. Group)	103 (74%)	900
All Sandstones	48 (58%)	1100
All Limestones	64 (76%)	1100
All Samples	234 (72%)	920
All Samples (Except Woodford & Miss. Group)	215 (78%)	990

In the section where the chemistry of thallium was discussed, it was stated that one important difference in the chemical properties of rubidium and thallium was the extremely low solubility of thallium sulphide in neutral and alkaline solutions. It is known that some sedimentary environments have high concentrations of sulphide ions. Therefore, it seems possible that this sparingly soluble sulphide should influence the distribution of thallium in sediments. The writer believes that Figs. 71 and 72 present evidence in support of this viewpoint although it is of a somewhat indirect nature. In Fig. 71, the  $Rb_2O/Tl_2O$  abundance ratio is plotted against percent organic carbon for the Cherokee and Nodular Shale samples. In both formations there is an inverse correlation between these two variables although it is more pronounced for the Cherokee samples. In Fig. 72 the average abundance ratio is plotted against the average organic carbon content for the various formations. This plot also shows a definite tendency for the average  $Rb_2O/Tl_2O$  abundance ratio to decrease with increasing content of organic matter.

One possible explanation for this negative correlation and one that cannot be ruled out on the basis of present evidence is that the marine organisms which contributed the organic matter to the sediments concentrated thallium in their bodies. Such a concentration of an element through biological activity was considered the most plausible

Figure - 71

Relationship between the  $\text{RB}_2\text{O}/\text{TR}_2\text{O}$  abundance ratio and organic carbon content

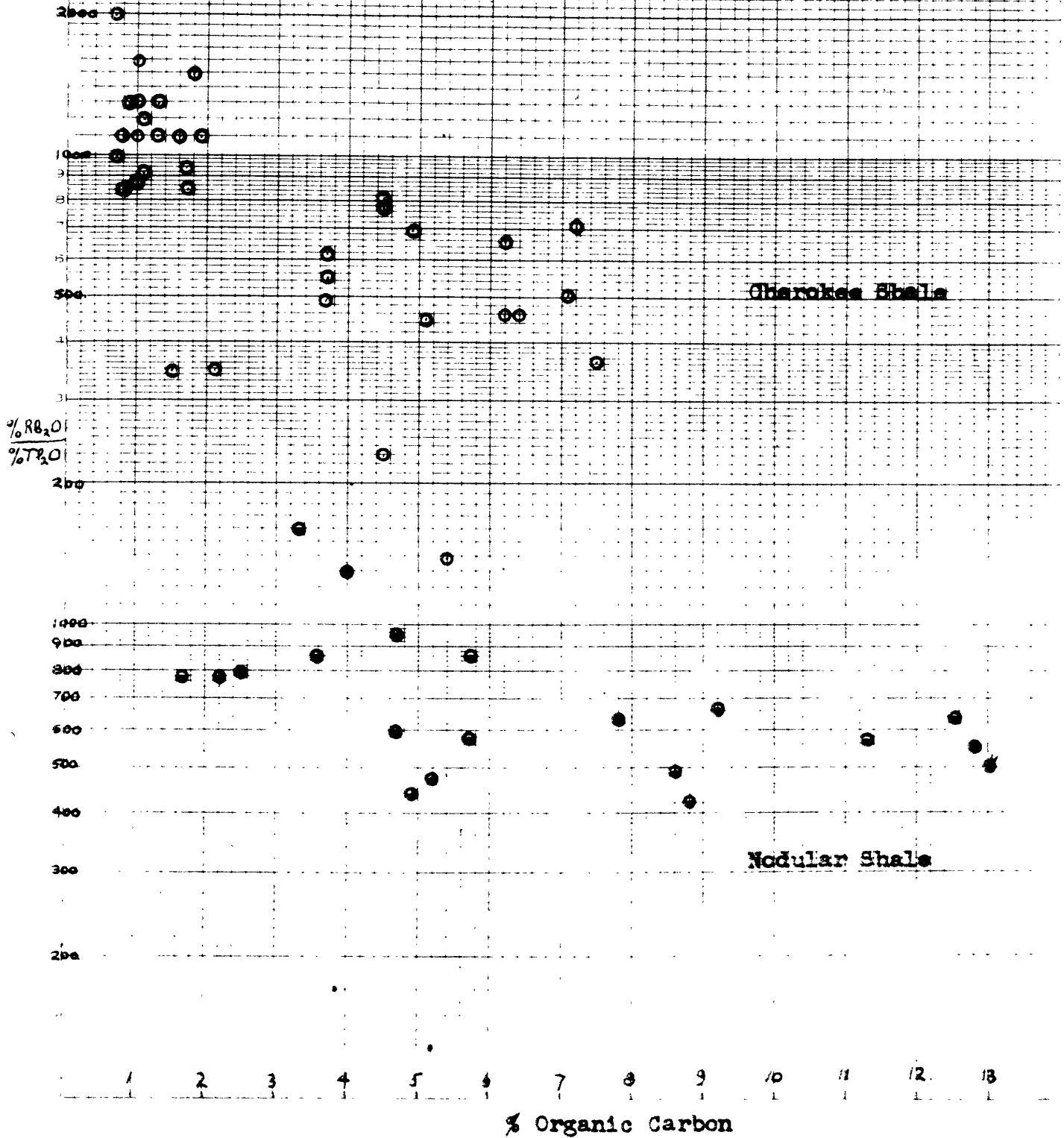
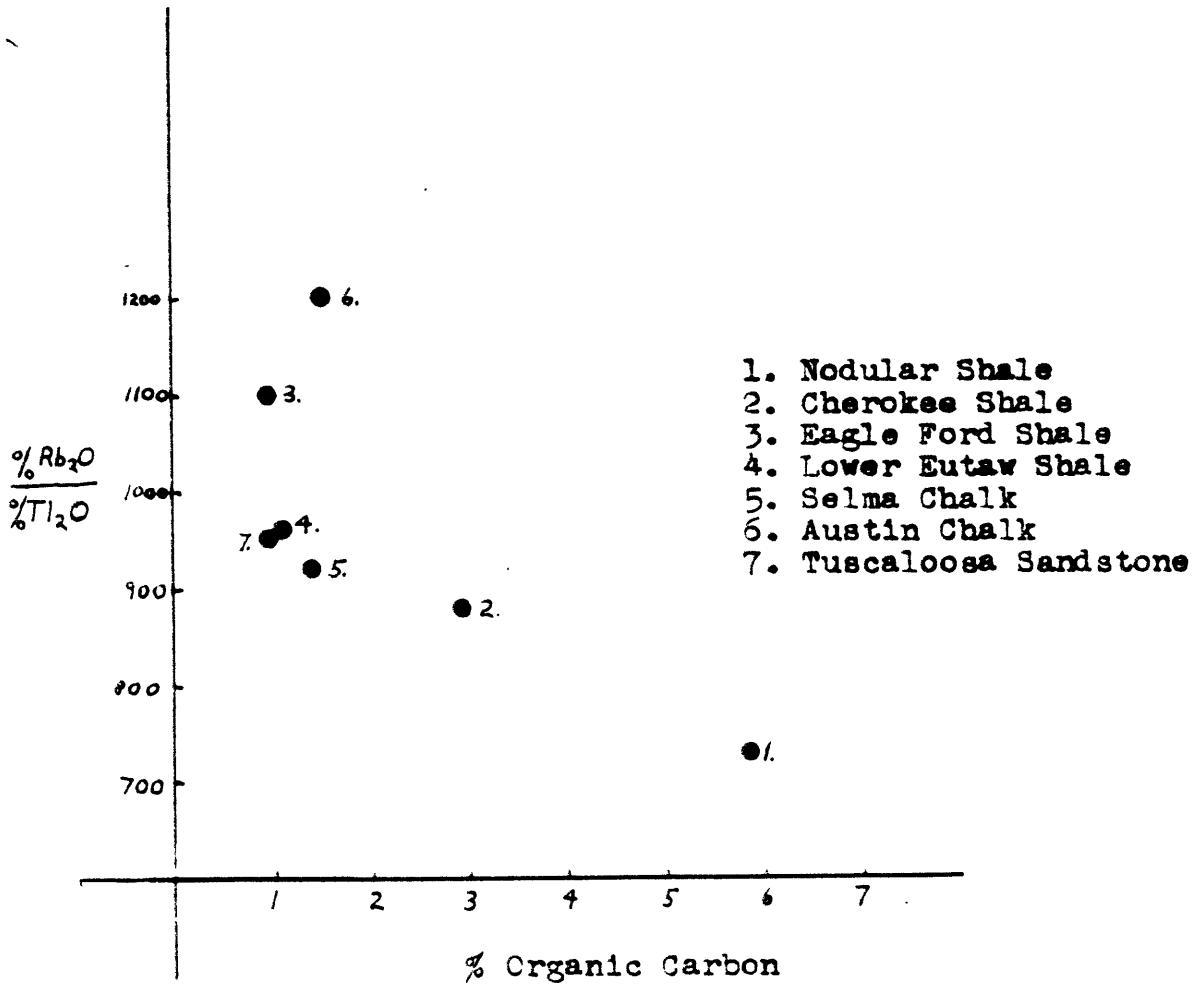


Fig. 72

Relationship between average  $\%Rb_2O/\%Tl_2O$  abundance ratio and average organic carbon content





mechanism for explaining the positive correlation between the  $K_2O/Rb_2O$  ratio and organic matter. However, the writer believes that the negative correlation between organic content and the  $Rb_2O/Tl_2O$  ratio is perhaps only incidental, and that the conditions responsible for the preservation of the organic matter are also responsible for the fixation of thallium in these highly organic sediments. It is generally believed that sedimentary environments most favorable for the preservation of organic material are those in which there is a lack of free circulation or where the burial is extremely rapid. Under these conditions the organic matter is only partially decomposed and turns into a putrefying ooze in which there is an abundance of hydrogen sulphide due to the action of sulphate reducing bacteria on the nitrogenous components of the organic matter. This hydrogen sulphide reacts with iron salts and precipitates iron sulphide. The association of iron sulphides (pyrite) and organic matter in sediments has been frequently reported and is apparently rather general. Therefore it seems probable that thallium would also be precipitated in these environments in view of the extremely low solubility of thalious sulphide and the probable high concentration of sulphide ion.

It seems reasonably clear therefore to say that the different properties of rubidium and thallium have influenced the degree of association of these two elements during

the sedimentary cycle. Some separation of thallium with respect to rubidium apparently takes place except in sulphide-rich environments where thallium tends to concentrate with respect to rubidium due to the low solubility of thalious sulphide.

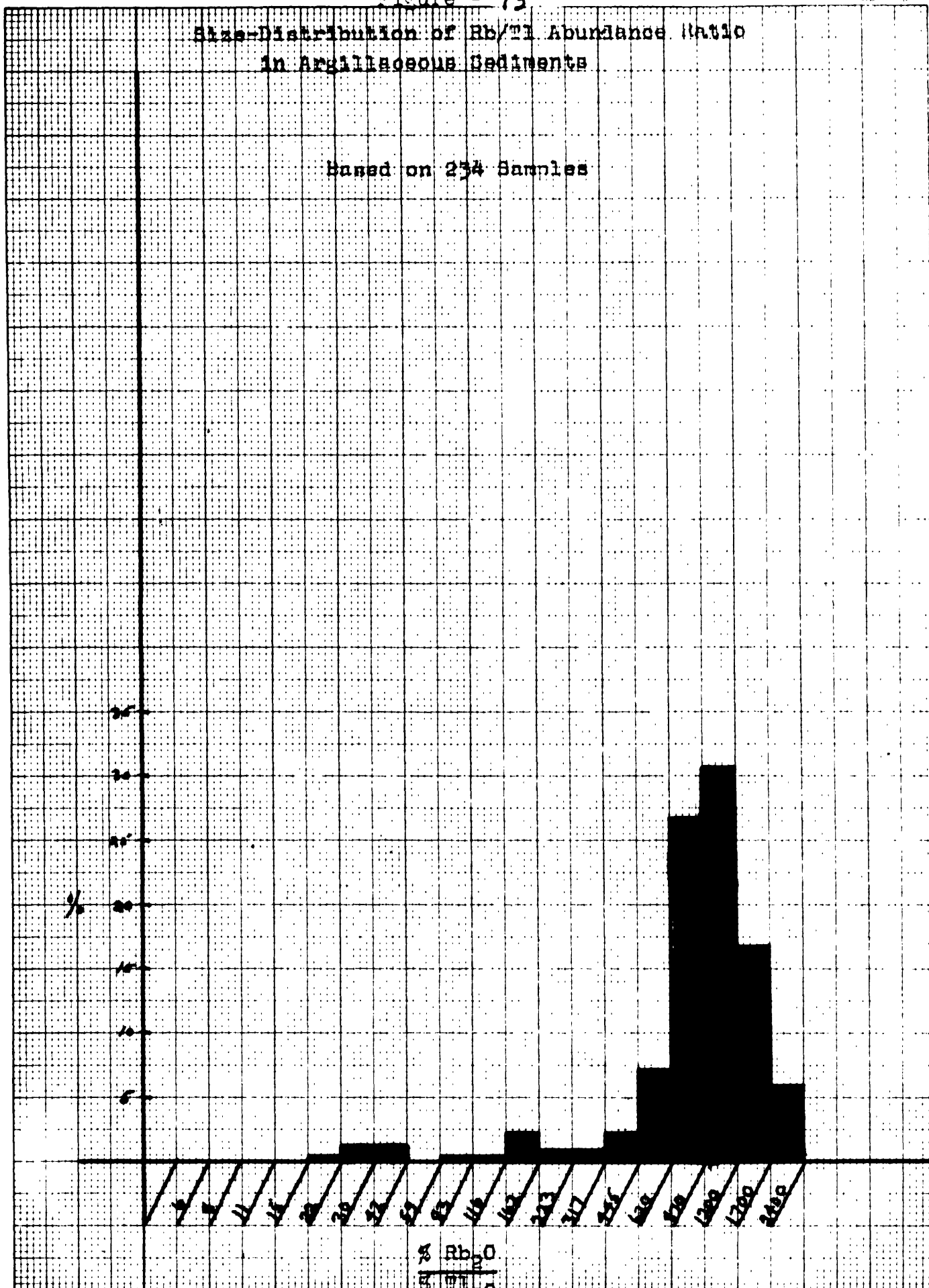
Histograms showing the distribution of the  $Rb_2O/Tl_2O$  ratio in the various formations are presented in Figs. 73 to 77 .

#### E. The $K_2O/Tl_2O$ abundance ratio

Little need be said about this ratio since the  $K_2O/Rb_2O$  and  $Rb_2O/Tl_2O$  ratios have been fully discussed. Table 17 tabulates average abundance ratios and Figs. 78 to 83 show the distribution of this ratio in the various formations. The average ratio is 59000, which is only about 20 per cent higher than the ratio in igneous rocks (48000), thus indicating that little separation of potassium and thallium takes place during the sedimentary cycle. Of course, environments rich in hydrogen sulphide will cause a considerable concentration of thallium and a consequent drop in this ratio. The low value of 8900 in the Woodford Shale is undoubtedly due to this cause.

### Size-Distribution of Rb/Tl Abundance Ratio in Argillaceous Sediments

Based on 254 Samples



$\frac{\% \text{ Rb}_2\text{O}}{\text{Rb/Tl}}$

Size-Distribution of Rb/Tl Ratio in  
Shales, Limestones, Sandstones

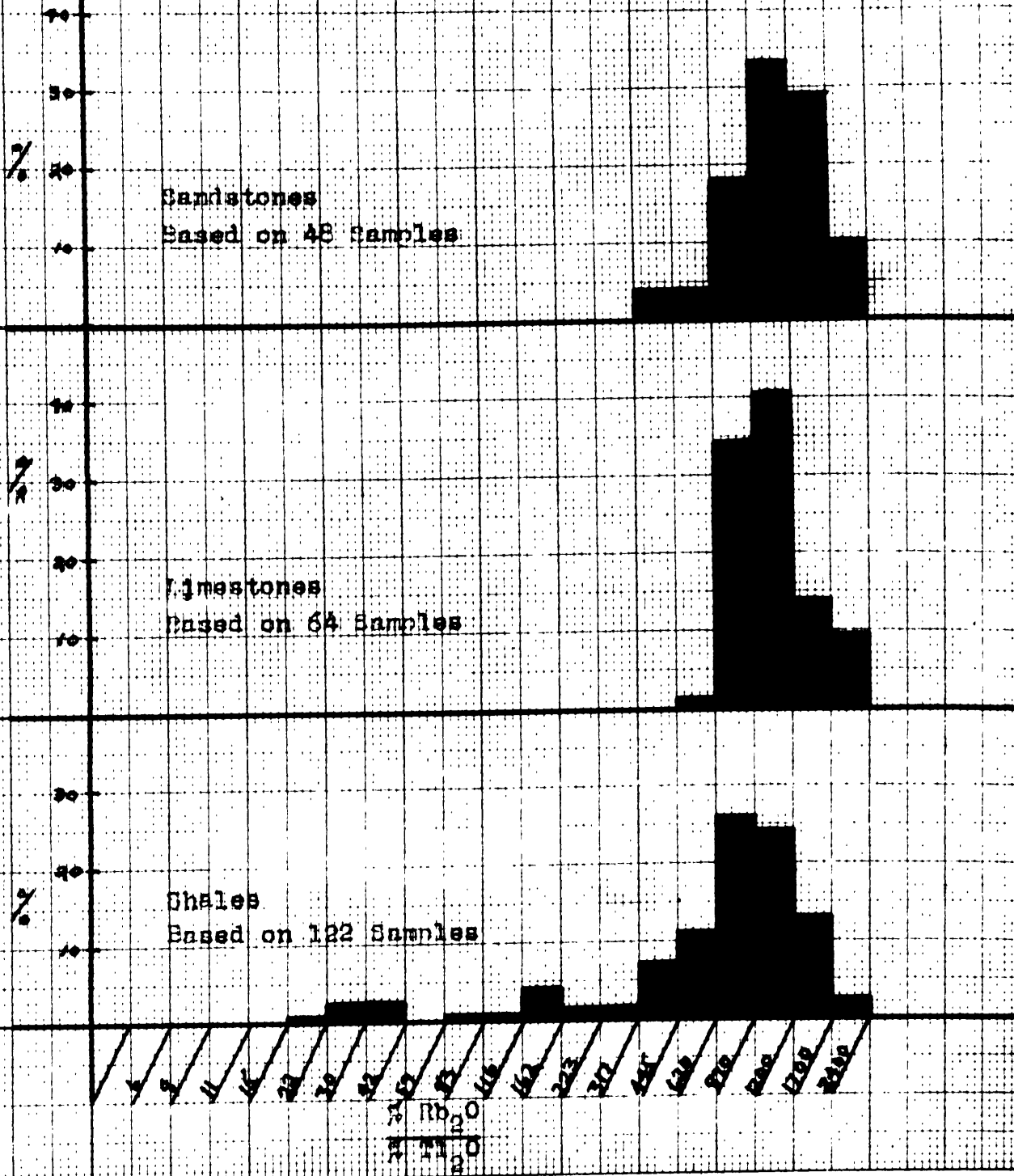
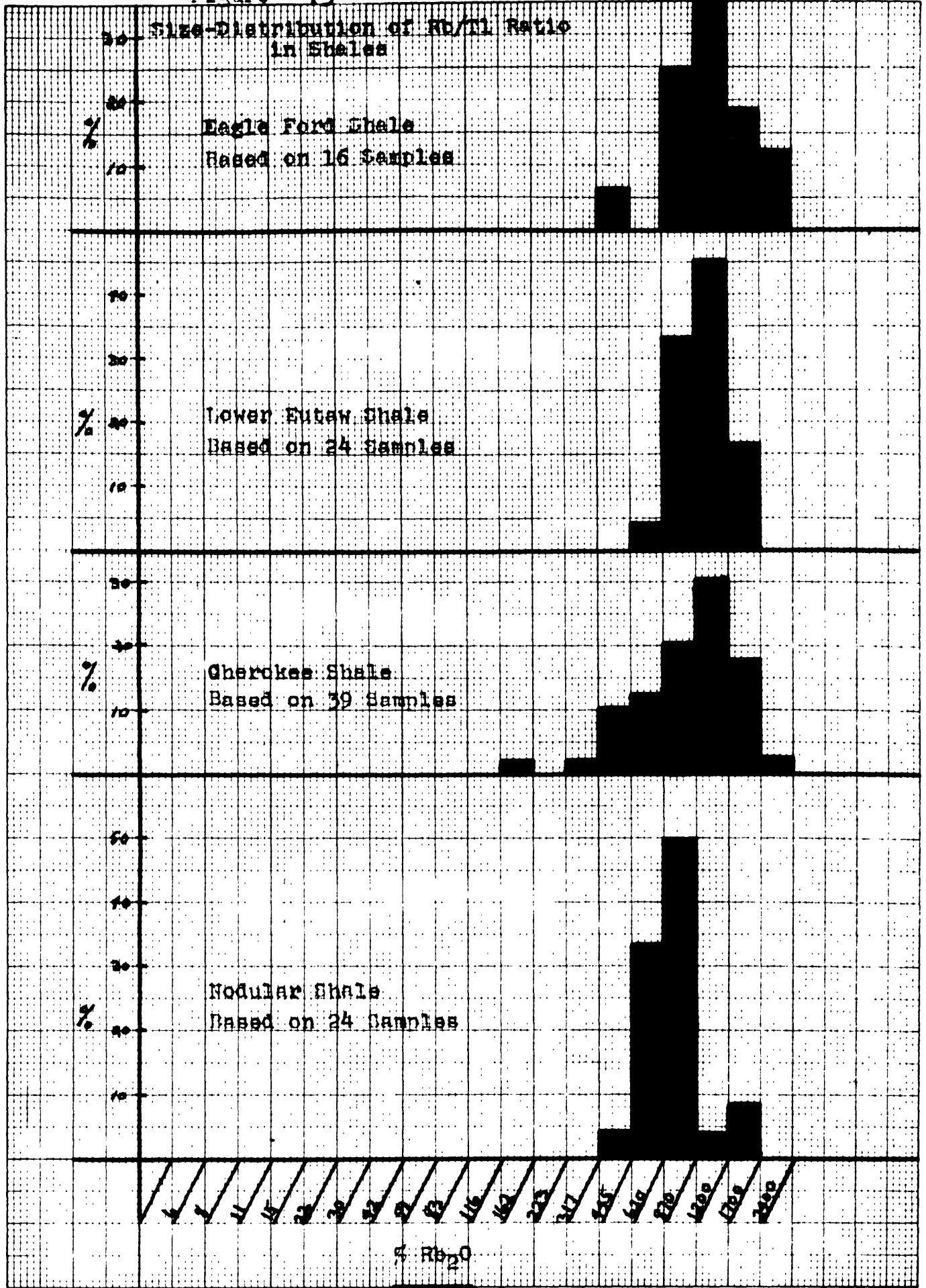


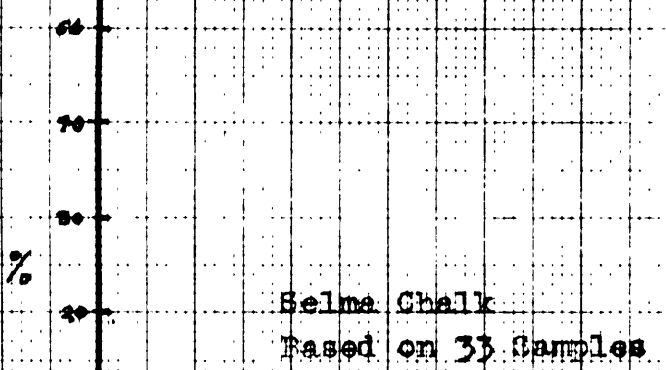
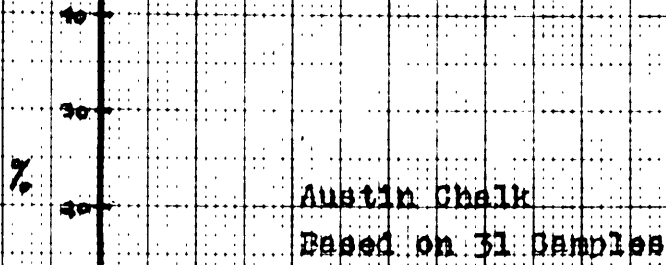
Figure - 75



10 MASS. AVE., CAMBRIDGE, MASS.

Rb/Tl  
1.0

Size-Distribution of Rb/Tl Ratio in Limestones



250  
 200  
 150  
 100  
 50  
 0

Size-Distribution of Rb/Th Ratio in Sandstones

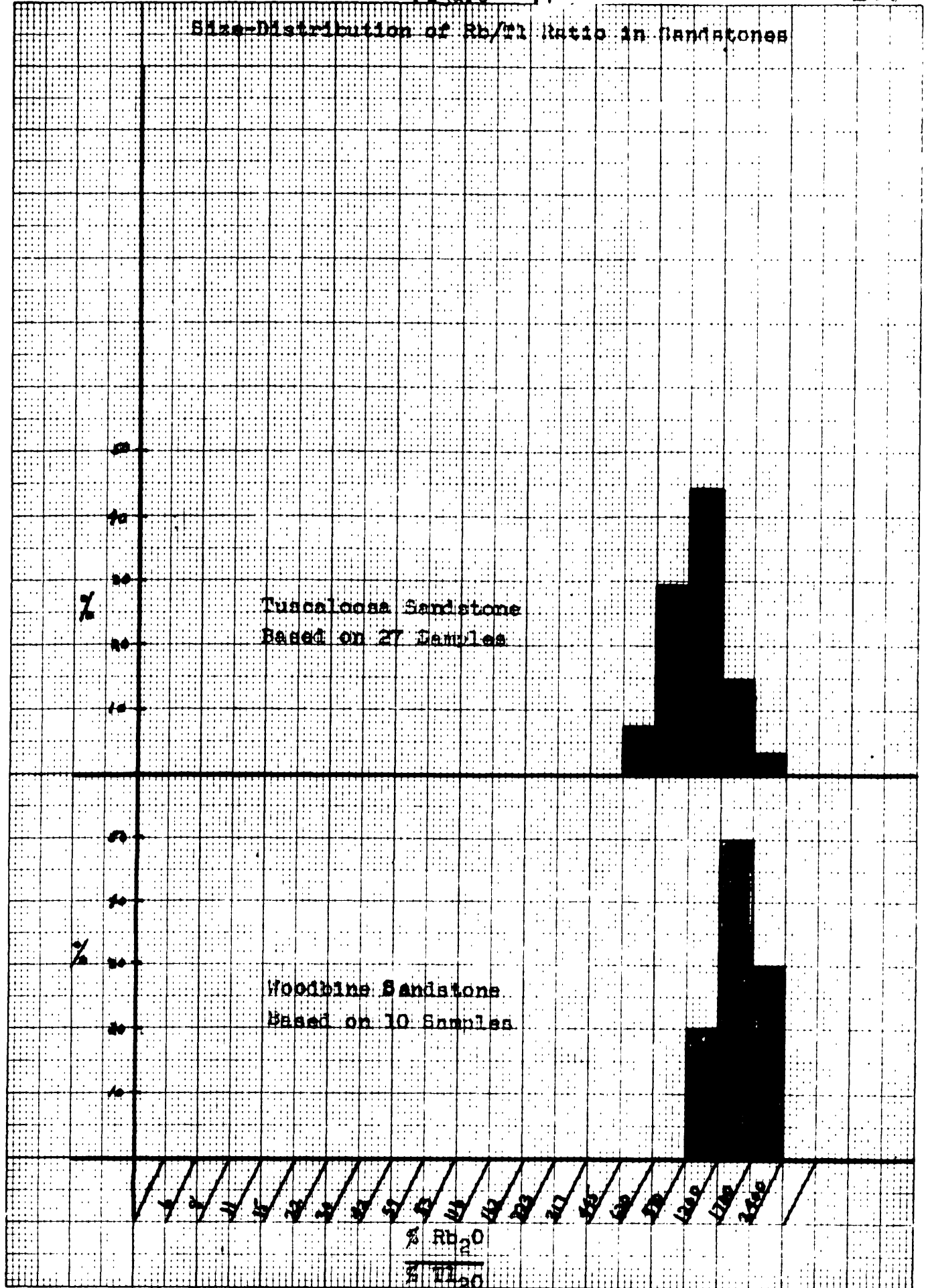


Table 17

The  $K_2O/Tl_2O$  abundance ratio in sediments

Formation	Average value $\frac{\%K_2O}{\%Tl_2O}$
Nodular Shale	53000
Cherokee Shale	60000
Woodford Shale	8900
Lower Eutaw Shale	60000
Eagle Ford Shale	68000
Woodbine Sandstone	85000
Tuscaloosa Sandstone	58000
Selma Chalk	60000
Austin Chalk	73000
All Shales	52000
All Shales (Except Woodford & misc. group)	60000
All Sandstones	70000
All Limestones	67000
All Samples	59000
All Samples (Except Woodford & misc. group)	64000



Figure - 78

### Size-Distribution of K/Tl Abundance Ratio in Argillaceous Sediments

Based on 238 Samples

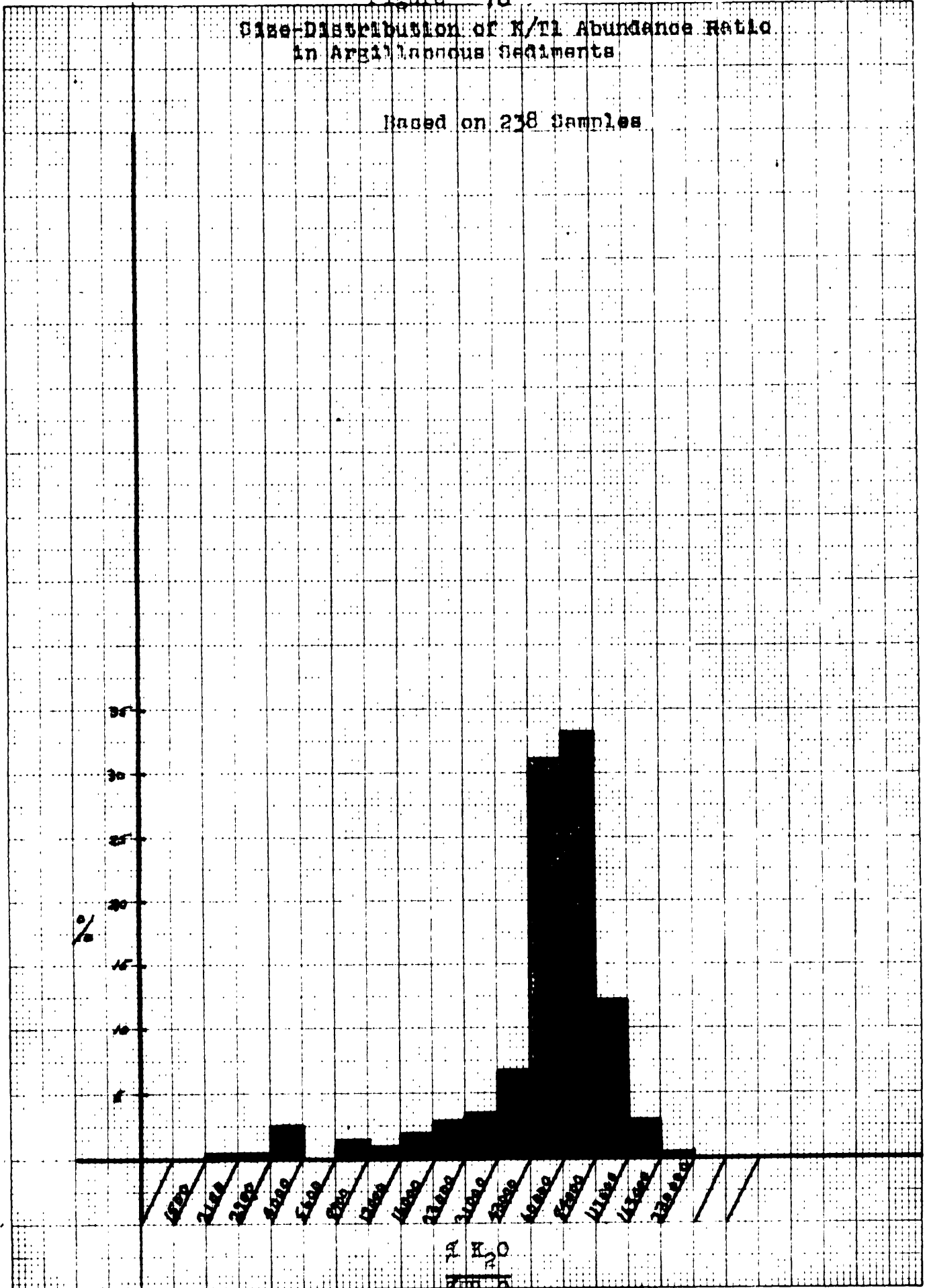
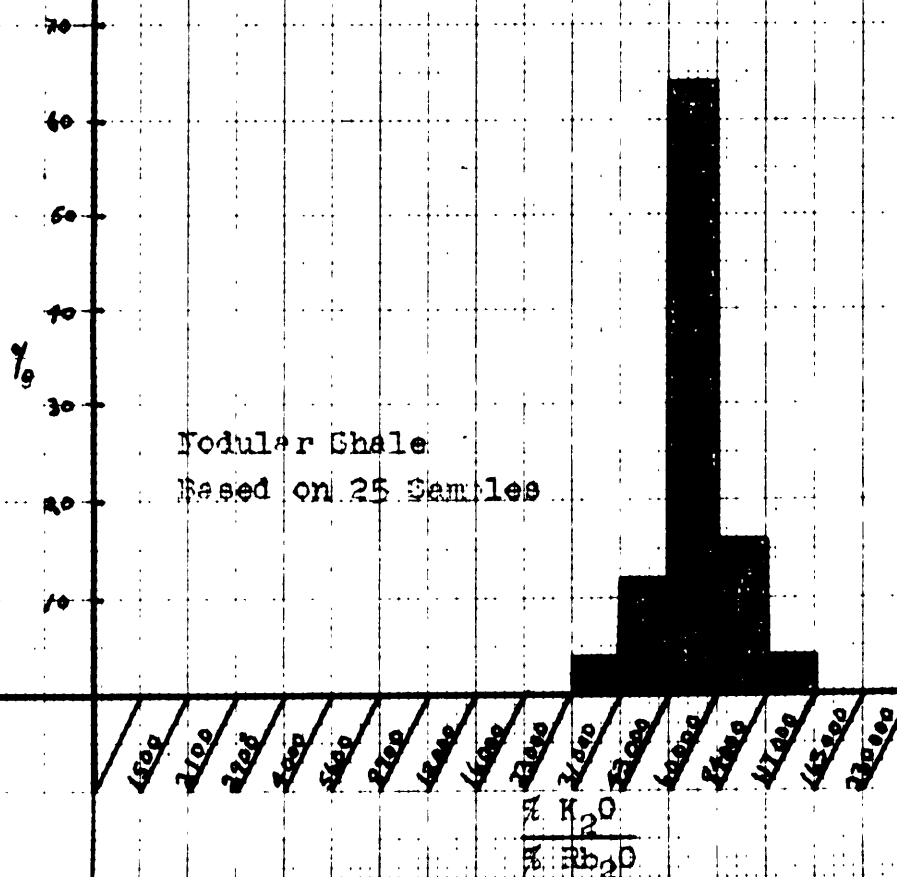
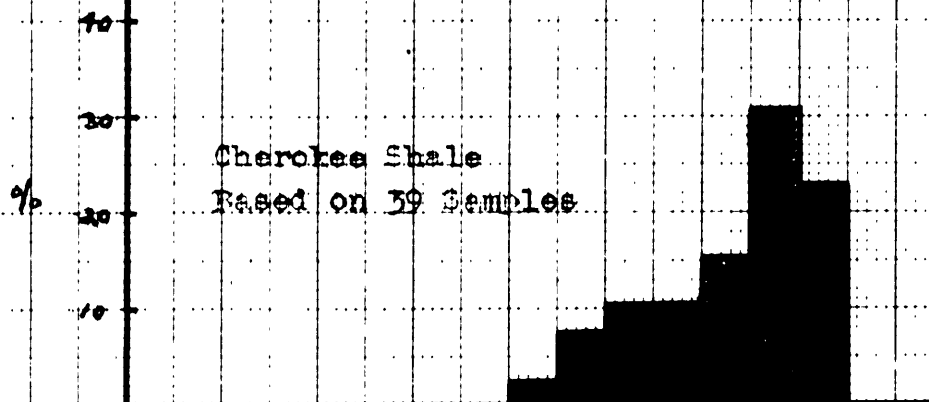




Figure - 80

Distribution of H/TI Ratio in Shales



1.50 1.75 2.00 2.25 2.50 2.75 3.00 3.25 3.50

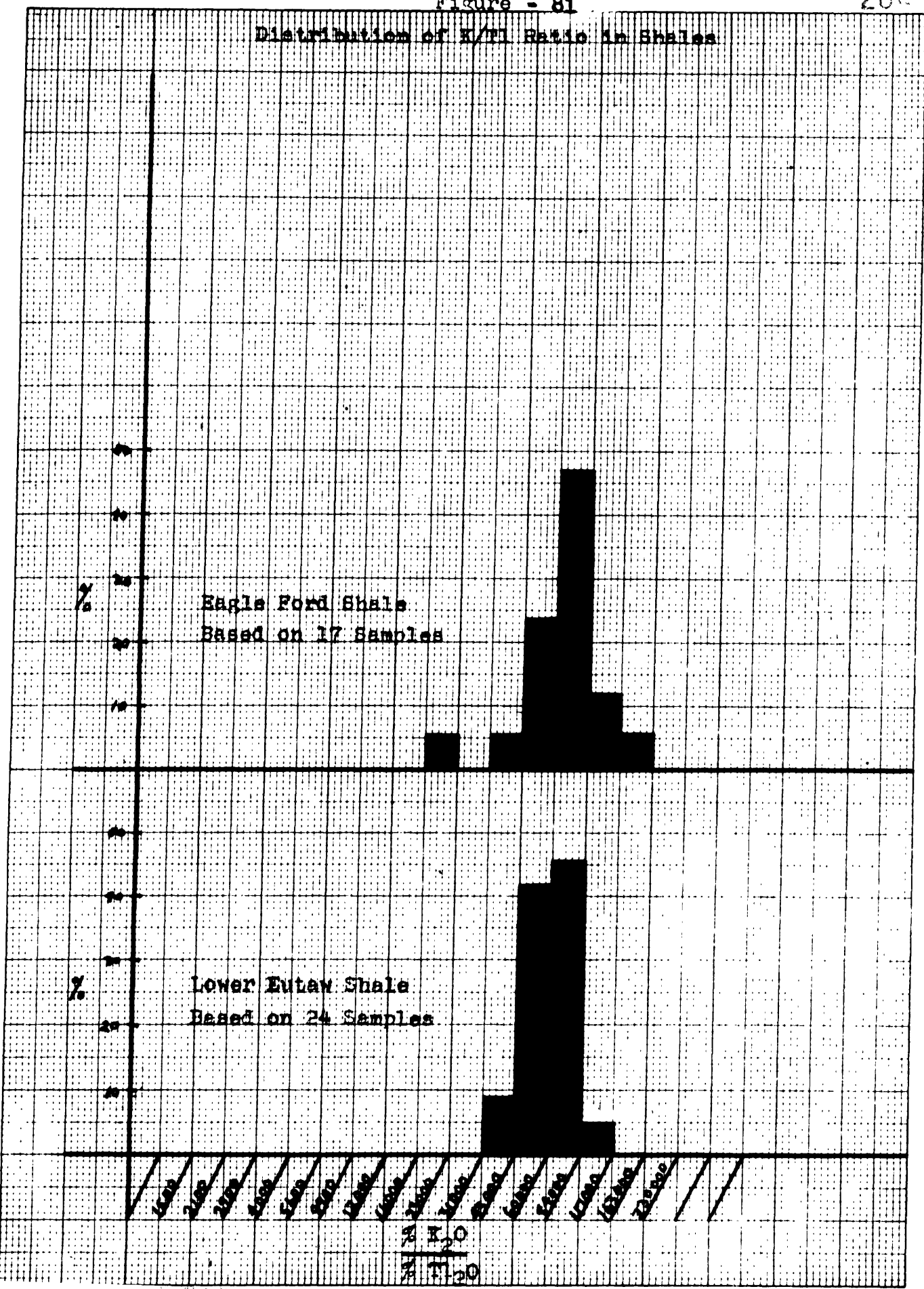
H/TI

Distribution of K/PI Ratio in Shales

40 MASS. AVE., CAMBRIDGE, MASS.

Eagle Ford Shale  
Based on 17 Samples

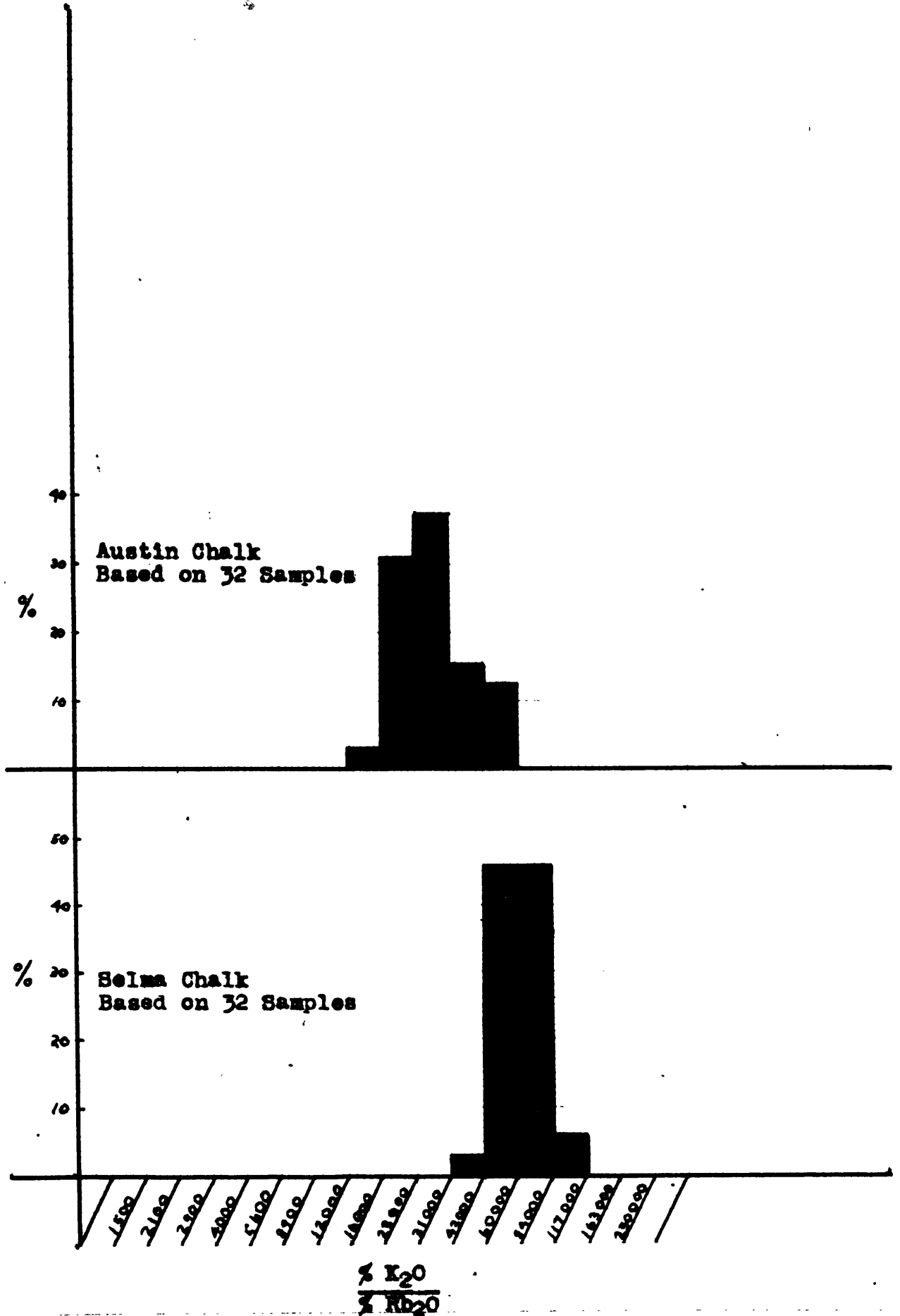
Lower Eutaw Shale  
Based on 24 Samples



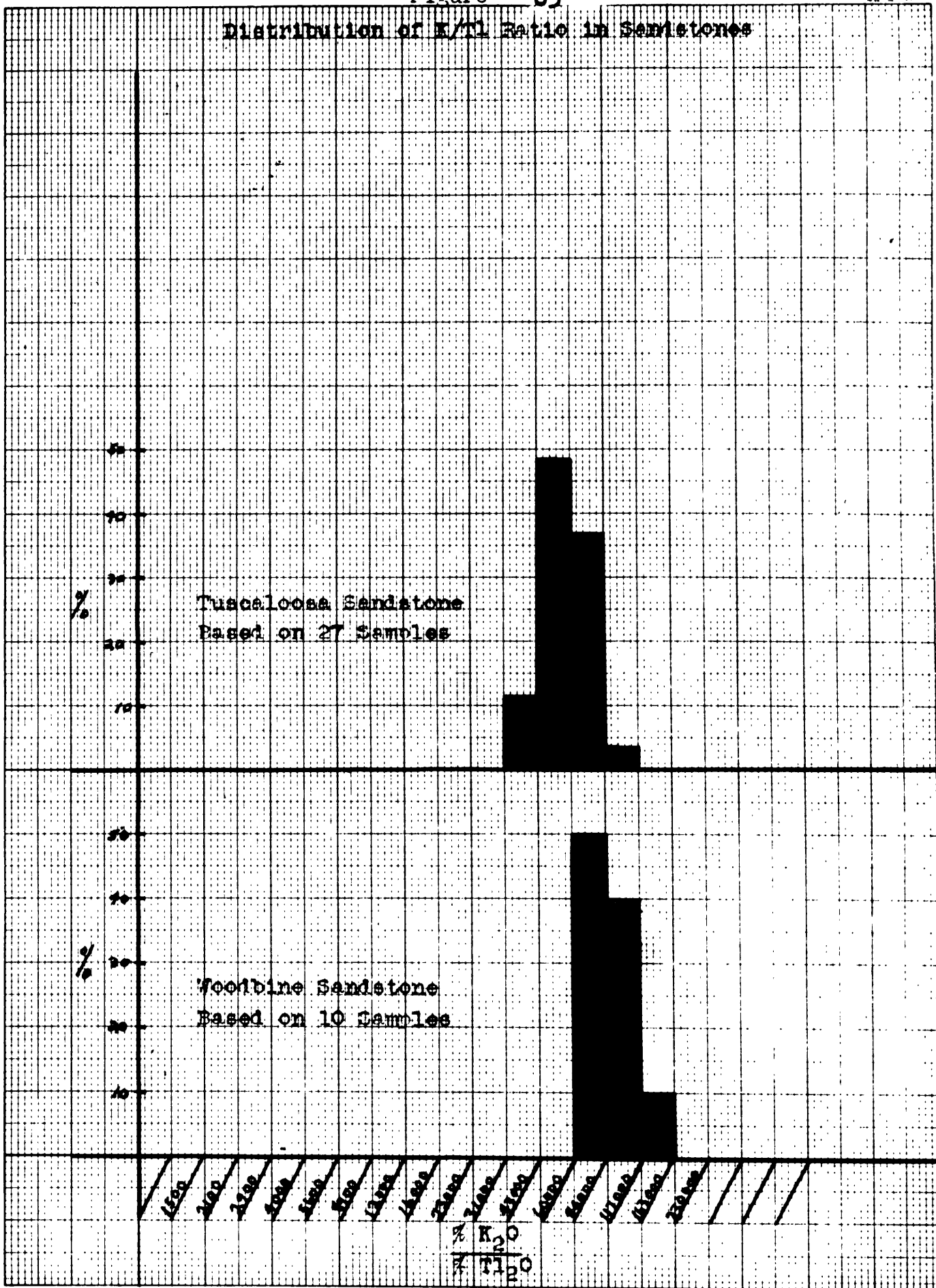
K/PI  
1.000  
1.125  
1.250  
1.375  
1.500  
1.625  
1.750  
1.875  
2.000  
2.125  
2.250

Figure - 82

Distribution of  $K_2O/Tl_2O$  Ratio in Limestones



Distribution of K/Al Ratio in Sandstones



## X. Discussion of Results

The evidence in the preceding section clearly indicates that rubidium and cesium are concentrated in argillaceous sediments to a greater extent than is potassium. The order of relative enrichment is:  $Cs > Rb > K$ . In this series, thallium normally follows potassium except in environments where large concentrations of hydrogen sulphide are possible.

It was also brought out in other sections that these four elements are undoubtedly present in sediments in more than one form. The following seemed to be the more important possibilities:

1. In structure sites in unweathered igneous minerals.
2. In structure sites in authigenic minerals.
3. As precipitated inorganic compounds.
4. In organic matter.
5. As adsorbed ions on various types of colloidal material such as the clay minerals.

Which of the above is the most important depends of course on the composition of the sediments. However, for the normal argillaceous sediment, most authorities agree that the alkali metals (and thallium) are primarily fixed through the mechanism of adsorption by the clay-like material present in the sediment.

There is a voluminous literature on the general subject

of the adsorption of cations by clay minerals. Most of these studies were searching for some relationship between relative adsorbability and properties of the ions. In perusing this large mass of literature, the writer found a hodgepodge of conflicting opinions and complicated equations. No useful purpose would be served by discussing the various theories propounded. The majority of the papers generally concluded with a simple qualitative statement to the effect that adsorption affinities seemed to be determined chiefly by the magnitude of the charge and the hydration of the ions involved.

The writer believes that the adsorption affinities of potassium, rubidium, cesium, and thallium as evidenced by the data collected in this investigation can be explained on the basis of a few simple facts. In all argillaceous sediments, the most important group of minerals are the "clay minerals", which result from the weathering of the various silicate minerals present in primary igneous rocks. The mineralogy of this material is an extremely complex subject but it need not be discussed here as it really is not pertinent. The importance of the "clay minerals" lies in the fact that their grain size generally is in the colloidal range of dimensions and that they carry a net negative charge. By being in the colloidal range of dimensions, the "clay minerals" have a tremendous surface area with consequent great surface energy. The net negative charge that



this material carries results from the fact that each crystal generally has a multitude of sites where there are unsatisfied negative valence forces. The reasons for the presence of these sites and their locations are not really pertinent to this discussion. The essential point is that they do exist. As soon as possible after formation, this material attempts to attain a lower energy state by adsorbing cations from the surrounding medium at all sites where there are these unsatisfied negative valence forces.

It is generally believed that adsorption of ions from aqueous solutions is controlled largely by electrostatic forces. Size considerations, which are so important in crystal chemistry, are relatively unimportant in adsorption phenomena since practically all adsorption sites are external to the structural framework, at least in the "clay mineral" group. Therefore the writer believes that it should be relatively easy to predict which cation of a given series will be preferentially adsorbed. It seems logical that if a group of different cations of the same charge are competing for the same site, the cation with the greatest positive electrostatic potential at the surface of the ion will be the successful competitor for the site. Ahrens ( 3 ) has recently suggested that a measure of the electrostatic potential existing at the surface of an ion was given by what he called the "field function". For any ion this was defined as equal to  $\frac{V_1}{R}$ , where  $V_1$  was the

ionization potential and  $R$  was the radius of the ion. Thus it seemed logical that the adsorbability of an ion should be proportional to its "field function". The "field functions" of the alkali metals and thallium are listed below:

Element	Ionization potential (Electron volts)	Crystal radius (Angstroms)	Field function (Volts per Å)
Li	5.36	0.68	7.06
Na	5.12	0.98	5.22
K	4.32	1.33	3.25
Rb	4.16	1.49	2.80
Cs	3.87	1.65	2.34
Tl	6.07	1.49	4.08

The field functions for the monovalent alkali metals are seen to decrease with increasing atomic weight in apparent contradiction to expectations based on experimental evidence.

The important fact that has to be considered here is one that was often neglected by research workers in this field. This is the fact that most cations are hydrated in aqueous solutions. When a series of ions such as the alkali metals are released from their parent silicate minerals by weathering processes, they enter an essentially aqueous medium in the form of stable cations. However, these cations probably have only a transitory existence as unhydrated ions. The water molecules, which as permanent dipoles, become oriented and attracted by the cations. The number of water dipoles associated with any cation will clearly be a function

of the positive electrostatic potential (or field function) existing at the surface of the ion. Therefore, for a given series such as the alkali metals, relative hydration should decrease according to the series: Li, Na, K, Rb, and Cs, which is the order of decreasing values of the field function. Several experimental methods have been used to find the degree of hydration of ions, but generally they have given widely varying results as far as absolute values go. However all methods agree that relative hydration does decrease with increasing atomic weight for the alkali metal series. These hydration shells are permanently attached to the cations as long as they remain in an aqueous environment and have the important effect of increasing the ionic radius. According to Gedroiz ( 8 ) the hydrated radii of the alkali metal ions are:

Li	3.65A
Na	2.80A
K	1.90A
Rb	1.80A

No value was reported for cesium, but according to Boyd et al ( 5 ), cesium is so large that it is not appreciably hydrated.

As these water hulls have effectively increased the radii of the cations, it is logical to use the hydrated radii in computing field function values for these ions in aqueous solution. When this is done for the alkali metal ions the following values result:

Cation	Field function $\frac{V_1}{R}$ (hydrated)
Li	1.47
Na	1.83
K	2.27
Rb	2.31
Cs	2.33

The question of how to compute a value for thallium posed a problem in view of the fact that no value for its hydrated radius could be located in the literature. Its crystal radius is identical with that of rubidium, but in view of its much greater ionization potential (6.07 volts) and consequent field function (4.08), its hydrated radius should be considerably greater than that of rubidium. A value was interpolated from a plot of  $\frac{V_1}{R}$  (hydrated) versus  $\frac{V_1}{R}$  for the alkali metal series and found to be approximately 2.10, which placed it between potassium and sodium.

Earlier in this section, it was mentioned that the writer believed that adsorption affinities are determined chiefly by the magnitude of the field functions of the ions. Thus on the basis of these recomputed values, relative adsorbability for the alkali metals and thallium should be according to the following series:



Since this was generally the order of relative enrichment found in argillaceous sediments, theory and fact are apparently in excellent agreement.

## Appendix A

Tables Giving Values of  $D_0/D$  ( $D_0 = 100$ ) for  
Values of  $D$  From 0 to 70

	0	1	2	3	4	5	6	7	8	9
1	100.00	90.91	83.33	76.92	71.43	66.67	62.50	58.82	55.56	52.63
2	50.00	47.62	45.45	43.48	41.67	40.00	38.46	37.04	35.71	34.48
3	33.33	32.36	31.25	30.30	29.41	28.57	27.78	27.03	26.32	25.64
4	25.00	24.39	23.81	23.26	22.73	22.22	21.74	21.28	20.83	20.91
5	20.00	19.61	19.23	18.87	18.52	18.18	17.86	17.54	17.24	16.95
6	16.67	16.39	16.13	15.87	15.63	15.38	15.15	14.93	14.71	14.49
7	14.29	14.08	13.89	13.70	13.51	13.33	13.16	12.99	12.82	12.66
8	12.50	12.35	12.20	12.05	11.90	11.76	11.63	11.49	11.36	11.24
9	11.11	10.99	10.87	10.75	10.64	10.53	10.43	10.31	10.20	10.10
10	10.00	9.90	9.80	9.71	9.62	9.52	9.43	9.35	9.26	9.17
11	9.09	9.01	8.93	8.84	8.77	8.70	8.62	8.54	8.47	8.40
12	8.32	8.26	8.20	8.13	8.06	8.00	7.94	7.87	7.81	7.75
13	7.69	7.63	7.57	7.52	7.46	7.41	7.35	7.30	7.25	7.19
14	7.14	7.09	7.04	6.99	6.94	6.90	6.85	6.80	6.76	6.71
15	6.67	6.62	6.58	6.54	6.49	6.45	6.41	6.37	6.33	6.29
16	6.25	6.21	6.17	6.13	6.10	6.06	6.02	5.99	5.95	5.92
17	5.88	5.85	5.81	5.78	5.75	5.71	5.68	5.65	5.62	5.59
18	5.56	5.52	5.49	5.46	5.43	5.41	5.38	5.35	5.32	5.29
19	5.26	5.24	5.21	5.18	5.15	5.13	5.10	5.08	5.05	5.03
20	5.00	4.97	4.95	4.93	4.90	4.88	4.85	4.83	4.81	4.78
21	4.76	4.74	4.72	4.69	4.67	4.65	4.63	4.61	4.59	4.57
22	4.54	4.52	4.50	4.48	4.46	4.44	4.42	4.41	4.39	4.37
23	4.35	4.33	4.31	4.29	4.27	4.26	4.24	4.22	4.20	4.18
24	4.17	4.15	4.13	4.12	4.10	4.08	4.07	4.05	4.03	4.02
25	4.00	3.98	3.97	3.95	3.94	3.92	3.91	3.89	3.88	3.86
26	3.85	3.83	3.82	3.80	3.79	3.77	3.76	3.75	3.73	3.72
27	3.70	3.69	3.68	3.66	3.65	3.64	3.62	3.61	3.60	3.58
28	3.57	3.56	3.55	3.53	3.52	3.51	3.50	3.48	3.47	3.46
29	3.45	3.44	3.42	3.41	3.40	3.39	3.38	3.37	3.36	3.34
30	3.33	3.32	3.31	3.30	3.29	3.28	3.27	3.26	3.25	3.24
31	3.23	3.22	3.21	3.19	3.18	3.17	3.16	3.15	3.14	3.13
32	3.13	3.12	3.11	3.10	3.09	3.08	3.07	3.06	3.05	3.04
33	3.03	3.02	3.01	3.00	2.99	2.99	2.98	2.97	2.96	2.95
34	2.94	2.93	2.92	2.92	2.91	2.90	2.89	2.88	2.87	2.87
35	2.86	2.85	2.84	2.83	2.82	2.82	2.81	2.80	2.79	2.79
36	2.78	2.77	2.76	2.75	2.75	2.74	2.73	2.72	2.72	2.71
37	2.70	2.70	2.69	2.68	2.67	2.67	2.66	2.65	2.64	2.64
38	2.63	2.62	2.62	2.61	2.60	2.60	2.59	2.58	2.58	2.57
39	2.56	2.56	2.55	2.54	2.54	2.53	2.53	2.52	2.51	2.51
40	2.50	2.49	2.49	2.48	2.48	2.47	2.46	2.46	2.45	2.44
41	2.44	2.43	2.43	2.42	2.42	2.41	2.40	2.40	2.39	2.39
42	2.38	2.38	2.37	2.36	2.36	2.35	2.35	2.34	2.34	2.33
43	2.33	2.32	2.31	2.31	2.30	2.30	2.29	2.29	2.28	2.28
44	2.27	2.27	2.26	2.26	2.25	2.25	2.24	2.24	2.23	2.23
45	2.22	2.22	2.21	2.21	2.20	2.20	2.19	2.19	2.18	2.18
46	2.17	2.17	2.16	2.16	2.16	2.15	2.15	2.14	2.14	2.13
47	2.13	2.12	2.12	2.11	2.11	2.11	2.10	2.10	2.09	2.09
48	2.08	2.08	2.07	2.07	2.07	2.06	2.06	2.05	2.05	2.04
49	2.04	2.04	2.03	2.03	2.02	2.02	2.02	2.01	2.01	2.00

	0	1	2	3	4	5	6	7	8	9
50	2.00	2.00	1.99	1.99	1.98	1.98	1.98	1.97	1.97	1.96
51	1.96	1.96	1.95	1.95	1.95	1.94	1.94	1.93	1.93	1.93
52	1.92	1.92	1.92	1.91	1.91	1.90	1.90	1.90	1.89	1.89
53	1.89	1.88	1.88	1.88	1.87	1.87	1.87	1.86	1.86	1.86
54	1.85	1.85	1.85	1.84	1.84	1.83	1.83	1.83	1.82	1.82
55	1.82	1.81	1.81	1.81	1.81	1.80	1.80	1.80	1.79	1.79
56	1.79	1.78	1.78	1.78	1.77	1.77	1.77	1.76	1.76	1.76
57	1.75	1.75	1.75	1.75	1.74	1.74	1.74	1.73	1.73	1.73
58	1.72	1.72	1.72	1.72	1.71	1.71	1.71	1.70	1.70	1.70
59	1.69	1.69	1.69	1.69	1.68	1.68	1.68	1.68	1.67	1.67
60	1.67	1.66	1.66	1.66	1.66	1.65	1.65	1.65	1.64	1.64
61	1.64	1.64	1.63	1.63	1.63	1.63	1.62	1.62	1.62	1.62
62	1.61	1.61	1.61	1.61	1.60	1.60	1.60	1.59	1.59	1.59
63	1.59	1.58	1.58	1.58	1.58	1.57	1.57	1.57	1.56	1.56
64	1.56	1.56	1.56	1.56	1.55	1.55	1.55	1.55	1.54	1.54
65	1.54	1.54	1.53	1.53	1.53	1.53	1.52	1.52	1.52	1.52
66	1.52	1.51	1.51	1.51	1.51	1.50	1.50	1.50	1.50	1.49
67	1.49	1.49	1.49	1.49	1.48	1.48	1.48	1.48	1.47	1.47
68	1.47	1.47	1.47	1.46	1.46	1.46	1.46	1.46	1.45	1.45
69	1.45	1.45	1.45	1.44	1.44	1.44	1.44	1.43	1.43	1.43
70	1.43	1.43	1.42	1.42	1.42	1.42	1.42	1.41	1.41	1.41

**Appendix B****Tables Giving the Quantitative Analyses of All  
Samples Studied in This Investigation\***

\* Sample numbers are the ones assigned by the  
American Petroleum Institute Research Project 43C.

The Rb, Cs, and Tl determinations were made by the  
writer. The K determinations were made by personnel  
of the American Petroleum Institute Research Project  
43C.



**Explanation of symbols**

- n. a. - not analyzed
- n. d. - not detected
- n. d. (1) - not detected - but excessive background  
and/or interference present
- n. d. (2) - not detected but burn was poor
- v. - faint line visible but background and/or  
interference generally of such nature  
that no accurate determination was possible

Sample No.	Per Cent			
	K <sub>2</sub> O	Rb <sub>2</sub> O	Cs <sub>2</sub> O	Tl <sub>2</sub> O
45001	1.48	0.023	0.00089	n. a.
45004	0.74	0.0096	v.	n. d. (1)
45005	0.86	0.014	0.00072	0.000018
45006	0.60	0.0060	v.	n. a.
45012	2.64	0.029	v.	0.000042
45014	2.44	0.025	v.	0.000017
45018	2.41	0.022	v.	0.000022
45029	2.58	0.033	v.	0.000033
45033	1.87	0.018	v.	0.000010
45042	2.39	0.029	v.	0.000018
45054	3.29	0.042	0.00061	0.000034
45057	3.44	0.048	0.00066	0.000040
45064	3.30	0.045	0.00066	0.000037
45080	1.38	0.018	n. d.	n. d.
45085	1.39	0.016	n. d.	0.000036
45089	1.36	0.017	n. d.	0.000048
45124	3.83	0.051	0.0012	0.00012
45125	7.78	0.048	0.0027	0.00021
45126	4.79	0.051	0.0017	0.00024
45127	2.45	0.039	0.00096	0.00029
45128	2.00	0.019	n. d.	0.00012
45129	2.41	0.033	v.	0.00030
45130	3.48	0.051	0.00099	0.00039
45131	4.57	0.054	0.0011	0.00031
45132	1.96	v.	n. d. (1)	0.00060

Sample No.	Per Cent			
	K <sub>2</sub> O	Rb <sub>2</sub> O	Cs <sub>2</sub> O	Tl <sub>2</sub> O
45133	4.72	0.060	0.0011	0.00046
45134	1.24	0.011	0.00027	0.00016
45135	0.24	v.	n. d.	n. d. (1)
45140	2.11	0.033	0.00028	0.000023
45174	1.92	0.026	0.0013	v.
45182	1.09	0.013	0.00064	v.
45183	2.38	0.036	0.00077	0.000038
45184	2.34	0.036	0.0010	0.000039
45192	1.57	0.024	0.00069	0.000025
45203	0.50	0.0069	0.00029	n. d.
45216	0.41	0.0090	v.	n. d. (2)
45239	2.02	0.036	0.00064	0.000039
45248	2.09	0.039	0.00077	0.000033
45256	2.16	0.023	0.00059	0.000041
45267	0.35	0.0060	0.00012	0.0000049
45272	1.25	0.018	0.00035	v.
45280	2.48	0.042	0.00097	0.000023
45290	1.36	0.021	0.00044	0.000019
45294	2.26	0.036	0.00064	0.000045
45298	2.10	0.029	0.00086	0.000032
45303	1.75	0.025	0.00057	0.000036
45304	1.82	0.025	0.00074	0.000015
45308	1.81	0.026	0.00051	0.000032
45312	2.45	0.042	0.00071	0.000031
45320	1.75	0.027	n. d. (1)	v.

Sample No.	Per Cent			
	K <sub>2</sub> O	Rb <sub>2</sub> O	Cs <sub>2</sub> O	Tl <sub>2</sub> O
45323	0.19	n. d. (1)	n. d. (1)	n. d.
45328	1.94	0.029	0.00049	0.000032
45332	2.16	0.036	0.00063	0.000035
45337	2.08	0.033	0.00062	0.000039
45344	0.54	0.0054	n. d. (1)	n. d.
45345	0.96	v.	n. d. (1)	n. d.
45349	1.03	n. d. (1)	n. d. (1)	n. d.
45354	3.67	0.075	0.0017	0.000095
45355	0.34	0.0060	0.00019	0.000016
45362	0.67	v.	n. d. (1)	n. d.
45363	0.74	v.	n. d. (1)	n. d.
45412	2.02	0.033	n. d.	n. d.
45414	0.17	n. d. (1)	n. d. (1)	n. d.
45441	1.72	0.025	n. d. (1)	0.000015
45454	2.11	0.029	0.00067	0.000029
45467	1.26	0.016	n. d. (1)	n. d.
45490	1.90	0.026	0.00044	0.000027
45491	1.69	0.026	0.00062	0.000012
45492	0.28	0.0035	n. d.	n. d.
45493	1.81	0.039	v.	n. d. (2)
45494	0.14	n. d.	n. d.	n. d.
45499	0.90	0.015	0.00083	0.000018
45500	0.66	n. a.	n. a.	0.000013
45501	1.28	0.020	n. d. (1)	n. d.
45518	1.87	0.027	0.00055	0.000022

Sample No.	Per Cent			
	K <sub>2</sub> O	Rb <sub>2</sub> O	Cs <sub>2</sub> O	Tl <sub>2</sub> O
45522	1.97	0.033	n. d. (1)	0.000026
45529	1.68	0.027	0.00078	0.000012
45531	0.20	v.	n. d.	n. d. (2)
45538	0.07	n. d. (1)	n. d. (1)	n. d.
45552	0.71	0.014	0.00052	n. d. (2)
45554	0.36	0.0063	n. d.	n. d.
45555	1.68	0.026	n. d. (1)	v.
45557	0.76	0.0084	0.00047	n. d. (2)
45609	0.85	0.011	0.00058	v.
45671	0.17	0.0018	n. d. (1)	n. d.
45710	0.24	n. a.	n. a.	n. d. (2)
45718	3.01	0.054	0.0015	0.000046
45720	2.46	0.042	0.0017	v.
45722	1.99	0.029	0.00066	0.000024
45724	2.03	0.030	0.00061	v.
45729	2.23	0.042	0.00087	0.000031
45756	1.87	0.027	0.00069	0.000032
45757	1.69	0.025	0.00089	0.000014
45759	2.72	n. d. (2)	n. d. (2)	v.
45762	1.92	0.029	0.00067	0.000026
45763	2.11	0.028	0.00063	0.000041
45766	2.21	0.030	0.00061	0.000025
45767	0.28	0.0060	v.	n. d. (2)
45768	0.73	n. d. (1)	n. d. (1)	0.000010
45771	1.73	0.025	0.00076	0.000027

Sample No.	Per Cent			
	K <sub>2</sub> O	Rb <sub>2</sub> O	Cs <sub>2</sub> O	Tl <sub>2</sub> O
45784	0.30	n. d. (1)	n. d. (1)	n. d.
45790	2.00	0.030	0.00037	0.000028
45791	0.94	v.	n. d. (1)	n. d.
45830	2.47	0.042	0.00091	0.000037
45843	2.12	0.029	0.0012	0.000035
45851	2.39	0.033	0.00088	0.000044
45861	2.59	0.039	0.0010	0.000048
45871	2.24	0.036	0.00065	0.000032
45881	2.18	0.030	0.0011	0.000032
45891	2.45	0.033	0.0011	0.000036
45892	2.47	0.036	0.0011	0.000037
45900	2.10	0.030	0.00095	0.000043
45901	1.99	0.030	0.00083	0.000037
45902	2.04	0.030	0.0010	0.000036
45904	2.24	0.033	0.00091	0.000045
45906	2.22	0.033	0.00095	0.000042
45907	2.40	0.036	0.0011	0.000038
45921	0.47	n. d. (1)	n. d. (1)	n. d.
45961	0.56	0.0090	0.00024	n. d. (2)
45962	1.19	0.022	0.00064	0.000027
45964	1.18	0.016	n. d. (1)	n. d.
45982	1.80	0.026	0.00074	0.000029
45985	1.86	0.027	0.00091	0.000032
45990	2.03	0.030	0.00096	0.000034
45994	2.29	0.033	0.00082	0.000037

Sample No.	Per Cent			
	K <sub>2</sub> O	Rb <sub>2</sub> O	Cs <sub>2</sub> O	Tl <sub>2</sub> O
45999	2.59	0.036	0.00091	0.000050
46000	2.41	0.033	0.00076	0.000039
46007	2.03	0.030	0.00093	0.000039
46010	1.90	0.025	0.00092	0.000028
46014	2.16	0.036	0.0013	0.000026
46016	2.22	0.033	0.00098	0.000054
46020	2.40	0.042	0.0011	0.000059
46023	2.27	0.036	0.00096	0.000040
46030	2.15	0.036	0.00086	0.000038
46032	2.39	0.042	0.00094	0.000033
46035	2.27	0.033	0.00072	0.000036
46037	2.41	0.036	0.00094	0.000043
46039	2.28	0.039	0.00086	0.000044
46041	2.44	0.042	0.00089	0.000046
46043	2.42	0.039	0.0011	0.000048
46045	2.39	0.042	0.00082	0.000042
46049	2.44	0.039	0.00091	0.000044
46053	2.32	0.039	0.00071	0.000047
46057	2.38	0.039	0.00057	0.000042
46059	2.60	0.045	0.00082	0.000044
46062	2.45	0.039	0.00061	0.000041
46064	2.48	0.045	0.00077	0.000039
46068	2.46	0.039	0.00057	0.000033
46072	2.27	0.039	0.00060	0.000037
46076	2.45	0.042	0.00094	0.000040

Sample No.	Per Cent			
	K <sub>2</sub> O	Rb <sub>2</sub> O	Cs <sub>2</sub> O	Tl <sub>2</sub> O
46081	2.59	0.045	0.00082	0.000024
46085	2.72	0.045	0.0010	0.000043
46087	2.70	0.042	0.0012	0.000046
46088	2.38	0.036	0.0010	0.000048
46091	2.59	0.042	0.0012	0.000038
46095	2.60	0.042	0.0011	0.000036
46097	2.70	0.048	0.0014	0.000045
46107	2.50	0.036	0.0011	0.000032
46114	1.63	0.026	0.0011	0.000017
46117	2.26	0.033	0.0010	0.000041
46125	2.35	0.033	0.00088	0.000037
46126	2.36	0.039	0.0011	0.000036
46127	2.29	0.036	0.0010	0.000024
46128	2.38	0.039	0.0013	0.000042
46135	2.33	0.036	0.0013	0.000041
46136	2.35	0.036	0.0011	0.000049
46137	2.48	0.039	0.0013	0.000057
46141	2.23	0.033	0.0010	0.000054
46146	2.47	0.039	0.0012	0.000050
46155	1.99	0.036	0.00091	0.000042
46165	2.00	0.030	0.0010	0.000027
46175	2.28	0.039	0.00073	0.000037
46182	2.10	0.033	0.00070	0.000035
46185	2.32	0.039	0.00060	0.000044
46194	2.23	0.039	0.00071	0.000030



Sample No.	Per Cent			
	K <sub>2</sub> O	Rb <sub>2</sub> O	Cs <sub>2</sub> O	Tl <sub>2</sub> O
46202	1.92	0.033	0.0010	0.000031
46203	1.52	0.024	0.00079	0.000018
46211	1.86	0.030	0.00098	0.000023
46212	1.70	0.026	0.00082	0.000023
46216	2.11	0.036	0.00093	0.000043
46222	2.12	0.036	0.00062	0.000036
46226	2.45	0.039	0.00061	0.000048
46230	2.06	0.036	0.00064	0.000043
46237	2.02	0.033	0.00062	0.000030
46239	2.04	0.033	0.00071	0.000053
46242	2.26	0.036	0.00060	0.000053
46244	2.15	0.033	0.00048	0.000046
46247	1.74	0.028	0.00045	v.
46249	2.04	0.033	0.00049	0.000054
46253	1.88	0.030	0.00046	0.000046
46255	2.03	0.033	0.00064	v.
46256	2.05	0.030	0.00034	0.000038
46259	1.81	0.030	v.	0.000035
46261	1.93	0.030	v.	0.000026
46262	1.56	0.025	0.00052	0.000019
46267	1.68	0.026	0.00042	0.000021
46272	1.68	0.026	0.00059	0.000031
46277	1.62	0.025	v.	0.000026
46282	1.99	0.029	0.00035	0.000028
46287	2.00	0.030	0.00057	0.000022

Sample No.	Per Cent			
	K <sub>2</sub> O	Rb <sub>2</sub> O	Ca <sub>2</sub> O	Tl <sub>2</sub> O
46292	1.86	0.030	0.00068	0.000021
46297	2.03	0.033	0.00076	0.000017
46302	1.97	0.030	0.00074	v.
46312	1.97	0.028	0.00061	0.000018
46317	1.75	0.029	0.00073	v.
46322	1.62	0.026	0.00057	0.000038
46327	1.85	0.036	0.00077	v.
46332	1.87	0.036	0.00089	0.000015
46337	1.92	0.030	0.00059	0.000019
46342	2.06	0.036	0.00076	0.000020
46352	1.80	0.029	0.00053	0.000029
46357	1.49	0.025	0.00072	0.000026
46367	1.67	0.026	v.	n. d.
46368	1.91	0.029	n. d.	n. d.
46369	2.11	0.034	n. d.	n. d.
46370	1.13	0.019	n. d.	n. d.
46371	2.69	0.038	n. a.	0.000019
46377	1.03	n. d.	n. d. (1)	n. d.
46382	1.46	0.023	0.00054	n. d.
46387	1.04	v.	v.	n. d.
46393	1.02	0.017	0.0014	n. d. (2)
46397	1.45	0.016	0.0053	n. d.
46402	0.16	v.	n. d.	n. d. (2)
46407	1.00	v.	n. d. (1)	n. d.
46412	1.36	0.036	0.0012	0.000019

Sample No.	K <sub>2</sub> O	Rb <sub>2</sub> O	Cs <sub>2</sub> O	Tl <sub>2</sub> O
46417	0.66	v.	n. d. (1)	n. d.
46422	0.08	n. d.	n. d. (1)	n. d.
46427	1.17	0.018	n. d. (1)	n. d.
46432	0.20	n. d.	n. d. (1)	n. d.
46437	0.12	n. d.	n. d. (1)	n. d.
46442	0.31	0.0045	0.00016	n. d.
46447	0.10	n. d.	n. d.	n. d.
46462	1.87	0.027	n. d. (1)	v.
46467	0.74	v.	n. d. (1)	n. d.
46472	2.08	0.033	n. d. (1)	0.000023
46475	0.0	n. d.	n. d. (1)	n. d.
46476	1.68	0.028	0.00083	0.000017
46479	1.73	0.030	0.00095	0.000023
46480	1.78	0.030	0.00093	n. a.
46485	0.89	0.014	0.00052	v.
46486	0.83	0.014	0.00038	0.000017
46490	2.05	0.036	0.00079	0.000042
46491	1.10	0.018	0.00039	v.
46494	1.07	0.024	0.00045	v.
46495	1.98	0.030	0.00051	0.000039
46500	2.12	0.030	0.00062	0.000039
46503	2.15	0.033	0.00075	0.000043
46508	1.49	0.022	0.00041	v.
46510	1.90	0.028	0.00063	n. a.
46512	1.72	0.025	0.00046	0.000042

Sample No.	Per Cent			
	K <sub>2</sub> O	Rb <sub>2</sub> O	Cs <sub>2</sub> O	Tl <sub>2</sub> O
46515	1.90	0.028	0.00063	0.000035
46518	2.02	0.030	0.00074	0.000035
46519	1.92	n. a.	n. a.	0.000030
46520	1.13	0.018	v.	v.
46525	1.02	0.013	v.	0.000029
46531	0.52	0.0072	0.00029	n. d. (1)
46536	0.48	0.0077	v.	0.000016
46538	0.95	0.0074	0.00023	v.
46539	0.59	0.0054	n. d. (1)	n. d. (1)
46541	0.30	0.0024	n. d. (1)	n. d. (1)
46542	2.12	0.019	0.00055	0.000039
46544	0.88	0.013	v.	v.
46549	0.64	0.0087	0.00022	0.000015
46555	1.34	0.021	v.	v.
46559	1.31	0.020	v.	0.000021
46561	1.85	0.028	v.	0.000042
46568	1.34	0.015	0.00047	0.000037
46573	1.60	0.022	0.00059	0.000035
46582	0.67	0.010	0.00021	v.
46591	1.70	0.017	0.00057	n. d. (1)
46593	1.39	0.014	0.00043	0.000028
46599	1.45	0.015	0.00051	0.000026
46600	1.55	0.016	0.00055	0.000022
46603	1.10	0.011	0.00036	0.000020
46608	1.26	0.014	0.00044	0.000022

Sample No.	Per Cent			
	K <sub>2</sub> O	Rb <sub>2</sub> O	Cs <sub>2</sub> O	Tl <sub>2</sub> O
46609	1.80	0.020	0.00027	0.00014
46613	2.24	0.028	0.00064	0.000036
46616	3.68	0.051	0.00095	0.000047
46619	2.27	0.030	0.00059	0.000032
46622	3.12	0.042	0.00078	0.000046
46625	3.36	0.045	0.00084	0.000042
46627	2.45	0.039	0.00077	0.000024
46630	3.36	0.048	0.00092	0.000042
46632	3.00	0.042	0.00075	0.000039
46635	3.25	0.042	0.00081	0.000037
46637	2.69	0.036	0.00058	0.000030
46640	3.19	0.039	0.00064	0.000045
46643	3.20	0.045	0.00090	0.000035
46644	2.53	0.036	0.00068	0.000027
46646	3.22	0.048	0.00078	0.000036
46648	3.25	0.045	0.00076	0.000037
46650	2.98	0.028	0.00082	0.0012
46653	3.00	0.029	0.00092	0.0010
46657	3.07	0.030	0.00074	0.0010
46661	3.08	0.029	0.00095	0.00096
46664	2.96	0.027	0.00099	0.00098
46667	2.82	0.030	0.0011	0.0019
46670	3.01	0.028	0.00098	0.00094
46673	3.18	0.045	0.0010	0.000022
46677	3.77	0.057	0.0013	0.000055

Sample No.	Per Cent			
	K <sub>2</sub> O	Rb <sub>2</sub> O	Ca <sub>2</sub> O	Tl <sub>2</sub> O
46679	3.14	0.042	0.00091	0.000050
46682	3.54	0.048	0.0012	0.000045
46684	3.55	0.048	0.0011	0.000042
46685	3.58	0.048	0.0010	0.000045
46690	3.79	0.054	0.0013	0.000035
46692	2.80	0.036	0.00093	0.000079
46695	2.59	0.042	0.00090	0.000059
46698	2.77	0.039	0.00090	0.00011
46705	2.96	0.045	0.00099	0.000068
46707	3.05	0.048	0.0012	0.000087
46708	2.83	0.042	0.00099	0.000093
46714	2.41	0.036	0.0013	0.000078
46715	3.64	0.054	0.0018	0.000067
46716	2.92	0.045	0.0013	0.000088
46719	2.65	0.039	0.0013	0.000046
46720	3.95	0.057	0.0018	0.000082
46724	3.18	0.042	0.0017	0.000068
46729	3.05	0.045	0.0012	0.00011
46731	2.64	0.033	0.0011	0.000089
46734	2.09	0.033	0.0014	0.000094
46736	1.50	0.018	0.00084	0.000078
46743	3.43	0.054	0.0011	0.00015
46745	3.16	0.042	v.	0.00016
46747	3.24	0.042	0.0011	0.00011

**Appendix C**

**Tables Giving the Abundance Ratios  
for All Samples**

Sample No.	$\frac{\%K_2O}{\%Rb_2O}$	$\frac{\%K_2O}{\%Cs_2O}$	$\frac{\%K_2O}{\%Tl_2O}$	$\frac{\%Rb_2O}{\%Tl_2O}$
45001	64	1660	-	-
45004	77	-	-	-
45005	62	1190	48000	780
45006	100	-	-	-
45012	91	-	63000	690
45014	98	-	14000	1470
45018	110	-	110000	1000
45029	78	-	78000	1000
45033	104	-	180000	1800
45042	82	-	130000	1610
45054	78	5400	97000	1240
45057	72	5210	86000	1200
45064	73	5000	89000	1220
45080	77	-	-	-
45085	87	-	38000	440
45089	80	-	28000	350
45124	75	3100	32000	430
45125	162	2880	37000	230
45126	94	2820	20000	210
45127	63	2560	8500	130
45128	105	-	17000	160
45129	73	-	8000	110
45130	68	3520	8900	130
45131	85	4160	15000	170
45132	-	-	3300	-



Sample No.	$\frac{\%K_2O}{\%Rb_2O}$	$\frac{\%K_2O}{\%Cs_2O}$	$\frac{\%K_2O}{\%Tl_2O}$	$\frac{\%Rb_2O}{\%Tl_2O}$
45133	79	4300	10000	130
45134	113	4600	7800	69
45135	-	-	-	-
45140	64	7540	92000	1400
45174	74	1480	-	-
45182	84	1720	-	-
45183	66	3100	63000	950
45184	65	2340	60000	920
45192	66	2270	63000	960
45203	73	1720	-	-
45216	46	-	-	-
45239	56	3160	52000	920
45248	54	2720	63000	1200
45256	94	3660	53000	560
45267	58	2920	71000	1200
45272	69	3580	-	-
45280	59	2560	110000	1800
45290	65	3090	72000	1100
45294	63	3530	50000	800
45298	73	2440	66000	910
45303	70	3070	49000	700
45304	73	2460	120000	1700
45308	69	3550	57000	810
45312	58	3450	79000	1400
45320	65	-	-	-

Sample No.	$\frac{\%K_2O}{\%Rb_2O}$	$\frac{\%K_2O}{\%Cs_2O}$	$\frac{\%K_2O}{\%Tl_2O}$	$\frac{\%Rb_2O}{\%Tl_2O}$
45323	-	-	-	-
45328	67	3960	61000	910
45332	60	3420	62000	1000
45337	63	3360	53000	850
45344	100	-	-	-
45345	-	-	-	-
45349	-	-	-	-
45354	49	2160	39000	790
45355	57	1780	21000	370
45362	-	-	-	-
45363	-	-	-	-
45412	61	-	-	-
45414	-	-	-	-
45441	69	-	110000	1700
45454	73	3150	73000	1000
45467	79	-	-	-
45490	73	4320	70000	960
45491	65	2730	140000	2200
45492	80	-	-	-
45493	46	-	-	-
45494	-	-	-	-
45499	60	1080	50000	830
45500	-	-	51000	-
45501	64	-	-	-
45518	69	3400	85000	1200

Sample No.	$\frac{\%K_2O}{\%Rb_2O}$	$\frac{\%K_2O}{\%Cs_2O}$	$\frac{\%K_2O}{\%Tl_2O}$	$\frac{\%Rb_2O}{\%Tl_2O}$
45522	60	-	76000	1300
45529	62	2150	14000	2300
45531	-	-	-	-
45538	-	-	-	-
45552	51	1360	-	-
45554	57	-	-	-
45555	65	-	-	-
45557	90	1620	-	-
45609	77	1460	-	-
45671	94	-	-	-
45710	-	-	-	-
45718	56	2000	66000	1200
45720	59	1450	-	-
45722	69	3020	83000	1200
45724	68	3330	-	-
45729	53	2560	72000	1400
45756	70	2710	58000	850
45757	68	1900	120000	1800
45759	-	-	-	-
45762	66	2860	74000	1100
45763	75	3340	51000	680
45766	74	3620	89000	1200
45767	47	-	-	-
45768	-	-	73000	-
45771	69	2280	64000	930

Sample No.	$\frac{\%K_2O}{\%Rb_2O}$	$\frac{\%K_2O}{\%Cs_2O}$	$\frac{\%K_2O}{\%Tl_2O}$	$\frac{\%Rb_2O}{\%Tl_2O}$
45784	-	-	-	-
45790	67	5410	71000	1100
45791	-	-	-	-
45830	59	2720	67000	1100
45843	73	1770	61000	830
45851	72	2720	54000	750
45861	66	2590	54000	810
45871	62	3440	70000	1100
45881	73	1960	68000	940
45891	74	2220	68000	940
45892	69	2240	67000	970
45900	70	2210	49000	700
45901	66	2400	54000	810
45902	68	2040	57000	830
45904	68	2460	50000	730
45906	67	2340	53000	790
45907	67	2180	63000	950
45921	-	-	-	-
45961	62	2330	-	-
45962	54	1860	44000	820
45964	74	-	-	-
45982	69	2440	62000	900
45985	69	2040	58000	850
45990	68	2110	60000	880
45994	69	2800	62000	890

Sample No.	$\frac{\%K_2O}{\%Rb_2O}$	$\frac{\%K_2O}{\%Cs_2O}$	$\frac{\%K_2O}{\%Tl_2O}$	$\frac{\%Rb_2O}{\%Tl_2O}$
45999	72	2840	52000	720
46000	73	3170	62000	850
46007	68	2180	52000	770
46010	76	2060	68000	890
46014	60	1660	83000	1400
46016	67	2260	41000	610
46020	57	2180	41000	710
46023	63	2360	57000	900
46030	60	2500	57000	950
46032	57	2540	72000	1300
46035	69	3160	63000	920
46037	67	2570	56000	840
46039	59	2650	52000	890
46041	58	2740	53000	910
46043	62	2200	50000	810
46045	57	2920	57000	1000
46049	63	2680	55000	890
46053	60	3270	49000	830
46057	61	4180	57000	930
46059	58	3170	59000	1000
46062	63	4020	60000	950
46064	55	3090	64000	1200
46068	63	4310	75000	1200
46072	58	3780	61000	1100
46076	58	2610	61000	1100

Sample No.	$\frac{\%K_2O}{\%Rb_2O}$	$\frac{\%K_2O}{\%Cs_2O}$	$\frac{\%K_2O}{\%Tl_2O}$	$\frac{\%Rb_2O}{\%Tl_2O}$
46081	58	3160	110000	1900
46085	60	2720	63000	1000
46087	64	2250	60000	930
46088	66	2380	50000	750
46091	62	2160	68000	1100
46095	62	2360	72000	1200
46097	56	1930	60000	1100
46107	70	2270	78000	1100
46114	63	1480	96000	1500
46117	69	2260	55000	810
46125	71	2680	64000	890
46126	61	2150	66000	1100
46127	64	2290	96000	1500
46128	61	1830	57000	930
46135	65	1790	57000	880
46136	65	2140	48000	740
46137	64	1910	44000	680
46141	68	2230	41000	610
46146	63	2060	49000	780
46155	55	2190	47000	860
46165	67	2000	74000	1100
46175	59	3130	62000	1100
46182	64	3000	60000	940
46185	60	3870	53000	890
46194	57	3140	74000	1300

Sample No.	$\frac{\%K_2O}{\%Rb_2O}$	$\frac{\%K_2O}{\%Cs_2O}$	$\frac{\%K_2O}{\%Tl_2O}$	$\frac{\%Rb_2O}{\%Tl_2O}$
46202	58	1920	62000	1100
46203	63	1930	85000	1300
46211	62	1900	81000	1300
46212	65	2070	74000	1100
46216	59	2260	49000	840
46222	59	3420	59000	1000
46226	63	4010	51000	810
46230	57	3220	48000	840
46237	61	3260	67000	1100
46239	62	2880	39000	620
46242	63	2760	43000	680
46244	65	4490	47000	720
46247	62	3870	-	-
46249	62	4160	38000	610
46253	63	4090	41000	650
46255	62	3170	-	-
46256	68	6030	54000	790
46259	60	-	52000	860
46261	64	-	74000	1200
46262	62	3010	32000	1300
46267	65	4000	30000	1200
46272	65	2840	54000	840
46277	65	-	63000	960
46282	69	5690	70000	1000
46287	67	3510	91000	1400

Sample No.	$\frac{\%K_2O}{\%Rb_2O}$	$\frac{\%K_2O}{\%Cs_2O}$	$\frac{\%K_2O}{\%Tl_2O}$	$\frac{\%Rb_2O}{\%Tl_2O}$
46292	62	2740	89000	1400
46297	62	2670	120000	1900
46302	66	2660	-	-
46312	70	3230	110000	1600
46317	60	2400	-	-
46322	62	2840	43000	680
46327	51	2400	-	-
46332	52	2100	120000	2400
46337	64	3250	100000	1600
46342	57	2710	100000	1800
46352	62	3390	62000	1000
46357	60	2070	57000	960
46367	64	-	-	-
46368	66	-	-	-
46369	62	-	-	-
46370	60	-	-	-
46371	71	-	140000	2000
46377	-	-	-	-
46382	64	2710	-	-
46387	-	-	-	-
46393	60	7300	-	-
46397	91	2740	-	-
46402	-	-	-	-
46407	-	-	-	-
46412	38	1130	72000	1900



Sample No.	$\frac{\%K_2O}{\%Rb_2O}$	$\frac{\%K_2O}{\%Ca_2O}$	$\frac{\%K_2O}{\%Ti_2O}$	$\frac{\%Rb_2O}{\%Ti_2O}$
46417	-	-	-	-
46422	-	-	-	-
46427	65	-	-	-
46432	-	-	-	-
46437	-	-	-	-
46442	69	1940	-	-
46447	-	-	-	-
46452	69	-	-	-
46457	-	-	-	-
46472	63	-	90000	1400
46475	-	-	-	-
46475	60	2020	99000	1600
46479	58	1820	75000	1300
46480	60	1910	-	-
46485	62	1710	-	-
46485	59	2190	49000	820
46490	57	2590	49000	860
46491	61	2820	-	-
46494	45	2380	-	-
46495	66	3880	51000	770
46500	71	3420	54000	770
46503	65	2870	50000	770
46508	68	3640	-	-
46510	68	3020	-	-
46512	69	3740	41000	600

Sample No.	$\frac{\%K_2O}{\%Rb_2O}$	$\frac{\%K_2O}{\%Cs_2O}$	$\frac{\%K_2O}{\%Tl_2O}$	$\frac{\%Rb_2O}{\%Tl_2O}$
46515	68	3020	54000	800
46518	67	2730	58000	860
46519	-	-	64000	-
46520	63	-	-	-
46525	79	-	35000	450
46531	72	1790	-	-
46536	62	-	30000	480
46538	128	4130	-	-
46539	109	-	-	-
46541	125	-	-	-
46542	112	3860	54000	490
46544	68	-	-	-
46549	73	3910	43000	580
46555	64	-	-	-
46559	65	-	63000	950
46561	66	-	44000	670
46568	89	2850	35000	410
46573	73	2710	46000	630
46582	67	3190	-	-
46591	100	2980	-	-
46593	99	3230	50000	500
46599	97	2840	56000	580
46600	97	2820	71000	730
46603	99	3050	55000	550
46608	90	2860	57000	640

Sample No.	$\frac{\%K_2O}{\%Rb_2O}$	$\frac{\%K_2O}{\%Cs_2O}$	$\frac{\%K_2O}{\%Tl_2O}$	$\frac{\%Rb_2O}{\%Tl_2O}$
46609	90	6660	16000	140
46613	80	3500	62000	780
46616	72	3880	78000	1100
46619	76	3850	71000	940
46622	74	4000	68000	910
46625	75	4000	80000	1100
46627	63	3180	100000	1600
46630	70	3650	80000	1100
46632	72	4000	77000	1100
46635	78	4020	88000	1100
46637	75	4640	90000	1200
46640	82	5000	71000	870
46643	71	3560	92000	1300
46644	71	3720	94000	1300
46646	67	4130	90000	1300
46648	72	4280	88000	1200
46650	106	3640	2500	23
46653	103	3260	3000	29
46657	102	4150	3000	30
46661	106	3240	3000	30
46664	110	2990	3000	28
46667	101	2560	1500	15
46670	108	3070	3200	30
46673	71	3180	140000	2000
46677	66	2820	68000	1000

Sample No.	$\frac{\%K_2O}{\%Rb_2O}$	$\frac{\%K_2O}{\%Cs_2O}$	$\frac{\%K_2O}{\%Tl_2O}$	$\frac{\%Rb_2O}{\%Tl_2O}$
46679	75	3460	63000	840
46682	74	2940	79000	1100
46684	74	3220	85000	1100
46686	75	3580	80000	1100
46690	70	2920	110000	1500
46692	78	3010	35000	460
46696	62	2880	44000	710
46698	71	3080	25000	350
46705	66	2990	44000	660
46707	64	2540	35000	550
46708	67	2860	30000	450
46714	67	1850	31000	460
46715	68	2020	54000	810
46716	65	2250	33000	510
46719	68	2040	58000	850
46720	69	2190	48000	700
46724	76	1870	47000	620
46729	68	2540	28000	410
46731	80	2400	30000	370
46734	63	1490	22000	350
46736	83	1780	19000	230
46743	64	3120	23000	360
46745	75	-	20000	260
46747	77	2940	29000	380

Appendix D

Location of Samples

Sample No.	Formation	Sample No.	Formation
45001	Miocene Nodular Shale	45133	Mt. Glen Shale
45004	" " "	45134	-- (Bl. Sh.)
45005	" " "	45135	--
45006	" " "	45140	Eagle Ford Shale
45012	Frio Sandstone	45174	" " "
45014	" " "	45182	" " "
45018	" " "	45183	" " "
45029	" " "	45184	" " "
45033	" " "	45192	Woodbine Sandstone
45042	" " "	45203	" "
45054	" " "	45216	Austin Chalk
45057	" " "	45239	Eagle Ford Shale
45064	" " "	45248	Woodbine Sandstone
45080	" " "	45256	Tuscaloosa Sandstone
45085	" " "	45267	Eagle Ford Shale
45089	" " "	45272	" " "
45124	Chattanooga Shale	45280	" " "
45125	-- (Bentonite)	45290	" " "
45126	Chattanooga Shale	45294	" " "
45127	-- (Bl. Sh.)	45298	Austin Chalk
45128	Woodford Shale	45303	" "
45129	-- (Bl. Sh.)	45304	" "
45130	Chattanooga Shale	45308	" "
45131	" "	45312	Eagle Ford Shale
45132	Woodford Shale	45320	Woodbine Sandstone

Sample No.	Formation	Sample No.	Formation
45323	Woodbine Sandstone	45522	Woodbine Sandstone
45328	Austin Chalk	45529	Austin Chalk
45332	Eagle Ford Shale	45531	" "
45337	" " "	45538	Woodbine Sandstone
45344	Austin Chalk	45552	Austin Chalk
45345	Woodbine Sandstone	45554	Woodbine Sandstone
45349	Eagle Ford Shale	45555	" "
45354	" " "	45557	Austin Chalk
45355	" " "	45609	" "
45362	Woodbine Sandstone	45671	" "
45363	" "	45710	" "
45412	" "	45718	Woodbine Sandstone
45414	" "	45720	Eagle Ford Shale
45441	" "	45722	Austin Chalk
45454	Austin Chalk	45724	" "
45467	Woodbine Sandstone	45729	" "
45490	Austin Chalk	45756	" "
45491	Woodbine Sandstone	45757	" "
45492	Austin Chalk	45759	" "
45493	Woodbine Sandstone	45762	" "
45494	" "	45763	" "
45499	Austin Chalk	45766	Woodbine Sandstone
45500	" "	45767	Austin Chalk
45501	Woodbine Sandstone	45768	Eagle Ford Shale
45518	" "	45771	Austin Chalk

Sample No.	Formation	Sample No.	Formation
45784	Woodbine Sandstone	45999	Lower Eutaw Shale
45790	Austin Chalk	46000	" " "
45791	Woodbine Sandstone	46007	" " "
45830	Eagle Ford Shale	46010	" " "
45843	Selma Chalk	46014	" " "
45851	" "	46016	" " "
45861	" "	46020	" " "
45871	" "	46023	" " "
45881	" "	46030	" " "
45891	" "	46032	Tuscaloosa Sandstone
45892	" "	46035	" "
45900	" "	46037	" "
45901	" "	46039	" "
45902	" "	46041	" "
45904	" "	46043	" "
45906	" "	46045	" "
45907	" "	46049	" "
45921	Woodbine Sandstone	46053	" "
45961	Austin Chalk	46057	" "
45962	" "	46059	" "
45964	Woodbine Sandstone	46062	" "
45982	Selma Chalk	46064	" "
45985	" "	46068	" "
45990	" "	46072	" "
45994	Lower Eutaw Shale	46076	" "



Sample No.	Formation	Sample No.	Formation
46081	Tuscaloosa Sandstone	46202	Lower Eutaw Shale
46085	" "	46203	" " "
46087	Selma Chalk	46211	" " "
46088	" "	46212	" " "
46091	" "	46216	" " "
46095	" "	46222	" " "
46097	" "	46226	" " "
46107	" "	46230	" " "
46114	" "	46237	Tuscaloosa Sandstone
46117	" "	46239	" "
46125	" "	46242	" "
46126	" "	46244	" "
46127	" "	46247	" "
46128	" "	46249	" "
46135	" "	46253	" "
46136	" "	46255	" "
46137	" "	46256	Eagle Ford Shale
46141	" "	46259	Tuscaloosa Sandstone
46146	" "	46261	" "
46155	Lower Eutaw Shale	46262	--
46165	" " "	46267	--
46175	" " "	46272	Austin Chalk
46182	" " "	46277	" "
46185	" " "	46282	" "
46194	" " "	46287	" "

Sample No.	Formation	Sample No.	Formation
46292	Austin Chalk	46417	Woodbine Sandstone
46297	" "	46422	" "
46302	" "	46427	" "
46312	" "	46432	" "
46317	" "	46437	" "
46322	" "	46442	" "
46327	" "	46447	" "
46332	" "	46462	Eagle Ford Shale
46337	" "	46467	Woodbine Sandstone
46342	" "	46472	" "
46352	" "	46475	" "
46357	" "	46476	Miocene Nodular Shale
46367	Eagle Ford Shale	46479	" " "
46368	" " "	46480	" " "
46369	" " "	46485	" " "
46370	" " "	46486	" " "
46371	" " "	46490	" " "
46377	Woodbine Sandstone	46491	" " "
46382	" "	46494	" " "
46387	" "	46495	" " "
46393	Austin Chalk	46500	" " "
46397	" "	46503	" " "
46402	" "	46508	" " "
46407	Eagle Ford Shale	46510	" " "
46412	Woodbine Sandstone	46512	" " "

Sample No.	Formation	Sample No.	Formation
46515	Miocene nodular shale	46609	Cherokee shale
46518	"	46613	"
46519	"	46616	"
46520	"	46619	"
46525	"	46622	"
46531	"	46625	"
46536	"	46627	"
46538	"	46630	"
46539	"	46632	"
46541	"	46635	"
46542	"	46637	"
46544	"	46640	"
46549	"	46643	"
46555	"	46644	"
46559	"	46646	"
46561	"	46648	"
46568	"	46650	Woodford shale
46573	"	46653	"
46582	"	46657	"
46591	"	46661	"
46593	"	46664	"
46599	"	46667	"
46600	"	46670	"
46603	"	46673	Cherokee shale
46608	"	46677	"

Sample No.	Formation	Sample No.	Formation
46679	Cherokee Shale	46715	Cherokee Shale
46682	" "	46716	" "
46684	" "	46719	" "
46686	" "	46720	" "
46690	" "	46724	" "
46692	" "	46729	" "
46696	" "	46731	" "
46698	" "	46734	" "
46705	" "	46736	" "
46707	" "	46743	Antrim Shale
46708	" "	46745	" "
46714	" "	46747	" "

## Location of New England Granites

## Sample No.

2A4 Roadcut, Route 128, Dedham, Mass.  
 6A8 Westwood Quarry, Westwood, Mass.

15A2 Bow St. Quarry, Freeport, Maine  
 15A12 Outer Latti Quarry, Pownal, Maine

15A19 Long Cove Quarry, South Thomaston, Maine  
 15A23 Neehan Quarry, Clark Island, Maine

16A10 American Granite Co. Quarry, North Jay, Maine  
 16A12 Maine & N. H. Granite Co. Quarry, North Jay, Maine

16A13 Perry Quarry, Hallowell, Maine  
 16A16 Jim Bailey Quarry, Hallowell, Maine

16A22 New Westerly Quarry, Milford, N. H.  
 16A28 Old Tonella Quarry, Milford, N. H.

18A18 Chapman Quarry, Westerly, R. I.  
 18A25 Calder & Carnie Quarry, Westerly, R. I.

19A5 Sullivan Granite Co. Quarry, Bradford, R. I.  
 19A8 Klondike Quarry, Bradford, R. I.

19A13 Webb-Fitzwilliam Quarry, Fitzwilliam, N. H.  
 19A22 North Pole Quarry, Fitzwilliam, N. H.

20A11 Wetmore-Morse Quarry, Barre, Vt.  
 20A26 Rock of Ages Quarry, Barre, Vt.

21A1 Woodbury Granite Corp. Quarry, Woodbury, Vt.  
 21A7 Drennan Quarry, Woodbury, Vt.

21A11 Blanchard Quarry, Concord, N. H.  
 21A16 State Prison Quarry, Concord, N. H.

22A11 Porcupine Quarry, North Sullivan, Maine  
 22A4 Havey-Robertson Quarry, North Sullivan, Maine

24A20 Blue Hill Granite Co., Blue Hill, Maine  
 24A24 Kinch Mt. Quarry, South Brookville, Maine

25A8 Wallace Cove Quarry, Jonesport, Maine  
 25A12 Booth Bros. Quarry, Jonesboro, Maine

## Biography

**Name:** Frank Cogswell Canney

**Date of Birth:** October 8, 1920

**Place of Birth:** Ipswich, Massachusetts

**Parents:** Ruth E. Canney and Frank T. Canney

**Wife:** Married Isabel Chandler Oliver  
on December 23, 1944

**Education:** Public Schools of Ipswich,  
Massachusetts

Massachusetts Institute of Technology,  
1937-1942. S.B. Degree in Chemistry  
April 27, 1942

Massachusetts Institute of Technology,  
1947-1952. Graduate Study

**Assistantships:** Research Assistant in Geology, 1948-  
1951

**Honors:** Society of the Sigma Xi

**Military Experience:** U. S. Navy, 1942-1947

1. Ahrens, L. H. (1945). Geochemical studies on some of the rarer elements in South African minerals and rocks. II. The geochemical relationship between thallium and rubidium in minerals of igneous origin. Trans. Geol. Soc. S. Afr., 48, 207.
2. Ahrens, L. H. (1950). Spectrochemical analysis. Addison-Wesley Press, Inc., Cambridge, Mass.
3. Ahrens, L. H. (1951). Private communication.
4. Barton, J. M. (1945). Pre-Permian axes of maximum deposition in West Texas. Bull. Am. Assoc. Petr. Geol. 29, 1356.
5. Boyd, G. E. et al (1947). Ion-exchange equilibria. J. Am. Chem. Soc. 69, 2818.
6. Cholak, J. and Story, R. V. (1941). Spectrochemical determination of trace metals in biological material. J. Opt. Soc. Am., 31, 730.
7. Clarke, F. W. (1924). The data of geochemistry. 5th Ed. U. S. Geol. Survey Bull. 770.
8. Gedroiz, K. K. (1918-19). Contribution to our knowledge of the absorptive capacity of the soil. Translated from Russian by S. A. Waksman, mimeographed and distributed by the U. S. D. A. Published originally in Zhur. Opt. Agron., 19, 269-322; 20, 31-58.
9. Goldschmidt, V. M., Bauer, H. and Witte, H. (1934). Geochemistry of the alkali metals. II. Nachr. Ges. Wiss. Göttingen, Math-Phys. Kl., 1, 39.
10. Harrison, G. R., Lord, R. G. and Loebnow, J. R. (1948). Practical Spectroscopy. Prentice-Hall, New York.
11. Hoote, H. W., Blount, A. L. and Jones, P. H. (1935). Marine oil shale, source of oil in Playa del Rey field, California. Bull. Am. Assoc. Petr. Geol., 19, 172.

## Bibliography - Continued

12. Kaiser, H. (1941). *Spectrochim. Acta.*, 2, 1.
13. McGlothlin, T. (1944). General geology of Mississippi. *Bull. Am. Assoc. Petr. Geol.* 28, 29.
14. Minor, H. E. and Hanna, M. A. (1941). East Texas oil field. In *Stratigraphic Type Oil Fields - A Symposium*. Am. Assoc. Petr. Geol., Tulsa, Okla.
15. Mitchell, R. L. (1948). The Spectrographic Analysis of Soils, Plants, and Related Materials. Technical Communication No. 44 of the Commonwealth Bureau of Soil Science, Harpenden, England.
16. Nachtrieb, N. H. (1950). *Principles and Practice of Spectrochemical Analysis*. McGraw-Hill, New York.
17. Preuss, E. (1940). Determination of Zn, Cd, Hg, In, Tl, Ge, Sn, Pb, Sb, and Bi by fractional distillation. *Zeit. Angew. Mineral.*, 3, 8.
18. Rankama, E. and Sahama, Th. G. (1950). *Geochemistry*. University of Chicago Press.
19. Sawyer, R. A. (1944). *Experimental Spectroscopy*. Prentice-Hall, New York.
20. Strock, L. W. (1936). *Spectrum Analysis with the Carbon Arc Cathode Layer*. Adam Hilger, London.
21. Trask, P. D. (1942). *Source Beds of Petroleum*. Am. Assoc. Petr. Geol., Tulsa, Okla.
22. ----- (1951). *Processing and Formulas*. 4th Ed. Eastman Kodak Co., Rochester, N. Y.